University of Nevada, Reno

Intimations on the Regulation of Myometrial Functions: Lessons from the Proteome and S-nitrosoproteome in Human Preterm Labor

A dissertation submitted in partial fulfillment of the
requirements for the degree of Doctor of Philosophy in
Biochemistry

by

Craig C. Ulrich

Dr. Iain L.O. Buxton/ Dissertation Advisor

May, 2013

University of Nevada, Reno
Statewide • Worldwide

THE GRADUATE SCHOOL

We recommend that the dissertation
prepared under our supervision by

CRAIG C. ULRICH

entitled

Intimations On The Regulation Of Myometrial Functions: Lessons From The Proteome And S-Nitrosoproteome In Human Preterm Labor

be accepted in partial fulfillment of the
requirements for the degree of

DOCTOR OF PHILOSOPHY

Iain L.O. Buxton, PharmD, Advisor

Josh Baker, PhD, Committee Member

Grant R. Cramer, PhD, Committee Member

Kathleen Schegg, PhD, Committee Member

Cherie Singer, PhD, Graduate School Representative

Marsha H. Read, Ph. D., Dean, Graduate School

May,

ABSTRACT

The molecular mechanisms involved in uterine quiescence during gestation and those responsible for induction of labor are not completely known. More than 10% of babies born worldwide are premature and one million die each year. Preterm labor results in preterm delivery in 50% of cases in the US explaining 75% of fetal morbidity and mortality. There is no FDA-approved treatment available to prevent preterm delivery. Nitric oxide relaxes uterine smooth muscle in a manner disparate from other smooth muscles since global elevation of cGMP following activation of soluble guanylyl cyclase does not relax the muscle. S-nitrosation, the covalent addition of an NO-group to a cysteine thiol is a likely mechanism to explain the ability of NO to relax myometrium. This work is the first to describe the myometrial S-nitrosoproteome in both the pregnant and non-pregnant tissue states. Using the guinea pig model, we show that specific sets of proteins involved in contraction and relaxation are S-nitrosated in laboring and non-laboring muscle and that many of these proteins are uniquely S-nitrosated in only one state of the tissue. In particular, we show that S-nitrosation of the intermediate filament protein desmin is significantly increased (5.7 fold, $p < 0.005$) in pregnancy and that this increase cannot be attributed solely to the increase in protein expression (1.8 fold, $p < 0.005$) that accompanies pregnancy. Elucidation of the myometrial S-nitrosoproteome provides a list of mechanistically important proteins that can constitute the basis of hypotheses formed to explain the regulation of uterine contraction-relaxation.

Identification and semi-quantification of proteomic changes during pregnancy will allow for targeted research into how the induction of labor occurs. We have recently performed two dimensional liquid chromatography coupled with tandem mass

spectrometry on myometrial proteins isolated from pregnant human patients in labor, pregnant patients not in labor, and pregnant patients in pre-term labor. Using a conservative false discovery rate of 1% we have identified 2132 protein groups using this method and semi-quantitative spectral counting shows 201 proteins that have disparate levels of protein expression in the preterm laboring samples. To our knowledge this is the first large scale proteomic project on human uterine smooth muscle and this initial work has provided a target list for future experiments into how changing levels of proteins are involved in the induction of labor.

Employing S-nitrosoglutathione as a nitric oxide donor, we identified 110 proteins that are S-nitrosated in one or more states of human pregnancy. Using area under the curve of extracted ion chromatograms as well as normalized spectral counts to quantify relative expression levels for 62 of these proteins, we show that 26 proteins demonstrate statistically significant differences in myometrium from spontaneously laboring preterm patients and non-laboring patients. We identified proteins that were up-S-nitrosated as well as proteins that were down-S-nitrosated in preterm laboring tissues. Identification and relative quantification of the S-nitrosoproteome provides a fingerprint of mechanistically important proteins that can form the basis of hypothesis-directed efforts to understand the regulation of uterine contraction-relaxation and the development of new treatment for preterm labor.

ACKOWLEDGEMENTS

My road to graduate school was a very winding and precipitous route. This incredible experience would have never been made possible without the understanding and support of many incredible people whom I am forever indebted to and who will always be in my heart.

My parents, Rob and Cheri, have provided more than I could ever ask for or need. I am particularly grateful that they remained strong and supportive through the many trials and tribulations that life has thrown our way. My grandparents, John, Patty, Bob, and Gail have provided the utmost support and love throughout my life and graduate training. The rest of my family, you are my inspiration and I appreciate all that you have done for me. I am fortunate enough that the list is too long to name you all!

Dealing with me throughout graduate school was not an easy task and I especially want to thank Jie for all her love and support through both the good and bad times. You really helped motivate me to finish and I thank you for that!

My friends in Alaska, Washington, and Reno, thank you for all the good times and motivating words! Without such great friends I never would have been able to succeed and I wish you all the best success in your lives as well. A special thanks to AK and Senny for their great support and friendship. I want to give a huge thanks to Dr. Chad Cowles for many great discussions the best of which occurred either on a boat or on the Truckee River.

I want to thank my graduate research committee; Drs. Josh Baker, Grant Cramer, Kathy Schegg, and Cherie Singer. Your help and guidance during my entire graduate education has been invaluable. I greatly appreciate the helpful insight and direction that

all of you provided. It was a great pleasure working with all of you! I would also like to thank Dr. David Quilici and Rebekah Woolsey for help and education concerning all of the mass spectrometry data.

The Buxton lab group is like a family to me. In no particular order I would like to thank; Dr. Nucharee Yakdong, Yi-Ying Wu, Scott Barnett, Dr. Heather Burkin, and Dr. Nate Heyman. A very special thanks to Sara Thompson, both professionally and personally you are irreplaceable.

Dr. Buxton deserves more thanks than can possibly be provided. You are one of the smartest and most caring individuals that I have ever interacted with. I am forever grateful for both the professional mentoring as well as the personal help and guidance that you have provided me. I hope to emulate your passion and knowledge in my career in hopes that someday I can be as accomplished as you. Thank you!

TABLE OF CONTENTS

LIST OF FIGURES

LIST OF TABLES

CHAPTER I:

INTRODUCTION

1.1 Preterm Labor

Preterm birth is defined as any birth that occurs before the 37th week of pregnancy. Preterm labor (PTL) results in preterm birth in over 50% of cases and affects approximately 13 million, or 9.6% of all births worldwide, every year (Beck, Wojdyla et al. 2010). Of all early neonatal deaths (deaths within the first 7 days of life) that are not related to congenital malformations, 28% are due to preterm birth (Lawn, Wilczynska-Ketende et al. 2006). This devastating outcome has no known cause, treatment, or cure.

In most cases of spontaneous preterm birth (sPTB) a precise pathogenetic mechanism cannot be established. There is evidence for the association of many maternal or fetal factors that increase the risk of sPTB including the following; intrauterine infection which can lead to activation of the innate immune system, stress and immune disorders, genetic risk factors, uteroplacental insufficiency, uterine overdistension, and cervical insufficiency(Voltolini, Torricelli et al. 2013). Each individual case of sPTB may have a different etiopathology but the end result leads to a common pathway that triggers uterine contractility and premature delivery. This process is poorly understood in both full term labor and PTL. What is known is that induction of labor, regardless of gestational age, is a complex signaling cascade involving mechanical and endocrine mechanisms, immune system responses, inflammatory signals, and release of molecules such as prostaglandins, cytokines, and oxytocin. This complex pathway leads in some way to uterine contractions that eventually expel the fetus.

The treatment of PTL and sPTB currently relies on the use of either hydroxyprogesterone caproate or tocolytics (anti-contraction medications), which have the goal of prolonging pregnancy. Hydroxyprogesterone caproate recently gained

approval from the US Food and Drug Administration as a supplementation during pregnancy to reduce the risk of recurrent preterm birth in women with a history of at least one prior spontaneous delivery. However, it has not been shown that hydroxyprogesterone caproate has any beneficial effect on treating acute PTL. This limits the treatment only to those individuals who are known to be at high risk of recurrent sPTB and furthermore does not address the issue of treating PTL once it has initiated.

There is no evidence that current tocolytic therapy has any direct favorable effect on neonatal outcomes or that any prolongation of pregnancy afforded by tocolytics actually translates into statistically significant neonatal benefit(2012). The most common current tocolytic agents are calcium-channel antagonists (nicardipine and nifedipine), β-adrenergic-receptor agonists (ritodrine, salbutamol, and terbutaline), magnesium sulfate, cyclooxygenase inhibitors (indomethacin), and oxytocin-receptor antagonists (atosiban).

The goal of this research was to identify novel potential therapeutic targets for PTL through the study of the proteome and S-nitrosoproteome of human uterine smooth muscle tissue. This approach allowed us to identify the total proteome and S-nitrosoproteome in disparate states of human pregnancy as well as allowing us to identify signature proteins that are regulated disparately in PTL, compared to term labor whether at the level of the total proteome or the S-nitrosoproteome. This knowledge will encourage future hypothesis-driven research to delineate the molecular mechanisms and biochemical pathways that are altered by these disparities.

1.2 Nitric Oxide and Thiol Chemistry

Nitric oxide (NO) is a gaseous free radical with unique chemical properties that impart vast chemical and physiological effects in the cell. When considering the chemistry and physiological effects of NO, it should be remembered that NO is a highly diffusible second messenger that can elicit effects relatively far from its site of production (Davis, Martin et al. 2001). Due to the wide ranging effects of NO, both beneficial and pathological in many different cells and tissues, I will limit the discussion here to the chemistry involved in modifying thiol side chains of cysteine residues. There are many authoritative reviews of the biology of NO. The field has grown so explosively since the pioneering work of Robert Furchgott (Furchgott and Zawadzki 1980) that even reviews are now specialized to a tissue or condition.

NO is chemically unable to directly oxidize amino acid side-chains at any meaningful biological rate and therefore NO-dependent amino acid oxidation occurs via secondary reactions following the oxidation of NO to nitrogen dioxide, dinitrogen trioxide or peroxynitrite. S-nitrosation is therefore often an indirect reaction of NO that results in a chemical modification of a thiol group and not a reversible association of NO with a thiol (Broniowska and Hogg 2012).

These indirect effects are produced through the interaction of NO with either O_2 or $O_2^{\bullet-}$ and include S-nitrosation (when NO+ is added to a thiol), oxidation (when one or two e- are removed from a substrate), or nitration (when NO_2+ is added to a molecule) (Davis, Martin et al. 2001). NO can undergo autoxidation (i.e. reaction with O_2) to produce N_2O_3; this compound can undergo hydrolysis to form nitrite (Malinski, Taha et al. 1993). Both NO and O_2 are 6-20 times more soluble in lipid layers compared with aqueous fractions and therefore the rate of autoxidation is increased dramatically in the

lipid phase (Malinski, Taha et al. 1993). This increased rate argues for compartmentalized chemistry, a phenomenon first described in cardiac muscle (Buxton and Brunton 1983) and known to occur for cyclic nucleotide signaling in myometrium (Buxton, Milton et al. 2010), specific to individual signaling pathways and could explain the anomalous thiol specificity of non-enzymatic S-nitrosation. In addition to autoxidation, NO can also react with $O_2^{\bullet-}$ to produce peroxynitrite ($ONOO^-$), which is a known potent oxidant in biological systems (Huie and Padmaja 1993). $ONOO^-$ acts as both a nitrating agent and a powerful oxidant to modify proteins.

Cysteine (Cys), with its thiol side chain, is a very unique and reactive amino acid. The thiol group is nucleophilic, acidic (pKa ~ 8) and redox active due to its hybridized p- and d-orbitals. Structural deviations in proteins are also able to modify the reactivity of active site Cys residues by lowering its pKa by several orders of magnitude (from 8 to 5 or 6) via tertiary interactions with basic groups that promote thiol deprotonation.

The unique reactivity of Cys allows for multiple biologically relevant modifications including, but not limited to: disulfide formation (e.g. glutathionylation), S-oxides (e.g. sulfenic, sulfinic, and sulfonic acids), and the focus of this work S-nitrosation. These biologically relevant modifications are depicted in Figure 1.1.

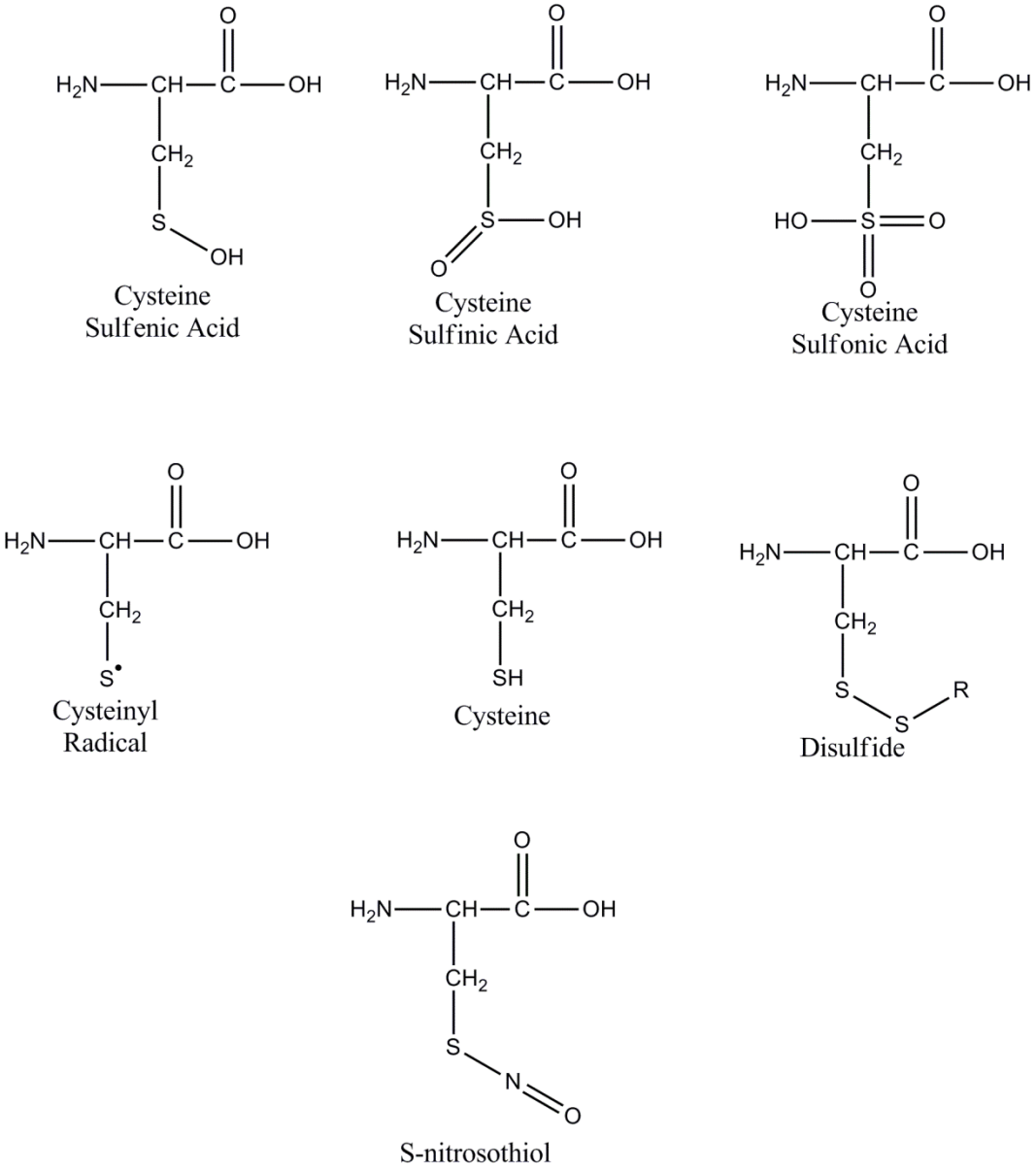

Figure 1.1: Several physiologically-relevant cysteine modifications. Depicted is a cysteine backbone with modifications to the thiol side chain. Clockwise, the modifications to the thiol side chain include S-OH, OS-OH, OOS-OH, S$^{\bullet}$, SH, S-S, S-NO.

1.3 Nitric Oxide Induced, cGMP Independent, Relaxation in the Uterus

NO induced relaxation of smooth muscle has canonically been considered to be a cyclic guanosine 3'-5'-monophosphate (cGMP)-dependent pathway. The molecular mechanism of cGMP-mediated smooth muscle relaxation is thought to revolve around cGMP-dependent protein kinase (PKG) activation. Active PKG is able to phosphorylate several key target proteins, including ion channels, ion pumps, receptors, and enzymes all involved in the control of intracellular Ca^{2+} concentration (Carvajal, Germain et al. 2000). Phosphorylation of these target proteins triggers a reduction in the intracellular Ca^{2+} concentration and results in relaxation of smooth muscle.

Uterine smooth muscle (USM) has been previously shown to relax in a manner disparate from other smooth muscle tissues. NO relaxes uterine smooth muscle in a dose-dependent, cGMP-independent manner (Kuenzli, Bradley et al. 1996; Bradley, Buxton et al. 1998; Buxton, Kaiser et al. 2001). The inhibitory concentration 50% for the transnitrosating agent cysteine-NO to relax human myometrium in tissue bath experiments is approximately 1 μM(Buxton, Kaiser et al. 2001). Elevations in cGMP that accompany NO stimulation can be prevented by pretreatment of tissues with inhibitors of soluble guanylyl cyclase such as 1H-[1,2,4]oxadiazolo[4,3-a]quinoxalin-1-one (ODQ),(Buxton, Kaiser et al. 2001); 6-anilino-5,8-quinolinedione (LY 83583),(Kuenzli, Buxton et al. 1998); or 3,7-bis(dimethylamino) phenothiazin-5-ium (methylene blue),(Kuenzli, Bradley et al. 1996). Stimulation of ODQ treated myometrial tissues with NO-donors results in relaxation without cyclic GMP elevation (Figure 1.2).

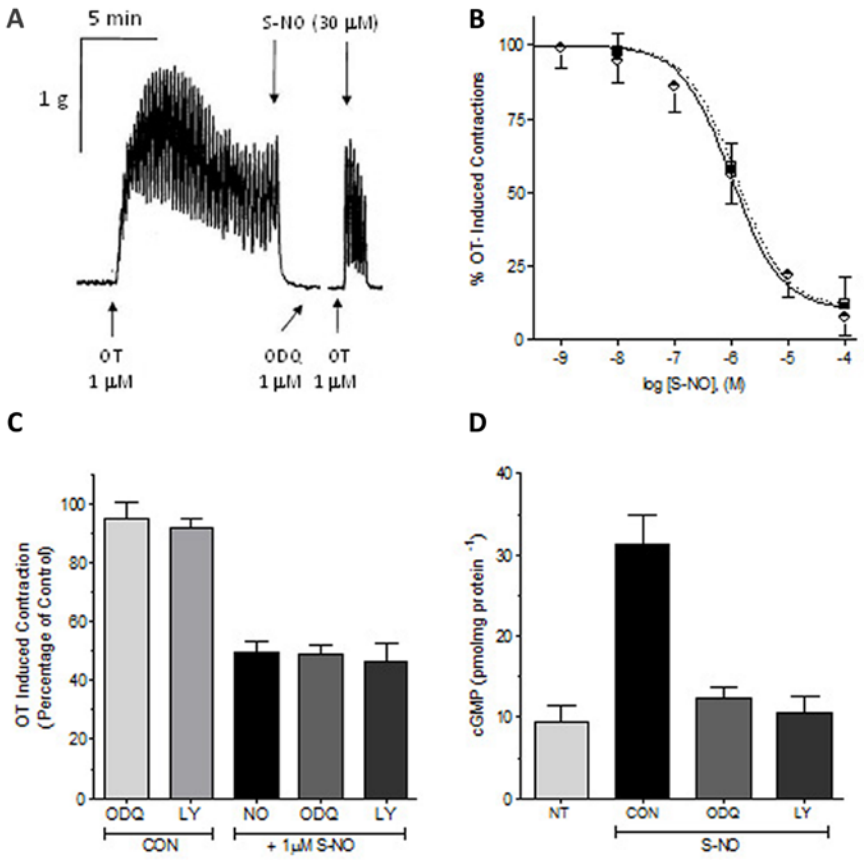

Figure 1.2: cGMP independent relaxation in the uterus stimulated by GSNO. (A,B) Strips of near-term pregnant non-laboring myometrium taken from consenting women at the time of caesarean section were hung in organ baths and tension recorded as described (*3*). Addition of oxytocin (1 µM) produced contraction (2.4 ± 0.76 g/mm^3, n=8) that was completely relaxed by S-NO as cysteine-NO (Cys-NO; IC_{50} = 1 µM). In the presence of 1 µM ODQ, relaxations to Cys-NO were unaffected. Data are mean ± SEM, n=8 and shown with permission (Wiley Publishers) (C) Addition of the GC inhibitors ODQ (1µM) or LY-83583 (10 µM) had little effect on OT-induced contractions (CON), while addition of Cys-NO (1µM) caused significant relaxation regardless of pre-treatment with the GC inhibitors. Data are mean ± SEM, n = 6-8. (D) OT-stimulated myometrial tissues were snap frozen under tension and basal cyclic GMP content (9 ± 2.1 pmol mg protein^{-1}) determined by ELISA as previously described (*3*). OT stimulation (1 µM) had no effect on cyclic GMP content (NT, 9.5 ± 1.9 pmol mg protein^{-1}), while Cys-NO stimulation (30 µM) led to a significant elevation in cyclic GMP (31.3 ± 3.6 pmol mg protein^{-1}) that was blocked by prior treatment of tissues with GC inhibitors ODQ (1 µM) or LY-83583 (10 µM). Data are mean ± SEM, n = 6.

It is now clearly established from our work and that of others that NO-mediated relaxation of USM is independent of global cGMP elevation or activation of its cognate kinase, PKG type I(Tichenor, Malmquist et al. 2003), no matter whether this is studied in animal(Kuenzli, Bradley et al. 1996), primate(Kuenzli, Buxton et al. 1998) or human(Bradley, Buxton et al. 1998).

The fact that NO signals non-classically in the uterus offers a persuasive justification for alternate research approaches to identify the disparate pathways involved in NO induced HUSM relaxation. Our approach was to look at one of the less canonical ways in which NO can modify signaling pathways, and that is by the post-translational protein modification known as S-nitrosation.

1.4 S-Nitros(yl)ation

There is significant confusion in the literature regarding the correct nomenclature for the reaction resulting in the addition of NO to a thiol side chain, with many groups using the term S-nitrosylation in place of S-nitrosation. The use of nitrosylation in this context is wrong. Smith and Marletta make a convincing argument that the nitroso group, not the nitrosyl group, is transferred during S-nitrosation reactions (Smith and Marletta 2012). We therefore have adopted this nomenclature to describe the conversion of a thiol to a nitrosothiol. Our early work did not reflect this nomenclature and the manuscript that represents Chapter 2 used the term S-nitrosylation in the published manuscript. I have modified the wording in Chapter 2 to represent the correct nomenclature.

As stated before, NO is chemically unable to directly oxidize amino acid side-chains at any meaningful biological rate and therefore NO-dependent amino acid oxidation occurs via secondary reactions(Broniowska and Hogg 2012). S-nitrosation requires a

one-electron oxidation of the initial addition complex between NO and a thiol. S-nitrosothiol formation can take place through NO autooxidation to N_2O_3, radical recombination between NO and a thiyl radical, and transition metal catalyzed pathways as long as an electron sink is present.

Another method of S-nitrosation is the transfer of an NO moiety from one protein or low molecular weight thiol to a different protein or low molecular weight thiol and is known as transnitrosation. Transnitrosation is a reversible second-order reaction between a nitrosothiol and a thiol. Transnitrosation proceeds through nucleophilic attack of a thiolate anion at the nitrosothiol nitrogen resulting in a nitroxyl disulfide intermediate or transition state. The overall mechanism of transnitrosation resembles an S_N2 reaction (Smith and Marletta 2012).

Our experiments employed the use of the physiologically relevant NO donor and transnitrosating agent S-nitrosoglutathione (GSNO). GSNO is the S-nitrosated version of the most abundant cellular thiol, glutathione. GSNO has been shown to transnitrosate various thiols with a second order rate constant in the range of 1-300 $M^{-1}s^{-1}$(Meyer, Kramer et al. 1994).

There is strong evidence for multiple membrane transporters of glutathione but there is not sufficient evidence to prove that GSNO is directly transported into cells; however, extracellular addition of GSNO does cause increases to intracellular S-nitrosothiol levels in multiple conditions(Broniowska, Diers et al. 2013). One hypothesis of how NO crosses the cellular membrane is that GSNO decomposes in the extracellular space to release NO, which based on its solubility can diffuse through the membrane and S-nitrosate intracellular targets (Ramachandran, Jacob et al. 1999; Ramachandran, Root et

al. 2001). The physiological rate of GSNO decomposition is debated. This rate is likely to be condition and system dependent. In myometrial smooth muscle, at a GSNO concentration of 300 μM, GSNO will produce ~5 μM reactive NO over 15-20 min without reactive NO accumulation(Cleeter, Cooper et al. 1994). Our studies were not reliant on NO crossing the membrane as exogenous treatment was done post membrane rupture and protein isolation. This process could easily be recapitulated in an intact cell or tissue considering the following mechanism of NO delivery to the S-nitrosothiol targets in the cell.

1.5 NO Production, Delivery, and Cellular Uptake in the Myometrium

There is some debate as to the origin of NO signaling in the myometrium. Here I will propose several possible sources as well as routes of cellular uptake for NO. Multiple groups argue for the presence of nitric oxide synthases (NOS's) in rodent myometrium(Kakui, Itoh et al. 2004; Suzuki, Mori et al. 2009) while others have found no evidence for any of the NOS isoforms in smooth muscle cells of human myometrium(Bartlett, Bennett et al. 1999). Our experiments have shown certain NOS isoforms to be present in myometrial tissue preparations. We cannot unambiguously say that these are present in the myometrial muscle cells; however, their presence in the tissue preparations argues for direct proximity and therefore physiological relevance.

There are three major mammalian isoforms of NOS: endothelial (eNOS), neuronal (nNOS), and inducible (iNOS). These mammalian NOSs have specific activities of NO generation that rank as follows iNOS ≥ nNOS ≥ eNOS, with nNOS activity being 4 times that of eNOS. However, if one considers their actual rates of NO biosynthesis (the speed at which each NOS makes one NO) then it has been shown that nNOS is at least twice as

fast as iNOS and about 30 times faster than eNOS(Stuehr, Santolini et al. 2004). This discrepancy is explained by the global kinetic model and the different enzyme distribution pattern of each NOS in the steady state(Santolini, Adak et al. 2001; Santolini, Meade et al. 2001). The reaction catalyzed by all NOS isozymes is to hydroxylate a guanidino nitrogen of arginine and then oxidize the N^{ω}-hydroxy-L-arginine intermediate to NO and L-citrulline. This reaction involves the following 5 cofactors: tetrahydrobiopterin, nicotinamide adenine dinucleotide phosphate, flavin adenine dinucleotide, flavin mononucleotide, and heme. If we assume that one or more of these NOS isozymes are present in the myometrium then the NO formed by this reaction would be directly available for downstream signaling, including S-nitrosation of target thiols.

NO need not be produced by NOS inside the uterine smooth muscle cells to have an intracellular action. The primary route of uptake involves the transnitrosation of the thiol containing amino acid L-cysteine by one of several NO carriers (e.g. GSNO, S-nitoso-albumin, and s-nitrosohemoglobin). This transnitrosation results in the formation of S-nitroso-L-cysteine (L-CysNO) which is a good substrate for uptake through the amino acid transporter L system (Broniowska, Diers et al. 2013). Once inside the cell L-CysNO can either transnitrosate the abundant glutathione (reaching levels of 5 mM in some conditions) to form GSNO or directly S-nitrosate protein targets to elicit cellular responses. The extracellular source of NO for this process can come from multiple sources some of which I will cover in detail below (Figure 1.3).

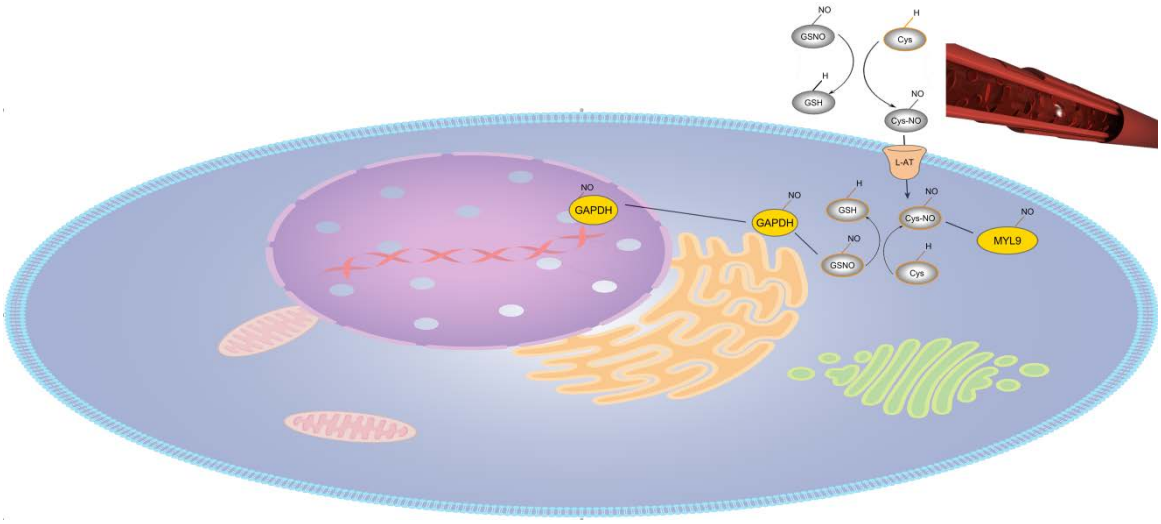

Figure 1.3: Human uterine smooth muscle cellular S-nitrosothiol uptake. NO carriers such as S-nitrosoglutathione (GSNO) can transnitrosate free L-cysteine (Cys) to form S-nitroso-L-cysteine (Cys-NO). Cys-NO can then be shuttled across the membrane throgh the amino acid transporter system L (L-AT). Once inside the cell Cys-NO can transnitrosate either glutathione (GSH) to regenerate GSNO intracellularly or it can directly transnitrosate target proteins such as myosin regulatory light chain 9 (MYL9). Regenerated GSNO can also transnitrosate target proteins such as glyceraldehyde 3-phosphate dehydrogenase (GAPDH) leading to downstream signaling such as nuclear transport and gene regulation. (Note that either albumin-SNO or hemoglobin-SNO could also transnitrosate Cys to Cys-NO)

NO can be generated by the immune system derived invading cells such as macrophages that have been shown to increase in number in the myometrium during the progression of pregnancy(Ivanisevic, Segerer et al. 2010). NO's classical role in the immune system was simply defined: NO is a product of macrophages that are activated by cytokines, microbial compounds or both. Macrophage produced NO is derived from the amino acid L-arginine by the enzymatic activity of iNOS and functions as a tumoricidal and antimicrobial molecule(Nathan 1992). Recent evidence argues for a broader role of NO produced from not only macrophages but also multiple other immune derived cells.

It has also come to light that the activity of NO is not restricted to the site of its production. Not only are •NO radicals highly diffusible but it has also been shown that low-molecular weight S-nitrosothiols (e.g. GSNO), S-nitrosated proteins, and nitrosyl-metal complexes can function as long-distance NO vehicles(Gaston and Stamler 1999). These NO carriers can liberate NO either spontaneously or after cleavage by ectoenzymes found on cells such as T and B lymphocytes(Henson, Nichols et al. 1999). Furthermore, N^{ω}-hydroxy-L-arginine, which is secreted by cells and detectable in the plasma, can be oxidized to citrulline and NO by a number of hemoproteins (such as peroxidases and cytochrome P450) as well as superoxide anions(Wu and Morris 1998). Likewise, circulating nitrite (NO_2^-), a stable product of the NOS reaction, can be reduced to •NO under mildly acidic conditions and is a substrate of the peroxidase pathways of neutrophils and eosinophils that can lead to the formation of novel NO derived oxidants at distant sites(Eiserich, Hristova et al. ; MacPherson, Comhair et al. 2001). This data makes it evident that NO production is not limited to antimicrobial activity when the

source is immune system derived and argues for a route of NO delivery into the myometrial smooth muscle cells.

Whatever the source of NO, it is evident that NO can and does have an effect on relaxation in the myometrium (Figure 1). Therefore it is critical to study what molecular mechanisms are subserved by NO signaling and how these can generate disparate outcomes during labor and preterm labor. In order to do this it is necessary to first identify the protein targets of NO and to delineate which of these are regulated differently in different states of human pregnancy. The following section will explain the experimental approach we have used to identify specific protein targets of NO in human myometrium.

1.6 Biotin Switch and Fluorescent Switch

The determination of S-nitrosothiols in biological samples represents an analytical challenge due to the following technical obstacles: metal-catalyzed S-nitrosothiol decomposition, reduction of the S-NO bond by thiols (transnitrosation), homolytic cleavage of the S-NO bond, photolytic S-N bond cleavage, and hydrolysis. These challenges necessitate differentially modifying both free thiols and the S-nitrosothiols with stable adjuncts in order to identify the state of all thiols. In 2001 Jaffrey and Snyder proposed an elegant solution to this problem. In the first step of their biotin switch method, they blocked all free thiols with the thiol-specific methylthiolating agent methyl methanethiosulfonate (MMTS) which does not react with S-nitrosothiols. N-ethylmaleimide can be used in place of MMTS and the rational for this modification will be explained later. The blocking reactions are shown in Figure 1.4.

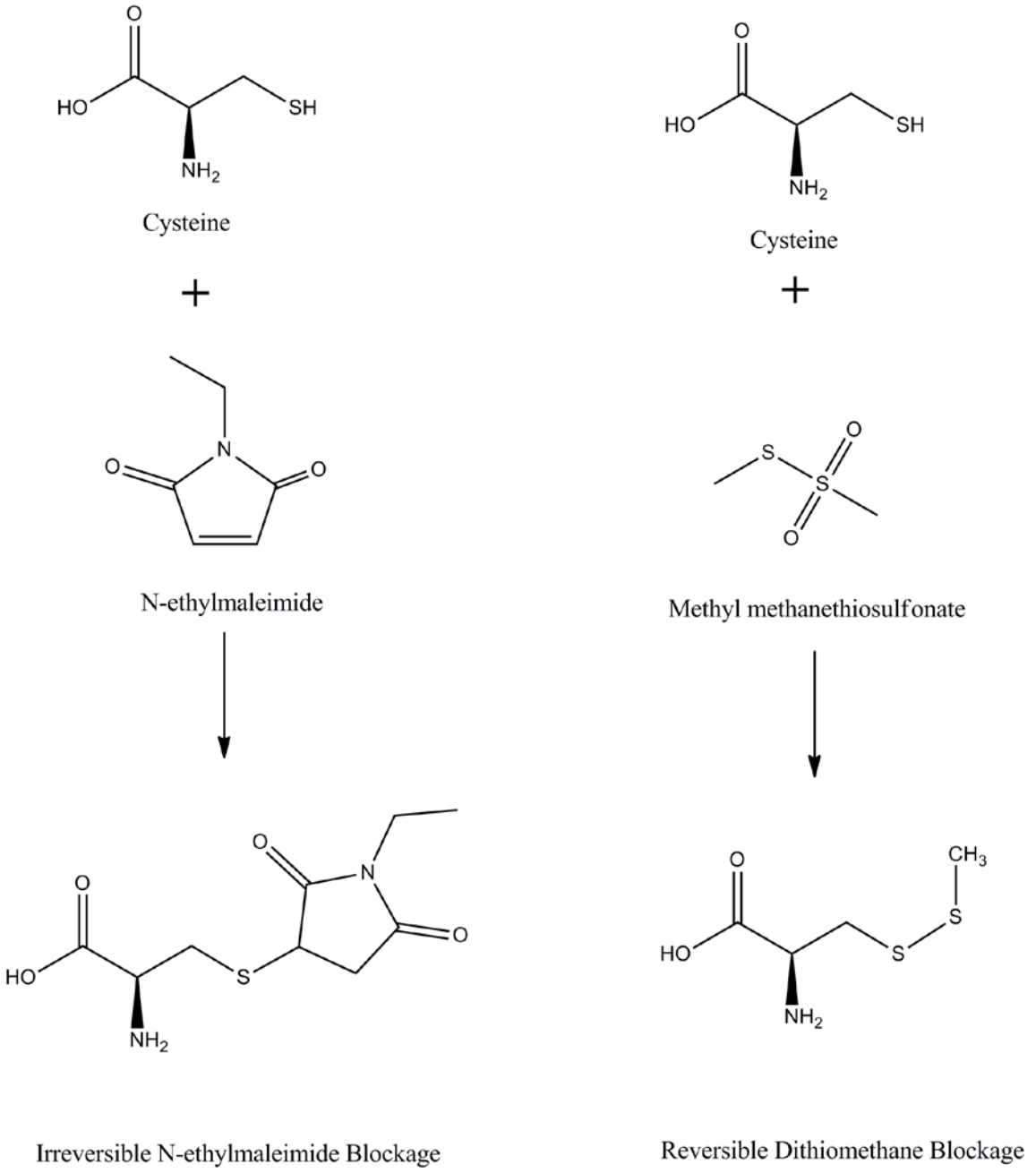

Figure 1.4: Specific blockers of free thiols used in the biotin switch reaction. The reaction on the left shows N-ethylmaleimide forming an irreversible thioether bond with a free thiol (represented here by cysteine). The reaction on the right shows methyl methanethiosulfonate forming a reversible dithiomethane bond with a free thiol. Unlike the thioether bond this disulfide bond can be reduced by agents such as β-mercaptoethanol or dithiothreitol.

After blocking and removal of MMTS by acetone precipitation and acetone washes, S-nitrosothiols are selectively decomposed with ascorbate, which results in the reduction of S-nitrosothiols to thiols. In the last step, the newly formed free thiols are reacted with N-[6-(biotinamido)hexyl]-3′-(2′-pyridyldithio)propionamide (biotin-HPDP), a sulfhydryl-specific biotinylating reagent(Jaffrey and Snyder 2001). The biotin-tagged proteins can then be enriched by streptavidin-affinity chromatography for downstream applications such as SDS-PAGE or mass spectrometry based identification. Figure 1.5 shows the selective chemistry involved in ascorbate reduction and biotin-HPDP labeling of S-nitrosothiols.

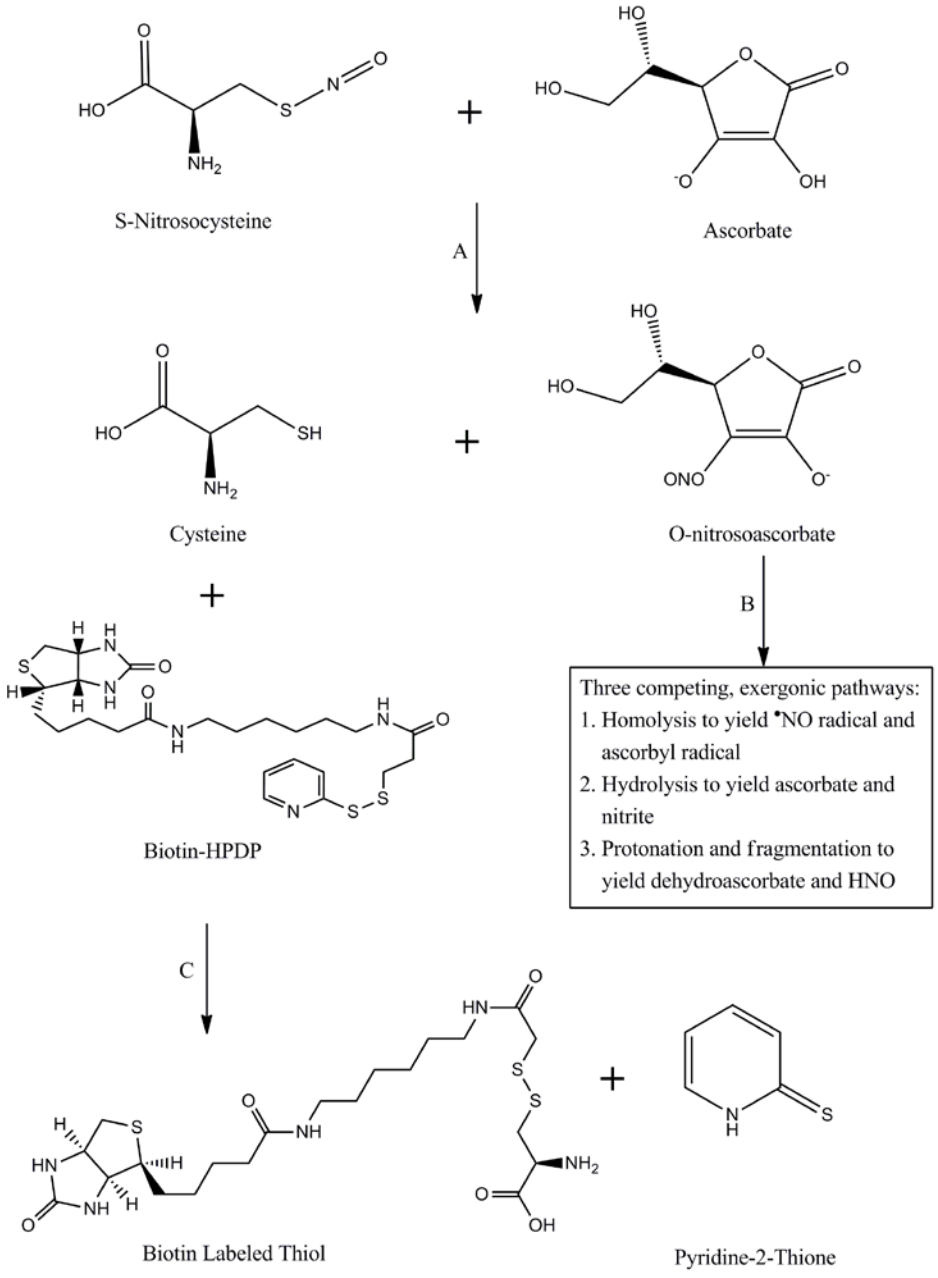

Figure 1.5: Ascorbate reduction and biotin-HPDP labeling of S-nitrosothiols. In reaction A ascorbate acts as a target nucleophile for the S-nitrosothiol (represented here as Cys-NO) resulting in the formation of O-nitrosoascorbate and a free thiol on the cysteine. O-nitrosoascorbate then breaks down by three competing, exergonic pathways (reaction B). The free thiol generated from the S-nitrosothiol can then be labeled with the sulfhydryl specific agent biotin-HPDP for downstream analysis.

One drawback to the biotin switch is that the biotin-tag will be removed in the presence of reducing agents such as β-mercaptoethanol or dithiothreitol. This is a problem if one wants to analyze differential S-nitrosation through a technique such as 2-dimensional differential in gel electrophoresis (2D-DIGE). This technique allows for multiple samples to be labeled, mixed together, and separated on identical gels. This helps solve the problem of gel-to-gel variation that is seen in classical 2D-PAGE gels. We recognized this and designed a modified biotin switch that we refer to as the fluorescent switch, in which we replace both the MMTS and biotin-HPDP with maleimide derivatives (N-ethylmaleimide in place of MMTS and one of three Alexa Fluor® maleimide conjugated fluorophores in place of biotin-HPDP). The maleimide group reacts specifically with sulfhydryl groups when the pH of the reaction mixture is between pH 6.5 and 7.5 resulting in the formation of a stable thioether linkage that is not cleaved by reducing agents. Using this modified technique we developed a highly sensitive assay that we named 2D-NitrosoDIGE, which allowed for direct comparison of S-nitrosation levels in different states of pregnancy. The results from the 2D-NitrosoDIGE experiments are described in Chapter 2 and a schematic of the different labeling techniques is shown in Figure 1.6.

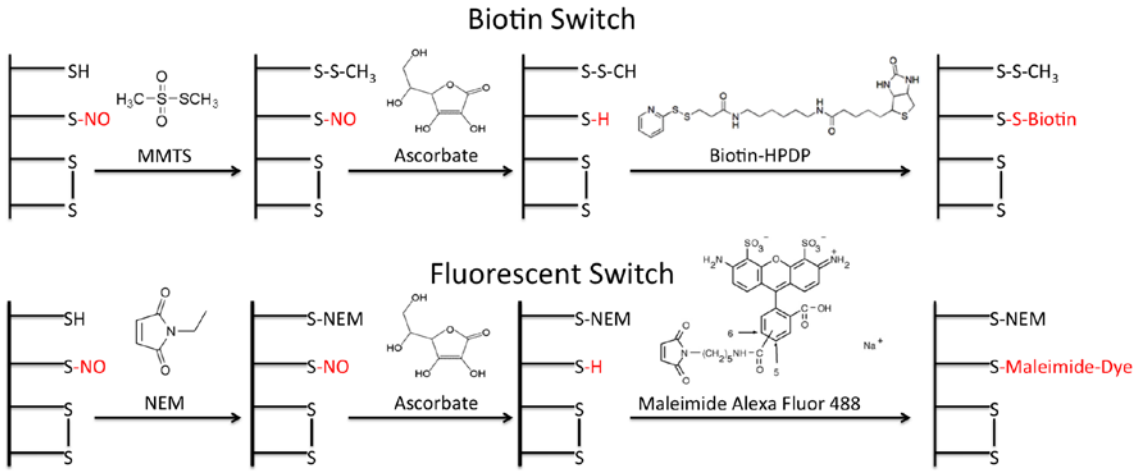

Figure 1.6: Schematic of the biotin switch and the fluorescent switch. Proteins that have been previously S-nitrosated can be either labeled with biotin-HPDP or an Alexa Fluor-maleimide dye. Step one involves blocking of all free thiols with either methyl methanethiosulfonate (MMTS) for the biotin switch or N-ethyl maleimide (NEM) for the fluorescent switch. Step 2 involves the reduction of all S-nitrosated thiols with ascorbate. Reduced thiols, which were originally S-nitrosated, are then labeled with biotin-HPDP or an Alexa Fluor-maleimide dye. The Alex Fluor dye in step 3 of the fluorescent switch can also be 555 or 647 maleimide dyes.

2D-NitrosoDIGE was a very promising technique and worked well for quantification of disparately regulated proteins. The main drawback of this technique is that not all proteins focus and separate in a manner that is conducive with spot cutting and mass spectrometry based identification. This limits the number of quantifiable proteins as it is impossible to determine which protein or proteins are changing if more than one protein is identified in a spot. If full separation could be achieved (e.g. with a subset of S-nitrosated proteins that had been previously isolated by the biotin switch and streptavidin purification) then this would be an ideal quantification method as it is easily understood and visually pleasing. However, it is not well suited to discovery of specific proteins in complex proteomic mixtures. Therefore, we decided to employ a purely mass spectrometry based technique that will be described next.

1.7 Quantitative Proteomics

A main goal of this research was to identify proteins that differ in their S-nitrosation in one or another state of human pregnancy, or in the level of S-nitrosation seen in a given protein. In order to ensure that measurement of disparate levels of S-nitrosation in a given protein are due to increases or decreases in the number of post-translational modifications rather than a misleading result due to increased protein expression of that protein in pregnancy, it was necessary to quantify the total protein levels for all of the S-nitrosated proteins identified. This would be a rather cumbersome task to undertake without a large-scale proteomic approach. In collaboration with Dr. David Quilici and the Nevada Proteomics Center, we undertook the task of mapping the myometrial smooth muscle proteome using two-dimensional liquid chromatography coupled with tandem mass spectrometry (2D LC/MS/MS). This is an emerging technique that separates

proteins by both strong cation exchange and reverse phase HPLC into multiple fractions that are then subjected to MS/MS analysis (Figure 1.7).

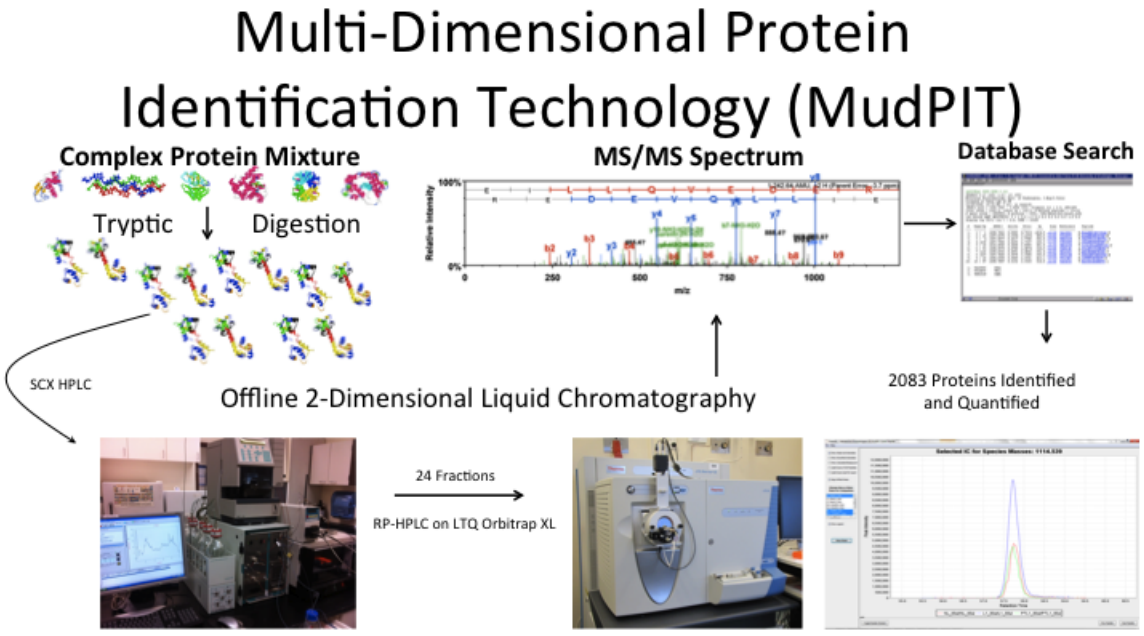

Figure 1.7: Multi-dimensional protein identification technology. Total protein was isolated from human uterine smooth muscle tissue strips and enzymatically digested with trypsin. Tryptic fragments were separated in two-dimensions; the first dimension used a 50 minute run on a strong cation exchange (SCX) column. Fractions were collected every two minutes for a total of 24 fractions. Each of these fractions was then separated by reverse phase HPLC and injected into an Orbitrap-LTQ mass spectrometer. Output spectra were then identified by database matching and analyzed using ProteoIQ® software.

This technique has been successfully used to map the proteome of *S. pombe*(Brill, Motamedchaboki et al. 2009) at a level that had not been previously achieved. No laboratory has performed these experiments in human myometrium making our findings unique and of particular interest and relevance to the field of smooth muscle biology as well as offering insight into opportunities for clinical-translational research to generate effective tocolytics. Indeed, since NO so effectively relaxes the pregnant myometrium in a manner that is demonstrably different than is the case in other smooth muscles, it is entirely likely that one or more proteins that we discover as disparately S-nitrosated in tissues from women in preterm labor may constitute a therapeutic target for drug development.

This undertaking produced an immense amount of data that not only provided the correlating protein expression of the S-nitrosoproteome but also provided an additional several thousand proteins measured at a quantitative level on which we were able to perform expression and pathway analysis. This cutting edge technique allowed us to be the first group to map the proteome of myometrial tissue in different states of pregnancy at a level that had not been previously accomplished. The major benefit of collecting this proteomic data is that it allows us to analyze the actual expression of protein levels in different states of pregnancy. Examining the proteome is of particular benefit. While there are approximately 30,000 genes in the human genome, one cannot know what genes are activated to make proteins in a given tissue without far more information than can be deduced from the genetic code alone (Glaser 2010). It is known that genomic and transcript data while of high value, don't necessarily correlate with the actual level of transcribed protein(Contopoulos-Ioannidis et al., 2007). What is needed therefore to

investigate a problem such as spontaneous preterm labor is to know the specific proteins that are altered and their abundance in pregnancy and labor and preterm labor. This approach gave us a relative quantification between states that could be used to identify proteins and pathways that are perturbed during labor and preterm labor. The procedure and results of these analyses can be found in Chapter 3.

Although our dataset was comprised of a couple thousand proteins we realize that there are tens of thousands more that we were not able to positively identify using our current protein extraction and separation techniques. This in no way diminishes the value of our dataset as even this fraction of proteins allows us to generate a preliminary proteome map that is extremely useful in directing future hypothesis-driven research. Ahrens et al. reviewed this concept of creating multiple levels of proteome coverage and integrating all of the different proteomic data into a "map"(Ahrens, Brunner et al. 2010). We have created a baseline proteome map of HUSM as well as another layer describing the S-nitrosoproteome which will allow future research to add more in depth layers until ultimately completing the entire proteomic profile of HUSM in different states of pregnancy and labor. This will be an immensely useful tool for researchers and clinicians alike.

The use of high-resolution mass spectrometry as well as improvements in MS based data analysis software allow for several different quantification options. The two most popular MS based quantification techniques are spectral counting (SC) and area under the curve of extracted ion chromatograms (AUC). SC infers the quantity of protein indirectly from the number of peptide-to-spectrum matches (PSMs; spectrum count) obtained for each protein(Bantscheff, Lemeer et al. 2012). Intensity-based label free quantification

(e.g. AUC) employs the MS signal response of intact peptides and, by inference, that of proteins for quantification(Bantscheff, Lemeer et al. 2012). AUC is accomplished by integrating the ion intensities of any given peptide over its chromatographic elution profile. This measure of MS1 intensity is potentially a more accurate mode of label-free quantification as it can provide measurements in the low abundance range since every sequenced peptide is observed with an intensity. This information is lost in SC, which limits quantification of the low abundance proteins identified by low numbers of MS/MS spectra only(Choi, Glatter et al. 2012).

We utilized both SC and AUC in our analysis of the MS/MS data from the identified S-nitrosoproteome and found good agreement between both data analysis. Two-dimensional liquid chromatography separation of the total proteome resulted in a relatively large elution profile shift for two of the NL samples. This shift (~4 minutes) resulted in peptides eluting in different fractions than the other 7 samples and therefore inhibiting our ability to compare the corresponding MS1 chromatograms for these two samples. Therefore, we applied a pure SC approach to semi-quantify the levels of protein expression between each group. One of the benefits of SC is that quantification is mostly independent of elution fraction due to the fact that as long as an MS2 event is triggered the peptide scoring match will be counted to the matching protein no matter what fraction that it is identified in. We realize that using dynamic exclusion in order to identify a greater number of proteins limits the quantitation that can be performed using SC. However, trends in protein abundance can still be realized and therefore a semi-quantitative analysis that provides trends can be performed. Chapter 3 explains both the technique and rationale of this mass spectrometry based approach in further detail.

CHAPTER 2:

UTERINE SMOOTH MUSCLE S-NITROSOPROTEOME IN PREGNANCY

This chapter is based on a manuscript published in *Molecular Pharmacology*.

Ulrich, C., Quilici, D.R., Schegg, K., Woolsey, R., Nordmeier, A., & Buxton, I.L.O. Uterine Smooth Muscle S-Nitrosylproteome in Pregnancy. *Mol Pharm.* February 2012 vol. 81 no. 2 143-153

2.1 Introduction

Preterm labor affects 12.5% of obstetric practice in the United States, leads to preterm delivery in over 50% of cases and this inexplicable tragedy(Buxton, Crow et al. 2000; Buxton 2004) in which 20,000 fetuses die annually appears to be increasing in frequency and disproportionally affects African American (18%) mothers(Behrman and Butler 2006). Despite decades of interest, over half of cases of preterm labor are spontaneous and unexplained. The molecular mechanisms involved in the induction of labor are still unknown. Uterine smooth muscle (USM) has been previously shown to relax in a manner disparate from other smooth muscle tissues. Nitric oxide (NO) relaxes uterine smooth muscle in a dose-dependent, cyclic guanosine 3'-5'-monophosphate (cGMP)-independent manner(Buxton, Kaiser et al. 2001). The inhibitory concentration 50% for the transnitrosylating agent cysteine-NO to relax human myometrium in tissue bath experiments is approximately 1 μM(Buxton, Kaiser et al. 2001). Elevations in cGMP that accompany NO stimulation can be prevented by pretreatment of tissues with inhibitors of soluble guanylyl cyclase such as 1H-[1,2,4]oxadiazolo[4,3-a]quinoxalin-1-one (ODQ), 6-anilino-5,8-quinolinedione (LY 83583), or 3,7-bis(dimethylamino) phenothiazin-5-ium (methylene blue). Stimulation of ODQ treated myometrial tissues with NO-donors results in relaxation without cyclic GMP elevation. It is now clearly established from our work and that of others that NO-mediated relaxation of uterine muscle is independent of global cGMP elevation or activation of its cognate kinase, PKG type I(Tichenor, Malmquist et al. 2003), no matter whether this is studied in animal(Kuenzli, Bradley et al. 1996), primate (Kuenzli, Buxton et al. 1998) or human(Bradley, Buxton et al. 1998).

NO could potentially signal as an endogenous tocolytic, but there is no certainty that NO is present as an endogenous myometrial relaxing factor and this need not be the case for proteomic experiments to be important. NO could be available from uterine arterial endothelium or released from syncytiotrophoblasts(Valdes and Corthorn 2011). Moreover, Suzuki *et al.* have recently suggested that NO is generated in rat uterus(Suzuki, Mori et al. 2009). The fact that NO signals non-classically in the uterus and that it may selectively S-nitrosate proteins associated with pregnancy is the compelling feature of our work. If certain proteins enjoy a pregnancy-state specific nitrosation, then we may learn more about both the function of S-nitrosated proteins and the basic regulation of uterine relaxation. Such S-nitrosated proteins may reveal themselves or their interactions with other proteins as "druggable" and thus may reveal new therapeutic targets.

The importance of the fact that an effect of NO to relax the uterus is independent of global cGMP accumulation means that there is hope for discovery of therapeutic targets in the myometrium that are absent or disparately regulated in other smooth muscles and thus, can permit a reasoned line of investigation to find uterine-specific tocolytics.

We have hypothesized that NO-mediated relaxation is dependent on S-nitrosation of specific and critical proteins involved in the relaxation of USM. We further hypothesize that these critical proteins are S-nitrosated disparately in pregnant and non-pregnant USM consistent with the development of regulation of contraction-relaxation signaling. S-nitrosation is a mechanistically important, NO-dependent, post translational modification that can alter smooth muscle relaxation/contraction dynamics(Dalle-Donne, Milzani et al. 2000). The terms nitrosation and nitrosylation are often used interchangeably and the

difference in terminology only refers to the mechanism of formation. Considering that we are not studying the chemistry of the reaction, only the posttranslational modification, we use the term S-nitrosation to refer to the modified proteins that we have identified.

S-nitrosation has been shown to alter the function of many proteins including the activity of several enzymes(Hess, Matsumoto et al. 2005). Based on the striking cGMP-independence of NO-mediated USM relaxation and with the benefit of prior research establishing that S-nitrosation is a source of NO bioactivity, we propose that NO-mediated relaxation in USM is the result of protein S-nitrosation. Moreover, whether or not it is NO that acts endogenously to mediate uterine quiescence during gestation, it is reasonable to determine the S-nitrosation of proteins in myometrium on the basis that such efforts could identify targets associated with uterine quiescence and thus useful in the effort to prevent preterm delivery.

We employed the myometrium from guinea pig, the small animal model proposed as the most appropriate for studies of human parturition(Mitchell and Taggart 2009), to identify disparate S-nitrosation between the pregnant and non-pregnant state of the tissue. The goal of the work presented here is to describe proteins in USM that are S-nitrosated by a physiologically relevant NO donor and then to identify a subset of these proteins that are disparately S-nitrosated in pregnant vs. non-pregnant USM. We show that multiple proteins known to be integral to smooth muscle relaxation/contraction dynamics are S-nitrosated in USM. Furthermore, our work shows that a large subset of these proteins show disparate abilities to be S-nitrosated when comparing pregnant to non-pregnant USM tissue.

2.2 Methods

Chemicals-Sodium ascorbate, N-2-Hydroxyethylpiperazine-N'-2-ethanesulfonic acid (HEPES), neocuproine, N-ethylmaleimide (NEM), methyl methanethiosulfonate (MMTS), 3-(3-cholamidopropyl)dimethylammonio-1-propanesulfonate (CHAPS), sodium dodecyl sulfate (SDS), and all other chemicals unless specified, were obtained from Sigma (St Louis, MO). N-[6-(biotinamido)hexyl]-3'-(2'-pyridyldithio) propionamide (biotin-HPDP) was from Thermo Scientific (Rockford, IL).

Animal Care-Female virgin Dunkin-Hartley guinea pigs were estrogen primed as described previously and sacrificed the following morning under a protocol approved by the local Institutional Review Board. Term-pregnant Dunkin-Hartley guinea pigs were sacrificed between day 65 and 70 of pregnancy and the uterine horns removed and placed in ice cold phosphate buffered saline. Muscles were carefully prepared for smooth muscle protein isolation from regions between placentas by dissection of serosa and scraping away endometrium/epithelium revealing muscle.

Biotin Switch and Streptavidin Pull-down-Protein isolates from term-pregnant and non-pregnant guinea pigs (1.8 ml 0.8 mg/ml in HEN buffer: 25 mM HEPES-NaOH, 1 mM EDTA, 0.1 mM neocuproine, pH 7.7) were incubated with 300 µM GSNO (1,746 µl of sample + 54 µl of 10 mM GSNO prepared in the dark) for 20 min at room temperature. At this concentration, GSNO will produce ~5 µM reactive NO over 15-20 min without reactive NO accumulation(Cleeter, Cooper et al. 1994). Non cysteinyl nitrosation events would not be appreciated due to the reactive chemistry of ascorbate reduction; a nucleophilic attack at the nitroso-nitrogen atom leading to thiol and *O*-nitrosoascorbate (reaction 1)

$$RSNO + ASC^- \rightarrow RSH + NOASC^-$$

which breaks down by various competitive pathways; the dominant one at physiological pH yields dehydroascorbic acid and nitroxyl which decomposes at physiological pH to nitrous oxide(Kirsch, Buscher et al. 2009) (reaction 2).

$$NOASC^- + H^+ \rightarrow DHA + HNO$$

$$2HNO \rightarrow HON=NOH$$

$$HON=NOH \rightarrow N_20 + H_2O$$

Neither biotin-HPDP nor a maleimide dye would lead to false positives because the amines or tyrosines would not be labeled even if they were nitrosated. The biotin switch assay and streptavidin pulldown were performed as described in reference 39. Final protein pellets were washed and dried and then delivered to the University of Nevada Proteomics Center for LC/MS/MS analysis.

Fluorescent Switch-The fluorescent switch technique is a variation of the biotin switch pioneered by Jaffrey et al.(Jaffrey and Snyder 2001). This technique is used to selectively label S-nitrosated proteins using thiol reactive dyes. All procedures are performed in the dark in amber tubes. Total protein extracts were S-nitrosated using 300 µM GSNO (Sigma) for 20 min at room temperature. SDS was added along with NEM (Sigma) to a final 2.0 ml volume with 2.5% SDS and 30 mM NEM. Samples were incubated at 50°C in the dark for 20 min with frequent vortexing. Four volumes of cold acetone (8 ml) were added to each sample and proteins were precipitated for 1 hr at −20°C and collected by centrifugation at 3000 x g for 10 min. The clear supernatant was aspirated and the protein pellet gently washed with 70% acetone (4 × 1 ml). After resuspension in 0.24 ml HENS buffer, the material was transferred to fresh 1.7-ml

microfuge tubes containing 100 µM maleimide-Alexa fluor dye (Invitrogen, Carlsbad CA). The labeling reaction was initiated by adding 30 µl of 200 mM sodium ascorbate (final 20 mM ascorbate) with gentle shaking at room temperature for 1 hr. Un-reacted dye was removed by acetone precipitation and proteins were pelleted and washed with 70% acetone (4 x 1 ml) and air dried.

Nitrosyl-DIGE-Dried samples were lyophilized for 15 min and 360 µl of Elution Buffer 3 (EB3) was added. The samples were vortexed a number of times and sonicated for 10 min over a period of 1 hr 50 min. The samples were spun at 10,000 x g, 22^{o}C, for 2 min. The supernatants, along with 1/3 dilutions of each supernatant in EB3, were assayed by EZQ protein quantification (Molecular Probes, Eugene, OR). Proteins were equilibrated to 244 µg total protein per 300 µl of a mixture containing protein, EB3, DeStreak reagent (Amersham Biosciences, Uppsala, Sweden), and bromophenol blue 0.1%. Equal amounts of total protein from laboring, non-laboring, and total control (containing a mixture of all samples) were used to rehydrate 17 cm 3-10 IPG strips by overnight passive rehydration. The strips were transferred to an isoelectric focusing plate and run as follows: 250 V, linear, 20 minutes; 10,000 V, linear, 2 hr 30 min; 10,000 V, rapid until 40,000 V-hr; 500 V, rapid, 24 hr. The strips were equilibrated for electrophoresis and placed on 8-16% Protean II gels (Bio-Rad) and electrophoresis performed under the following conditions: 5 mA er gel constant, 30 min; 16 mA constant, 30 min; 24 mA constant, 4 hr 45 min. Gels were then transferred to low fluorescence plates and scanned on the Typhoon Trio (GE, Piscataway, NJ). Images were analyzed using DeCyder software (GE) and proteins of interest were excised, trypsin digested, and analyzed by either MS or LC/MS/MS at the University of Nevada Proteomics Center.

Protein Digestion and Mass Spectrometry-Nevada Proteomics Center analyzed selected proteins by trypsin digestion and MALDI TOF/TOF or LC/MS/MS analysis. Spots were digested using a previously described protocol with some modifications(Rosenfeld, Capdevielle et al. 1992). Samples were washed twice with 25 mM ammonium bicarbonate (ABC) and 100% acetonitrile, reduced and alkylated using 10 mM dithiothreitol and 100 mM iodoacetamide and incubated with 75 ng sequencing grade modified porcine trypsin (Promega, Fitchburg WI) in 25 mM ABC for 6 hr at 37^{o}C. Samples were spotted onto a MALDI target with ZipTip µ-C_{18} (Millipore Corp., MA). Samples were eluted with 70% acetonitrile, 0.2% formic acid and overlaid with 0.5 µl 5 mg/ml MALDI matrix (α-cyano-4-hydroxycinnamic acid, 10 mM ammonium phosphate). All mass spectrometric data were collected using an ABI 4700 Proteomics Analyzer MALDI TOF/TOF mass spectrometer (Applied Biosystems, Foster City, CA), using their 4000 Series Explorer software v. 3.6. The peptide masses were acquired in reflectron positive mode (1-keV accelerating voltage) from a mass range of 650 - 4000 Daltons; 1250 laser shots were averaged for each mass spectrum. Each sample was internally calibrated on trypsin's autolysis peaks 842.51 and 2211.10 to within 20 ppm. Any sample failing to internally calibrate was analyzed under default plate calibration conditions of 150 ppm. Raw spectrum filtering/peak detection settings were S/N threshold of 3, and cluster area S/N optimization enabled at S/N threshold 10, baseline subtraction enabled at peak width 50. The twenty most intense ions from the MS analysis, which were not on the exclusion list, were subjected to MS/MS. The MS/MS exclusion list included known trypsin masses: 842.51, 870.54, 1045.56, 1126.56, 1420.72, 1531.84, 1940.94, 2003.07, 2211.10, 2225.12, 2239.14, 2283.18, 2299.18, 2678.38, 2807.31,

2914.51, 3094.62, 3337.76, 3353.75. For MS/MS analysis the mass range was 70 to precursor ion with a precursor window resolution of -1 to +4 Da with an average 2500 laser shots for each spectrum, CID on, metastable suppressor on. Raw spectrum filtering/peak detection settings were S/N threshold of 5, and cluster area S/N optimization enabled at S/N threshold 6, baseline subtraction enabled at peak width 50. The data were then stored in an Oracle database (Oracle database schema v. 3.19.0 Data version 3.90.0).

MALDI Data Analysis-Peak lists were also created using ABI's 4000 Series Explorer software v. 3.6 Peaks to MASCOT feature. MS peak filtering included mass range 650-4000 Da, minimum S/N filter 10. A peak density filter of 50 peaks per 200 Da with a maximum number of peaks set to 200 was used. MS/MS peak filtering included mass range of 60 Da to 20 Da below each precursor mass. Minimum S/N filter 10, peak density filter of 50 peaks per 200 Da, cluster area filter used with maximum number of peaks 200. The filtered data were searched by Mascot v 2.1.03 (Matrix Science) using NCBI nr database (NCBI 20090319), containing 8,080,522 sequences. Searches were performed without restriction to protein species, M_r, or pI and with variable oxidation of methionine residues and carbamidomethylation of cysteines. Maximum missed cleavage was set to 1 and limited to trypsin cleavage sites. Precursor mass tolerance and fragment mass tolerance were set to 20 ppm and ± 0.2 Da, respectively.

MALDI data were collected for both trypsin digested spots from Nitro-DIGE as well as streptavidin pull down of biotin labeled samples. We acquired LC/MS/MS capability during this study and therefore, identification of samples was initially done only on the MALDI and then on the LC/MS/MS when it was available. Single protein identifications

were recorded for the 6 spots cut and the additional proteins identified by MALDI in Table S1 are from the streptavidin pull down samples.

LC/MS/MS Data Analysis- For LC/MS/MS analysis, trypsin digestion was carried out as detailed above for MALDI/TOF/TOF. The labels introduced in the Biotin Switch are removed when the disulfide linking Biotin-HPDP to the protein is cleaved after addition of beta-mercaptoethanol and is therefore not considered during database searching. The samples were in solution digested, as outlined in the Protein Digestion and Mass Spectrometry section, the samples were reduced and alkylated using 10 mM DTT and 100 mM iodoacetamide. These steps lead to carbamidomethylation of cysteines. Peptides were first separated by Michrom Paradigm Multi-Dimensional Liquid Chromatography (MDLC) instrument (Magic C_{18}AQ 3µ 200Å (0.2 x 50 mm) column, (Michrom Bioresources Inc., Auburn, CA) with an Agilent ZORBAX 300SB-C_{18} 5µ (5 x 0.3 mm) trap (Agilent Technologies, Santa Clara, CA)). The step gradient employed 0.1% formic acid in water (Pump A) and 0.1% formic acid in Acetonitrile (Pump B) as follows (Time (min), Flow (µl/min), Pump B(%): (0.00, 4.00, 5.00), (5.00, 4.00, 5.00), (95.00, 4.00, 45.00), (95.10, 4.00, 80.00), (96.10, 4.00, 80.00), (96.20, 4.00, 5.00). Eluted peptides were analyzed using a Thermo Finnigan LTQ-Orbitrap using Xcalibur v 2.0.7. MS spectra (*m*/*z* 300–2000) were acquired in the positive ion mode with resolution of 60,000 in profile mode. The top 6 data-dependent signals were analyzed by MS/MS with CID activation, minimum signal of 50,000, isolation width of 3.0, and normalized collision energy of 35.0. The reject mass list included known trypsin fragments: 323.2040, 356.0690, 371.1010, 372.1000, 373.0980, 374.0970, 445.1200, 523.2840, 536.1650, 572.5680, 747.3510, 824.4870, 930.1760. Dynamic exclusion settings were used with a

repeat count of 2, repeat duration of 10 seconds, exclusion list size of 500 and exclusion duration of 30 seconds.

Criteria for Protein Identification-Scaffold (V3.00.07, Proteome Software Inc., Portland, OR) was used to validate MS/MS based peptide and protein identifications. Peptide identifications were accepted if they could be established at greater than 95.0% probability as specified by the Peptide Prophet algorithm(Keller, Nesvizhskii et al. 2002). Protein identifications were accepted if they could be established at greater than 95.0% probability and contained at least 2 identified peptides. Protein probabilities were assigned by the Protein Prophet algorithm(Nesvizhskii, Keller et al. 2003). Proteins that contained similar peptides and could not be differentiated based on MS/MS analysis alone were grouped to satisfy the principles of parsimony.

Western Blot- Pregnant and non-pregnant USM protein isolated for Nitroso-DIGE and the biotin switch was used to measure total levels of desmin. Protein isolates were separated by SDS-PAGE (10%) transferred to nitrocellulose and blotted with rabbit anti-desmin [Y266] (Abcam) and labeled with anti-rabbit Alexa-Fluor 680 (Invitrogen). Blots were visualized using the Licor Odyssey imaging system.

Identification of Previously Characterized S-nitrosated Proteins-The lack of a central comprehensive online database for the classification of characterized S-nitrosated proteins makes classification of novel S-nitrosated proteins difficult. We used two methods to determine if our identified proteins had been previously classified as being S-nitrosated. First we methodically searched Xue et al.'s compiled database that was generated for their SNO identification algorithm(Xue, Liu et al. 2010). We included hits from both the experimentally identified database as well as the inferred database.

Second, we performed a search in PubMed and Google Scholar using the protein of interest as a key word with "nitrosylation or nitrosation" as the second keyword. Results are listed in Table S2.1 with the PubMed ID of the most relevant paper that hit to each keyword search.

Controls-Stringent controls were performed in order to avoid false positive identification of non S-nitrosated cysteine's that could have been mislabeled during the experimental procedures. These controls are standard when performing the biotin switch procedure and include removal of GSNO and/or ascorbate during the biotin or fluorescent switch. A small number of proteins were shown to be constitutively S-nitrosated and were labeled without the addition of GSNO, this is a common and expected result. Removal of ascorbate during the biotin or fluorescent switch removed any signal that was seen when ascorbate was present. The fluorescent switch or streptavidin purification of biotin switched proteins removes any signal from naturally biotinylated proteins and these are therefore not present in our analysis. Streptavidin purification and LC/MS/MS analysis of ascorbate negative samples were shown to only contain the contaminating keratin proteins, trypsin and serum albumin. Therefore, our ascorbate positive sample identification contains almost no non-specific binding proteins. Dye swapping and calibration with identical samples was performed on Nitrosyl-DIGE samples and it was determined that differences more than 1.5 fold as determined by DeCyder software were real.

Data Analysis-All data was analyzed using GraphPad Prism 5 and GraphPad Instat 3. Student's T-Test and one way ANOVA were used with $p < 0.05$ considered significant.

2.3 Results

The first step in identifying differentially S-nitrosated proteins in USM was to elucidate the overall USM S-nitrosylproteome. We used the biotin switch technique (Figure 2.1) coupled with streptavidin pull-down to isolate all S-nitrosated proteins from both pregnant and non-pregnant USM tissue.

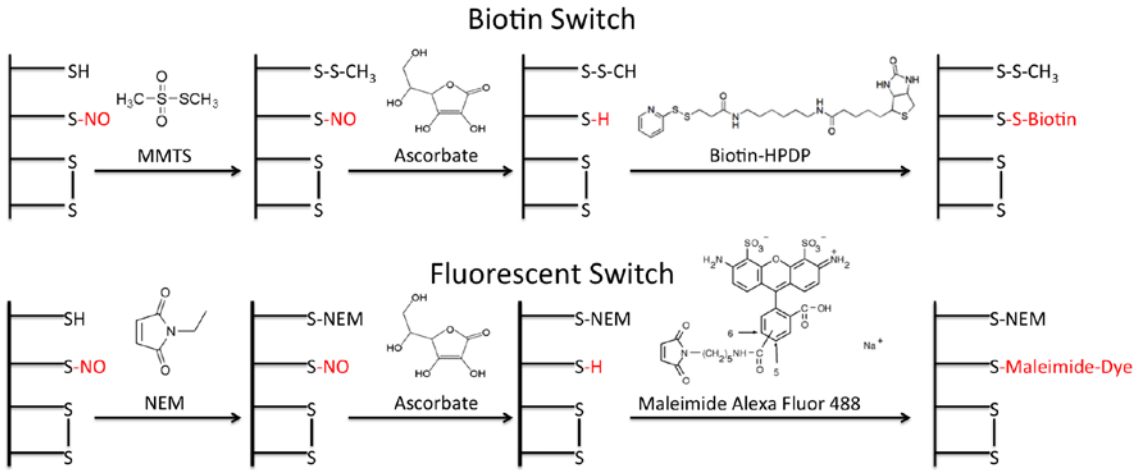

Figure 2.1*:* Schematic of the biotin switch and the fluorescent switch. Proteins that have been previously S-nitrosated can be either labeled with biotin-HPDP or an Alexa Fluor-maleimide dye. Step one involves blocking of all free thiols with either methyl methanethiosulfonate (MMTS) for the biotin switch or N-ethyl maleimide (NEM) for the fluorescent switch. Step 2 involves the reduction of all S-nitrosated thiols with ascorbate. Reduced thiols, which were originally S-nitrosated, are then labeled with biotin-HPDP or an Alexa Fluor-maleimide dye. The Alex Fluor dye in step 3 of the fluorescent switch can also be 555 or 647 maleimide dyes.

Isolated samples were identified on an LTQ-Orbitrap LC/MS/MS; all biological samples were examined in triplicate to avoid false positives. Three different biological samples were used for each group (NP and P). Each of these samples was subjected to multiple analysis involving nitrosyl-DIGE and LC/MS/MS after biotin switch and streptavidin pulldown. Only proteins that were present in a minimum of 2 of the 3 LC/MS/MS analyses or present in all nitrosyl-DIGE gels were included in Table 1 (see Appendices Section 1). Note that endogenously biotinylated proteins such as CoA-carboxylase remain attached to the beads after the proteins of interest are eluted and are thus not seen (see Methods). In order to identify proteins that show disparate levels of S-nitrosation, we utilized a technique that we are calling "nitrosyl-DIGE". Briefly, S-nitrosation of pregnant and non-pregnant samples is induced with the biologically relevant NO donor GSNO and samples are "fluorescently switched" so that the induced S-NO is exchanged for S-maleimide dye as described in Methods. The labeled samples are then separated using 2-dimensional in-gel electrophoresis (2-D DIGE) and analyzed for increases/decreases in spot intensity as compared to a control sample that contains a mixture of every sample in the entire experiment. Differences greater than 1.5 fold were determined to be statistically significant based on rigorous controls. Spots of interest (Figure 2.2) were excised, trypsin digested and analyzed by MS/MS or LC/MS/MS and identified using Mascot® and Scaffold® software.

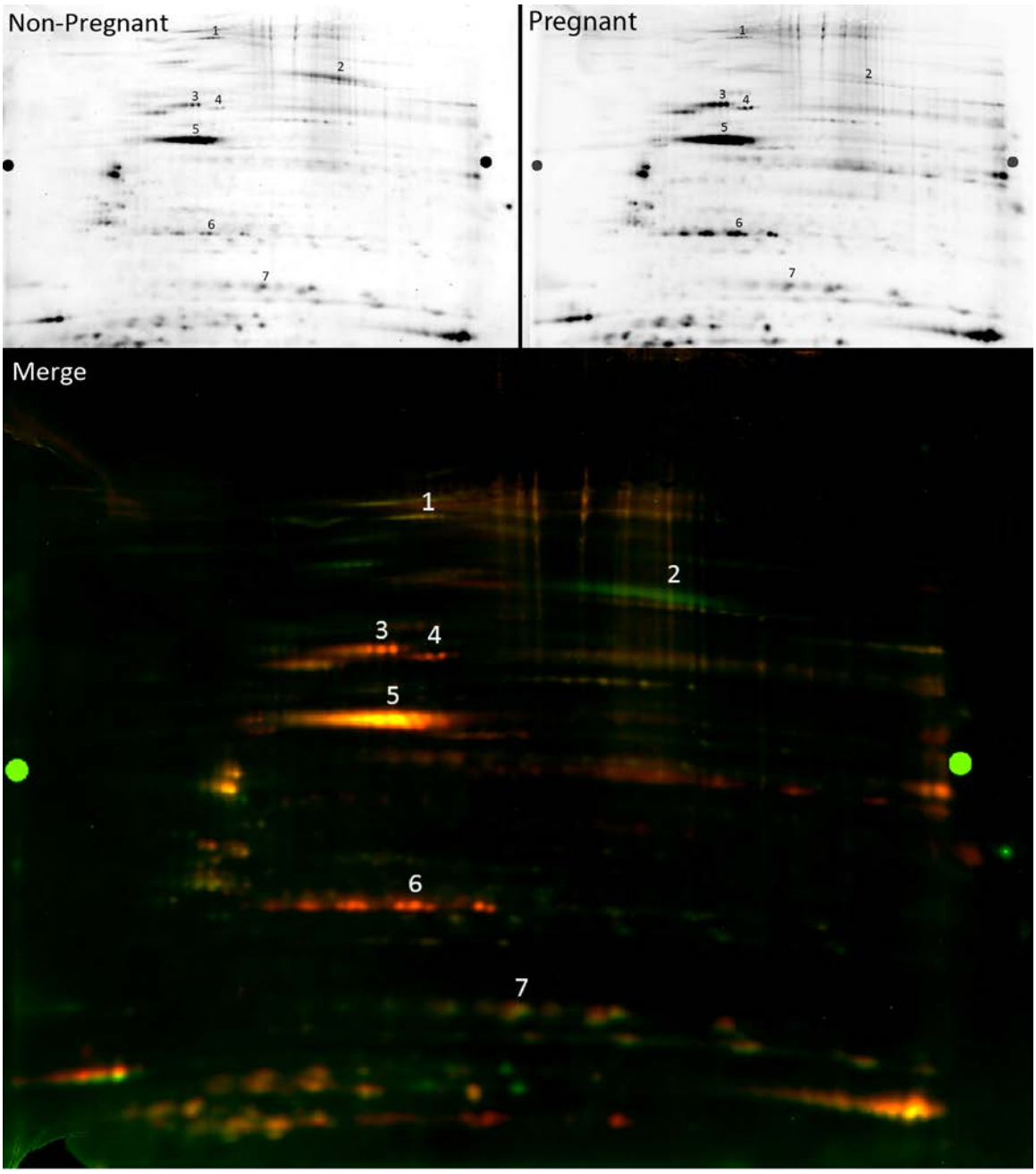

Figure 2.2: Nitrosyl-DIGE analysis of non-pregnant and pregnant guinea pig USM. A representative Nitrosyl-DIGE showing individual channels channels (Red Flor = Pregnant, Green Flor = Non-pregnant) as well as the two-dye overlay. Numbered spots were cut, trypsin digested, and identified by MS analysis. 1=Transitional endoplasmic reticulum ATPase 2=Serotransferrin 3=Vimentin 4=Desmin 5=Actin 6=Hsp27 7=Transgelin.

Spots that were repeatedly identified from multiple nitrosyl-DIGE gels with high confidence are included in Table S2.1 (see Appendices Section 1).

Our list of S-nitrosated USM proteins is the first from USM tissue and includes a number of interesting and functionally important proteins involved in USM contraction/relaxation dynamics (Table S2.2, see Appendices Section 1). Of the 118 unique S-nitrosated proteins that we identified, 51 are novel targets of S-nitrosation not previously described and several, including desmin, transgelin, myosin light polypeptide 9, and myosin light chain kinase (MYLK) are known to have important roles in smooth muscle contraction/relaxation dynamics(Tang 2008; Han, Dong et al. 2009).

Two methods were used to identify disparate protein S-nitrosation in USM. The "biotin switch" coupled with streptavidin pull-down and LC/MS/MS analysis of proteins labeled in non-pregnant and pregnant USM was used to identify the complete S-nitrosylproteome of each tissue. Of the 118 total proteins identified, 10 were found to be unique to non-pregnant tissue, 75 were found to be unique to pregnant tissue, and 33 were found to be present in both non-pregnant and pregnant tissue (Table S2.1, see Appendices Section 1). This list contains numerous proteins that are integral to smooth muscle contraction/relaxation dynamics including desmin, vimentin, heat shock protein beta-1 (Hsp27), transgelin, myosin, actin, MYLK, and guanine nucleotide-binding protein G_i subunit alpha-2 (Table S2.1, see Appendices Section 1).

The nitrosyl-DIGE technique identified several candidate proteins that exceeded the significant 1.5 fold difference in spot intensity. Specifically, we determined that desmin (5.9 fold increase in pregnancy), vimentin (3.8 fold increase in pregnancy) and transgelin (4.6 fold increase in pregnancy) all showed a statistically significant difference in S-

nitrosated state when comparing pregnant and non-pregnant USM tissue. Western blot analysis of total levels of desmin protein in pregnant and non-pregnant samples showed an approximately two-fold increase in total protein levels of desmin, this is in agreement with previous analysis of intermediate filament (IF) increases during pregnancy(Leoni, Carli et al. 1990). However, the increase in protein level was not alone sufficient to account for the near six-fold increase in the level of S-nitrosation seen (Figure 2.3).

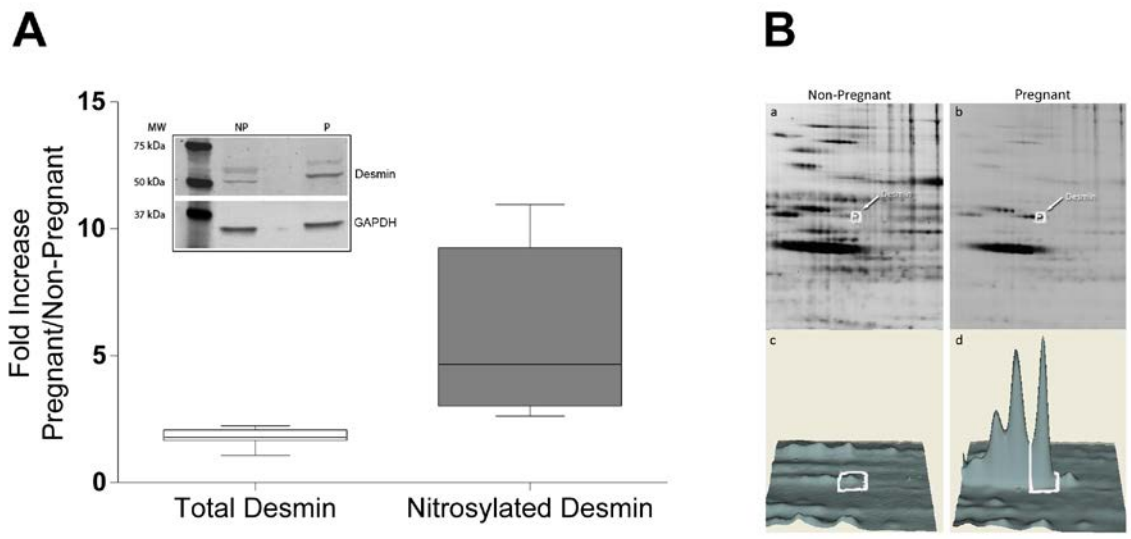

Figure 2.3: **Comparison of increased levels of total desmin protein vs. total levels of S-nitrosated desmin.** A) Total desmin protein level from non-pregnant and pregnant USM was separated by SDS-PAGE and a western blot was performed using a desmin specific antibody. Total desmin was normalized to GAPDH and the fold increase was calculated to be 1.792. B) Total desmin S-nitrosation was determined from 3 independent nitrosyl-DIGE experiments using DeCyder software and the fold increase was calculated to be 5.733. A students T-test was performed to analyze the difference in means between groups and the result was shown to be statistically significant with a p value of 0.0005.

Desmin has a single cysteine (Cys-333) that could undergo S-nitrosation and therefore any increase in measured levels indicates an increase in total S-nitrosated desmin rather than an increase in the number of S-nitrosation events per protein.

Our data demonstrate an increase in the percentage of total S-nitrosated desmin during pregnancy. Vimentin, Hsp27, and transgelin similarly all have only a single cysteine and therefore changes in S-nitrosation expression correlate with changing levels of total S-nitrosated protein. We therefore conclude that S-nitrosation levels change in a fashion disparate from total protein levels for desmin and that the overall levels of S-nitrosation for vimentin, Hsp27 and transgelin all increase in a statistically significant manner in pregnant USM when compared to the non-pregnant state of the tissue. This observation leads us to hypothesize that this change in S-nitrosation level has functional relevance and future work can now be directed at determining how this post-translational modification affects the function of these proteins.

2.4 Discussion

Elucidation of the guinea pig USM S-nitrosylproteome is the first step in identifying mechanistically important proteins regulated by S-nitrosation. The novel relaxation cascade induced by nitric oxide donors in USM argues for a tissue specific role of S-nitrosation. To our knowledge this is the first work examining the S-nitrosylproteome in USM tissue. Disparate levels of S-nitrosation identified in pregnant versus non-pregnant USM argue for a possible role of S-nitrosation regulation of relaxation during the progression of pregnancy.

It has been suggested by Kirsch *et al.* that the ascorbate-dependent reduction of S-nitrosated thiols should be performed under hypoxic conditions at pH 11.9(Kirsch,

Buscher et al. 2009). We agree that chemically this is the ideal reaction, however we are focused on elucidating the biologically relevant modifications and therefore suggest that the possible depletion of free thiols by nitroxyl intermediate that would occur at neutral pH *in vitro* would also be depleted *in vivo* and therefore less likely to identify functionally irrelevant S-nitrosation modifications.

We have employed GSNO at seemingly high concentration if one compares the effort to S-nitrosylate target proteins in our work to the classic action of NO as an activator of purified soluble guanylyl cyclase (sGC). This however is not the best comparison for the non-classical effects of NO in nitrosating proteins on cysteine residues. Direct effects of NO on purified sGC are in the nanomolar range(Cary, Winger et al. 2006), but nanomolar stimulation of cGMP accumulation in tissues by NO-donors *in vitro* is ineffective due to the many factors associated with time-dependent NO-radical delivery (estimated for 300 µM GSNO at 5 nmols/min/ml, exhausted after 15 min)(Cleeter, Cooper et al. 1994), the presence or absence of thiol reagents and penetration into the tissue. Our experiments employing 300 µM GSNO with tissue lysates then will expose proteins to 5 µM reactive $^{\bullet}$NO ($^{\bullet}$NO is highly reactive and will not accumulate). Some effects of NO such as those of GSNO on mitochondrial function require concentrations from 100 to 500 µM(Cleeter, Cooper et al. 1994). Generally, the relaxant actions of NO-donors in smooth muscle are half-maximal in the 1-10 micromolar range(Norman and Cameron 1996; Buxton, Kaiser et al. 2001; Modzelewska and Kostrzewska 2005), although notably, a 300 µM median effective dose of NO-donor was required to relax rat myometrium in studies by Buhimschi *et al.*(Buhimschi, Buhimschi et al. 1997)

In examining non-classical effects of NO, it is not possible to readily predict the levels of NO as liberated from NO-donors at the protein level. One can however, model the levels of NO that may be available physiologically. The model prepared by Lim *et al.* predicts [GSNO] ranging from 1 to 5 μM(Lim, Dedon et al. 2008). These predictions for [GSNO] are reasonable, given the micromolar levels determined in various tissues from humans and animal models of human disease. For example, Kluge *et al.* measured [GSNO] of 6-8 μM in normal rat cerebellum(Kluge, Gutteck-Amsler et al. 1997), while Stamler and co-workers have found nitrosothiol levels in general ranging from 7 μM in blood(Stamler, Jaraki et al. 1992) to 15-20 μM in pulmonary fluids(Gaston, Reilly et al. 1993). This range does not factor in possible compartmentalization or increased levels of nitosothiols during nitrosative stress or activated NO signaling. Higher concentrations are likely in the cell and are necessary for some physiological effects of S-nitrosation. For example, Padgett and Whorton found that half maximal inhibition of GAPDH by S-nitrosation using GSNO occurred between 200-700 μM increasing in the presence of DTT(Padgett and Whorton 1995). There is also evidence that GSNO, GSH, and S-nitrosothiols are in a dynamic equilibrium and a high concentration of GSNO will push the balance towards the highest number of S-nitrosated proteins. In order to identify specificity as well as the maximum number of candidate S-nitrosated proteins, we chose to use a high-physiological (300 μM) concentration of GSNO.

Desmin and vimentin are IF proteins that have been shown to be involved in regulation of smooth muscle contraction/relaxation of USM cells(Leoni, Carli et al. 1990). Smooth muscles are unique in that in response to external stimulation, they are able to adjust their contraction/relaxation status by reorganizing the actin cytoskeleton

and the IF network(Tang 2008). We have shown that levels of S-nitrosated desmin increase in a statistically significant manner in pregnant tissue when compared to non-pregnant tissue (Figure 2.3). We propose that one method of regulation of contraction/relaxation is through selective S-nitrosation of desmin and reorganization of the cytoskeleton. Vimentin is thought to be involved in force development in smooth muscle tissues(Wang, Li et al. 2006) arguing that regulation by S-nitrosation could involve inhibition of the contractile state and therefore promotion of relaxation.

HSP27 has been shown to have a regulatory role in smooth muscle contraction(Somara, Gilmont et al. 2009). Its regulatory interaction with thin filaments has been studied in several smooth muscle systems with postsecondary modifications (i.e. phosphorylation) being the main process of regulation(Kostenko and Moens 2009). HSP27 has also been shown to be S-nitrosated under varying conditions leading to the possibility that regulation of HSP27 could be dependent on its nitrosated state(Shi, Feng et al. 2008). HSP27 has also been shown to be highly induced in the myometrium during pregnancy and labor(White, Williams et al. 2005). Therefore we consider HSP27 to be a prime candidate for future studies regarding the possible role of S-nitrosation being a regulatory mechanism for HSP27 action.

Transgelin (also designated SM22α and p27) is a 22-kDA smooth muscle protein that physically associates with cytoskeletal actin filament bundles in contractile smooth muscle cells. Studies in transgelin knockout mice have demonstrated a pivotal role of transgelin in the regulation of Ca^{2+}-independent contractility(Je and Sohn 2007). Transgelin has also been implicated in induction of actin polymerization and/or stabilization of F-actin and is proposed to be necessary for actin polymerization and

bundling(Han, Dong et al. 2009). We show S-nitrosation of transgelin in USM tissue and also that it is only able to be S-nitrosated during pregnancy. This argues for a plausible role of modulating the contractile state of USM through S-nitrosation of transgelin during pregnancy.

Myosin and actin have both been shown to be S-nitrosated in skeletal muscle with myosin being reversibly inhibited by S-nitrosation with GSNO(Nogueira, Figueiredo-Freitas et al. 2009). Exposure of skeletal and cardiac myosins to physiological concentrations of nitrogen oxides, including the endogenous nitrosothiol S-nitroso-L-cysteine, reduced the velocity of actin filaments over myosin in a dose-dependent and oxygen-dependent manner, caused a doubling of force as measured in a laser trap transducer, and caused S-nitrosation of cysteines in the myosin heavy chain(Evangelista, Rao et al. 2010). Inhibition of the Mg^{2+}-ATPase activity of myosin and actomyosin by GSNO provides a plausible explanation for the functional effects of SNO donors in muscle fibers(Nogueira, Figueiredo-Freitas et al. 2009). We show for the first time that myosin-11 and myosin regulatory light peptide 9 are able to become S-nitrosated during pregnancy but not in non-pregnant USM. Calponin-1 was shown to be S-nitrosated only in non-pregnant USM and its interaction with actin and inhibition of the actomyosin Mg^{2+}-ATPase activity argue for a plausible role in the regulation of relaxation during pregnancy. Further research into what role these pregnancy state-dependent S-nitrosations play in the regulation of contraction/relaxation needs to be completed in order to understand how they affect the progression of pregnancy. Our work described here provides a starting point.

MYLK is a serine/threonine protein kinase whose role is to phosphorylate myosin regulatory light chain which in turn initiates actin–myosin ATPase on myosin heavy chains and thus myometrial cross-bridge cycling and contraction(Kamm and Stull 1989). We have shown that MYLK is able to be S-nitrosated in pregnant USM but not in non-pregnant USM. The effect of this modification is currently unknown and could plausibly play a role in inhibiting phosphorylation of myosin light chain and hence promote relaxation of pregnant USM during periods of quiescence. Further research should probe this interesting question in order to identify the mechanistic role of MYLK S-nitrosation.

One of the hypothesized modes for maintaining quiescence in the uterus is by activation of adenylate cyclases and the production of cyclic AMP (cAMP). cAMP is thought to promote the relaxation of myometrial, and other smooth muscle cells via activation of cAMP-dependent protein kinase (PKA) and downstream phosphorylation of MYLK(Price and Bernal 2001). Guanine nucleotide-binding protein G_i subunit alpha-2 ($G_i\alpha$) is an inhibitor of adenylate cyclases shown to be present in the myometrium and hence promotes contraction(Yuan and Lopez Bernal 2007). We have shown for the first time that $G_i\alpha$ is S-nitrosated in USM and that it is selectively S-nitrosated only during pregnancy. This leads to the possibility that S-nitrosation of $G_i\alpha$ could maintain the uterus in a quiescent state by preventing inhibition of adenylate cyclase and hence production of cAMP. This notwithstanding, a major role for cAMP action in uterine quiescence is controversial since it is well known that β_2 agonists such as ritodrine (Yutopar®) have little effect as tocolytics and no longer enjoy an FDA indication for the treatment of preterm labor. Yutopar® has been discontinued by the manufacturer.

We show for the first time the S-nitrosoproteome of non-pregnant and pregnant guinea pig USM. We unambiguously identified 118 proteins of which 10 were found to be unique to non-pregnant tissue, 75 were found to be unique to pregnant tissue, and 33 were found to be present in both non-pregnant and pregnant tissue. Of these 118 proteins we believe that 51 are novel targets of S-nitrosation not previously identified in the searchable literature. This list also includes an interesting subset of proteins known to be involved in smooth muscle contraction/relaxation dynamics. Current work is being performed to isolate biologically significant SNO proteins that will then be used to unambiguously localize S-nitrosation sites. However, the identification of the overall S-nitrosoproteome is important first, as it allows investigators to identify proteins of interest to further study mechanistic changes induced by S-nitrosation. Further research needs to be performed to elucidate the mechanisms involved in the S-nitrosation of these proteins and how this important post-translational modification affects their function.

CHAPTER 3:

SEMI-QUANTITATIVE PROTEOMIC AND PATHWAY ANALYSIS OF HUMAN UTERINE SMOOTH MUSCLE IN PREGNANCY, LABOR, AND PRETERM LABOR

This chapter is based on a manuscript that is currently being prepared for submission to *Molecular and Cellular Proteomics.*

Ulrich, C., Quilici, D., Buxton, I.L.O. Semi-quantitative proteomic and pathway analysis of human uterine smooth muscle in pregnancy, labor, and preterm labor *Mol Cell Prot USA, In Preparation,* (2013).

3.1 Introduction

The consensus is that both labor and preterm labor (PTL) are unexplained events. In order to combat the elusive problem of PTL it is critical that we understand the "machinery" involved in the induction of labor and how this is disparately activated in preterm labor. The basis of this "machinery" is the myometrial proteome and its post-translationally modified derivatives. These molecules are at the heart of induction of labor and must be understood in order to identify the anomalous events that take place in early induction of labor. In order to understand these proteins we must first identify them and semi-quantitatively measure how they are changing in different states of pregnancy. By identifying and semi-quantitating we will begin to amass a differentially expressed data set that can help guide us to the pathways most likely perturbed in our diseased state. This will allow for a directed approach to comprehensively quantitate those proteins of interest that we show to be anomalous in the diseased state.

Although our dataset was comprised of a couple thousand proteins we realize that there are thousands more that we were not able to positively identify using our current protein extraction and separation techniques. This in no way diminishes the value of our dataset as even this fraction of proteins allows us to generate a scaled out proteome map that is extremely useful in directing future hypothesis driven research. Ahrens et al reviewed this concept of creating multiple levels of proteome coverage and integrating all of the different proteomic data into a "map"(Ahrens, Brunner et al. 2010). We have created a baseline proteome map of human uterine smooth muscle (HUSM) that will allow future research to add more in depth layers until ultimately completing the

proteomic profile of HUSM in different states of labor. This will be an immensely useful tool for researchers and clinicians alike.

The use of high resolution mass spectrometry (MS) as well as improvements in MS based data analysis software allow for several different quantification options. The two most popular label-free MS based quantification techniques are spectral counting (SC) and area under the curve of extracted ion chromatograms (AUC). SC infers the quantity of protein indirectly from the number of peptide-to-spectrum matches (PSMs; spectrum count) obtained for each protein(Bantscheff, Lemeer et al. 2012). Intensity-based label free quantification (e.g. AUC) employs the MS signal response of intact peptides and, by inference, that of proteins for quantification(Bantscheff, Lemeer et al. 2012). AUC is accomplished by integrating the ion intensities of any given peptide over its chromatographic elution profile. This measure of MS1 intensity is potentially a more accurate mode of label-free quantification as it can provide measurements in the low abundance range since every sequenced peptide is observed with intensity. This information is lost in SC, which limits quantification of the low abundance proteins identified by low numbers of MS/MS spectra only (Choi, Glatter et al. 2012). We attempted to utilize both analysis techniques but chromatographic shifts during the two-dimensional LC prevented us from aligning all samples for MS1 quantitation. The reason for this is that not all samples elute at exactly the same time and during 24 fractionations there are shifts that leave some peptides in different fractions (Figure 3.1).

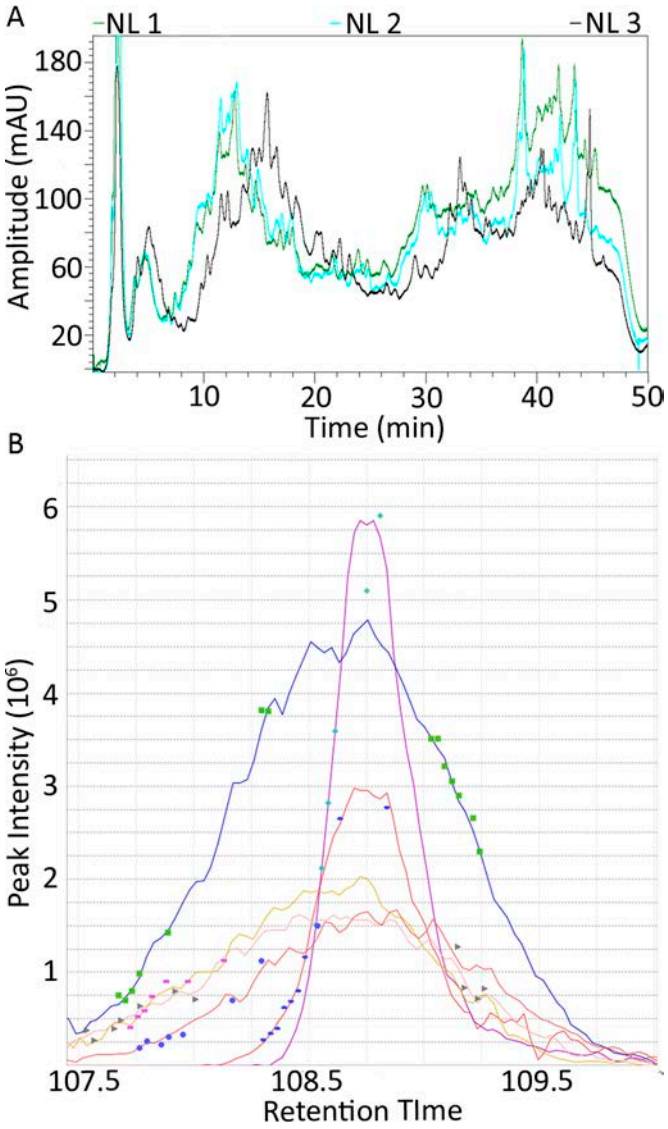

Figure 3.1: Chromatography variations necessitate quantificationation by spectral counting. (A) UV trace of first dimension SCX separation, 7 of 9 groups showed variation of ± 15 seconds of retention time on the SCX column (Black line is NL 1 which is representative of the other 6 samples). NL2 and NL3 showed a non-linear shift of ≥ 4 minutes. This resulted in peptides running in different fractions during the second dimension reverse phase separation and inability to overlap the MS1 chromatograms. (B) MS1 chromatograms from L and PTL were extracted and analyzed. This chromatogram shows PTL traces (the largest three blue, purple, and red) versus L traces (the smallest three orange, pink, and yellow) and confirms that this peptide was more highly expressed in PTL. Trends identified by spectral counting were recapitulated in the AUC analysis of L and PTL.

This does not affect SC quantification as the identifying peptides will be seen no matter what fraction they are in. Alignment was possible for 3 PTL and 3 L samples, therefore we performed an AUC analysis on these to compare to the low abundance spectral count proteins and found good agreement between the two analyses when there were enough spectral counts to positively identify a protein.

3.2 Experimental Procedures

Chemicals-Sodium ascorbate, N-2-Hydroxyethylpiperazine-N'-2-ethanesulfonic acid (HEPES), neocuproine, 3-(3-cholamidopropyl)dimethylammonio-1-propanesulfonate (CHAPS), sodium dodecyl sulfate (SDS), and all other chemicals unless specified, were obtained from Sigma (St Louis, MO).

Tissue Collection-All research was reviewed and approved by the University of Nevada Biomedical Review Committee (IRB) for the Protection of Human Subjects. Human uterine myometrial biopsies were obtained with written informed consent from mothers undergoing elective Cesarean section in preterm labor without infection or rupture of membranes, at term in labor or at term not in labor. Tissues were transported to the laboratory immediately in cold physiological buffer, microdissected under magnification to isolate smooth muscle, snap frozen in liquid nitrogen, and stored at -80^{o}C. The average age for patients in the pregnant laboring group was 28.9 ± 5.6 years, in the non-laboring group 28.0 ± 5.1 years, and in the preterm laboring group 30.8 ± 10.2 years. Pregnant laboring and non-laboring patients ranged from 37-41 weeks gestation, with the mean at 39 weeks for both laboring and non-laboring groups. Preterm laboring patients ranged from 29.2-36 weeks gestation, with the mean being 33.5 weeks. Patients

represented a range of ethnicities and were 52% Caucasian, 30% Hispanic, 7.4% African American, and 11% other.

Protein Isolation-To isolate total protein, myometrial muscle samples from 12 patients in each pregnancy state were ground to a powder under liquid nitrogen and reconstituted in 20 ml HEN buffer (25 mM HEPES-NaOH, 1 mM EDTA, 0.1 mM neocuproine, pH 7.7). Samples were sonicated (10 X 2 sec bursts, 70% duty cycle) and brought to 0.4% CHAPS. Samples were then centrifuged at 2000 x g for 10 min at 4°C. Protein concentration was determined by the bicinchoninic acid (BCA) assay and samples diluted to 0.8 mg/ml in HEN buffer. This procedure was followed in order to mimic the conditions used for protein isolation during measurement of the human uterine smooth muscle S-nitrosoproteome.

Protein Digestion and Mass Spectrometry- The Nevada Proteomics Center analyzed selected proteins by trypsin digestion and two-dimensional LC/MS/MS analysis. Samples were digested and desalted according to L.M. Brill et al. (Brill, Motamedchaboki et al. 2009). Peptides from ca. 1 mg of protein were re-suspended in 200 µl of 95% solvent C/5% solvent D (Solvent C = 5% acetonitrile/0.1% formic acid in H2O; Solvent D = 25% acetonitrile/0.1% formic acid in H2O, containing 500 mM KCl (Sigma–Aldrich)). The peptide mixture was vortexed at maximum speed for 30 seconds, vortexed at setting 6 for 30 min at room temperature, vortexed at maximum speed for 30 seconds and sonicated for 20 minutes. The peptide mixture was centrifuged for 10 minutes at 14,000 rpm, room temperature. The supernatant containing soluble peptides was transferred to a deactivated, Qsert snap cap glass sample vial, which includes caps with PTFR/silicone septa (Waters, P/N 186001124DV), sealed and immediately stored at

4° C. Peptides were separated using SCX as soon as possible after preparation, within 1 hour or less, as described below. The peptides were subjected to fractionation by strong cation exchange (SCX) chromatography followed by reversed phase HPLC-tandem mass spectrometry [3]. SCX peptides were separated over a 50 minute gradient on a Paradigm Multi-Dimensional Liquid Chromatography (MDLC) instrument (Michrom Bioresources Inc., Auburn, CA) using a polysulfoethyl A, 5µ 200Å (2.0 x 150 mm) column, (PolyLC, Inc., Columbia, MD) at a flow rate of 200 µl/min producing a total of twenty-four fractions collected by a Probot fraction collector (LC Packings, Netherlands). The SCX fractions were then loaded into a Paradigm AS1 (Michrom Bioresources Inc., Auburn, CA) autosampler. The autosampler stored the fractions at 4^0C during for the duration of the analysis. Fifty microliters of the SCX fraction was loaded onto the vented trap prior to HPLC analysis. A Paradigm Multi-Dimensional Liquid Chromatography (MDLC) instrument (Magic C_{18}AQ 3µ 200Å (0.2 x 50 mm) column, (Michrom Bioresources Inc., Auburn, CA) with an Agilent ZORBAX 300SB-C_{18} 5µ (5 x 0.3 mm) trap (Agilent Technologies, Santa Clara, CA) was used. The gradient employed was 0.1% formic acid in water (Pump A) and 0.1% formic acid in Acetonitrile (Pump B) as follows (Time (min), Flow (µl/min), Pump B(%): (0.00, 2.00, 5.00), (6.00, 2.00, 5.00), (185.00, 2.00, 35.00), (188.00, 2.00, 80.00), (190.00, 2.00, 80.00), (193.00, 2.00, 5.00), (200.00, 2.00, 5.00). Eluted peptides were analyzed using a Thermo Finnigan LTQ-Orbitrap using Xcalibur v 2.0.7. MS spectra (*m*/*z* 300–2000) were acquired in the positive ion mode with resolution of 60,000 in profile mode. The top 4 data-dependent signals were analyzed by MS/MS with CID activation, minimum signal of 2,000, isolation width of 3.0, and normalized collision energy of 35.0. Dynamic exclusion settings were used with

a repeat count of 2, repeat duration of 10 seconds, exclusion list size of 500 and exclusion duration of 30 seconds.

Database Searching-Tandem mass spectra were extracted; charge state deconvolution and deisotoping were not performed. All MS/MS samples were analyzed using Sequest (Thermo Fisher Scientific, San Jose, CA, version v.27, rev. 11). Sequest was initiated to search the database containing ipi.HUMAN.v3.87, the Global Proteome Machine cRAP v.2012.01.01, and random decoy sequences (183158 entries) assuming the digestion enzyme trypsin. Sequest was searched with a fragment ion mass tolerance of 1.00 Da and a parent ion tolerance of 10 ppm. Oxidation of methionine and iodoacetamide derivative of cysteine were specified in Sequest as variable modifications.

Criteria for Protein Identification-PROTEOIQ (V2.6, www.nusep.com) was used to validate MS/MS based peptide and protein identifications. Peptides were parsed before analysis with a minimum Xcorr value of 1.5 and a minimum length of 6 amino acids. Results were parsed based on the following criteria; FDR $\leq$ 1.0, minimum of 2 peptides per group, minimum of 5 spectra per peptide, minimum of 66% of replicates. Peptide identifications were accepted if they could be established at greater than 95.0% probability as specified by the Peptide Prophet algorithm (Keller, Nesvizhskii et al. 2002). Protein identifications were accepted if they could be established at greater than 95.0% probability and contained at least two identified peptides with 5 spectra per peptide. Protein probabilities were assigned by the Protein Prophet algorithm (Nesvizhskii, Keller et al. 2003). Proteins that contained similar peptides and could not be differentiated based on MS/MS analysis alone were grouped to satisfy the principles of parsimony.

Semi-Quantification and Data Analysis-SC data were analyzed using the in program statistical package provided with ProteoIQ. The statistical significance level for 3-way comparisons of spectral counts measures was pre-determined as 0.05.

Pathway Analysis - In conjunction with our bioinformatics core we used Ingenuity computational pathway analysis (IPA®) (Ingenuity systems; Redwood City, CA) software to elucidate the global implications of differentially expressed proteins in PTL patients. IPA® was applied to identify potentially perturbed molecular pathways and networks in PTL patients. The IPA program uses a knowledge database derived from the literature to relate the proteins to each other, based on their interaction and function. The knowledge base consists of a high quality expert-curated database containing 1.5 million biological findings consisting of more than 42,000 mammalian genes and pathway interactions extracted from the literature. In brief, proteins that were confidently identified and showed a statistically significant change ($\pm\log_2$ 1, $p > 0.05$) were considered for IPA® analysis. The IPA® software then used these proteins and their identifiers to navigate the curated literature database and extract overlapping network(s) between the candidate proteins. Associated networks were generated, along with a score representing the log probability of a particular network being found by random chance. Top canonical pathways associated with the uploaded data were presented, along with a p-value. Furthermore, upstream regulators that are likely to be responsible for the observed changes were predicted to be activated or inhibited. The p-values were calculated using right-tailed Fisher's exact tests. IPA® also uses a z-score algorithm to reduce the chance that random data will generate significant predictions.

3.3 Results

This work describes the HUSM proteome in 3 distinct states of pregnancy: term non laboring, full term laboring, and preterm laboring. In order to identify as many proteins as possible we chose to separate digested peptides by 2-dimensional high performance liquid chromatography(HPLC)-electrospray ionization(ESI)-tandem mass spectrometry(MS/MS) that demonstrates high sensitivity and robust operation as described by Brill et al.(Brill, Motamedchaboki et al. 2009). The peptides were first separated by strong cation exchange, during which 24 fractions were collected at intervals of 2 minutes. The 24 fractions were each then separated by reversed phase and directly coupled to ESI-MS/MS. Using this method we unambiguously identified a total of 2132 protein groups in these samples with the following breakdown: 1869 proteins identified in term laboring tissue samples, 1963 proteins identified in term non laboring tissue samples, and 2102 proteins identified in preterm laboring samples (Figure 3.2).

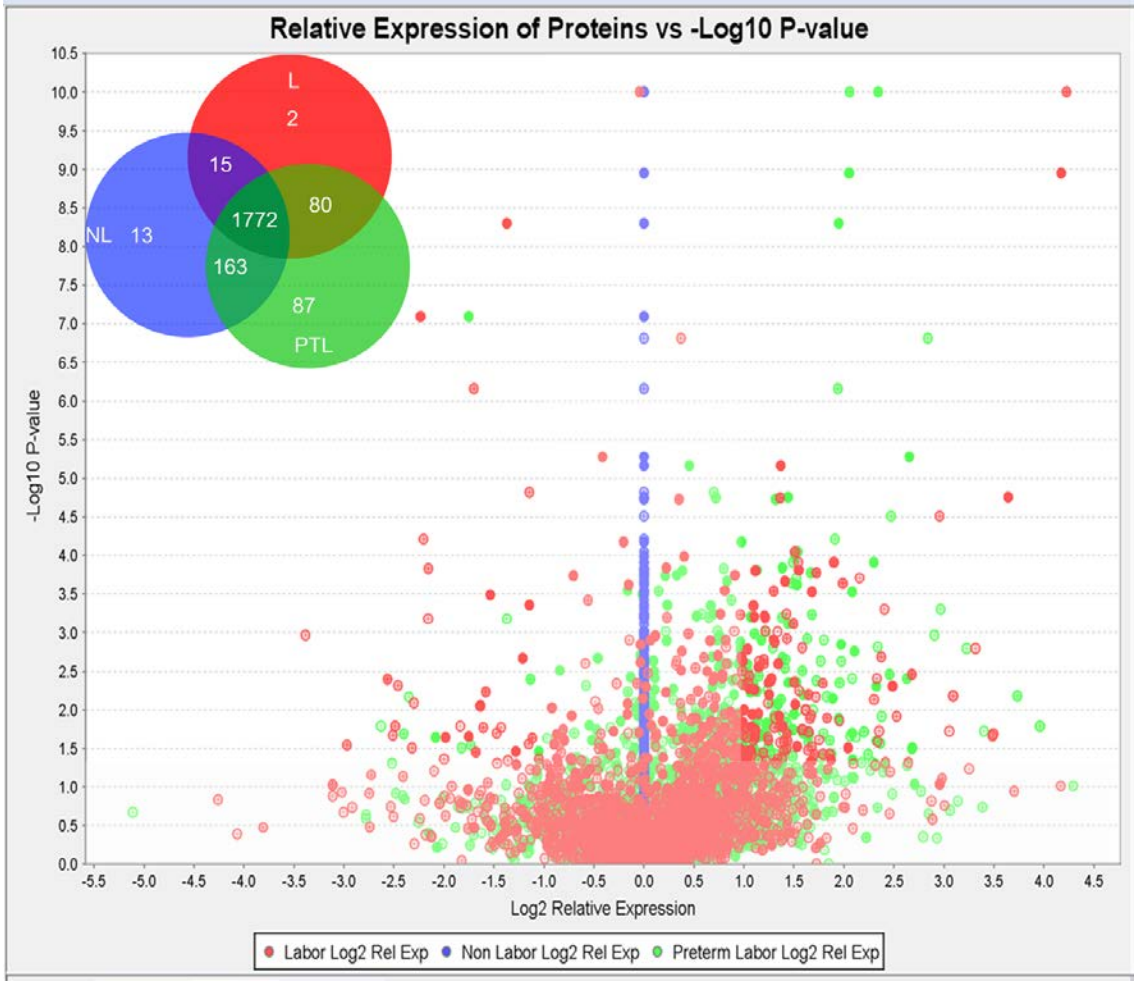

Figure 3.2: Relative quantification of the human uterine smooth muscle proteome: Volcano plot showing disparate regulation of L (red dots) and PTL (green dots) as compared to NL (blue dots). Proteins were considered significant and interesting if they fell outside of the shaded boxes. This area represents those proteins that showed a $\log_2$ change of ± 1 with a p-value ≤ 0.05. Venn diagram inset shows the group distribution of proteins identified in each state of pregnancy.

We show that 201 of these 2132 proteins show disparate regulation in the PTL state as evidenced by a $\log_2$ relative expression of ± 1 and $p \leq 0.05$ as compared to the NL state when measured by semi-quantitative spectral counting (Figure 3.3). We identified 41 proteins specific to PTL that met our statistical criteria, and another 55 that were specific to PTL and L (Figure 3.3 Inset).

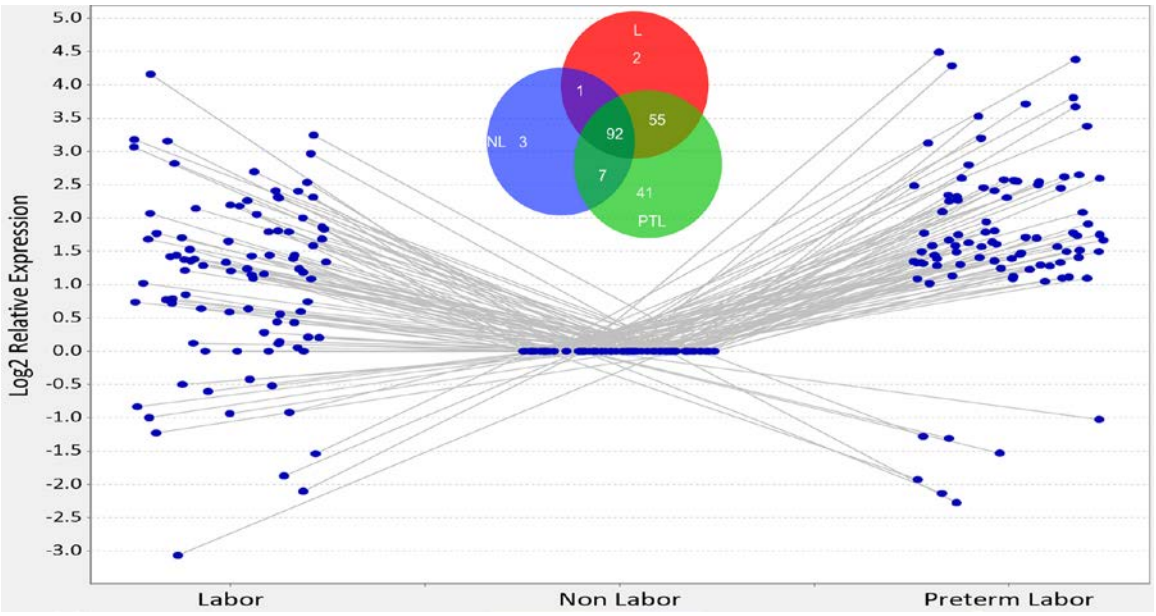

Figure 3.3: Changes in protein expression during PTL. Scatter plot representing the 92 proteins that were identified in all 3 states of pregnancy and showed a $\log_2$ change of ± 1 with a p-value ≤ 0.05. Venn diagram inset represents all 201 proteins that showed a $\log_2$ change of ± 1 with a p-value ≤ 0.05. Proteins that were not represented in all groups are not shown on the scatterplot; these proteins all had a $\log_2$ relative expression of ±10 in at least one of the groups (See Table S3.1 for all expression values).

This is the most comprehensive semi-quantitative proteomic study done in human myometrium and provides a useful set of protein expression data in different states of pregnancy. We initially attempted to analyze our data using both area under the curve of extracted ion chromatograms (AUC) and spectral counting (SC). Unfortunately, the process of separating peptides in 2-dimensions led to shifts in the chromatography peaks that are used to integrate the AUC data and therefore AUC analysis was not possible with this data set. However, SC data analysis allows for identification of specific trends that show disparate levels of protein between groups. In order to better understand the relevance of the disparate levels of protein expression that we see we employed IPA® to help delineate the molecular networks and pathways that were most likely perturbed by these proteomic changes. Network analysis of perturbed biological function highlighted an increase in the inflammatory response in PTL as compared to NL (Table 3.1 and Fig. 3.4).

Functions Annotation	p-Value	Predicted Activation State	Activation z-score	# Molecules	Molecules
accumulation of myeloid cells	4.00E-07	Increased	3.11	12	CTSG, ELANE, HMOX1, ITGA6, ITGB2, LAMA5, NT5E, POSTN, PRTN3, S100A8, S100A9, THBS1
accumulation of phagocytes	4.64E-07	Increased	3.106	11	CTSG, ELANE, HMOX1, ITGA6, ITGB2, LAMA5, NT5E, PRTN3, S100A8, S100A9, THBS1
activation of leukocytes	5.08E-04	Increased	3.061	20	CD14, CD276, CTSG, ELANE, FKBP1A, FN1, HMOX1, HSPH1, ITGB2, LCN2, LTBP1, LTF, MPO, NT5E, PRG2, PRTN3, S100A8, S100A9, SERPINB9, THBS1
activation of myeloid cells	5.97E-07	Increased	2.896	15	CD14, ELANE, FKBP1A, FN1, HMOX1, ITGB2, LCN2, LTBP1, LTF, MPO, PRG2, PRTN3, S100A8, S100A9, THBS1
accumulation of neutrophils	4.08E-07	Increased	2.789	8	CTSG, ELANE, ITGA6, ITGB2, LAMA5, PRTN3, S100A8, S100A9
accumulation of granulocytes	2.02E-06	Increased	2.789	9	CTSG, ELANE, ITGA6, ITGB2, LAMA5, POSTN, PRTN3, S100A8, S100A9
activation of phagocytes	1.01E-04	Increased	2.579	13	CD14, ELANE, FKBP1A, FN1, HMOX1, LCN2, LTBP1, LTF, MPO, PRG2, PRTN3, S100A9, THBS1
activation of granulocytes	4.59E-06	Increased	2.377	9	CD14, ELANE, FKBP1A, HMOX1, ITGB2, LCN2, LTF, PRG2, PRTN3
chemotaxis of leukocytes	1.86E-03	Increased	2.253	12	CTSG, ELANE, FLT1, FN1, GIT2, ITGB2, LSP1, PIGR, PRTN3, S100A8, S100A9, THBS1
activation of neutrophils	5.71E-06	Increased	2.157	8	CD14, ELANE, FKBP1A, HMOX1, LCN2, LTF, PRG2, PRTN3
cell movement of phagocytes	1.71E-03	Increased	2.106	16	COL1A1, CTSG, ELANE, FLT1, FN1, GIT2, HARS, HMOX1, ITGB2, LSP1, PIGR, PRTN3, S100A8, S100A9, SWAP70, THBS1
chemotaxis of phagocytes	1.15E-03	Increased	2.035	11	CTSG, ELANE, FLT1, GIT2, ITGB2, LSP1, PIGR, PRTN3, S100A8, S100A9, THBS1
chemotaxis of myeloid cells	8.86E-04	Increased	2.035	11	CTSG, ELANE, FLT1, GIT2, ITGB2, LSP1, PIGR, PRTN3, S100A8, S100A9, THBS1
quantity of monocytes	8.52E-03	Decreased	-2.19	5	ITGB2, LCN2, MPO, PRTN3, THBS1

Table 3.1: IPA® generated biological function analysis. The inflammatory response in PTL as compared to NL was identified as the most perturbed biological function based on the provided protein expression profile. Both the p-Value and activation z-score are used to identify perturbations in protein expression of known biological networks. UNIPROT identifiers for the listed molecules can be found in Table S3.1.

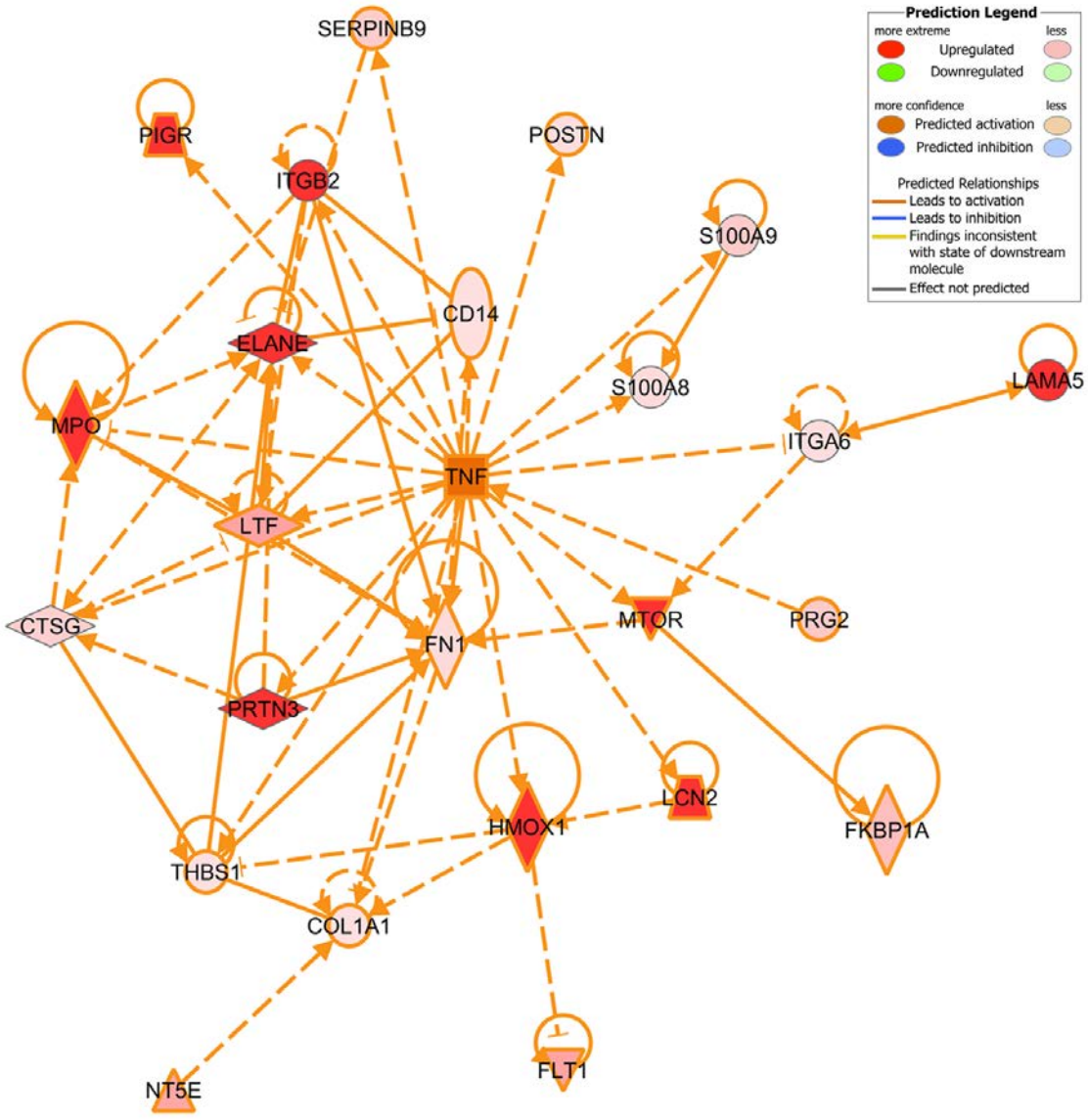

Figure 3.4: Inflammatory response proteins up-regulated in PTL: IPA® generated network of select proteins involved in the inflammatory response regulated by TNFα. This protein expression pattern is consistent with the predicted activation of TNFα and downstream regulation of these and other proteins.

The molecular activation prediction algorithm available in IPA® identified tumor necrosis factor (TNFα) as an upstream regulator of the majority of proteins that were up-regulated in PTL. Included in this group was serine/threonine-protein kinase mTOR (mTOR) as well as several more proteins integral to the canonical mTOR signaling pathway which was among the top scored perturbed pathways in our pathway analysis.

3.4 Discussion

HUSM Proteome: The pattern of proteomic regulation during PTL is skewed toward an increase in the majority of disparately regulated proteins. It is currently unclear why the majority of proteins that showed a significant difference trend to an increase in PTL. What is clear from the protein expression data is that PTL is in a perturbed state in which some of the regulatory pathways involved in the induction of labor are affected. Of particular interest, we show that laminin subunit alpha-5 (LAMA5), integrin alpha-6 (ITGA6), and fibronectin (FN1) are all up-regulated in PTL patients. These proteins are involved in extracellular matrix remodeling as well as transducing signals from the extracellular environment. The role these proteins have during the induction of labor is not currently known, however this data is in accord with these proteins having an integral function during the switch from uterine quiescence to the contractile state.

Pathway Analysis: Perturbation of the TNFα signaling network during PTL is of great interest considering the thought that pregnancy is likely an inflammatory state and therefore the myometrial reaction to this state must be integral to the progression of pregnancy and induction of labor. TNFα protein, mRNA, and receptors are present in multiple reproductive tissues throughout pregnancy, including the endometrium (Tabibzadeh 1991; Hunt, Chen et al. 1992) and myometrium (Dudley 1999; Alexander,

Sooranna et al. 2012). It has been shown that myometrial TNFα receptors increase with gestation and labor (Alexander, Sooranna et al. 2012) arguing for a critical signaling role with advancing gestation and labor. Of particular interest, it has been shown that high concentrations of TNFα appear with the onset of labor that is unresponsive to tocolysis (Steinborn, Kuhnert et al. 1996). Multiple groups have shown that TNFα works synergistically with other inflammatory cytokines to release prostaglandins, which can induce uterine contractions and labor (Daher, Fonseca et al. 1999). Genetic analysis of pro-labor genes in a cell culture model showed that one of the most important modulators was TNFα (Tattersall, Engineer et al. 2008), however, the global proteome changes induced by TNFα during pregnancy, labor, and PTL have not previously been elucidated. Our present research shows that multiple proteins regulated by TNFα show increased expression in PTL patients when compared to NL patients. Of particular interest was the up-regulation of mTOR and its canonical signaling pathway in PTL (Figure 3.5).

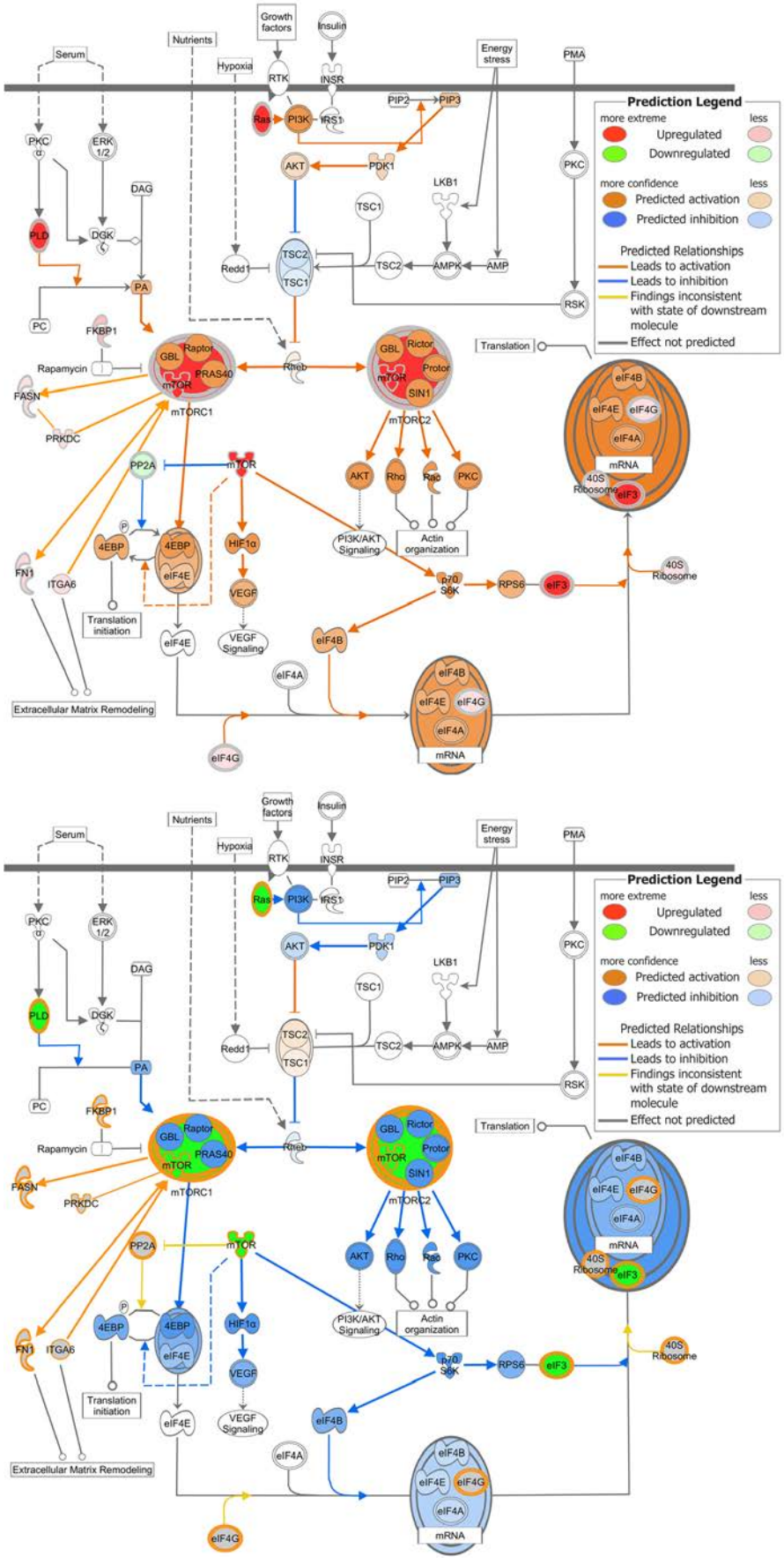
Growth factors
Insulin
Nutrients
Serum
Hypoxia
RTK
INSR
Energy stress
PMA
Ras
PI3K
IRS1
PIP2
PIP3
PKC
ERK 1/2
AKT
PDK1
LKB1
DAG
TSC1
PLD
DGK
TSC2
Redd1
AMPK
AMP
PA
RSK
PC
FKBP1
Raptor
GBL
PRAS40
mTOR
Rheb
Rictor
Protor
SIN1
Translation
Rapamycin
FASN
mTORC1
mTORC2
PRKDC
eIF4B
eIF4E
eIF4G
eIF4A
mRNA
40S Ribosome
eIF3
PP2A
Rho
Rac
4EBP
HIF1α
PI3K/AKT Signaling
Actin organization
FN1
ITGA6
VEGF
p70 S6K
RPS6
Translation initiation
VEGF Signaling
Extracellular Matrix Remodeling
Prediction Legend
more extreme
less
Upregulated
Downregulated
more confidence
Predicted activation
Predicted inhibition
Predicted Relationships
Leads to activation
Leads to inhibition
Findings inconsistent with state of downstream molecule
Effect not predicted

Figure 3.5: IPA® generated mTOR canonical pathway with molecular activation prediction. (A) Term not in labor mTOR pathway proteins show down regulation consistent with predicted inhibition of multiple down-stream processes. (B) Preterm labor mTOR pathway proteins show up regulation consistent with up regulation of multiple down-stream processes. Note, term in labor protein expression trended in the direction of up regulation but was not as pronounced as PTL (not shown).

The mTOR pathway has been previously shown in rat to be involved in the proliferative activity of uterine myocytes (Jaffer, Shynlova et al. 2009; Shynlova, Tsui et al. 2009). Our data suggests an alternate role for mTOR signaling during human gestation. The up-regulation of multiple proteins in the mTOR signaling pathway during PTL, including those involved in cytoskeletal rearrangement and extracellular matrix remodeling, argues for a plausible role for this pathway in the early induction of labor. The fact that the increase in mTOR pathway protein expression is greater in both L and PTL (with PTL having the greatest increase) than NL is intriguing. This is contrary to the idea that mTOR's main role in pregnancy is to transduce proliferative phenotype signaling.

In conclusion, we have identified a baseline HUSM proteome that can be used to guide directed research into how perturbation of specific proteomic networks affects uterine quiescence as well as the induction of labor. The obvious disparity in protein regulation between the laboring phenotypes and the non laboring phenotypes argue for a mechanistic role and future work will identify what function these perturbed networks have during the induction of labor.

CHAPTER 4:

The Human Uterine Smooth Muscle S-nitrosoproteome Fingerprint in Pregnancy, Labor and Preterm Labor

This chapter is based on a manuscript that is currently under review for *PLOS ONE*.

Ulrich, C., Quilici, D., Schlauch, K.A., Buxton, I.L.O. The human uterine smooth muscle S-nitrosoproteome fingerprint in pregnancy, labor, and preterm labor *PLOS ONE USA, Under Review,* (2013).

4.1 Introduction

Preterm labor affects one in eight pregnancies in the United States, leads to preterm delivery in over 50% of cases and this inexplicable tragedy (Buxton, Crow et al. 2000; Buxton 2004) in which 20,000 fetuses die annually disproportionally affects African American mothers (Behrman and Butler 2007). Over half of cases of preterm labor are spontaneous and unexplained. The problem is global and intolerable for civil society to bare (Kinney, Howsen et al. 2012). The molecular mechanisms involved in the induction of labor are incompletely known and therefore understanding preterm labor is largely without a mechanistic context. Human uterine smooth muscle (HUSM) has been previously shown to relax in a manner disparate from other smooth muscle tissues. Nitric oxide (NO) relaxes HUSM in a dose-dependent, cyclic guanosine 3'-5'-monophosphate (cGMP)-independent manner (Figure 4.1) suggesting that the mechanistic explanation for the actions of NO in myometrium will reveal new therapeutic targets to prevent preterm labor (Buxton, Kaiser et al. 2001).

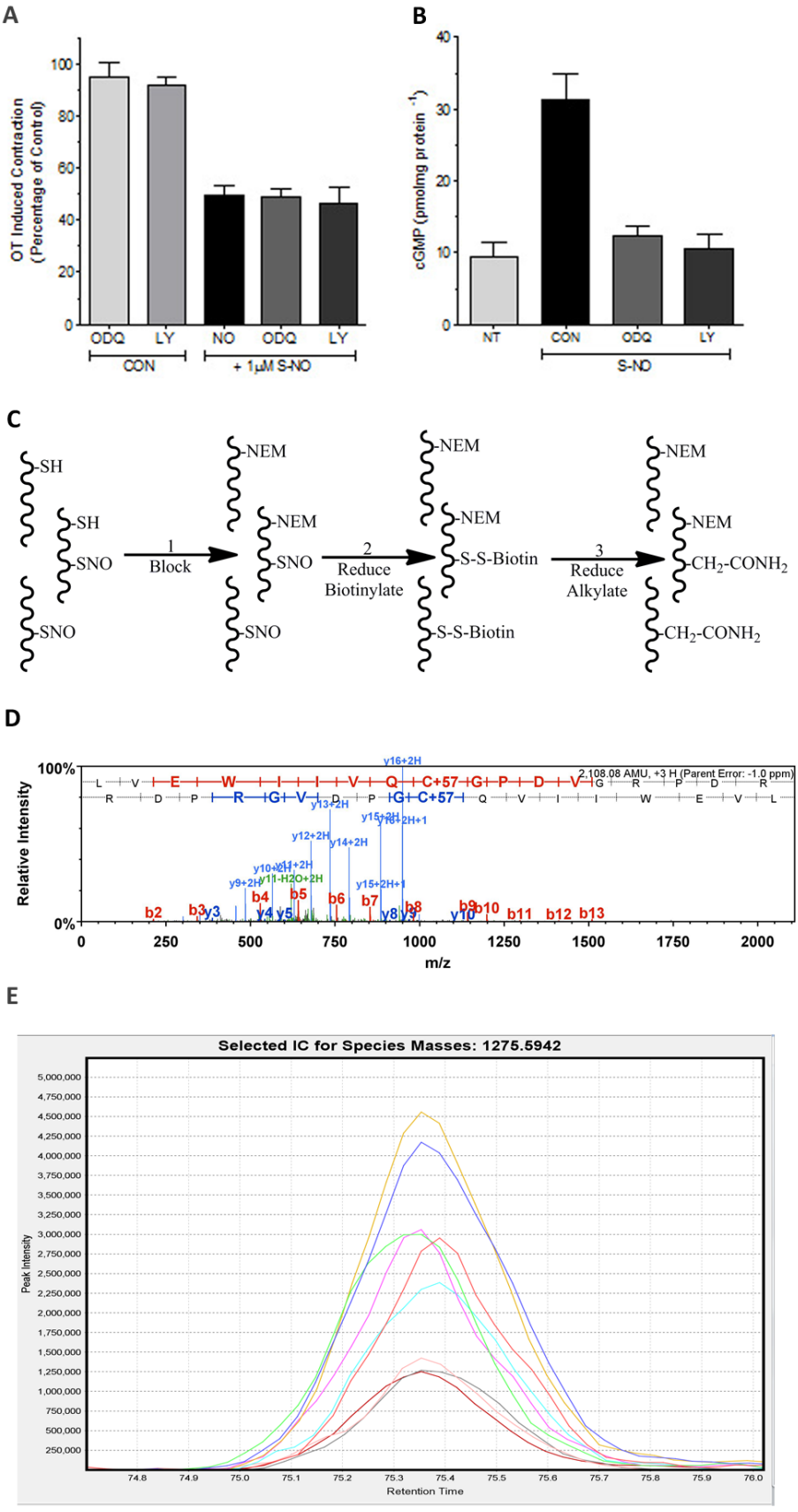
A
OT Induced Contraction (Percentage of Control)
ODQ
LY
NO
ODQ
LY
CON
+ 1μM S-NO
B
cGMP (pmol/mg protein -1)
NT
CON
ODQ
LY
S-NO
C
SH
SH
SNO
SNO
1
Block
NEM
NEM
SNO
SNO
2
Reduce
Biotinylate
NEM
NEM
S-S-Biotin
S-S-Biotin
3
Reduce
Alkylate
NEM
NEM
CH2-CONH2
CH2-CONH2
D
Relative Intensity
m/z
2,108.08 AMU, +3 H (Parent Error: -1.0 ppm)
E
Selected IC for Species Masses: 1275.5942
Peak Intensity
Retention Time

Figure 4.1: S-NO-mediated relaxation of agonist-induced contraction of pregnant myometrium is cGMP-independent. (A) Strips of near-term pregnant non-laboring myometrium from consenting women at the time of caesarean section were hung in organ baths and tension recorded as described [5]. Addition of oxytocin (1 μM) produced contraction (2.4 ± 0.76 g/mm^3, n=8) that was relaxed by cysteine-NO (Cys-NO; IC_{50} = 1 μM). Addition of the guanylyl cyclase inhibitor LY-83583 (10 μM) had no effect on OT-induced contractions (CON). In the presence of guanylyl cyclase inhibitors 1 μM ODQ or LY-83583 (10 μM), relaxations to Cys-NO were unaffected. Data are mean ± SEM, n = 6-8; All SNO treatments were significantly different ($p<0.001$). **(B)** OT-stimulated tissues were snap frozen under tension and basal cGMP content (9 ± 2.1 pmol mg protein^{-1}) determined by ELISA [5]. Cys-NO stimulation (30 μM) led to a significant elevation in cGMP (CON; 31.3 ± 3.6 pmol mg protein^{-1}) that was reduced to the leves of non-treated tissues (NT) by prior treatment of tissues with GC inhibitors ODQ (1 μM) or LY-83583 (10 μM). Data are mean ± SEM, n = 6. **(C)** A modified biotin-switch**;** (Step 1) NEM is used in place of MMTS to block free non-nitrosated thiols; (Step 2) S-nitrosated thiols are selectively reduced using ascorbate, labeled with a thiol reactive biotin tag, and purified using streptavidin resin. (Step 3) Biotin labeled thiols are reduced and alkylated to allow for identification of S-NO sites. **(D)** Representative MS/MS spectra of a carbamidomethyl labeled S-NO peptide from transgelin. Note the 57 Da shift on the identified cysteine which is indicative of carbamidomethylation. **(E)** Representative extracted ion chromatogram of a single peptide quantitated in all 9 replicates. Each line is indicative of an individual sample.

NO may signal as an endogenous tocolytic, but there is as yet no certainty that NO is present as an endogenous myometrial relaxing factor in women. What is clear is that NO relaxes human myometrium at concentrations (Buxton, Kaiser et al. 2001) that could be present locally from uterine arterial endothelium or released from placental syncytiotrophoblasts (Valdes and Corthorn 2011) or macrophages (Yellon, Mackler et al. 2003; Shynlova, Nedd-Roderique et al. 2012). Moreover, Suzuki *et al.* have recently suggested that NO is generated in rat uterus (Suzuki, Mori et al. 2009). The fact that NO signals non-classically in the uterus and that it may selectively and disparately *S*-nitrosate proteins associated with pregnancy outcomes is compelling. If certain proteins enjoy a pregnancy-state specific degree of S-nitrosation that is independent of the expression level for that protein, then we may learn more about both the function of S-nitrosated proteins and the basic regulation of uterine relaxation. Such S-nitrosated proteins may reveal themselves or their interactions with other proteins as "druggable". The importance of the fact that an effect of NO to relax the uterus is independent of global cGMP accumulation means that there is hope for discovery of therapeutic targets in the myometrium that are absent or disparately regulated in other smooth muscles and thus, can permit a reasoned line of investigation to find uterine-specific tocolytics.

The need for new therapeutic approaches to manage preterm labor and prevent preterm delivery cannot be overstated. There is no FDA-approved drug available for the treatment of preterm labor and current approaches are clearly inadequate. Treatments used, such as β_2-adrenergic agonists and calcium channel blockers, are borrowed from other suggested pharmacological use. If we are to improve outcomes for mothers and

their babies, and reduce the financial burden on societies, it is imperative that we focus on myometrial pharmacology already known to be unique (Buxton 2004).

We have demonstrated that NO-induced relaxation of HUSM is the result of a pathway independent of the canonical cGMP-induced relaxation pathway. This is an important signaling exception that offers an opportunity in the search for treatment of spontaneous preterm labor. We propose that myometrial NO-mediated relaxation is dependent on S-nitrosation of specific and critical proteins involved in the relaxation of HUSM. We further hypothesize that these critical proteins are S-nitrosated disparately in pregnant laboring and preterm laboring HUSM when compared to non-laboring HUSM. S-nitrosation is a mechanistically important, NO-dependent, post translational modification that can alter smooth muscle relaxation/contraction dynamics (Dalle-Donne, Milzani et al. 2000).

There has been some debate about the correct nomenclature for this reaction with many groups employing the term S-nitrosylation in place of S-nitrosation. Smith and Marletta make a convincing argument that the nitroso group, not the nitrosyl group, is transferred during protein nitrosation reactions (Smith and Marletta 2012). We therefore have adopted this nomenclature to describe the conversion of a thiol to a nitrosothiol. S-nitrosation has been shown to alter the function of many proteins including the activity of several enzymes (Hess, Matsumoto et al. 2005) and our previous work has shown disparate levels of S-nitrosation in guinea pig pregnancy (Ulrich, Quillici et al. 2012). Based on the striking cGMP-independence of NO-mediated HUSM relaxation and prior research establishing that S-nitrosation is an established source of NO bioactivity, we propose that NO-mediated relaxation in HUSM is the result of protein-specific S-

nitrosation. Moreover, whether or not it is NO that acts endogenously to mediate uterine quiescence during gestation, it is reasonable to determine the pregnancy state relaxation associated S-nitrosation of proteins in myometrium on the basis that such efforts could identify targets mechanistically associated with uterine quiescence and thus can be useful in the effort to prevent preterm delivery. Here we present proteins that can be S-nitrosated by S-nitrosoglutathione (GSNO) as candidates as belonging to contractile and inflammatory signaling pathways that can be examined in a hypothesis-directed fashion to find new therapeutic targets in the search for effective tocolytics.

4.2 Results and Discussion

4.2.1 The S-nitrosoproteome in disparate states of human pregnancy

With samples obtained under informed consent, we compared GSNO-mediated S-nitrosation in spontaneously laboring term (12 patients ranging from 37-41 weeks) and spontaneously laboring preterm myometrium (12 patients ranging from 29-36 weeks) to the non-laboring state of term pregnancy myometrium (12 patients ranging from 37-41 weeks) in women. By combining the biotin switch technique (Jaffrey and Snyder 2001), streptavidin purification, and high accuracy LC/MS/MS analysis, we unambiguously identified 110 HUSM proteins that can be S-nitrosated in one or more conditions of pregnancy (Table S4.1). The use of a differential blocking and labeling technique (Figure 4.1C) allowed us to identify the modified cysteine(s) that are either S-nitrosated or reversibly oxidized on 118 peptides corresponding to 56 of the identified proteins (Table S4.2). All known disulfide forming cysteines were removed from this list and we provide it as a supplementary guide to help identify those cysteines that are modified under the NO signaling conditions applied. Additionally, expression levels of 62 of the

110 proteins were quantified using normalized spectral counts and area-under-the-curve measures of extracted ion chromatograms (AUC). We employed both quantification measures because spectral counting while using dynamic exclusion limits the quantitative capability to a relative measurement between states and we wanted to verify that the number of MS2 events per peptide were indicative of the amount of peptide which was measured by AUC of the MS1 chromatograms. A simple ANOVA demonstrated that 26 of these proteins exhibited statistically significant differences across the three conditions, specified by an F-statistic p-value of $p<.05$. These proteins had $\log_2$ fold changes of at least ± 1 in preterm laboring patients compared to non-laboring patients (Figure 4.2).

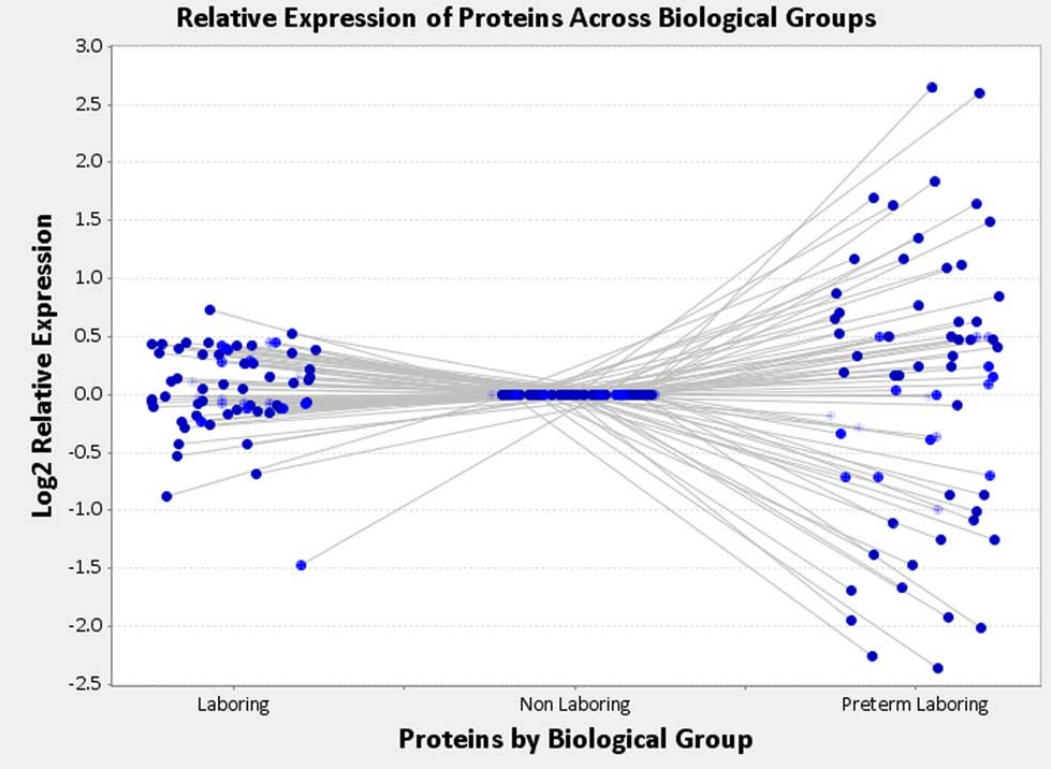

Figure 4.2: Relative expression profile of the human uterine smooth muscle S-nitrosoproteome in disparate states of pregnancy. Dots are representative of individual S-nitrosated proteins present in all three states of pregnancy. Non-laboring was designated as the baseline state and laboring and preterm laboring conditions are compared by Log_2 relative expression of area under the curve of extracted ion chromatograms.

The ability to S-nitrosate proteins in pregnant myometrium might reasonably be suggested to rely principally on the abundance of any particular protein and the availability of a free cysteine thiol. To verify that changes at the total protein level were not responsible for these results, we semi-quantitatively measured by spectral counting the relative changes of the total proteome in each condition of pregnancy using 2-D LC/MS/MS analysis. Our study showed clearly that changes in S-nitrosation were independent of changes in total protein levels among proteins identified. Thus, the difference in S-nitrosation levels of a given protein in one pregnancy state versus another is a consequence of the state of pregnancy and not the apparent availability of NO or the level of protein thiol substrate. Other putative distinctions that would permit increased or decreased S-nitrosation of a given protein in one or more states of pregnancy is not known, but may result in differences in the function of that protein. Such differences in myometrium from patients in labor preterm may be associated mechanistically with early labor.

4.2.2 Up-regulation of S-nitrosation in PTL

Examination of our findings using Ingenuity Pathway Analysis™ (IPA, Ingenuity Systems, Redwood City, CA) shows that several of the S-nitrosated proteins that are up S-nitrosated fit into functionally interesting protein groupings that are disparately regulated at the post-translational level. Interestingly, the pathway involving actin cytoskeleton dynamics (Figure 4.3) shows a statistically significant increase in S-nitrosation of several key regulatory proteins including calponin-1 (CNN1), profilin-1 (PFN1), myosin regulatory light polypeptide 9 (MYL9), myosin light polypeptide 6 (MYL6), thioredoxin (THIO), and transgelin (TAGLN).

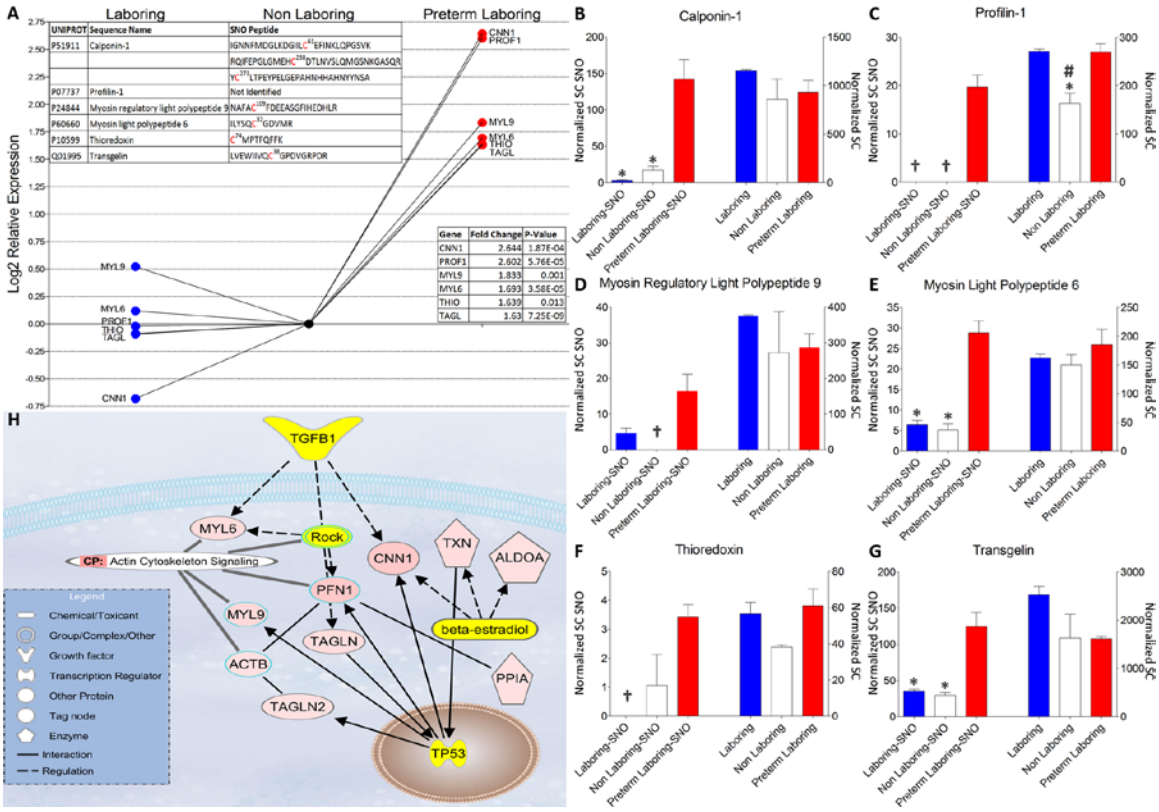

Figure 4.3: Proteins of interest that show a statistically significant increase in S-nitrosation during preterm labor. (A) Log_2 relative expression of the area under the curve of extracted ion chromatograms. Upper inset contains identification of protein as well as any S-nitrosated peptides that were identified by LC/MS/MS. Lower inset contains gene identification, log_2 fold change, and p-value for identified proteins. **(B-G)** Relative expression of normalized spectral counts of S-nitrosated protein levels (left three bars of each graph) and total protein levels (right three bars of each graph) from experiment matched samples. * signify $p<0.05$ when comparing NL and or L to PTL, # signify $p < 0.05$ when comparing NL to L and PTL, † signify no spectral counts were observed. **(H)** Ingenuity Pathway Analysis of statistically significant increased S-nitrosated proteins (red) as well as their nearest connecting neighbors (yellow).

The role of S-nitrosation in regulating these proteins is not completely understood particularly in the context of an interactome in pregnant myometrium. Each of these proteins has been shown to play a role in regulating smooth muscle contraction or nitric oxide signaling. *In vitro* S-nitrosation of skeletal muscle myosin, for example, increases the force of the acto-myosin interaction while decreasing its velocity indicative of the relaxed state (Evangelista, Rao et al. 2010). The calcium binding protein CNN1 has been shown to participate in regulating smooth muscle contraction by binding actin and inhibiting the actin-myosin interaction (Carmichael, Winder et al. 1994; Winder, Allen et al. 1998). This tonic inhibition the ATPase activity of myosin in smooth muscle is blocked by Ca^{2+}-calmodulin which inhibits CNN1-actin binding (Mezgueldi, Mendre et al. 1995). PFN1 is essential in signaling cascades that modulate smooth muscle contraction through regulation of actin polymerization rather than MYL9 phosphorylation (Tang 2008). Transgelin (also designated SM22α and p27) is a 22-kDA smooth muscle protein that physically associates with cytoskeletal actin filament bundles in contractile smooth muscle cells. Studies in transgelin knockout mice have demonstrated a pivotal role for transgelin in the regulation of Ca^{2+}-independent contractility (Je and Sohn 2007). Transgelin has also been implicated in induction of actin polymerization and/or stabilization of F-actin and is proposed to be necessary for actin polymerization and bundling (Han, Dong et al. 2009). Considered together, these proteins constitute a potential interactome and discovering their behavior as S-nitrosated proteins may further our understanding of contraction-relaxation signaling in myometrium.

4.2.3 Down-regulation of S-nitrosation in PTL

We unambiguously identified 14 proteins that showed a statistically significant decrease in S-nitrosation in PTL samples exposed to S-nitrosation by GSNO. Area under the curve measures of extracted ion chromatograms and spectral counting showed that these proteins differ significantly in the preterm state of labor (Figure 4, A-N). IPA identified nearest neighbor interactions with tumor necrosis factor (TNF), progesterone, and nitric oxide for 12 of these proteins and reveals an over representation of proteins involved in integrin signaling and cell morphology (Figure 4, O).

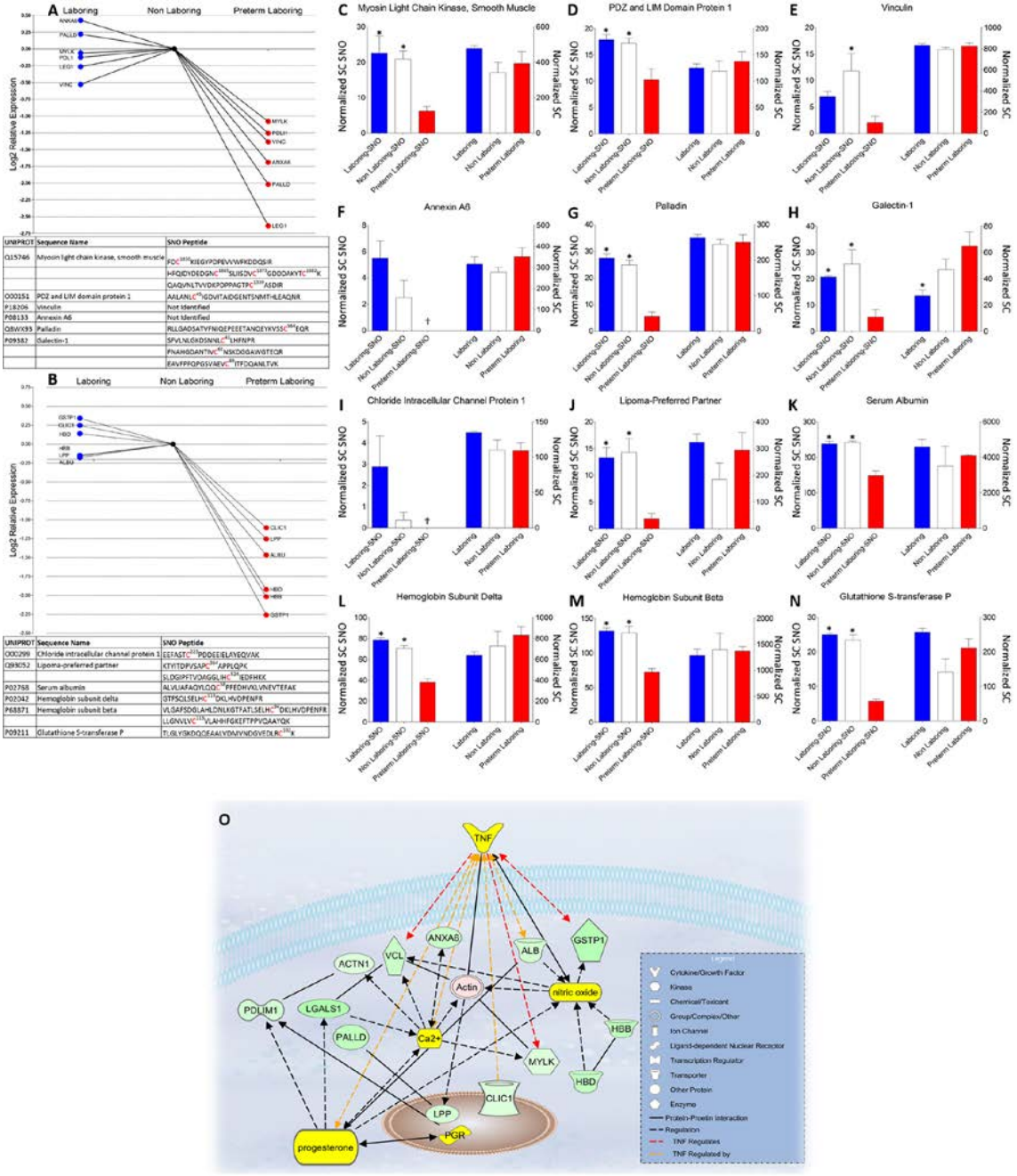

UNIPROT	Sequence Name	SNO Peptide
O15746	Myosin light chain kinase, smooth muscle	FDC[1435]KIEGYPDPEVVVNFKDDQSIR
		HFQICYDEDGNC[1693]SLISDVC[1870]GDDDAMYTC[1882]K
		QAQVNLTVVDEKDPPAGTPC[1933]ASDIR
O00151	PDZ and LIM domain protein 1	AALANLC[45]GDVITAIDGENTSNMTHLEAQNR
P18206	Vinculin	Not Identified
P08133	Annexin A6	Not Identified
Q8WX93	Palladin	RLLGADSATVFNIGEPEEETANQEYKVSSC[394]EQR
P09382	Galectin-1	SFVLNLGKDSNNLC[16]LHFNPR
		FNAHGDANTIVC[88]NSKDGAWGTEQR
		EAVFPFQPGSVAEVC[115]ITFDQANLTVK

UNIPROT	Sequence Name	SNO Peptide
O00299	Chloride intracellular channel protein 1	EEFASTC[35]PDQEEIELAYEQVAK
Q92052	Lipoma-preferred partner	KTYITDPVSAPC[394]APPLQPK
		SLDGIPFTVDAGGLIHC[150]EDFHKK
P02768	Serum albumin	ALVLIAFAQYLQQC[179]PFEDHVKLVNEVTEFAK
P02042	Hemoglobin subunit delta	STFPCLSELHC[111]DKLHVDPENFR
P68871	Hemoglobin subunit beta	VLSAFSDGLAHLDNLKGTFATLSELHC[88]DKLHVDPENFR
		LLGNVLVC[115]VLAHHFGKEFTPPVQAAYQK
P09211	Glutathione S-transferase P	TLGLYSKDQQFEAALVDMVNDGVEDLRC[35]K

Figure 4.4: Proteins involved in smooth muscle contraction showing a significant decrease in S-nitrosation during preterm labor. (A,B) Log_2 relative expression of the AUC of extracted ion chromatograms. Lower inset: identification of protein as well as any S-nitrosated peptides that were identified by LC/MS/MS. **(C-N)** Relative expression of normalized spectral counts of S-nitrosated protein levels (left three bars of each graph) and total protein levels (right three bars of each graph) from experiment matched samples. * signify $p<0.05$ when comparing NL and or L to PTL, † signify no spectral counts were observed. **(O)** Ingenuity Pathway Analysis of statistically significant decrease in S-nitrosated proteins (green) as well as their nearest connecting neighbors (yellow).

Of particular interest is the disparate regulation of myosin light chain kinase (MYLK) which is a key regulator of the acto-myosin interaction and therefore smooth muscle contraction/relaxation dynamics (Okagaki, Hayakawa et al. 1999). Disparate regulation of both MYLK and its smooth muscle target MYL9, the regulatory light chain, argues for a mechanistic role of S-nitrosation in the premature induction of labor.

That specific protein S-nitrosations are decreased in pregnancy myometrium when not the result of decreases in protein expression is unexpected and underscores the likelihood that our data offer a window into the unique nature of preterm myometrium.

While there are contrasting data on whether or not NO synthases are present in myometrial smooth muscle cells, they need not be present in the cell for NO availability during gestation. In PTL we show down regulation of S-nitrosation in 3 of the known transporters of NO: serum albumin (ALB) known to be available to tissues by paracellular transport from blood (Schnitzer and Oh 1994), hemoglobin subunit β (HBB), and hemoglobin subunit δ (HBD) proteins likely derived from macrophages that are included in the micro-dissected muscle strips derived from myometrial biopsies (Ivanisevic, Segerer et al. 2010). In conjunction with decreased S-nitrosation of glutathione S-transferase P (GSTP1), which has been shown to mediate NO storage and transport in cells (Lok, Suryo Rahmanto et al. 2012), this creates a convincing argument for an alteration in the NO transport, storage, and signaling pathways leading to a decreased availability for the relaxing effects of NO in PTL.

Cytoskeletal and thin-filament regulation play a critical role in contraction/relaxation dynamics in smooth muscle tissues. Here we showed that multiple proteins involved in regulation of cytoskeletal dynamics and thin-filament regulation are differentially S-

nitrosated in PTL patients. Vinculin (VCL) and α-actinin (ACTN1), both implicated in the physical coupling of actin filaments to β-integrins and hence involved in providing a direct mechanical coupling between integrin proteins and the actin cytoskeleton (Opazo, Zhang et al. 2004), showed decreased S-nitrosation in preterm samples. VCL has also been shown to be recruited to the cell membrane during contractile stimulation and inhibition of this recruitment inhibits force development (Opazo, Zhang et al. 2004). Galectin-1 (LEG1), also known as LGALS1, is notably down S-nitrosated in preterm laboring tissues when compared to non-laboring tissues. LEG1 has been shown to interact with VCL at focal adhesions, and expression of LEG1 mRNA is up-regulated by progesterone and down-regulated by estrogen in uterine tissue (Choe, Shim et al. 1997) consistent with myometrial quiescence.

Chloride intracellular channel protein 1 (CLIC1), that can insert into intracellular membranes and form chloride ion channels, is a homologue of the glutathione S-transferase superfamily that is redox regulated (Littler, Harrop et al. 2004) and has been shown to be strongly and reversibly inhibited by cytosolic F-actin (Singh, Cousin et al. 2007). Both redox regulation as well as cytoskeletal interaction argue for a possible functional role during disparate states of redox controlled S-nitrosation of CLIC1. A definitive functional role for CLIC1 has not been determined in pregnancy but our data argue for a plausible functional role in redox regulation during disparate states of pregnancy since CLC1 is down S-nitrosated in preterm labor.

Lipoma preferred partner (LPP) is a nucleocytoplasmic shuttling protein located in focal adhesions and associates with the actin cytoskeleton (Petit, Fradelizi et al. 2000). LPP can function as an adaptor protein that constitutes a platform that orchestrates

protein-protein interactions. LPP was seen to be down S-nitrosated in preterm laboring tissue and has been shown to play an important role in the motility of smooth muscle cells (Gorenne, Nakamoto et al. 2003). LPP is a mechano-sensitive protein that is down-regulated by stretch and apparently up-regulated by blockade of nitric oxide synthase (Hooper, Dash et al. 2012). This dependency argues for an important role in the mechano-regulation of the continuously expanding myometrium in human pregnancy and could be further examined as a target biomarker for PTL. Considered together, these proteins constitute a potential interactome and discovering their behavior as S-nitrosated proteins may further our understanding of contraction-relaxation signaling in myometrium.

4.3 Conclusion

The induction of labor in humans is a complex problem that will require multiple approaches to understand how to control and manipulate the process. There are no such approaches at present as evidenced by the lack of FDA approved tocolytics available for PTL. What obstetricians provide now in the US is off label and ineffective. The standard approach to the problem of PTL has been to adopt what has been established for the treatment of other medical conditions involving smooth muscle and apply it to women in labor too soon (Buxton 2004). In order to generate an opportunity to approach the problem of preterm labor that is unique to myometrial biochemistry, we provide here an NO-mediated “fingerprint” of post-translationally modified proteins integral to relaxation mechanisms that will allow directed research regarding the regulation of quiescence of the uterus during gestation. The identification of S-nitrosated proteins in the myometrium provides a platform from which to explore new and improved hypotheses for future

research by establishing a unique snapshot of how NO modifications are disparately changing in the PTL state. The aberrant PTL S-nitrosoproteome fingerprint visualized in Figure 4.2 provides us with multiple novel targets and putative biomarkers to help elucidate the disparate mechanisms involved in the premature induction of labor. Of particular interest is the disparity in S-nitrosation of the key known regulators of smooth muscle contraction in PTL samples, such as MYLK, MYL9 and PFN1. The functional role of this disparity has yet to be elucidated but we show convincing evidence that these proteins are regulated very differently by NO at the protein level independent of protein abundance. While much work is yet to be done, we believe that the research presented here will open new opportunities for study and directly addresses public policy and advocacy statements such as those of the American Public Health Association[1], the World Health Organization and March of Dimes as well as eventually lowering the burden on society as illustrated by the Institute of Medicine[2].

4.4 Materials and Methods

Chemicals-Sodium ascorbate, N-2-Hydroxyethylpiperazine-N'-2-ethanesulfonic acid (HEPES), neocuproine, N-ethylmaleimide (NEM), methyl methanethiosulfonate (MMTS), 3-(3-cholamidopropyl)dimethylammonio-1-propanesulfonate (CHAPS), sodium dodecyl sulfate (SDS), and all other chemicals unless specified, were obtained from Sigma (St Louis, MO). N-[6-(biotinamido)hexyl]-3'-(2'-pyridyldithio) propionamide (biotin-HPDP) was from Thermo Scientific (Rockford, IL).

[1] Reducing Racial/Ethnic and Socioeconomic Disparities in Preterm and Low Birthweight Births, Policy Date 11/08/2006 #20062.

[2] Institute of Medicine (US) Committee on Understanding Premature Birth and Assuring Healthy Outcomes; Behrman RE, Butler AS, editors. Preterm Birth: Causes, Consequences, and Prevention. Washington (DC): National Academies Press (US); 2007. 14, Public Policies Affected by Preterm Birth. Available from: http://www.ncbi.nlm.nih.gov/books/NBK11365/

Tissue Collection-All research was reviewed and approved by the University of Nevada Biomedical Review Committee (IRB) for the Protection of Human Subjects. Human uterine myometrial biopsies were obtained with written informed consent from mothers undergoing elective Cesarean section in preterm labor without infection or rupture of membranes, at term in labor or at term not in labor. Tissues were transported to the laboratory immediately in cold physiological buffer, microdissected under magnification to isolate smooth muscle, snap frozen in liquid nitrogen, and stored at -80^{o}C. The average age for patients in the pregnant laboring group was 28.9 ± 5.6 years, in the non-laboring group 28 ± 5.1 years, and in the preterm laboring group 30.8 ± 10.2 years. Pregnant laboring and non-laboring patients ranged from 37-41 weeks gestation, with the mean at 39 weeks for both laboring and non-laboring groups. Preterm laboring patients ranged from 29.2-36 weeks gestation, with the mean being 33.5 weeks. Patients represented a range of ethnicities and were 52% Caucasian, 30% Hispanic, 7.4% African American, and 11% other.

Protein Isolation-To isolate total protein, myometrial muscle samples from 12 patients in each pregnancy state were ground to a powder under liquid nitrogen and reconstituted in 20 ml HEN buffer (25 mM HEPES-NaOH, 1 mM EDTA, 0.1 mM neocuproine, pH 7.7). Samples were sonicated (10 X 2 sec bursts, 70% duty cycle) and brought to 0.4% CHAPS. Samples were then centrifuged at 2000 x g for 10 min at 4°C. Protein concentration was determined by the bicinchoninic acid (BCA) assay and samples diluted to 0.8 mg/ml in HEN buffer.

Biotin Switch and Streptavidin Pull-down- Each patient in all groups was independently isolated by biotin switch and streptavidin pulldown and then pooled for MS/MS analysis

(ie PTL1 4 pateints, PTL2 4 patients, PTL3 4 patients). Protein isolates (1.8 ml 0.8 mg/ml in HEN buffer) were incubated with 300 µM GSNO (1,746 µl of sample + 54 µl of 10 mM GSNO prepared in the dark) for 20 min at room temperature. At this concentration, GSNO will produce ~5 µM reactive NO over 15-20 min without accumulation (Cleeter, Cooper et al. 1994). Non cysteinyl nitrosation events would not be appreciated due to the reactive chemistry of ascorbate reduction; a nucleophilic attack at the nitroso-nitrogen atom leading to thiol and *O*-nitrosoascorbate (reaction 1)

$$RSNO + ASC^- \rightarrow RSH + NOASC^-$$

which breaks down, by various competitive pathways, the dominant of which at physiological pH yielding dehydroascorbic acid and nitroxyl radical which decomposes at physiological pH to nitrous oxide (Kirsch, Buscher et al. 2009) (reaction 2).

$$NOASC^- + H^+ \rightarrow DHA + HNO$$

$$2HNO \rightarrow HON=NOH$$

$$HON=NOH \rightarrow N_20 + H_2O$$

Neither biotin-HPDP nor a maleimide dye would lead to false positives because the amines or tyrosines would not be labeled even if they were nitrosated. SDS (0.2 ml of 25% SDS in water) was added along with 20 µl of 3 M NEM (final 2.0 ml at 2.5% SDS and 30 mM NEM). Samples were incubated at 50°C in the dark for 15 min with frequent vortexing. Three volumes of cold acetone (6 ml) were added to each sample. Proteins were precipitated for 1 hr at −20 °C and collected by centrifugation at 3,000 x g for 10 min. The clear supernatant was aspirated and the protein pellet gently washed with 70% acetone (4×5 ml). After resuspension in 0.24 ml HEN buffer with 1% SDS (HENS), the material was transferred to a fresh 1.7-ml microfuge tube containing 30 µl biotin–HPDP

(2.5 mg/ml). The labeling reaction was initiated by adding 30 µl of 200 mM sodium ascorbate (final 20 mM ascorbate). Four volumes of -20°C acetone was added to the labeled samples and incubated at -20°C for 20 min to remove biotin-HPDP. The samples were centrifuged at 3,000 x g for 10 min at 4°C and the supernatant discarded. The sides of the tube and the pellet were washed with -20° C acetone to remove traces of biotin-HPDP. The pellet was resuspended in 140 µl of HENS buffer. Neutralization buffer (20 mM Hepes, pH 7.7, 100 mM NaCl, 1 mM EDTA, 0.5% Triton X-100) was added (280 µl) along with 42 µl of streptavidin-agarose. Proteins were incubated for 1 hr at room temperature, washed five times with 1.5 ml of neutralization buffer with 600 mM NaCl. Beads were incubated with 100 µl elution buffer (neutralization buffer with 600 mM NaCl plus 100 mM beta-mercaptoethanol) to recover the bound proteins. This step releases the protein from the streptavidin bead leaving the biotin-HPDP tag bound to the bead as well as natively biotinylated proteins still bound to the bead. Four volumes of -20° C acetone were added and samples incubated for 1 hr at -20°C to re-precipitate proteins. Samples were centrifuged at 3000 x g. for 10 min at 4°C, the and supernatant discarded and the pellet washed and dried ready for proteomic analysis.

Protein Digestion and Mass Spectrometry-Nevada Proteomics Center analyzed selected proteins by trypsin digestion and LC/MS/MS analysis. Acetone precipitated pellets were washed twice with 25 mM ammonium bicarbonate (ABC) and 100% acetonitrile, reduced and alkylated using 10 mM dithiothreitol and 100 mM iodoacetamide and incubated with 75 ng sequencing grade modified porcine trypsin (Promega, Fitchburg WI) in 25 mM ABC overnight at 37°C. Peptides were first separated by Michrom Paradigm Multi-Dimensional Liquid Chromatography (MDLC) instrument (Magic C_{18}AQ 3µ 200Å (0.2 x

50 mm) column, (Michrom Bioresources Inc., Auburn, CA) with an Agilent ZORBAX 300SB-C_{18} 5µ (5 x 0.3 mm) trap (Agilent Technologies, Santa Clara, CA)). The gradient employed 0.1% formic acid in water (Pump A) and 0.1% formic acid in Acetonitrile (Pump B) as follows (Time (min), Flow (µl/min), Pump B(%): (0.00, 4.00, 5.00), (5.00, 4.00, 5.00), (95.00, 4.00, 45.00), (95.10, 4.00, 80.00), (96.10, 4.00, 80.00), (96.20, 4.00, 5.00). Eluted peptides were analyzed using a Thermo Finnigan LTQ-Orbitrap using Xcalibur v 2.0.7. MS spectra (*m*/*z* 300–2000) were acquired in the positive ion mode with resolution of 60,000 in profile mode. The top 4 data-dependent signals were analyzed by MS/MS with CID activation, minimum signal of 50,000, isolation width of 3.0, and normalized collision energy of 35.0. The reject mass list included: 323.2040, 356.0690, 371.1010, 372.1000, 373.0980, 445.1200, 523.2840, 536.1650, 571.5509, 572.5680, 575.5494, 677.6090, 737.7063, 747.3510, 761.7316, 763.8791, 767.0623, 824.4870, 832.1884, 930.1760, 1106.0552, 1106.0564, 1142.0940, 1150.0927. Dynamic exclusion settings were used with a repeat count of 2, repeat duration of 10 seconds, exclusion list size of 500 and exclusion duration of 30 seconds.

Database Searching-Tandem mass spectra were extracted; charge state deconvolution and deisotoping were not performed. All MS/MS samples were analyzed using Sequest (Thermo Fisher Scientific, San Jose, CA, version v.27, rev. 11). Sequest was set up to search database containing ipi.HUMAN.v3.87, the Global Proteome Machine cRAP v.2012.01.01, and random decoy sequences (183158 entries) assuming the digestion enzyme trypsin. Sequest was searched with a fragment ion mass tolerance of 1.00 Da and a parent ion tolerance of 10 ppm. Oxidation of methionine, iodoacetamide derivative of cysteine, and n-ethylmaleimide on cysteine were specified in Sequest as variable

modifications. The labels introduced in the Biotin Switch are removed when the disulfide linking Biotin-HPDP to the protein is cleaved after addition of beta-mercaptoethanol and is therefore not considered during database searching.

Criteria for Protein Identification-PROTEOIQ (V2.6, www.nusep.com) was used to validate MS/MS based peptide and protein identifications. Peptides were parsed before analysis with a minimum Xcorr value of 1.5 and a minimum length of 6 amino acids. There were no matches to the concatenated decoy database and therefore a false discovery value is not applicable. Peptide identifications were accepted if they could be established at greater than 95.0% probability as specified by the Peptide Prophet algorithm (Keller, Nesvizhskii et al. 2002). Protein identifications were accepted if they could be established at greater than 95.0% probability and contained at least 2 identified peptides with 5 spectra per peptide. Protein probabilities were assigned by the Protein Prophet algorithm (Nesvizhskii, Keller et al. 2003). Proteins that contained similar peptides and could not be differentiated based on MS/MS analysis alone were grouped to satisfy the principles of parsimony.

Controls-Stringent controls were performed in order to avoid false positive identification of non S-nitrosated cysteines that could have been mislabeled during the experimental procedures. These controls are standard when performing the biotin switch procedure and include removal of GSNO and/or ascorbate during the biotin switch. A small number of proteins were shown to be constitutively S-nitrosated and were labeled without the addition of GSNO, this is a common and expected result. Removal of ascorbate during the biotin switch removed any signal that was seen when ascorbate was present. Streptavidin purification of biotin switched proteins removes any signal from

naturally biotinylated proteins and these are therefore not present in our analysis. Streptavidin purification and LC/MS/MS analysis of ascorbate negative samples were shown to only contain the contaminating keratin proteins, trypsin and traces of serum albumin. Therefore, our ascorbate positive sample identification contains almost no non-specific binding proteins

Data Analysis-AUC data was analyzed using the in program statistical package provided with ProteoIQ. Spectral counting data was extracted from ProteoIQ and analyzed using GraphPad Prism version 5.00 for Windows, GraphPad Software, San Diego California USA, www.graphpad.com. Significance was set at $p < 0.05$ with NL set as a control baseline to measure changes in PTL and L. Table S4.3 provides statistical values for all quantitated proteins.

CHAPTER 5

CONCLUSION

5.1 Summary of Research and Developed Methods

The realization that NO induced relaxation in the myometrium is independent of guanylyl cyclase activation and cGMP production spawned the need for future research into this unknown mechanism of action of NO. Our approach utilized the recent identification of NO as a major biologically relevant post-translational modifier of specific cysteine residues. The proteins affected by NO modification in the myometrium had not been previously studied and therefore we found it pertinent to identify these proteins in multiple states of pregnancy and labor to determine if disparate regulation was present in the diseased state of PTL.

The biotin-switch assay is notoriously difficult due to the labile nature of the S-NO bond. It is necessary to use gentle extraction buffers and complete the entire assay in the dark to avoid reduction of the S-NO bond and false positive and/or negative results. This assay presented a challenge and took almost an entire year to optimize to work with our reagents and equipment. Through this trial and error process we developed two variations of the biotin switch that would better suit our equipment and experimental design. The first variation was to replace the biotin labeling agent with a maleimide derived fluorescent probe and therefore named the fluorescent switch, this assay was described in Chapter 2. The realization that 2D-NitrosoDIGE could not comprehensively identify and quantitate all labeled proteins due to challenges involved in achieving complete separation led us to pursue a purely mass spectrometry based approach for our human sample experiments. This led us to our second modification of the biotin-switch assay, which was to replace the reversible MMTS blocking agent with the irreversible

blocker NEM. This seemingly minor modification allowed us to differentiate between free thiols and reversibly S-nitrosated/oxidized thiols during MS analysis and therefore provided a list of modified cysteine residues in different states of pregnancy.

There is no legitimate, physiologically relevant, animal model of PTL and sPTB. However, delineating the disparities in the S-nitrosoproteome between the non-pregnant and pregnant state in an animal model directed us as to what protein groups were most likely involved in cellular regulation during pregnancy. We employed the myometrium from guinea pig, the small animal model proposed as the most appropriate for studies of human parturition(Mitchell and Taggart 2009), to study differences in the S-nitrosoproteome between the non-pregnant and pregnant states. This model allowed for identification of S-nitrosoproteins, some of which were novel S-nitrosation targets that hadn't been previously classified in any system. In order to further our knowledge we needed to analyze the disparity in S-nitrosation in PTL and unfortunately the guinea pig model is unable to replicate this diseased state.

PTL is a uniquely human disease and therefore necessitates studying a human population if one wants to identify the physiologically relevant targets involved in the induction of PTL. We were blessed with an amazing tissue collection specialist (Sara Thompson) who was able to acquire a sufficient number of HUSM tissue samples in all applicable states of pregnancy and labor. This allowed us to perform the necessary proteomic experiments, described earlier, to identify the S-nitrosoproteome as well as the total proteome in laboring, non laboring, and preterm laboring patients.

This information provides the first mechanistic proteomic and post-translational modification fingerprint of HUSM in different states of pregnancy. Moreover, we

provide regulatory network analysis to help guide future hypothesis driven research into what role protein and S-nitrosoprotein regulation has in the induction of labor and how the disparity evident in PTL is involved in the early induction of labor.

5.2 Future Research Directions

5.2.1 Future Directions for Biochemical Mechanisms of S-Nitrosation

The combination of global and post-translational proteomics has led to a plethora of future hypothesis driven research projects that aim to delineate the molecular mechanisms that are affected by the disparate regulation of the proteome and/or S-nitrosoproteome. The HUSM proteome and S-nitrosoproteome each have their own unique subset of targets that will be used to direct future research into how these disparities regulate the induction of L and PTL.

One of the future research projects into how the disparity of NO regulation affects PTL will attempt to identify how the S-nitrosation of MYL9 affects myosin-based actin sliding velocities/actin-myosin ATPase activity. Because MYL9 contains a single cysteine, S-nitrosation will reveal cys-109 S-nitrosation. The phosphorylation of MYL9 activates the myosin complex and permits actin/myosin cross-bridge cycling. Our preliminary results have determined that MYL9 is up S-nitrosated in PTL. A change in myosin-based actin sliding velocities/actin-myosin ATPase activity could significantly affect contractile dynamics. S-nitrosation may alter MYL9 phosphorylation or synergize with it.

Smooth muscle contractions require MYL9 phosphorylation and monomeric globular actin (G-actin) must polymerize to form filamentous polymeric actin (F-actin). PROF1 binds G-actin and is up S-nitrosated in PTL. PROF1 binds to G-actin in a 1:1 complex

and facilitates ADP/ATP exchange. We are planning to test the effects of PROF1 S-nitrosation on G-actin:PROF1 binding and F-actin polymerization and stabilization. At high concentrations, PROF1 prevents the polymerization of actin, and enhances it at low concentrations. PROF1 is inactivated when bound to phosphatidylinositol 4,5-bisphosphate (PIP2). By determining if S-nitrosated PROF1 alters the rate of polymerization or the G-actin/F-actin ratio, we will learn how S-nitrosation affects the binding and shuttling capability of PROF1. Both the rate of formation and the concentration of F-actin at equilibrium play an essential role in the cell's ability to contract.

While examining the effect of GSNO on the potassium channel subfamily K member 2 (TREK-1), which is thought to have a role in maintaining uterine quiescence, we determined that this channel is able to be post-translationally S-nitrosated by GSNO (Figure 5.1).

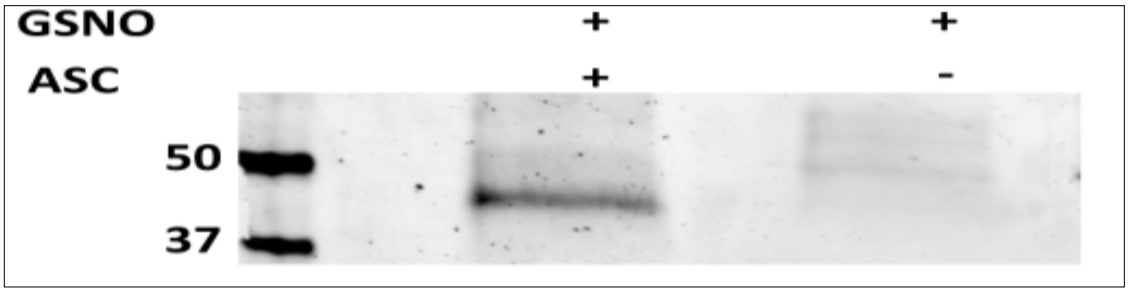

Figure 5.1: **In vitro S-nitrosation of FLAG tagged TREK-1.** Full length human TREK-1 was C-terminally tagged with the FLAG epitope and expressed in HEK 293 cells. Total cell lysates were treated with 100 µM GSNO and subjected to the Fluorescent Switch to label all S-nitrosated cysteines. TREK-1 was immunopurified with anti-FLAG coated agarose and subjected to SDS-PAGE. The negative control, in which ascorbate is absent during the labeling step, shows no TREK-1 labeling.

Thus, future research will determine the possibility that GSNO treatment of native human uterine myocytes alters the TREK-1 current and further define this in cells overexpressing both the wt-TREK-1 as well as co-expression of variant channels. Recently described variants of the TREK-1 channel are expressed in patients that deliver spontaneously preterm. Using the endogenous nitric oxide donor GSNO, we will determine the concentration-effect relationship for putative regulation of TREK-1 by S-nitrosation in both wt-TREK-1 expressing and variant co-expressing HEK cells and we will unambiguously define the fact of TREK-1 S-nitrosation.

Biochemical S-nitrosation of proteins such as TREK-1 whose activation will hyperpolarize membrane potential consistent with relaxation of the muscle would offer a therapeutic target for preventing preterm labor. Moreover, the existence of channel variants in women spontaneously in labor preterm suggests that basal inactivation of stretch-activated channel activity and or failure of an effect of endogenous NO signaling from a cellular compartment such as uterine artery/vascular endothelium/macrophages to activate variant channels may be associated with preterm labor as we propose.

If TREK-1 is S-nitrosated *in vivo* and S-nitrosation effects function, this can drive future research efforts to determine the S-nitrosation site(s) and mechanism of channel regulation. Only one paper on TREK-1 (KCNK2) nitrosation is currently available and suggests concentration dependent activation-inactivation(Koh, Monaghan et al. 2001). Their notion that NO confers cyclic GMP-dependence of activation is particularly interesting though no lab has repeated these results as yet. If the S-nitrosation were on Cys-207, it would be possible to implicate a mechanism of action since Cys-207 sits near the pore domain of TREK-1, or if a Cys at the C-terminal were S-nitrosated, it could

implicate activation-inactivation based on knowledge of the importance of this region (Sandoz, Bell et al. 2011). If both sites were S-nitrosated this could explain concentration dependence of channel regulation and we could determine the associated level of GSNO involved; the relaxation 50% concentration in human myometrium is 1 μM (Buxton, Kaiser et al. 2001).

Each of these projects will expand the knowledgebase of how NO affects the relaxation of myometrium in a way that is disparate from other smooth muscle tissues. Elucidating the biochemical regulation of NO induced relaxation will help lead to protein and pathway targets that can be used as a platform for the design of next-generation pharmaceuticals directed at combating PTL.

5.2.2 Future Directions for HUSM Proteomics

We have shown that both the TNF-α regulated inflammatory pathway and the mTOR-signaling pathway are perturbed in PTL patients. What has yet to be shown is how these perturbations affect the cellular and molecular process that these groups of proteins are involved in. Future work identifying other post-translational modifications, in particular the phosphoproteome, is necessary to understand the global signaling cascades that eventually lead to the induction of labor.

We are currently working on identifying the global HUSM phosphoproteome in different states of pregnancy as well us during specific pharmacological treatments to induce contraction or relaxation. These studies can be paired with the recently developed, iodoacetyl-activated, tandem mass tag technique (Thermo Scientific) to globally quantify the changes in phosphorylation and S-nitrosation in different states of pregnancy as well as during pharmacological treatment. The interaction of these two

important signaling pathways will help to further describe the molecular mechanisms involved during the induction of labor.

Preliminary studies performed on HUSM cells in a stretch-activation assay show that multiple regulatory phosphorylation cascades are initiated when a stretch is imposed and that some of these cascades show disparate regulation in PTL. These studies were directed at known pathways and done with a low-throughput western blot approach. Future work will examine the global phospho/S-nitroso proteomic changes that occur when HUSM cells are stretched to simulate the expanding uterus. We will use a high-throughput mass spectrometry based approach to capture the global changes and compare these to the changes we have identified using the western blot approach. The use of a cell culture model will allow for direct pharmacological manipulation to simulate induction of contractions as well as relaxation. These induced states can then be directly compared to a baseline state to identify the networks and pathways that are modified during stretch and/or pharmacological manipulation.

Our increased knowledge into better protein isolation and identification techniques will allow for a more robust global proteomic profile of HUSM in different states of pregnancy. The identification of changes in post-translational modifications will advance the field of HUSM cell physiology and shed light onto which molecular pathways are critical to the induction of labor.

5.3 Concluding Remarks

The exciting fields of S-nitrosation and quantitative proteomics are expanding rapidly. New technology for the site-specific identification of S-nitrosated cysteine residues continually makes the assessment of the S-nitrosoproteome in any system a

reality. Along this same line, advances in liquid chromatography and mass spectrometry continue to allow us to dig deeper into our proteome of interest as well as specifically quantify a group of peptides of interest. This has great clinical implication as it allows for direct quantification of identified biomarkers that can be associated to a disease.

It was a great pleasure to be allowed to learn these techniques and apply them to our model. Future research utilizing what we have discovered will undoubtedly bring us closer to defining how labor is initiated and what goes wrong in those patients that initiate labor prematurely.

APPENDICES

SECTION I Uterine Smooth Muscle S-Nitrosylproteome in Pregnancy

Table S2.1: The Myometrial Nitrosoproteome

Protein	Biological Process	Previously Identified	NP	P	UniProt	No. of Peptides	% Coverage
(40S ribosomal protein S11)*	Protein binding	Y C131 (PMID: 20585580)	Y	Y	P62280	3	22.8
(40S ribosomal protein S28)*	Protein binding	N	Y	N	P62857	2	33
(4-trimethylamino-butyraldehyde dehydrogenase)*	Metabolism	Y C(74, 173, 443) (PMID: 20585580)	N	Y	P49189	3	8.65
(60 kDa heat shock protein, mitochondrial)*	Protein Folding	Y C(237, 442, 447) (PMID: 20585580)	N	Y	P10809	2	9.95
(60S ribosomal protein L8)*	rRNA binding	N	Y	N	P62917	2	12.7
(6-phosphogluconate dehydrogenase, decarboxylation)*	Metabolism	N	N	Y	P52209	2	11.88
(Actin, alpha skeletal muscle)*	Cytoskeletal	Y (PMID: 10961840)	Y	Y	P68133	4	13.3
(Actin, cytoplasmic 1)*	Cytoskeletal	Y C(217, 272, 285) (PMID: 20585580)	Y	Y	P60709	29	76.13
(ADP-ribosylation factor 4)*	Transport	N	N	Y	P18085	3	36.67
(Aflatoxin B1 aldehyde reductase member 2)*	Metabolism	N	N	Y	O43488	2	10.46
(Alcohol dehydrogenase [NADP+])*	Metabolism	Y (PMID: 19738628)	N	Y	P14550	5	28.62
(Aldehyde dehydrogenase, mitochondrial)*	Metabolism	Y C66 (PMID: 20585580)	N	Y	P05091	2	8.83
(Aldose reductase)*	Metabolism	Y C299 (PMID: 20585580)	N	Y	P15121	3	28.48
(Alpha-2-HS-glycoprotein)*	Endocytosis	N	Y	N	P02765	2	10.61
(Alpha-actinin-1)*†	Cytoskeletal	Y C332 (PMID: 20585580)	N	Y	P12814	4	7.85
(Alpha-aminoadipic semialdehyde dehydrogenase)*	Metabolism	N	N	Y	P49419	2	10.57
(Alpha-enolase)*	Metabolism	Y C(119,357) (PMID: 20585580)	Y	Y	P06733	11	34.79
(Ankyrin-3)*	Cytoskeletal-membrane linker	Y C(1123, 1246, 1369, 2096, 2835, 3395, 3958, 3980, 4233, 4321) (PMID: 20585580)	Y	N	Q12955	2	0.25
(Annexin A1)*	Exocytosis and PLPA2 regulation	N	N	Y	P04083	8	35.84

Protein	Biological Process	Previously Identified	NP	P	UniProt	No. of Peptides	% Coverage
(Annexin A2)*†	Cytoskeletal adapter	Y (PMID: 12199706)	N	Y	P07355	16	53.69
(Annexin A3)*†	Inhibitor of PLPA2	N	N	Y	P12429	5	23.53
(Annexin A4)*	Exocytosis, membrane fusion	N	N	Y	P09525	2	14.33
(Annexin A5)*	Blood coagulation	N	N	Y	P08758	2	11.29
(ATP synthase subunit alpha, mitochondrial)*	Transport	Y (PMID: 20585580)	N	Y	P25705	2	4.73
(Calpain small subunit 1)*	Cytoskeletal remodeling and signal transduction	N	N	Y	P04632	4	34.98
(Calponin-1)*	Smooth muscle contraction. Interaction of calponin with actin inhibits actomyosin Mg-ATPase	N	Y	N	P51911	2	17.67
(Cell division cycle 42 (GTP binding protein, 25kDa))*	Cell division	N	N	Y	Q5JYX0	5	28.8
(Chloride intracellular channel protein 1)*	Ion Transport (redox regulated)	N	N	Y	O00299	2	18.26
(Cofilin-1)*	Cytoskeletal actin binding	N	Y	Y	P23528	6	56.02
(Corticosteroid-binding globulin)*	Transport	N	N	Y	P08185	2	14.07
(Creatine kinase B-type)*	Metabolism	Y (PMID: 18670085)	N	Y	P12277	8	50.66
(Cysteine and glycine-rich protein 1)*	Zinc ion binding	N	Y	Y	P21291	2	27.98
(Cysteine sulfinic acid decarboxylase)*	Metabolism	N	N	Y	Q9Y600	5	16.53
(Cysteine-rich protein 2)*	Zinc ion binding. Interacts with TGFB1I1	N	Y	Y	P52943	7	7.5
(Cytochrome C oxidase subunit 2)†	Electron Transport	Y (PMID: 15561762)	N	Y	P00403	4	19.38
(Desmin)*†	Cytoskeletal	Y C333 (PMID: 20585580)	Y	Y	P17661	18	50.21
(Destrin)*†	Actin de-polymerization	Y (PMID: 18670085)	N	Y	P60981	9	46.06
(dihydropyrimidinase-like 2)*	Hydrolase	N	N	Y	Q86U75	2	11.07
(Dihydropyrimidinase-related protein 2)*	Cell signaling	Y C504 (PMID: 16418269)	Y	N	Q16555	2	3.03
(Elongation factor 1-alpha 1)*	Protein biosynthesis	Y C(3234, 411) (PMID: 20585580)	N	Y	P68104	4	21.54
(Elongation factor 1-gamma)*	Protein biosynthesis	Y C194 (PMID: 20585580)	N	Y	P26641(	2	11.67
(Elongation factor 2)*	Translation elongation	Y C(41, 567) (PMID: 20585580)	Y	Y	P13639(	7	15.02
(Eukaryotic initiation factor 4A-I)*	Protein biosynthesis	N	N	Y	P60842	5	19.6
(Fatty acid-binding protein, epidermal)*	Transport	N	N	Y	Q01469	2	15.56
(Filamin-A)*	Cytoskeletal scaffold actin binding	Y C717 (PMID: 20585580)	Y	Y	P21333	33	19.74

Protein	Biological Process	Previously Identified	NP	P	UniProt	No. of Peptides	% Coverage
(Filamin-C)*	Cytoskeletal actin cross-linker	Y C (805, 1680, 2096, 2660) (PMID: 20585580)	N	Y	Q14315	10	6.93
(Galectin-1)*	Regulation of apoptosis, cell proliferation/differentiation	Y C61 (PMID: 20585580)	N	Y	P09382	5	39.26
(Glutaredoxin-1)*	Transport and thiol reduction	Y (PMID: 17355958)	N	Y	P35754	2	38.68
(Glutathione S-transferase Mu 2)*	Metabolism	Y (PMID: 20585580)	N	Y	P28161	5	23.96
(Glutathione S-transferase Mu 3)*	Metabolism	Y C3 (PMID: 20585580)	N	Y	P21266	2	16.59
(Glutathione S-transferase P)*	Metabolism	Y C(47, 101) (PMID: 11533048)	Y	Y	P09211	8	59.52
(Glyceraldehyde-3-phosphate dehydrogenase)*†	Metabolism	Y C(152, 156, 247) (PMID: 20585580)	N	Y	P04406	12	59.46
(Glycerol-3-phosphate dehydrogenase 1-like protein)*	Regulation of sodium current	N	N	Y	Q8N335	2	10.8
(Guanine nucleotide-binding protein G(i) subunit alpha-2)*	Signal transduction	N	N	Y	P04899	2	9.58
(Heat shock 105kDa/110kDa protein 1)*	Chaperone	N	N	Y	Q5TBM3	2	4.42
(Heat shock protein 90kDa alpha (cytosolic), class B member 1)*	Chaperone	N	Y	N	Q5T9W8	2	5.75
(Heat shock protein beta-1)*†	Cytoskeletal remodeling and signal transduction	Y (PMID: 18670085)	Y	Y	P04792	11	84.5
(Heat shock protein beta-6)*	Stress response (HSP20 family)	N	N	Y	O14558	4	51.85
(Heat shock protein HSP 90-alpha)†	Chaperone	Y C(481, 597, 598) (PMID: 20585580)	Y	Y	P07900	10	14
(Hemoglobin subunit alpha)*†	Oxygen Transport	Y C105 (PMID: 20585580)	Y	Y	P69905	8	57.04
(Hemoglobin subunit beta)*†	Oxygen Transport	Y C93 (PMID: 16594178)	Y	Y	P68871	13	90.48
(Histidine-rich glycoprotein)*	Blood coagulation	N	N	Y	P04196	2	3.68
(Kinesin family member 17)*	Microtubule-based movement	N	N	Y	A2A3Q7	2	4.91
(Lipoma-preferred partner)*	Cell signaling and protein scaffold	N	Y	Y	Q93052	14	31.97
(L-lactate dehydrogenase A chain)*	Metabolism	Y C163 (PMID: 20585580)	N	Y	P00338	10	54.14
(Malate dehydrogenase, cytoplasmic)†	Metabolism	Y C(137, 154) (PMID: 20585580)	Y	Y	P40925	12	194 Mowse

Protein	Biological Process	Previously Identified	NP	P	UniProt	No. of Peptides	% Coverage
(Myosin light chain kinase, smooth muscle)*	Smooth muscle contraction	N	N	Y	Q15746	3	3.45
(Myosin light polypeptide 6)*†	Smooth muscle contraction	? (PMID: 20585450)	Y	Y	P60660	9	51.66
(Myosin regulatory light polypeptide 9)*	Smooth muscle contraction	? (PMID: 20585450)	N	Y	P24844	4	45.35
(Myosin-11)*	Smooth muscle contraction	? (PMID: 20585450)	N	Y	P35749	6	5.27
(Neutral alpha-glucosidase AB)†	Metabolism	N	Y	Y	Q14697	4	3.91
(Nucleoside diphosphate kinase A)*	Metabolism and cell signaling	N	N	Y	P15531	2	25.47
(Oligoribonuclease, mitochondrial)*	Exonuclease	N	N	Y	Q9Y3B8	2	18.2
(PDZ & LIM domain protein 1)*	Cytoskeletal adapter (interacts with alpha-actinins 1,2, and 4)	N	N	Y	O00151	3	19.82
(Peptidyl-prolyl cis-trans isomerase A)*	Protein Folding	N	Y	Y	P62937	7	51.52
(Peroxiredoxin-1)*	Redox regulation	Y C(52, 173) (PMID: 20585580)	Y	Y	Q06830	6	36.14
(Phosphofructokinase, platelet)*	Metabolism	N	N	Y	Q5VSR7	3	4.8
(Phosphoglucomutase-like protein 5)*	Cytoskeletal, Interacts with cytoskeletal proteins dystrophin and utrophin	N	N	Y	Q15124	2	7.14
(Phosphoglycerate kinase 1)*	Metabolism	Y C50 (PMID: 20585580)	N	Y	P00558	9	42.82
(Phosphoglycerate mutase 1)*	Metabolism	Y C55 (PMID: 20585580)	N	Y	P18669	2	13.39
(Prefoldin subunit 3)*	Protein Folding	N	N	Y	P61758	2	28.43
(Preproalbumin precursor)*	Guinea pig specific	N	Y	Y	Q6WDN9	39	65.46
(Profilin-1)*	Cytoskeletal remodeling	Y (PMID: 18283105)	N	Y	P07737	3	22.86
(Prolow-density lipoprotein receptor-related protein 1)*	Endocytosis and cell signaling	N	N	Y	Q07954	2	0.9
(Prorelaxin H1)*	Signal transduction and tissue remodeling	N	N	Y	P04808	3	51.25
(Protein DJ-1)*	Transcriptional activator	N	N	Y	Q99497	5	38.62
(Protein S100-A10)*	Protein binding, induces the dimerization of ANXA2/p36	N	N	Y	P60903	2	37.5
(Protein S100-A11)*†	Calcium binding and signal transduction	Y C13 (PMID: 20585580)	N	Y	P31949	7	53.92
(Protein S100-A4)*†	Calcium binding	N	N	Y	P26447	2	11.88
(Protein S100-A9)*	Signal transduction	Y (PMID: 18832721)	N	Y	P06702	3	51.26
(Purine nucleoside phosphorylase)†	NAD biosynthesis	N	N	Y	P00491	4	28.82
(Pyruvate kinase isozymes M1/M2)*	Metabolism	Y C(326, 358, 423, 474) (PMID: 20585580)	Y	Y	P14618	14	47.27

Protein	Biological Process	Previously Identified	NP	P	UniProt	No. of Peptides	% Coverage
(Ras-related protein Rab-1A)*	Transport	N	N	Y	P62820	3	35.12
(Ras-related protein R-Ras)*	Cytoskeletal remodeling	N	N	Y	P10301	3	26.15
(Serotransferrin)*	Transport	Y C(58, 67, 137, 246, 387, 396, 469, 596, 615) (PMID: 20585580)	Y	Y	P02787	6	10.08
(Serpin peptidase inhibitor, clade B (ovalbumin), memb.6)*	Peptidase inhibitor	N	N	Y	Q5TD02	11	48.99
(S-formylglutathione hydrolase)*	Metabolism	N	N	Y	P10768	2	15.6
(SH3 domain-binding glutamic acid-rich-like protein)†	SH3 Binding	No Cys in Human	Y	Y	O75368	2	17.2
(Stress-70 protein, mitochondrial)*	Chaperone	Y C487 (PMID: 20585580)	N	Y	P38646	2	4.28
(Talin-1)*	Cytoskeletol-membrane connector	N	Y	Y	Q9Y490	13	10.27
(Testis derived transcript (3 LIM domains))*	Zinc ion binding	N	N	Y	A4D0U5	6	18.89
(Thioredoxin)†	S-nitrosation regulation	Y (62, 69, 73) (PMID: 20585580)	Y	Y	P10599	7	32
(Transforming growth factor β-1-induced transcript 1 protein)*	Molecular adapter at focal adhesion complexes	N	Y	Y	O43294	3	13.3
(Transforming protein RhoA)*	Signal transduction	N	N	Y	P61586	2	13.99
(Transgelin)*†	Actin Binding	N	N	Y	Q01995	10	59.7
(Transgelin-2)*	Protein binding	N	Y	Y	P37802	7	40.09
(Transitional endoplasmic reticulum ATPase)*†	Transport	Y C(77, 209, 695) (PMID: 20585580)	Y	N	P55072	2	11
(Transthyretin)*	Transport	Y (PMID: 16101296)	Y	N	P02766	2	26.19
(Tropomyosin alpha-4 chain)*	Smooth muscle contraction is regulated by interaction with caldesmon	Y C170 (PMID: 18992711)	N	Y	P67936	3	16.53
(Tropomyosin beta chain)*†	Smooth muscle contraction is regulated by interaction with caldesmon	Y C170 (PMID: 19447776)	Y	Y	P07951	4	29.58
(Tryptophanyl-tRNA synthetase, cytoplasmic)*	Protein biosynthesis	N	N	Y	P23381	2	12.13
(Tubulin beta chain)*†	Cytoskeletal	Y (PMID: 16418269)	Y	Y	P07437	18	54.05
(Tubulin beta-2B chain)*	Cytoskeletal	N	N	Y	Q9BVA1	15	46.07
(Tyrosine 3-monooxygenase/tryptophan 5-monooxygenase activation protein, beta polypeptide)*	Protein binding	N	N	Y	Q59EQ2	2	24.39

Protein	Biological Process	Previously Identified	NP	P	UniProt	No. of Peptides	% Coverage
(Vimentin)*†	Cytoskeletal remodeling	Y C328 (PMID: 20585580)	Y	Y	P08670	18	50.22
(Vinculin)*	Cytoskeletal actin binding	Y (PMID: 17704302)	N	Y	P18206	3	5.11
(Vitamin D-binding protein)*	Transport	N	Y	N	P02774	2	5.88
(Zinc finger protein 641)*	Transcriptional activator	N	Y	Y	Q96N77	13	40.69

118 unique proteins were identified, 62 of which have not been previously described as being S-nitrosated. 75 proteins were disparately S-nitrosated only during pregnancy and 10 were disparately S-nitrosated only during non-pregnancy. 33 proteins were S-nitrosated in both pregnancy and the non-pregnant tissue.
Proteins marked with * were identified by LTQ-Orbitrap LC/MS/MS, proteins marked with † were identified by MALDI TOF/TOF.
NP, non-pregnant estrogen primed guinea pig. P, Pregnant near term 60-67 day timed pregnant. Previously Identified Y, Yes; N, No.

Table S2.2: S-Nitrosated proteins identified in guinea pig USM that are involved in contraction/relaxation dynamics.

Protein	Biological Process	Previously Identified	NP	P	Uniprot
(Transgelin)*†	Actin Binding, Contraction	N	N	Y	Q01995 (TAGL_Hu)
(Destrin)*†	Actin depolymerization	Y (PMID: 18670085)	N	Y	P60981 (DEST_Hu)
(Tubulin beta chain)*†	Cytoskeletal	Y (PMID: 16418269)	Y	Y	P07437 (TBB5_Hu)
(Alpha-actinin-1)*†	Cytoskeletal	Y C332 (PMID: 20585580)	N	Y	P12814 (ACTN1_Hu)
(Desmin)*†	Cytoskeletal	Y C333 (PMID: 20585580)	Y	Y	P17661 (DESM_Hu)
(Actin, cytoplasmic 1)*	Cytoskeletal	Y (PMID: 20585580)	Y	Y	P60709 (ACTB_Hu)
(Actin, alpha skeletal muscle)*	Cytoskeletal	Y (PMID: 10961840)	Y	Y	P68133 (ACTS_Hu)
(Tubulin beta-2B chain)*	Cytoskeletal	N	N	Y	Q9BVA1 (TBB2B_Hu)
(Vinculin)*	Cytoskeletal actin binding	Y (PMID: 17704302)	N	Y	P18206 (VINC_Hu)
(Cofilin-1)*	Cytoskeletal actin binding	N	Y	Y	P23528 (COF1_Hu)
(Filamin-C)*	Cytoskeletal actin crosslinker	Y (PMID: 20585580)	N	Y	Q14315 (FLNC_Hu)
(Annexin A2)*†	Cytoskeletal adapter	Y (PMID: 12199706)	N	Y	P07355 (ANXA2_Hu)
(PDZ and LIM domain protein 1)*	Cytoskeletal adapter (interacts with alpha-actinins 1,2, and 4)	N	N	Y	O00151 (PDLI1_Hu)
(Profilin-1)*	Cytoskeletal remodeling	Y (PMID: 18283105)	N	Y	P07737 (PROF1_Hu)
(Vimentin)*†	Cytoskeletal remodeling	Y C328 (PMID: 20585580)	Y	Y	P08670 (VIME_Hu)
(Ras-related protein R-Ras)*	Cytoskeletal remodeling	N	N	Y	P10301 (RRAS_Hu)
(Calpain small subunit 1)*	Cytoskeletal remodeling and signal transduction	N	N	Y	P04632 (CPNS1_Hu)
(Heat shock protein beta-1)*†	Cytoskeletal remodeling and signal transduction	Y (PMID: 18670085)	Y	Y	P04792 (HSPB1_Hu)
(Filamin-A)*	Cytoskeletal scaffold actin binding	Y C717 (PMID: 20585580)	Y	Y	P21333 (FLNA_Hu)
(Phosphoglucomutase-like protein 5)*	Cytoskeletal, Interacts with dystrophin and utrophin	N	N	Y	Q15124 (PGM5_Hu)
(Ankyrin-3)*	Cytoskeletal-membrane linker	Y (PMID: 20585580)	Y	N	Q12955 (ANK3_Hu)
(Talin-1)*	Cytoskeletol-membrane connector	N	Y	Y	Q9Y490 (TLN1_Hu)
(Kinesin family member 17)*	Microtubule-based movement	N	N	Y	A2A3Q7 (A2A3Q7_Hu)
(Transforming growth factor beta-1-induced transcript 1 protein)*	Molecular adapter at focal adhesion complexes	N	Y	Y	O43294 (TGFI1_Hu)

Protein	Biological Process	Previously Identified	NP	P	Uniprot
(Protein S100-A10)*	Protein binding, induces the dimerization of ANXA2/p36	N	N	Y	P60903 (S10AA_Hu)
(Guanine nucleotide-binding protein G(i) subunit alpha-2)*	Signal transduction	N	N	Y	P04899 (GNAI2_Hu)
(Myosin regulatory light polypeptide 9)*	Smooth muscle contraction	? (PMID: 20585450)	N	Y	P24844 (MYL9_Hu)
(Myosin-11)*	Smooth muscle contraction	? (PMID: 20585450)	N	Y	P35749 (MYH11_Hu)
(Myosin light polypeptide 6)*†	Smooth muscle contraction	? (PMID: 20585450)	Y	Y	P60660 (MYL6_Hu)
(Myosin light chain kinase, smooth muscle)*	Smooth muscle contraction	N	N	Y	Q15746 (MYLK_Hu)
(Tropomyosin beta chain)*†	Smooth muscle contraction is regulated by interaction with caldesmon	Y C170 (PMID: 19447776)	Y	Y	P07951 (TPM2_Hu)
(Tropomyosin alpha-4 chain)*	Smooth muscle contraction is regulated by interaction with caldesmon	Y C170 (PMID: 18992711)	N	Y	P67936 (TPM4_Hu)
(Calponin-1)*	Smooth muscle contraction	N	Y	N	P51911 (CNN1_Hu)

Thirty-four S-nitrosated proteins were identified that are known to play a role in either cytoskeletal rearrangement or the regulation of contraction/relaxation in smooth muscle tissues; 15 of these are novel targets of S-nitrosation not previously identified; 20 are selectively S-nitrosated during pregnancy.
NP, non-pregnant estrogen primed guinea pig; P, Pregnant near term 60-67 day timed pregnant; Hu, human.
Previously Identified Y, Yes; N, No. Proteins marked with * were identified by LTQ-Orbitrap LC/MS/MS, proteins marked with † were identified by MALDI TOF/TOF.

SECTION II Semi-Quantitative Proteomic and Pathway Analysis of Human Uterine Smooth Muscle in Pregnancy, Labor, and Preterm Labor

Table S3.1: Relative expression levels of human uterine smooth muscle in pregnancy, labor, and preterm labor.

Sequence Id	Gene	Total Pep	% Seq Coverage	F-Statistic	P Value	L Pep	L Rel Ex	NL Pep	NL Rel Ex	PTL Pep	PTL Rel Ex
Q09666	AHNK	192	43.45	2.44	0.167	129	-0.32	154	0	176	0.37
P21333	FLNA	173	68.91	0.23	0.804	143	0.01	142	0	152	0.11
P35749	MYH11	155	58.27	0.61	0.575	117	-0.2	127	0	125	-0.28
Q14204	DYHC1	143	39.69	3.85	0.084	98	-0.25	107	0	121	0.47
Q14315	FLNC	130	61.58	1.77	0.249	88	-0.16	103	0	119	0.28
Q9Y490	TLN1	112	59.46	0.69	0.539	87	0.1	93	0	100	0.26
Q15149	PLEC	109	32.94	18.65	0.003	49	-0.85	72	0	99	0.66
P35579	MYH9	85	46.99	1.96	0.221	59	-0.49	72	0	61	-0.48
P02768	ALBU	85	83.25	0.57	0.594	65	0.3	58	0	68	0.42
P01024	CO3	72	54.84	0.54	0.611	48	0.13	50	0	68	0.26
Q00610	CLH1	67	47.16	8.56	0.017	40	-0.58	52	0	58	0.45
P18206	VINC	67	58.99	2.13	0.2	52	-0.27	55	0	59	0.06
Q13813	SPTA2	65	37.78	4.25	0.071	33	-1.29	42	0	59	0.21
P11532	DMD	62	23.72	18.52	0.003	28	-0.86	43	0	53	0.5
Q99715	COCA1	62	31.93	36.49	0	32	-0.7	36	0	58	0.84
Q9HBL0	TENS1	61	56.25	1.07	0.402	40	0.01	50	0	54	0.28
P02751	FINC	60	39.69	92.2	0	32	0.05	36	0	56	1.78
P46821	MAP1B	60	36.63	0.78	0.499	46	0.13	45	0	50	0.28
P12814	ACTN1	59	67.04	1.38	0.32	45	-0.2	50	0	56	0.4
P98160	PGBM	57	23.37	7.39	0.024	24	-0.78	41	0	49	0.29
P46940	IQGA1	56	46.11	2.96	0.127	38	-0.31	46	0	51	0.37
O43707	ACTN4	55	65.20	3.57	0.095	41	-0.53	47	0	54	0.45
O15061	SYNEM	54	47.80	7.79	0.021	30	-0.5	45	0	49	0.24
Q9NZM1	MYOF	53	34.06	3.91	0.082	26	-0.82	33	0	51	0.46
O75369	FLNB	53	28.48	0.62	0.569	30	-0.6	35	0	41	-0.31
P02787	TRFE	53	65.33	0.61	0.572	41	0.02	39	0	45	0.28
Q01082	SPTB2	52	33.93	10.09	0.012	28	-0.92	38	0	43	0.26
Q8IVF2	AHNK2	52	15.44	7.98	0.02	29	-0.07	26	0	37	0.43
Q02952	AKA12	50	49.16	2.16	0.196	29	-0.38	37	0	43	0.19
P12111	CO6A3	49	22.16	5.2	0.049	22	-0.08	27	0	47	1
P17661	DESM	49	76.60	7.44	0.024	30	-0.81	37	0	42	0.39
P68032	ACTC	49	88.86	0.59	0.582	45	0.54	36	0	36	0.54
P62736	ACTA	49	88.86	0.46	0.652	45	0.49	37	0	36	0.5

P63267	ACTH	48	89.10	0.48	0.64	45	0.52	38	0	34	0.51
Q05707	COEA1	47	34.69	2.08	0.206	36	0.16	39	0	39	-0.17
P01023	A2MG	46	46.81	0.97	0.432	33	-0.24	38	0	46	0.26
O95425	SVIL	45	31.07	3.45	0.1	21	-0.06	32	0	37	0.49
P08670	VIME	45	74.89	3.8	0.086	32	-0.64	35	0	41	0.07
P68133	ACTS	44	82.76	0.58	0.59	40	0.5	33	0	32	0.54
P60709	ACTB	43	89.33	0.06	0.938	37	0.03	29	0	31	0.16
Q01995	TAGL	42	89.05	0.48	0.641	31	0.42	31	0	29	0.13
P11216	PYGB	41	52.43	1.05	0.406	31	-0.18	31	0	36	0.4
Q9UMS6	SYNP2	39	55.08	0.42	0.672	28	0.1	29	0	37	0.24
P11047	LAMC1	37	32.82	74.05	0	18	-1.26	25	0	35	0.1
Q9BVA1	TBB2B	37	74.16	0.09	0.918	27	0.17	30	0	32	0.15
Q13885	TBB2A	37	73.26	0.07	0.931	28	0.16	30	0	32	0.13
P07437	TBB5	37	66.44	0.11	0.9	29	0.14	28	0	30	0.16
P08603	CFAH	36	46.63	4.66	0.06	21	0.23	30	0	30	0.37
P0C0L5	CO4B	36	30.39	0.2	0.821	22	0.08	23	0	32	0.19
P07942	LAMB1	35	31.91	8.68	0.017	16	-0.48	23	0	30	0.48
Q9BX66	SRBS1	35	33.05	1.2	0.365	19	-0.14	25	0	32	0.18
Q05682	CALD1	35	37.33	0.51	0.622	24	-0.09	24	0	33	0.08
P24821	TENA	35	26.08	2.55	0.158	25	-0.43	22	0	31	0.44
Q15746	MYLK	35	23.41	0.27	0.77	28	0.11	23	0	32	0.19
Q9NZN4	EHD2	35	72.01	2.04	0.21	29	-0.24	29	0	29	0.45
P35580	MYH10	34	23.08	0.98	0.427	17	-0.31	29	0	29	-0.28
P23634	AT2B4	34	32.23	7.89	0.021	21	-0.56	28	0	30	-0.01
P08133	ANXA6	34	58.99	2.09	0.205	24	-0.29	26	0	33	0.37
P14618	KPYM	34	67.98	0.23	0.801	31	0.17	30	0	30	0.13
P04114	APOB	33	11.26	7.74	0.022	9	-1.25	18	0	27	1.22
P14625	ENPL	33	45.21	1.05	0.406	22	-0.43	28	0	26	-0.09
Q93052	LPP	32	68.30	1.55	0.287	21	0.55	21	0	26	0.79
P01009	A1AT	32	66.03	1.34	0.33	23	0.33	23	0	29	0.3
P68371	TBB4B	32	62.25	0.11	0.9	26	0.19	26	0	28	0.16
Q96AC1	FERM2	31	47.94	0.82	0.485	23	-0.31	23	0	24	0.13
Q96Q06	PLIN4	31	35.89	1.54	0.289	23	-0.64	26	0	27	0.14
P55072	TERA	31	56.70	0.69	0.537	25	-0.07	24	0	27	0.28
Q15124	PGM5	31	61.38	1.06	0.402	25	-0.24	25	0	27	0.06
P51911	CNN1	31	76.43	0.17	0.851	27	0.2	21	0	27	0.17
P02545	LMNA	30	51.05	5.81	0.039	10	-0.86	21	0	30	0.48
Q07954	LRP1	30	9.18	3.55	0.096	16	-0.91	19	0	24	0.18
Q6UVK1	CSPG4	30	20.67	7.81	0.021	17	-0.53	22	0	27	0.45
P07900	HS90A	30	44.40	1.09	0.396	17	0.01	28	0	27	0.34
P22314	UBA1	30	44.80	2.14	0.199	20	-0.09	23	0	26	0.29
P09493	TPM1	30	57.75	0.85	0.473	22	-0.33	21	0	26	0.05

P50395	GDIB	30	72.13	1.95	0.222	24	-0.35	24	0	27	0.23
P14543	NID1	29	33.76	9.38	0.014	15	-0.85	24	0	27	0.32
P13639	EF2	29	44.52	1.6	0.278	16	-0.28	19	0	25	0.27
P06737	PYGL	29	38.25	6.93	0.028	18	-0.76	21	0	26	0.49
P08238	HS90B	29	46.13	2.78	0.14	19	-0.18	23	0	26	0.31
P00450	CERU	29	37.09	3.04	0.122	20	-0.22	20	0	28	0.53
Q14697	GANAB	29	44.81	3.29	0.108	20	0.08	22	0	24	0.61
P11142	HSP7C	29	50.00	0.11	0.896	24	-0.06	23	0	25	0.03
Q16363	LAMA4	28	23.53	6.06	0.036	14	-0.99	18	0	23	0.55
P27816	MAP4	28	32.64	0.49	0.637	19	-0.09	21	0	27	0.31
Q63ZY3	KANK2	28	50.76	0.97	0.432	22	-0.25	24	0	27	0.17
P68363	TBA1B	28	71.40	1.25	0.351	24	0.06	22	0	21	0.24
Q71U36	TBA1A	28	71.40	0.95	0.437	25	0.16	23	0	21	0.25
P30101	PDIA3	27	60.59	8.78	0.017	15	-0.26	19	0	27	0.49
P26038	MOES	27	50.26	6.02	0.037	17	-0.35	16	0	25	0.56
Q99798	ACON	27	45.64	1.63	0.273	18	0.07	17	0	23	0.54
O00159	MYO1C	27	35.18	6.47	0.032	18	-0.63	19	0	27	0.41
Q9Y4G6	TLN2	26	14.71	3.36	0.105	13	-0.69	22	0	20	-0.12
Q15582	BGH3	26	51.24	0.41	0.681	19	0.25	20	0	23	0.35
P12277	KCRB	26	67.45	3.96	0.08	21	0.48	19	0	20	0.6
Q9BUF5	TBB6	26	67.94	0.13	0.884	21	-0.07	19	0	23	0.16
P04350	TBB4A	26	54.95	0.1	0.906	22	0.16	22	0	23	0.14
Q14195	DPYL3	26	60.70	1.85	0.237	22	0.61	24	0	23	0.46
Q9BQE3	TBA1C	26	67.04	1.74	0.254	23	0.05	21	0	19	0.26
Q9H4M9	EHD1	25	59.36	0.73	0.519	15	-0.41	19	0	22	0.09
Q86VP6	CAND1	25	28.21	3.22	0.112	15	-0.35	21	0	24	0.36
P23142	FBLN1	25	46.37	0.52	0.617	16	0.17	20	0	25	0.27
P07951	TPM2	25	57.75	0.58	0.59	18	-0.45	15	0	24	-0.24
Q8WX93	PALLD	25	28.20	1.28	0.346	20	-0.23	19	0	22	-0.02
Q01813	K6PP	25	40.18	0.18	0.84	21	-0.09	21	0	25	0.09
Q14203	DCTN1	24	27.54	0.38	0.702	11	0.12	16	0	23	0.31
Q8WUM4	PDC6I	24	40.32	9.74	0.013	11	-0.57	18	0	18	0.06
P53621	COPA	24	28.10	14.54	0.005	12	-1.11	16	0	23	0.69
P06756	ITAV	24	30.63	1.83	0.239	12	-0.32	18	0	22	0.26
P07237	PDIA1	24	52.76	1.46	0.304	12	-0.1	20	0	21	0.33
P48681	NEST	24	21.28	70.84	0	13	0.28	11	0	24	1.59
P31150	GDIA	24	64.88	1.44	0.308	15	-0.24	18	0	18	0.31
P06396	GELS	24	48.72	3.7	0.09	16	-0.11	20	0	21	0.16
Q9BSJ8	ESYT1	24	34.15	7.54	0.023	17	-0.38	19	0	19	0.34
P68871	HBB	24	94.56	0.63	0.566	19	-0.4	19	0	17	0.03
P04083	ANXA1	24	66.76	1.41	0.315	19	-0.62	19	0	23	0.02
P54652	HSP72	24	48.20	1.62	0.273	19	-0.22	20	0	23	0.24

Q9NR12	PDLI7	24	60.83	0.52	0.62	20	0.09	17	0	15	-0.14
P07355	ANXA2	24	64.60	6.66	0.03	20	-0.55	23	0	22	0.43
P11021	GRP78	24	41.44	0.48	0.64	20	0	23	0	23	0.24
P08107	HSP71	24	50.39	1.27	0.346	21	-0.15	20	0	23	0.19
P53814	SMTN	23	34.79	0.86	0.471	12	-0.51	18	0	18	-0.04
Q96HC4	PDLI5	23	50.17	3.07	0.121	15	-0.42	16	0	20	-0.05
O43294	TGFI1	23	62.26	1.68	0.263	16	-0.32	22	0	19	0.3
Q13509	TBB3	23	46.00	0.09	0.917	17	0.1	15	0	20	0.18
O75083	WDR1	23	56.44	3.91	0.082	17	0.04	18	0	23	0.37
P06576	ATPB	23	53.50	1.09	0.396	20	-0.39	20	0	20	0.28
P08758	ANXA5	23	73.13	1.53	0.29	22	-0.57	19	0	22	0.02
P07996	TSP1	22	22.65	14.53	0.005	8	0.02	10	0	22	1.32
Q01518	CAP1	22	53.68	2.62	0.152	11	-0.77	13	0	21	0.02
P13796	PLSL	22	51.04	18.74	0.003	13	-1.07	14	0	21	0.68
P10809	CH60	22	52.53	2.59	0.155	13	-0.33	18	0	17	0.07
P67936	TPM4	22	58.06	0.17	0.852	15	-0.24	10	0	17	-0.14
P17655	CAN2	22	46.57	0.23	0.799	15	-0.03	20	0	18	0.08
P78559	MAP1A	22	14.70	3.71	0.089	16	0.54	12	0	18	0.75
P43121	MUC18	22	34.37	0.23	0.805	16	0.07	15	0	18	0.16
P06733	ENOA	22	66.13	8.58	0.017	16	0.23	17	0	17	0.44
P55786	PSA	22	33.19	9.67	0.013	17	-0.06	19	0	19	0.4
P02774	VTDB	22	49.58	4.31	0.069	20	0.26	13	0	20	0.31
Q9UPN3	MACF1	21	4.05	3.25	0.11	8	0.37	10	0	20	1.4
P28838	AMPL	21	58.57	1.23	0.358	9	-0.52	14	0	19	0.29
P40939	ECHA	21	40.76	1.18	0.369	10	-0.23	14	0	17	0.29
O94973	AP2A2	21	32.48	4.2	0.072	10	-0.57	16	0	19	0.71
Q14764	MVP	21	35.95	8.6	0.017	11	0.04	14	0	20	0.74
Q96QK1	VPS35	21	32.66	6.6	0.031	11	-0.34	14	0	20	0.54
P33176	KINH	21	30.43	2.89	0.132	13	-0.79	15	0	15	0.46
Q07065	CKAP4	21	47.51	1.54	0.288	14	-0.63	14	0	19	-0.12
O00151	PDLI1	21	81.46	0.85	0.472	14	-0.15	14	0	21	0.19
P00352	AL1A1	21	63.07	10.31	0.011	14	-0.47	15	0	19	0.32
P13489	RINI	21	66.38	1.7	0.26	14	-0.34	19	0	19	0.14
Q02218	ODO1	21	31.67	2.05	0.21	15	-0.02	14	0	20	0.96
P25705	ATPA	21	46.11	0.19	0.834	16	-0.18	18	0	18	-0.12
P04406	G3P	21	76.42	1.09	0.396	17	0.39	14	0	16	0.45
P68366	TBA4A	21	49.78	0.79	0.494	18	0.02	16	0	17	0.23
P20742	PZP	20	22.20	7.94	0.021	10	-0.25	10	0	19	0.89
P30153	2AAA	20	43.46	2.92	0.13	10	-0.47	16	0	16	0.28
P11217	PYGM	20	27.91	3.7	0.09	11	-0.61	12	0	18	0.43
P49748	ACADV	20	42.75	1.88	0.232	13	-0.13	15	0	17	0.52
P31939	PUR9	20	46.11	4.09	0.076	13	-0.43	16	0	18	0.41

P29401	TKT	20	46.55	1.23	0.358	14	0.01	13	0	20	0.32
P04792	HSPB1	20	76.10	3.7	0.09	15	0.52	18	0	18	0.56
P69905	HBA	20	83.80	0.63	0.566	15	-0.34	19	0	13	0.39
O00410	IPO5	20	27.44	1.17	0.373	16	0.03	13	0	17	0.55
P07384	CAN1	20	33.47	14.06	0.005	16	-0.39	16	0	15	0.21
P04075	ALDOA	20	72.80	2.16	0.197	16	0.67	17	0	18	0.27
P13645	K1C10	19	46.58	2.33	0.178	4	-2.2	15	0	15	0.41
P63010	AP2B1	19	24.55	3.6	0.094	5	-1.26	13	0	17	0.68
Q9UGI8	TES	19	51.78	0.56	0.6	9	0.38	11	0	18	0.36
Q9P2E9	RRBP1	19	20.71	9.12	0.015	10	-0.69	12	0	17	0.02
Q9UHD8	41526	19	47.10	5.54	0.043	10	-0.8	13	0	14	-0.34
Q14974	IMB1	19	32.53	0.86	0.47	10	-0.43	16	0	19	0.18
P04264	K2C1	19	31.37	3.81	0.086	11	-0.86	16	0	16	0.08
O95782	AP2A1	19	27.94	4.03	0.078	11	-0.7	16	0	16	0.72
P35573	GDE	19	16.97	3.32	0.107	12	-0.77	10	0	18	0.7
O60701	UGDH	19	52.23	1.64	0.27	12	-0.58	14	0	16	-0.2
Q92626	PXDN	19	20.96	1.66	0.267	13	-1.06	14	0	11	-0.82
P00338	LDHA	19	64.46	0.79	0.497	13	0.13	14	0	18	0.41
P02647	APOA1	19	56.55	0.48	0.64	13	-0.17	17	0	18	0.24
P30041	PRDX6	19	68.75	0.01	0.992	15	0.01	13	0	15	-0.05
P50454	SERPH	19	53.59	0.21	0.82	15	0.14	18	0	17	0.21
P48735	IDHP	19	42.04	0.28	0.763	16	-0.34	15	0	18	0.17
P00558	PGK1	19	58.03	1.02	0.415	16	0.41	15	0	19	0.49
Q16555	DPYL2	19	54.55	2.93	0.13	16	-0.2	17	0	17	0.33
P22105	TENX	18	6.48	1.31	0.337	5	-0.62	11	0	14	0.39
P27338	AOFB	18	48.08	4.52	0.064	7	-0.77	13	0	12	0.28
Q9NYU2	UGGG1	18	18.20	5.57	0.043	7	-1.54	14	0	14	-0.04
P16615	AT2A2	18	22.94	3.73	0.089	8	-0.76	13	0	13	0.33
P05556	ITB1	18	29.45	1.24	0.354	9	-0.68	13	0	17	0.15
Q07960	RHG01	18	59.91	4.46	0.065	10	-0.09	12	0	15	0.52
Q9Y3Z3	SAMH1	18	36.58	6.65	0.03	11	-0.03	11	0	14	0.94
P78371	TCPB	18	44.67	3.12	0.118	11	-1.55	12	0	14	0.05
O00429	DNM1L	18	36.01	0.34	0.722	11	0.11	12	0	15	0.34
P50990	TCPQ	18	41.97	1.41	0.314	11	-0.29	13	0	14	0.33
P06744	G6PI	18	41.58	0.58	0.588	11	0.06	13	0	15	0.26
P05091	ALDH2	18	48.74	0.28	0.762	12	-0.39	12	0	17	0.07
Q14BN4	SLMAP	18	18.72	0.98	0.428	13	-0.31	12	0	17	0.31
P00747	PLMN	18	37.53	0.31	0.744	14	-0.2	14	0	16	-0.16
P04843	RPN1	18	42.50	4.01	0.078	14	-0.67	16	0	18	0.21
P02790	HEMO	18	59.09	3.07	0.121	15	0.84	15	0	17	0.43
P08727	K1C19	17	46.75	12.91	0.023	0	-10	3	0	17	2.75
Q14643	ITPR1	17	8.45	2.3	0.196	4	-0.33	9	0	14	1.07

P46939	UTRO	17	7.25	4.07	0.077	5	0.47	6	0	15	2.15
Q96PK2	MACF4	17	4.04	5.15	0.05	6	0.43	8	0	16	1.61
P04040	CATA	17	38.14	7.42	0.024	6	-0.44	10	0	14	0.68
Q7L576	CYFP1	17	16.52	1.69	0.262	6	-0.76	10	0	14	1.07
P21980	TGM2	17	33.92	16.89	0.003	6	-2.91	16	0	11	-1.65
P07814	SYEP	17	18.72	0.65	0.556	7	-0.47	11	0	13	0.17
Q86UP2	KTN1	17	20.19	1.34	0.329	9	-0.19	10	0	14	0.55
P35606	COPB2	17	26.05	2.12	0.201	9	-0.81	11	0	13	0.72
Q6DD88	ATLA3	17	51.20	0.41	0.683	10	0.12	12	0	13	0.31
Q9Y696	CLIC4	17	71.15	0.5	0.632	10	0.53	13	0	17	-0.02
Q562R1	ACTBL	17	47.87	1.68	0.264	11	0.01	9	0	9	0.22
P02675	FIBB	17	50.92	0.59	0.582	11	-0.29	13	0	10	-0.13
P35609	ACTN2	17	17.23	2.87	0.134	11	-0.43	14	0	16	0.58
Q13418	ILK	17	40.93	0.47	0.644	12	0.47	14	0	15	0.01
P61158	ARP3	17	55.98	0.75	0.512	12	0.14	14	0	16	0.22
P21399	ACOC	17	28.35	3.15	0.116	13	0.69	8	0	14	0.68
P09525	ANXA4	17	52.35	6.46	0.032	13	-0.46	12	0	16	0.38
P08648	ITA5	17	22.12	0.22	0.807	13	0.16	14	0	17	0.14
P34932	HSP74	17	32.98	3.51	0.098	14	-0.5	14	0	13	0.19
P00734	THRB	17	35.37	3.85	0.084	15	0.42	9	0	16	0.84
P22897	MRC1	16	13.94	2.6	0.154	3	-1.17	7	0	14	0.89
Q9P0K7	RAI14	16	25.10	9.9	0.018	3	-2.03	10	0	10	0.78
Q7Z6Z7	HUWE1	16	6.15	4.77	0.069	5	0.57	4	0	14	1.86
Q99832	TCPH	16	46.78	8.84	0.016	5	-1.16	11	0	11	0.12
Q10567	AP1B1	16	22.55	1.75	0.252	7	-1.07	10	0	13	0.38
P49588	SYAC	16	23.24	0.51	0.623	7	-0.48	12	0	11	0.08
Q7KZF4	SND1	16	30.66	2.22	0.19	8	-0.97	10	0	12	-0.08
Q13045	FLII	16	17.57	1.49	0.298	8	-0.9	12	0	15	0.68
P22413	ENPP1	16	26.81	4.15	0.074	8	-1.41	13	0	14	0.73
P00738	HPT	16	43.10	1.03	0.412	8	-0.49	13	0	14	0.07
P23141	EST1	16	31.75	9.1	0.015	8	-1.62	14	0	10	-0.26
P13667	PDIA4	16	31.01	3.35	0.106	9	-0.83	8	0	11	-0.3
P60842	IF4A1	16	42.12	0.73	0.521	9	-0.5	12	0	16	0.02
Q8N3D4	EH1L1	16	19.89	1.17	0.373	10	0.25	9	0	13	0.84
P00367	DHE3	16	34.95	1.99	0.217	10	-0.12	9	0	14	0.38
P08237	K6PF	16	27.82	14.39	0.005	10	-0.28	10	0	14	0.85
P36871	PGM1	16	41.28	2.04	0.211	10	0.66	10	0	16	1.32
P63104	1433Z	16	60.00	0.68	0.544	10	-0.19	13	0	16	0.34
Q16853	AOC3	16	31.06	2.69	0.147	10	0.28	14	0	15	0.68
Q9Y678	COPG	16	25.74	3.49	0.099	10	-1.09	14	0	15	0.18
P11413	G6PD	16	42.91	11.36	0.009	11	-0.88	11	0	10	-0.16
P13797	PLST	16	37.94	1.1	0.392	11	-0.47	12	0	13	0.09

P40926	MDHM	16	59.17	1.68	0.264	11	0.01	12	0	15	0.39
P60174	TPIS	16	69.23	3.74	0.088	11	0.2	12	0	16	0.54
P38646	GRP75	16	29.46	0.29	0.757	11	-0.21	14	0	11	-0.01
P39060	COIA1	16	13.06	1.3	0.34	11	-0.27	14	0	14	0.15
Q9H4A4	AMPB	16	36.15	7.56	0.023	12	0.03	9	0	15	0.93
P50991	TCPD	16	39.89	6.58	0.031	12	-0.8	10	0	14	0.26
P62140	PP1B	16	51.68	1	0.422	12	-0.27	11	0	14	0.31
Q06830	PRDX1	16	72.36	0.32	0.741	12	0.02	11	0	14	0.23
Q6NZI2	PTRF	16	33.59	0.05	0.947	12	0.07	12	0	14	0.01
P45974	UBP5	16	26.69	1.46	0.305	12	-0.36	14	0	14	0.29
P68104	EF1A1	16	45.24	0.3	0.751	13	0.11	12	0	13	0.3
P30837	AL1B1	16	38.88	1.74	0.254	14	-0.22	15	0	15	0.2
Q15181	IPYR	16	75.09	0.84	0.475	16	0.5	14	0	13	0.33
Q9NVA2	41528	15	45.45	8.74	0.017	5	-1.84	7	0	14	-0.26
Q14240	IF4A2	15	44.23	1.74	0.253	6	-0.91	10	0	14	-0.36
P49327	FAS	15	11.15	4.5	0.064	7	1.38	5	0	14	1.62
Q6YHK3	CD109	15	15.43	3.54	0.096	7	-1.01	9	0	13	0.42
P35221	CTNA1	15	28.70	0.98	0.427	7	-0.41	10	0	12	0.47
P05023	AT1A1	15	20.92	17.96	0.003	7	-0.7	10	0	15	0.41
P26641	EF1G	15	39.13	3.27	0.11	7	-0.94	12	0	10	-0.1
P07195	LDHB	15	46.11	1.27	0.347	7	-0.54	13	0	14	0.41
Q04446	GLGB	15	27.49	1.2	0.364	8	0.13	8	0	11	0.47
Q13409	DC1I2	15	39.81	0.19	0.834	8	-0.02	9	0	12	0.24
P12956	XRCC6	15	34.15	3.5	0.098	8	-0.67	10	0	12	0.6
O94788	AL1A2	15	47.68	2.74	0.143	8	-0.61	11	0	11	-0.31
O00299	CLIC1	15	77.59	0.2	0.82	9	0.09	11	0	12	-0.09
P04899	GNAI2	15	50.99	1.84	0.238	9	-0.18	12	0	14	0.48
P62258	1433E	15	53.73	1.99	0.217	9	-1.44	13	0	15	0.17
P47895	AL1A3	15	36.33	3.14	0.117	10	-0.05	11	0	13	0.33
P02042	HBD	15	93.88	2.25	0.187	10	-0.6	12	0	15	0.22
P17858	K6PL	15	28.21	6.72	0.029	10	-0.75	13	0	11	0.36
Q16851	UGPA	15	41.14	0.95	0.437	11	-0.31	11	0	12	-0.07
P00751	CFAB	15	27.62	0.3	0.749	11	0.06	12	0	14	0.21
P49368	TCPG	15	38.17	2.37	0.174	12	-0.36	10	0	13	0.47
P16152	CBR1	15	67.15	0.59	0.583	13	0.01	10	0	13	0.21
P19801	ABP1	14	19.71	37.68	0.004	0	-10	2	0	14	4.17
Q9Y4L1	HYOU1	14	21.72	2.71	0.145	5	-1.6	9	0	14	0
Q8WUY3	PRUN2	14	8.23	2.95	0.128	6	0.61	3	0	12	1.98
O75746	CMC1	14	28.91	0.19	0.836	6	0.78	8	0	10	0.17
P19367	HXK1	14	21.26	10.71	0.01	6	-0.5	8	0	12	1.58
Q9UHG3	PCYOX	14	37.23	4.04	0.077	6	-0.83	9	0	11	0.11
O75874	IDHC	14	43.72	2.23	0.189	8	-0.41	11	0	11	0.72

P02679	FIBG	14	45.25	2.72	0.144	8	-0.66	12	0	12	-0.23
Q99460	PSMD1	14	21.30	0.31	0.745	10	-0.28	9	0	12	0.37
Q15019	41519	14	64.54	1.39	0.319	10	0.28	11	0	12	0.38
P23528	COF1	14	62.65	0.48	0.638	10	-0.39	11	0	14	-0.13
P28331	NDUS1	14	33.43	1.61	0.275	10	-0.29	11	0	14	0.57
P27348	1433T	14	52.65	0.92	0.447	10	-0.68	13	0	14	-0.06
P62136	PP1A	14	46.36	1.54	0.288	11	-0.42	9	0	12	0.42
P17987	TCPA	14	31.47	0.07	0.936	11	0.08	10	0	10	-0.02
P00915	CAH1	14	70.11	0.97	0.43	11	-0.1	11	0	12	0.52
P27824	CALX	14	25.51	0.19	0.83	11	-0.12	11	0	12	0.12
Q9ULC3	RAB23	14	71.31	0.01	0.989	11	0.05	11	0	13	0
Q92499	DDX1	14	28.24	1.32	0.334	11	-0.33	11	0	13	0.52
P49419	AL7A1	14	37.48	0.99	0.426	11	0.44	12	0	12	0.58
P21266	GSTM3	14	58.22	1.96	0.222	11	-0.48	12	0	12	0.14
P51888	PRELP	14	39.79	2.58	0.155	12	-0.98	13	0	14	-0.47
P00387	NB5R3	14	52.49	0.43	0.668	13	0.42	12	0	12	0.25
P62937	PPIA	14	70.91	3.1	0.119	13	0.6	12	0	14	0.48
P09960	LKHA4	14	34.21	0.02	0.98	13	0.06	14	0	11	0.12
P01857	IGHG1	14	52.42	0.07	0.933	14	0.03	13	0	13	-0.1
P02788	TRFL	13	24.65	7.4	0.032	1	0.83	1	0	13	3.71
P78527	PRKDC	13	4.68	8.7	0.017	2	-0.89	6	0	13	1.37
Q08211	DHX9	13	12.76	3.86	0.097	3	0.99	4	0	12	2.63
Q0ZGT2	NEXN	13	20.74	2.75	0.142	3	-1.3	9	0	11	0.25
P41252	SYIC	13	13.31	1.3	0.338	4	-0.48	7	0	12	0.92
P98095	FBLN2	13	15.37	3.55	0.096	4	-1.05	8	0	11	0.23
O43237	DC1L2	13	43.90	0.71	0.527	5	0.04	8	0	11	0.55
P31040	DHSA	13	34.04	1.92	0.226	5	0.84	8	0	11	1.83
P17812	PYRG1	13	29.10	7.39	0.024	5	-1.18	8	0	13	0.73
Q5T4S7	UBR4	13	4.46	0.66	0.55	5	-0.08	9	0	8	0.64
O94979	SC31A	13	17.54	2.97	0.127	5	-1.68	9	0	10	-0.12
Q15942	ZYX	13	34.79	6.07	0.036	5	0.37	9	0	11	0.9
P49591	SYSC	13	31.13	2.79	0.139	5	-0.97	9	0	12	0.41
P23526	SAHH	13	31.48	1.89	0.23	5	-1.79	10	0	12	0
Q86VB7	C163A	13	19.72	0.95	0.446	6	0.01	4	0	13	1.16
P53618	COPB	13	21.83	1.05	0.407	6	0.3	8	0	11	0.61
Q12805	FBLN3	13	39.76	0.43	0.671	6	-0.1	9	0	13	0.29
P48643	TCPE	13	34.94	2.98	0.127	6	-0.61	10	0	11	0.42
O43491	E41L2	13	24.28	9.43	0.014	6	-1.46	11	0	8	-0.49
O60763	USO1	13	19.65	0.93	0.445	7	0.51	7	0	10	0.77
P49411	EFTU	13	35.84	3.09	0.119	7	0.28	7	0	11	0.85
Q9H223	EHD4	13	26.62	5.9	0.038	7	-0.97	7	0	11	0.24
P43034	LIS1	13	47.07	0.26	0.778	7	0.08	8	0	12	0.26

O43776	SYNC	13	33.39	4.78	0.057	7	-0.93	9	0	12	0.63
Q15084	PDIA6	13	43.64	2.19	0.193	7	-0.3	10	0	13	0.34
O75923	DYSF	13	10.24	2.77	0.141	8	-0.15	5	0	10	0.94
Q04917	1433F	13	51.63	0.69	0.537	8	-0.9	8	0	10	0.25
P10301	RRAS	13	60.55	3.27	0.11	8	-1.31	9	0	13	-0.08
P27797	CALR	13	54.44	0.86	0.47	8	0.07	10	0	12	0.32
P04844	RPN2	13	33.91	7.05	0.027	8	-0.52	12	0	12	0.42
Q9BZQ8	NIBAN	13	23.49	5.69	0.041	9	1.13	5	0	10	0.41
P01008	ANT3	13	34.91	0.76	0.508	9	0.53	8	0	11	0.8
P50479	PDLI4	13	52.73	2.47	0.165	9	-0.37	8	0	12	0.52
Q08257	QOR	13	54.71	2.16	0.197	9	-0.06	8	0	13	0.55
Q6S8J3	POTEE	13	9.95	0.21	0.816	9	-0.24	10	0	10	-0.04
Q3ZCM7	TBB8	13	19.37	0.04	0.96	9	0.11	10	0	11	0.18
P36578	RL4	13	33.72	3.25	0.11	9	-0.27	11	0	11	0.22
Q00341	VIGLN	13	15.30	1.42	0.313	9	-0.68	12	0	12	0.2
P29536	LMOD1	13	25.67	1.03	0.411	10	0.16	8	0	12	0.6
P21796	VDAC1	13	64.31	25.87	0.001	10	-1.17	9	0	11	0.3
P21291	CSRP1	13	62.69	0.72	0.523	10	0.17	11	0	13	0.23
Q99536	VAT1	13	54.20	1.57	0.282	10	0.83	11	0	13	0.86
P13010	XRCC5	13	25.00	1.54	0.301	11	-0.13	7	0	11	0.62
P06753	TPM3	13	25.70	0.06	0.945	11	-0.07	8	0	11	0
P00488	F13A	13	25.27	16.06	0.004	11	0.09	10	0	13	0.93
P01860	IGHG3	13	41.11	0.35	0.72	11	-0.46	12	0	11	-0.13
Q9NVD7	PARVA	13	32.26	7.2	0.025	12	0.15	9	0	10	0.78
P63244	GBLP	13	61.20	2.56	0.157	12	-0.03	13	0	12	0.58
P08729	K2C7	12	24.52	87.89	0.003	0	-10	2	0	12	3.54
P24043	LAMA2	12	5.32	13.9	0.006	1	-2.66	7	0	9	0.06
Q92616	GCN1L	12	8.24	2.56	0.157	4	-1.4	5	0	9	0.47
O15144	ARPC2	12	48.67	4.66	0.06	4	-0.8	5	0	10	1.49
O75131	CPNE3	12	28.86	2.65	0.15	4	-1.02	9	0	7	-0.24
Q16891	IMMT	12	24.67	0.62	0.571	5	-0.14	6	0	12	0.45
P35611	ADDA	12	27.68	5.05	0.052	5	-2.64	7	0	10	-0.56
Q9NZN3	EHD3	12	24.86	3.88	0.083	5	-0.86	7	0	11	0.22
Q15075	EEA1	12	12.40	2.84	0.136	5	-1.02	8	0	7	0.86
O95479	G6PE	12	22.00	8.74	0.017	5	-1.01	8	0	11	-0.03
O14974	MYPT1	12	17.28	3.43	0.102	5	-1.29	9	0	11	0.18
Q13200	PSMD2	12	19.05	49.16	0	5	-2.68	10	0	9	1.07
O00231	PSD11	12	36.73	2.41	0.171	5	-0.85	10	0	11	0.21
P14868	SYDC	12	32.34	0.64	0.558	6	-0.13	7	0	10	0.63
Q16181	41524	12	40.05	5.97	0.037	6	-0.59	8	0	11	0.49
P19338	NUCL	12	21.41	1.01	0.418	6	-0.62	8	0	12	0.04
Q9ULV4	COR1C	12	31.22	14.14	0.005	6	-0.57	9	0	11	0.47

P01871	IGHM	12	31.42	2.45	0.167	6	-0.39	9	0	11	0.73
P12109	CO6A1	12	21.50	5.09	0.051	6	-0.56	9	0	12	1.09
O95373	IPO7	12	16.86	8.19	0.019	7	-0.29	5	0	10	0.96
Q13162	PRDX4	12	59.04	5.9	0.038	7	-0.07	7	0	10	0.86
P35241	RADI	12	25.90	1.3	0.339	7	-0.38	7	0	10	0.34
P46459	NSF	12	21.64	3.97	0.08	7	-0.5	7	0	10	0.58
Q13425	SNTB2	12	28.89	2.61	0.153	7	-0.31	7	0	10	0.48
P39656	OST48	12	36.62	1.77	0.249	7	-0.56	7	0	12	0.42
P15311	EZRI	12	24.57	1.7	0.259	7	-0.49	7	0	12	0.34
P26639	SYTC	12	23.51	2.34	0.178	7	-0.93	8	0	11	0.99
Q06124	PTN11	12	33.17	5.67	0.041	7	-1.08	9	0	12	0.33
Q9Y6N5	SQRD	12	35.33	1.79	0.246	7	-0.49	10	0	10	-0.5
Q08043	ACTN3	12	12.87	3.32	0.107	7	-0.54	10	0	12	0.55
P23396	RS3	12	60.08	1.27	0.348	7	-0.4	10	0	12	0.24
Q13228	SBP1	12	33.26	1.91	0.229	8	1.05	6	0	11	2.19
P07099	HYEP	12	34.29	2.62	0.152	8	0.38	8	0	8	0.66
P36955	PEDF	12	36.60	0.19	0.834	8	0.05	10	0	10	0.23
Q15417	CNN3	12	39.21	13.3	0.006	8	0.65	10	0	10	0.28
P40763	STAT3	12	26.23	4.11	0.075	9	0.23	7	0	12	1.08
P54920	SNAA	12	59.66	1.44	0.309	9	-1.12	8	0	11	-0.42
Q16881	TRXR1	12	32.82	1.12	0.386	9	0.37	9	0	11	0.54
P19823	ITIH2	12	21.04	2.39	0.172	9	0.21	9	0	12	0.62
P02511	CRYAB	12	78.29	0.25	0.785	9	-0.22	9	0	12	0.09
P55084	ECHB	12	29.11	0.32	0.736	9	0.13	11	0	10	0.25
P22695	QCR2	12	37.97	0.69	0.54	9	-0.64	12	0	9	-0.42
P42224	STAT1	12	21.33	3.29	0.109	10	-1.02	9	0	9	0
O14558	HSPB6	12	93.75	1.27	0.348	10	0.14	12	0	11	0.49
P01019	ANGT	12	30.10	2.22	0.189	11	0.11	9	0	10	0.29
P01042	KNG1	12	21.74	0.23	0.8	11	-0.21	10	0	11	-0.04
O60506	HNRPQ	12	23.27	1.82	0.241	11	-0.4	11	0	12	0.28
P09211	GSTP1	12	69.05	1.27	0.347	12	0.63	10	0	10	0.57
Q07157	ZO1	11	9.10	4.29	0.07	2	-1.2	4	0	9	1.16
P35908	K22E	11	17.84	5	0.053	2	-2.67	9	0	9	-0.3
P23229	ITA6	11	13.72	66.93	0	3	-1.28	2	0	11	1.64
Q13596	SNX1	11	23.95	4.44	0.066	3	-1.52	7	0	9	0.21
P42025	ACTY	11	53.72	5.07	0.051	4	-2.07	7	0	8	-0.11
O60749	SNX2	11	26.97	4.24	0.071	4	-0.8	7	0	8	0.55
P61978	HNRPK	11	39.09	2.64	0.15	5	-0.18	5	0	11	0.34
Q6PCE3	PGM2L	11	25.40	9.12	0.015	5	-1.33	5	0	11	1.11
Q15907	RB11B	11	52.75	1.75	0.253	5	-0.66	6	0	11	0.29
P08865	RSSA	11	49.15	12.13	0.008	5	-0.08	7	0	10	0.61
P49589	SYCC	11	17.11	3.39	0.104	5	-0.96	7	0	10	0.54

O43242	PSMD3	11	28.46	2.46	0.166	5	-0.59	8	0	8	0.56
Q9HCB6	SPON1	11	20.94	11.11	0.01	5	0.63	9	0	9	0.97
P31948	STIP1	11	23.02	1.77	0.249	6	-0.5	5	0	10	0.5
Q86TX2	ACOT1	11	38.95	3.07	0.121	6	0.11	6	0	9	1.03
P49753	ACOT2	11	33.95	3.07	0.121	6	0.11	6	0	9	1.03
P54578	UBP14	11	34.62	14.95	0.005	6	-0.91	7	0	8	0.03
P23381	SYWC	11	36.09	1.19	0.367	6	0.64	7	0	10	1.42
P51659	DHB4	11	24.86	26.22	0.001	6	0.38	7	0	11	1.55
Q99623	PHB2	11	45.82	3.81	0.086	6	-0.73	8	0	10	1.01
Q8NBS9	TXND5	11	33.33	1.2	0.365	6	-0.72	8	0	11	0.13
Q9BTV4	TMM43	11	37.50	2.19	0.193	6	-0.18	9	0	10	0.62
Q7Z406	MYH14	11	5.01	1.07	0.4	6	-0.45	10	0	8	-0.39
P50148	GNAQ	11	37.33	4.69	0.059	7	-0.64	6	0	9	0.6
Q12797	ASPH	11	21.77	0.15	0.868	7	0.16	6	0	10	-0.06
Q96CX2	KCD12	11	46.15	2.84	0.136	7	-0.25	6	0	10	0.61
Q92973	TNPO1	11	17.71	2.06	0.209	7	0.5	7	0	9	1.35
P14314	GLU2B	11	34.28	0.23	0.805	7	-0.16	7	0	10	0.16
O43852	CALU	11	45.71	2.27	0.185	7	-0.56	8	0	7	0.68
P19971	TYPH	11	36.72	6.23	0.034	7	-0.74	8	0	7	0.18
Q13561	DCTN2	11	35.66	3.51	0.098	7	-0.57	8	0	8	0.27
P48059	LIMS1	11	38.15	0.83	0.481	7	-0.12	8	0	10	0.79
P31946	1433B	11	55.28	0.38	0.697	7	-0.44	8	0	11	-0.05
P04439	1A03	11	41.92	1.91	0.228	7	-0.59	9	0	6	-0.37
P35237	SPB6	11	38.03	1.27	0.346	7	-0.02	9	0	8	0.61
P00505	AATM	11	36.74	6.35	0.033	7	-0.31	9	0	9	0.66
P04217	A1BG	11	33.94	0.32	0.739	7	-0.17	9	0	11	0.16
P01876	IGHA1	11	56.09	1.94	0.224	7	0.6	10	0	10	0.43
Q9BZL4	PP12C	11	26.98	2.5	0.163	8	-0.24	6	0	10	0.43
P40227	TCPZ	11	30.89	0.62	0.568	8	-0.71	7	0	9	-0.18
P17980	PRS6A	11	36.90	0.18	0.837	8	-0.23	7	0	9	0.13
Q9Y3F4	STRAP	11	51.14	1.45	0.306	8	-1.14	7	0	10	0.89
P61163	ACTZ	11	50.00	0.76	0.508	8	0.31	8	0	9	0.1
Q96AQ6	PBIP1	11	20.25	0.49	0.636	8	0.04	8	0	9	0.52
P60981	DEST	11	64.24	0.14	0.875	8	0.01	8	0	11	0.21
Q15365	PCBP1	11	57.87	0.37	0.707	8	-0.17	9	0	7	0.02
O60664	PLIN3	11	43.32	3.69	0.09	8	0.21	9	0	8	0.65
P54136	SYRC	11	22.27	1.12	0.385	8	-0.41	9	0	8	0.15
Q99714	HCD2	11	75.10	12.16	0.008	8	-0.28	9	0	9	0.33
P09104	ENOG	11	46.08	1.92	0.227	8	0.36	9	0	10	0.26
P37802	TAGL2	11	65.33	11.45	0.009	8	-0.47	9	0	10	0.36
P45880	VDAC2	11	50.00	3.82	0.085	8	-0.79	9	0	11	0.37
Q9Y3I0	RTCB	11	27.72	0.71	0.527	8	-0.51	9	0	11	0.12

P11940	PABP1	11	22.80	3.92	0.081	8	-0.55	10	0	9	0.65
P40925	MDHC	11	45.21	0.4	0.689	8	-0.23	10	0	10	-0.01
P23284	PPIB	11	44.91	2.56	0.157	8	-0.57	10	0	10	0.19
P51149	RAB7A	11	62.32	3.49	0.099	9	-0.28	8	0	9	0.29
P47756	CAPZB	11	45.85	0.01	0.988	9	-0.05	9	0	9	-0.01
P24844	MYL9	11	62.79	0.21	0.813	9	0.34	9	0	10	0.3
P46439	GSTM5	11	42.66	1.51	0.294	10	0.88	7	0	7	-0.12
A6NKZ8	YI016	11	20.16	0.01	0.987	10	0.04	7	0	9	0.1
Q16647	PTGIS	11	29.80	0.12	0.89	10	-0.1	10	0	10	0.02
P47755	CAZA2	11	62.59	0.63	0.563	10	0.09	11	0	11	0.39
P05787	K2C8	10	20.70	16.04	0.007	1	-1.04	2	0	10	1.88
P02671	FIBA	10	14.20	0.84	0.475	2	-0.76	4	0	9	0.43
O14980	XPO1	10	13.26	0.09	0.915	2	0.7	5	0	10	0.02
Q07866	KLC1	10	21.82	1.31	0.338	2	-0.91	6	0	9	0.17
O00203	AP3B1	10	11.97	3.77	0.087	3	0.3	5	0	9	1.25
Q9Y224	CN166	10	52.05	2.64	0.151	3	-1.79	7	0	7	0.46
P35527	K1C9	10	27.29	1.45	0.307	3	-0.75	7	0	8	0.5
P58107	EPIPL	10	3.61	23.09	0.002	4	1.35	3	0	10	2.86
P43652	AFAM	10	20.53	9.97	0.012	4	2.63	4	0	10	3.51
O95817	BAG3	10	31.30	0.21	0.817	4	0.33	6	0	8	0.53
O76024	WFS1	10	15.28	1.05	0.406	4	0.91	7	0	6	0.21
Q7Z4I7	LIMS2	10	36.36	2.63	0.151	4	-0.42	7	0	9	0.33
P07954	FUMH	10	30.39	0.67	0.547	5	0.37	4	0	8	0.06
Q9P2J5	SYLC	10	10.03	1.25	0.35	5	-0.89	5	0	8	0.53
Q969G5	PRDBP	10	31.03	1.2	0.365	5	-0.02	5	0	9	0.76
P07093	GDN	10	26.38	4.5	0.076	5	1.16	5	0	10	2.31
A1X283	SPD2B	10	16.36	1.4	0.316	5	-0.31	6	0	7	0.84
Q16204	CCDC6	10	24.47	4.47	0.065	5	-0.69	6	0	9	0.25
P29992	GNA11	10	33.70	0.85	0.472	5	-0.46	7	0	9	0.29
P62424	RL7A	10	30.45	3.83	0.085	5	-1.61	7	0	9	0.16
P02748	CO9	10	24.15	1.23	0.357	5	-0.16	7	0	10	1
P49189	AL9A1	10	23.28	0	0.998	5	0.02	8	0	8	0.03
O60716	CTND1	10	16.01	3.77	0.087	5	0.03	8	0	9	1.31
Q96G03	PGM2	10	23.04	1.93	0.225	6	0.44	4	0	7	1.24
P18669	PGAM1	10	41.34	1.57	0.284	6	0.47	5	0	10	0.65
P35998	PRS7	10	33.49	1.31	0.338	6	0.49	6	0	7	1.2
P01011	AACT	10	26.48	6.83	0.028	6	-0.24	6	0	9	0.58
P78344	IF4G2	10	13.56	4.63	0.061	6	-0.65	6	0	9	0.66
P13804	ETFA	10	47.45	4.56	0.062	6	-1.08	6	0	10	0.14
O43399	TPD54	10	63.11	1.02	0.415	6	-0.68	7	0	7	-0.15
P12236	ADT3	10	37.92	1.34	0.331	6	-0.72	7	0	10	0.26
Q99497	PARK7	10	62.43	4.22	0.072	6	0.17	8	0	9	0.37

P12235	ADT1	10	38.93	0.89	0.458	6	-0.44	8	0	10	0.28
Q5JWF2	GNAS1	10	10.22	3.17	0.115	6	-0.93	9	0	7	-0.6
P63092	GNAS2	10	26.90	3.17	0.115	6	-0.93	9	0	7	-0.6
P07585	PGS2	10	36.21	6.83	0.028	6	-1.31	9	0	10	-0.17
P56199	ITA1	10	13.74	0.87	0.466	7	-0.6	6	0	9	0.52
P05452	TETN	10	53.96	0.11	0.893	7	-0.02	7	0	8	0.07
P31930	QCR1	10	33.33	1.08	0.397	7	-0.27	7	0	10	0.41
P62701	RS4X	10	37.64	7.82	0.021	7	-0.27	7	0	10	0.59
Q9Y281	COF2	10	57.23	0.55	0.601	7	-0.46	8	0	7	-0.18
Q14152	EIF3A	10	10.56	10.06	0.012	7	-0.83	8	0	8	-0.03
P35232	PHB	10	57.72	4.82	0.057	7	-0.2	8	0	9	0.53
P32119	PRDX2	10	59.09	0.81	0.488	7	0	9	0	9	0.42
Q06323	PSME1	10	42.97	3.09	0.12	7	-0.62	9	0	9	0.59
P06727	APOA4	10	31.57	2.11	0.203	7	-0.32	10	0	6	-0.8
P55060	XPO2	10	14.21	2.83	0.136	8	0.1	7	0	6	0.48
P53004	BIEA	10	39.19	4.45	0.065	8	-1.25	7	0	8	0.3
Q9UJ70	NAGK	10	41.86	1.51	0.294	8	-0.38	7	0	10	0.56
P84077	ARF1	10	58.56	2.21	0.191	8	0.42	7	0	10	0.39
P61204	ARF3	10	58.56	2.21	0.191	8	0.42	7	0	10	0.39
Q9NQC3	RTN4	10	13.00	4.43	0.066	8	-0.71	8	0	8	-0.42
P30044	PRDX5	10	55.61	0.68	0.544	8	0.11	9	0	8	0.55
P21964	COMT	10	56.83	2.76	0.141	8	-0.04	9	0	9	0.43
P34931	HS71L	10	21.84	1.21	0.363	8	-0.19	9	0	10	0.22
P20810	ICAL	10	24.15	0.2	0.821	8	0.21	9	0	10	0.24
Q96KP4	CNDP2	10	30.74	3.71	0.089	8	0.46	10	0	9	1.09
P48147	PPCE	10	22.68	4.58	0.062	9	0.88	5	0	10	1.8
P07737	PROF1	10	65.71	10.17	0.012	9	0.36	6	0	7	0.75
P02749	APOH	10	39.71	0.05	0.954	9	0.08	7	0	8	0.07
P30086	PEBP1	10	72.19	4.81	0.057	9	0.83	7	0	9	0.27
P62873	GBB1	10	38.82	2.01	0.215	9	-0.24	8	0	9	0.28
P60660	MYL6	10	65.56	1.28	0.345	9	-0.25	8	0	9	0.27
P09488	GSTM1	10	42.66	23.74	0.001	10	2.1	3	0	8	0.89
P01859	IGHG2	10	35.28	1.65	0.269	10	0.48	9	0	9	0.01
P17948	VGFR1	9	8.74	175.72	0.006	0	-10	2	0	8	3.49
Q9H3U1	UN45A	9	15.36	3.4	0.358	1	-1	3	0	7	-0.21
Q93008	USP9X	9	4.82	0.22	0.811	1	0.29	3	0	8	0.64
P69892	HBG2	9	67.35	7.72	0.022	1	-0.27	4	0	9	0.93
Q9Y4F1	FARP1	9	12.82	1.25	0.379	2	-0.56	2	0	9	0.74
P10644	KAP0	9	27.30	1.92	0.227	2	-0.86	4	0	8	1.1
P80723	BASP1	9	63.44	3.87	0.083	2	-1.75	4	0	9	0.06
O14617	AP3D1	9	11.80	28.09	0.004	2	-2.38	5	0	6	0.53
Q16531	DDB1	9	13.86	5.24	0.048	2	-1.55	5	0	8	0.8

P05106	ITB3	9	14.97	1.97	0.234	2	-1.85	6	0	7	0.53
Q92597	NDRG1	9	35.03	3.37	0.118	2	-2.39	7	0	7	-1.05
P49821	NDUV1	9	33.84	6.34	0.043	3	0.09	4	0	8	1.38
Q13492	PICAL	9	20.25	1.49	0.298	3	-0.41	5	0	8	0.86
P12110	CO6A2	9	13.15	1.74	0.253	3	-0.47	6	0	8	0.78
Q9Y6C9	MTCH2	9	40.26	4.08	0.076	3	1.12	6	0	8	1.85
P07858	CATB	9	36.58	14.98	0.005	3	-1.43	6	0	9	0.44
P13611	CSPG2	9	3.83	2.02	0.213	3	-1.71	7	0	6	0.11
Q1KMD3	HNRL2	9	15.13	7.13	0.026	3	-2.07	7	0	6	-0.14
Q02878	RL6	9	33.33	1.99	0.217	4	-0.58	3	0	9	1.38
P00739	HPTR	9	26.44	1.44	0.308	4	-0.25	4	0	7	0.49
P00390	GSHR	9	32.76	3.68	0.091	4	-0.29	4	0	8	0.92
Q14624	ITIH4	9	15.48	6.76	0.029	4	-0.45	5	0	8	0.75
P27695	APEX1	9	47.17	0.92	0.455	4	-1.05	5	0	8	0.1
Q92945	FUBP2	9	16.74	1.39	0.318	4	0.26	5	0	9	1.31
Q15111	PLCL1	9	13.33	4.38	0.067	4	-0.62	6	0	6	-0.15
P22626	ROA2	9	30.59	2.14	0.199	4	-0.72	6	0	8	0.14
P52209	6PGD	9	25.47	2.71	0.145	4	-0.54	6	0	9	0.24
Q9H2G2	SLK	9	14.33	1.14	0.38	4	-0.95	7	0	4	-0.04
Q9Y305	ACOT9	9	28.47	1.61	0.275	4	-1.41	7	0	5	0.75
O75116	ROCK2	9	7.85	1.38	0.322	4	-0.89	7	0	6	0.16
P04220	MUCB	9	34.78	1.66	0.267	4	-0.14	7	0	8	0.74
P28482	MK01	9	30.83	2.1	0.217	5	1.6	3	0	9	1.83
P30622	CLIP1	9	7.37	0.91	0.453	5	-0.05	3	0	9	0.99
P22102	PUR2	9	16.24	0.02	0.977	5	0.06	4	0	8	-0.1
P39059	COFA1	9	7.42	2.02	0.214	5	-0.35	4	0	9	0.6
P52788	SPSY	9	39.34	0.95	0.439	5	-0.71	5	0	7	-0.24
Q9Y2D5	AKAP2	9	22.58	4.85	0.056	5	-0.72	5	0	7	1.36
Q9BR76	COR1B	9	34.76	1.93	0.225	5	0.47	5	0	9	0.75
Q16401	PSMD5	9	24.01	0.76	0.509	5	1.11	5	0	9	1.38
Q9NQR4	NIT2	9	51.45	0.48	0.638	5	0.87	6	0	6	1.08
P35222	CTNB1	9	18.31	10.89	0.01	5	-1.64	6	0	7	0.79
Q05639	EF1A2	9	16.63	0.22	0.808	5	-0.01	6	0	7	0.24
P26196	DDX6	9	27.33	3.6	0.094	5	1.15	6	0	9	1.87
Q15113	PCOC1	9	30.73	2.12	0.201	5	-0.9	7	0	8	0.08
O75489	NDUS3	9	42.05	4.94	0.054	5	-0.4	7	0	9	0.98
P28161	GSTM2	9	48.17	0.43	0.668	5	0.04	8	0	6	-0.34
O94919	ENDD1	9	26.80	0.38	0.697	5	0.12	8	0	7	0.32
Q15691	MARE1	9	48.13	0.32	0.737	5	-0.21	8	0	8	0.03
P30043	BLVRB	9	65.53	1.93	0.226	6	0.52	6	0	7	0.01
P48444	COPD	9	22.70	2.2	0.192	6	-0.33	6	0	7	0.86
P24752	THIL	9	35.13	2.47	0.165	6	-0.45	6	0	8	0.56

P05141	ADT2	9	28.86	2.07	0.207	6	-0.39	6	0	8	0.67
P60228	EIF3E	9	23.37	1.12	0.386	6	-0.9	6	0	8	0.46
P55209	NP1L1	9	25.83	3.23	0.111	6	0.26	6	0	9	0.71
O43390	HNRPR	9	17.38	44.27	0	6	-1.18	6	0	9	0.64
P50552	VASP	9	30.00	0.43	0.669	6	-0.37	7	0	6	0.06
P16188	1A30	9	33.70	3.1	0.119	6	-0.84	7	0	7	-0.27
P62195	PRS8	9	32.76	0.2	0.824	6	-0.16	7	0	7	0.41
P10768	ESTD	9	51.42	3.04	0.123	6	0.26	7	0	8	1.03
Q9NY33	DPP3	9	21.71	2.31	0.18	6	-0.77	7	0	8	0.03
Q96IZ0	PAWR	9	47.65	1.07	0.4	6	-0.15	7	0	8	0.2
P05388	RLA0	9	41.96	0.14	0.868	6	0.14	7	0	9	0.23
Q15435	PP1R7	9	36.94	0.59	0.584	6	-0.49	8	0	6	0.22
P13861	KAP2	9	33.42	0.92	0.449	6	0.26	8	0	6	-0.49
P62879	GBB2	9	36.47	2.67	0.148	6	-0.53	8	0	7	0.22
Q53GG5	PDLI3	9	38.19	4.25	0.071	6	-0.64	8	0	9	0.11
Q92598	HS105	9	15.50	6.46	0.032	7	1.74	5	0	5	2.14
P50995	ANX11	9	19.60	2.54	0.159	7	-0.41	6	0	7	0.58
P01877	IGHA2	9	56.47	6.34	0.033	7	0.17	6	0	8	0.38
O00629	IMA4	9	34.74	2.87	0.133	7	-0.22	7	0	8	0.61
P61981	1433G	9	51.01	0.8	0.493	7	-0.67	7	0	9	0.01
P05413	FABPH	9	57.89	0.76	0.509	7	-0.42	8	0	8	0.25
P52907	CAZA1	9	52.45	5.24	0.048	7	-0.72	8	0	9	-0.09
Q92747	ARC1A	9	34.59	6.69	0.03	7	0.27	8	0	9	1.2
P01889	1B07	9	34.81	1.57	0.283	7	-0.54	9	0	8	-0.02
P51884	LUM	9	32.25	0.45	0.658	7	-0.26	9	0	9	-0.17
O94875	SRBS2	9	12.27	0.29	0.762	8	-0.46	3	0	7	0.15
P14550	AK1A1	9	44.92	2.02	0.213	8	0.42	7	0	8	0.9
Q01469	FABP5	9	64.44	3.23	0.112	8	1.21	7	0	8	1.51
P19105	ML12A	9	62.57	0.42	0.674	8	0.36	8	0	9	0.57
O14950	ML12B	9	62.21	0.42	0.674	8	0.36	8	0	9	0.57
P01861	IGHG4	9	44.04	0.09	0.917	8	0.1	9	0	7	-0.04
O00571	DDX3X	9	18.43	0.86	0.47	8	-0.32	9	0	9	0.42
P05387	RLA2	9	73.91	1.33	0.332	9	0.01	6	0	7	0.53
P02766	TTHY	9	68.71	5.55	0.043	9	1.12	8	0	9	0.9
Q13642	FHL1	9	34.67	2.33	0.179	9	0.19	9	0	9	-0.09
O15230	LAMA5	8	3.27	0	-1	0	-10	0	-10	8	10
P11586	C1TC	8	11.34	0.29	0.617	0	-10	5	0	6	0.25
P26640	SYVC	8	7.91	3.11	0.185	1	0.21	2	0	6	2.51
Q8N8S7	ENAH	8	17.43	0.62	0.595	1	-0.5	2	0	8	1.49
P28074	PSB5	8	33.08	3.09	0.155	1	-1.16	3	0	6	0.85
Q13219	PAPP1	8	7.93	0.61	0.599	1	0.42	3	0	7	1.49
P63096	GNAI1	8	26.84	3.81	0.086	1	-2.19	3	0	7	-0.27

P23246	SFPQ	8	15.70	2.2	0.206	1	-1.03	4	0	6	1.21
Q15063	POSTN	8	16.27	5.05	0.052	2	-0.05	3	0	8	1.33
P36776	LONM	8	12.83	0.72	0.557	2	-1.29	4	0	5	0.34
Q5SSJ5	HP1B3	8	17.72	6.45	0.032	2	-1.08	5	0	5	-0.15
Q6NUK1	SCMC1	8	21.17	2.34	0.177	2	-1.53	5	0	6	0.42
P62495	ERF1	8	21.97	5.79	0.04	2	-1.61	7	0	8	1.3
Q709C8	VP13C	8	3.30	44.02	0.006	3	-0.58	1	0	6	1.8
Q14008	CKAP5	8	4.87	0.16	0.855	3	0.63	3	0	7	0.65
Q14192	FHL2	8	32.26	1.5	0.296	3	-0.77	3	0	8	0.64
Q13464	ROCK1	8	8.27	0.17	0.848	3	-0.45	4	0	4	-0.34
P22059	OSBP1	8	20.82	0.74	0.517	3	-0.86	4	0	5	-0.89
P15144	AMPN	8	11.89	2.05	0.21	3	-0.59	4	0	7	1.15
P13727	PRG2	8	39.19	18.43	0.003	3	0.2	4	0	8	2.6
P48960	CD97	8	11.62	4.12	0.075	3	-0.56	5	0	7	0.81
Q9Y230	RUVB2	8	23.11	2.94	0.129	3	-1.58	5	0	7	0.36
P84095	RHOG	8	48.17	3.84	0.084	3	-0.95	5	0	8	0.04
Q8TD19	NEK9	8	11.75	5.02	0.052	3	-1.25	5	0	8	0.72
Q9NPQ8	RIC8A	8	18.27	21.53	0.003	3	-2.75	6	0	7	0.86
P02730	B3AT	8	12.73	3.94	0.081	3	-2.29	7	0	6	0.02
P09486	SPRC	8	31.35	1.1	0.391	3	-0.27	8	0	6	-0.37
P15121	ALDR	8	39.24	2.6	0.168	4	1.09	2	0	8	2.4
P31943	HNRH1	8	26.06	10.88	0.01	4	0.22	4	0	6	0.78
P08754	GNAI3	8	25.99	4.65	0.06	4	-1.48	4	0	7	0.06
P47897	SYQ	8	12.77	0.42	0.679	4	0.89	4	0	8	0.27
P61247	RS3A	8	31.06	5.54	0.043	4	-0.81	4	0	8	0.09
O60443	DFNA5	8	24.80	9.53	0.014	4	-1.16	5	0	5	0.19
Q08380	LG3BP	8	21.54	3.68	0.091	4	-0.95	5	0	6	1.4
P61106	RAB14	8	50.23	7.83	0.021	4	-0.93	5	0	6	-0.26
P62906	RL10A	8	36.87	1.11	0.39	4	-0.57	5	0	6	0.3
P02765	FETUA	8	33.79	0.63	0.566	4	0.43	5	0	8	0.3
P30085	KCY	8	47.45	1.22	0.359	4	-0.22	5	0	8	0.66
Q9P289	MST4	8	21.88	0.44	0.666	4	-0.19	6	0	6	0.34
O95810	SDPR	8	25.65	3.7	0.09	4	-1.2	6	0	7	-0.29
P20618	PSB1	8	42.74	1.68	0.264	4	-0.16	6	0	8	0.55
Q13131	AAPK1	8	21.11	3.95	0.08	4	-0.86	7	0	6	1.12
Q14247	SRC8	8	20.73	0.06	0.938	4	-0.11	7	0	7	0.01
Q00325	MPCP	8	23.76	2.54	0.159	4	-1.34	8	0	6	-0.11
Q9UBG0	MRC2	8	10.21	1.02	0.415	5	-0.39	3	0	6	0.47
P04179	SODM	8	72.52	4.29	0.07	5	0.91	3	0	7	1.38
Q13423	NNTM	8	11.88	0.48	0.641	5	0.64	4	0	6	0.63
P09651	ROA1	8	22.04	1.23	0.357	5	-0.2	4	0	7	0.45
P08294	SODE	8	54.17	1.29	0.341	5	-0.39	4	0	8	0.98

P31937	3HIDH	8	26.79	0.32	0.736	5	0.19	5	0	6	0.5
O95831	AIFM1	8	21.86	0.31	0.741	5	0.6	5	0	7	0.8
Q04760	LGUL	8	46.74	4.55	0.063	5	0.22	5	0	7	1.79
P30740	ILEU	8	29.02	6.41	0.032	5	-0.51	5	0	8	1.32
P63241	IF5A1	8	46.10	1.55	0.286	5	0.21	6	0	7	0.72
P51991	ROA3	8	23.02	17.09	0.003	5	-1.4	6	0	7	0.05
O15143	ARC1B	8	33.33	31.76	0.001	5	0.3	6	0	7	1.59
P48506	GSH1	8	18.52	0.48	0.643	5	-0.59	6	0	7	0.14
Q9Y265	RUVB1	8	25.88	0.63	0.563	5	-0.65	6	0	8	0.05
Q16795	NDUA9	8	29.44	0.51	0.625	5	-0.43	6	0	8	0.18
P60900	PSA6	8	35.37	0.81	0.49	5	-0.67	7	0	6	0.41
P40123	CAP2	8	27.46	1.31	0.338	5	-0.12	7	0	7	0.88
Q96AG4	LRC59	8	41.37	2.13	0.201	5	0.34	7	0	8	0.17
P05534	1A24	8	32.60	4.16	0.073	5	-0.8	8	0	5	-0.8
Q9BQS8	FYCO1	8	9.95	0.34	0.726	6	0.08	3	0	6	0.53
Q14194	DPYL1	8	23.95	1.65	0.269	6	0.71	3	0	6	0.44
Q96TA1	NIBL1	8	20.24	1.51	0.294	6	-0.03	3	0	8	0.76
P42765	THIM	8	32.24	0.02	0.978	6	-0.05	4	0	6	0.05
P67775	PP2AA	8	36.89	0.88	0.463	6	0	5	0	7	0.53
P62714	PP2AB	8	36.89	0.9	0.457	6	0.17	5	0	7	0.63
P09936	UCHL1	8	46.64	0.51	0.625	6	-0.44	5	0	7	0.41
P11766	ADHX	8	35.29	0.56	0.601	6	0.02	6	0	7	0.19
P41091	IF2G	8	25.21	1.71	0.259	6	0.27	6	0	7	0.5
Q9UBX5	FBLN5	8	24.55	1.11	0.388	6	-0.22	6	0	7	0.66
Q15404	RSU1	8	53.79	2.2	0.192	6	-0.33	6	0	8	0.33
P28066	PSA5	8	51.87	3.61	0.094	6	-0.57	6	0	8	0.74
Q96FW1	OTUB1	8	34.69	0.56	0.597	6	0.09	6	0	8	0.34
P13591	NCAM1	8	13.17	11.89	0.008	6	0.54	7	0	5	-0.69
P50570	DYN2	8	13.79	0.07	0.935	6	0.13	7	0	7	0.12
P00568	KAD1	8	47.42	0.23	0.804	6	0.04	7	0	8	0.17
P51452	DUS3	8	57.84	1.18	0.37	6	-0.43	8	0	7	0.32
Q15436	SC23A	8	15.42	1.6	0.277	7	0.41	5	0	7	0.62
P30711	GSTT1	8	31.25	1.03	0.413	7	-0.88	6	0	6	-0.36
Q9NZU5	LMCD1	8	28.77	1.63	0.272	7	0.16	6	0	6	0.63
Q13555	KCC2G	8	25.63	0.81	0.487	7	0.13	6	0	8	0.83
P61160	ARP2	8	28.93	0.21	0.814	7	0.12	7	0	8	0.4
O95336	6PGL	8	48.84	1.38	0.321	7	-0.15	8	0	7	0.21
Q04826	1B40	8	34.81	6.68	0.03	7	-0.94	8	0	8	-0.35
P18085	ARF4	8	52.22	5.64	0.042	7	0.41	8	0	8	0.47
P21589	5NTD	7	15.51	0	-1	0	-10	0	-10	7	10
P05164	PERM	7	11.14	0	-1	0	-10	0	-10	7	10
O76094	SRP72	7	17.29	0.21	0.681	0	-10	3	0	6	0.74

Q7Z7G0	TARSH	7	8.37	1.75	0.277	0	-10	6	0	2	-1.9
Q92900	RENT1	7	9.74	1.39	0.348	1	-0.37	3	0	7	1.7
Q15008	PSMD6	7	22.11	2.65	0.149	1	-0.95	4	0	7	1.26
Q9Y5S2	MRCKB	7	5.79	0.61	0.598	1	-1.72	6	0	3	0.36
P01031	CO5	7	6.32	0.45	0.659	2	-0.27	2	0	7	1.01
Q9H2D6	TARA	7	3.59	3.42	0.102	2	-1.27	3	0	5	0.5
Q02978	M2OM	7	23.89	6.5	0.031	2	-0.28	3	0	7	2.55
P48668	K2C6C	7	15.60	2.26	0.2	2	-1.32	4	0	4	0.39
P02538	K2C6A	7	15.60	2.26	0.2	2	-1.32	4	0	4	0.39
Q16270	IBP7	7	36.17	0.19	0.83	2	-0.3	4	0	5	0.07
Q9ULA0	DNPEP	7	25.68	7.29	0.033	2	1.83	4	0	5	2.22
Q99873	ANM1	7	23.27	1.02	0.426	2	-1.75	4	0	6	-0.4
Q9UQ80	PA2G4	7	23.10	5.85	0.049	2	-3.21	4	0	6	-0.74
P40261	NNMT	7	43.18	3.15	0.116	2	-1.57	4	0	7	0.6
P39019	RS19	7	31.03	2.68	0.147	2	-0.38	4	0	7	0.91
Q92841	DDX17	7	13.69	1.1	0.415	2	0.26	4	0	7	1.6
P05455	LA	7	22.55	7.05	0.027	2	-2.36	5	0	6	0.28
O94905	ERLN2	7	29.20	2.96	0.128	2	-1.49	5	0	7	0.35
P04275	VWF	7	3.20	6.1	0.046	2	-1.39	6	0	6	0.24
P09382	LEG1	7	70.37	7.21	0.025	2	-1.32	6	0	7	0.39
Q14766	LTBP1	7	6.80	0	-1	3	10	0	-10	6	10
O15031	PLXB2	7	6.42	0.84	0.483	3	0.06	2	0	6	1.23
O94855	SC24D	7	12.11	0.4	0.686	3	-0.14	3	0	3	0.63
Q9UEY8	ADDG	7	14.87	1.24	0.381	3	-0.6	3	0	5	0.58
P08779	K1C16	7	16.91	0.31	0.756	3	-0.88	3	0	5	0.01
A0AVT1	UBA6	7	8.17	0.95	0.44	3	-0.44	3	0	6	0.99
P12081	SYHC	7	17.49	12.33	0.007	3	-0.8	3	0	7	1.46
Q12884	SEPR	7	12.24	0.2	0.827	3	-0.51	3	0	7	0.24
Q86UY8	NT5D3	7	15.88	0.09	0.919	3	0.17	4	0	4	0.25
P17252	KPCA	7	18.45	1.66	0.267	3	0.01	4	0	5	1.01
Q13724	MOGS	7	12.54	1.85	0.236	3	-0.88	4	0	5	0.23
P04259	K2C6B	7	14.36	2.29	0.197	3	-1.41	4	0	5	0.25
P04003	C4BPA	7	14.24	11.5	0.009	3	-0.52	4	0	6	0.64
P54577	SYYC	7	15.91	5.66	0.042	3	-2.33	4	0	7	0.65
P62333	PRS10	7	23.91	0.44	0.666	3	-0.56	5	0	5	-0.38
A0FGR8	ESYT2	7	11.40	0.21	0.82	3	0.22	5	0	5	0.04
O00154	BACH	7	26.58	0.11	0.897	3	-0.41	5	0	5	0.02
Q9NZ08	ERAP1	7	8.93	3.5	0.112	3	-1.54	5	0	5	-1.45
P53992	SC24C	7	9.05	1.57	0.282	3	-0.99	5	0	5	0.31
Q12792	TWF1	7	36.00	1.78	0.248	3	-0.28	5	0	6	0.24
P04632	CPNS1	7	38.06	0.39	0.691	3	-0.42	5	0	6	-0.05
P37837	TALDO	7	23.44	2.09	0.205	3	-0.66	5	0	6	0.35

Q9UNM6	PSD13	7	25.27	2.05	0.21	3	-0.39	5	0	6	1.14
Q8WVM8	SCFD1	7	18.85	2.53	0.16	3	-1.58	6	0	4	0.31
P25311	ZA2G	7	33.89	2.12	0.201	3	-0.18	7	0	6	1.53
Q32MZ4	LRRF1	7	14.48	0.61	0.577	4	1.07	2	0	6	0.64
Q86UE4	LYRIC	7	15.12	0.3	0.756	4	-0.66	3	0	5	-0.64
Q7Z4H8	KDEL2	7	21.89	0.41	0.683	4	-0.16	3	0	5	-0.8
P55735	SEC13	7	40.37	19.66	0.002	4	0.75	3	0	6	0.69
Q14103	HNRPD	7	14.08	1.61	0.276	4	-0.59	4	0	5	0.41
Q6IBS0	TWF2	7	31.23	8.59	0.017	4	0.19	4	0	6	0.88
P10909	CLUS	7	21.83	2.05	0.21	4	-0.92	4	0	7	-0.04
P60953	CDC42	7	42.41	2.71	0.145	4	-1.76	4	0	7	-0.1
Q16658	FSCN1	7	19.47	14.84	0.005	4	-0.3	4	0	7	0.92
Q7L2H7	EIF3M	7	25.94	0.33	0.732	4	-0.21	5	0	4	0.77
P55010	IF5	7	23.90	0.6	0.58	4	-0.2	5	0	4	0.3
P53396	ACLY	7	10.45	0.96	0.436	4	0.03	5	0	6	0.6
P10155	RO60	7	17.66	1.06	0.412	4	-1.7	5	0	6	-0.06
O94874	UFL1	7	11.21	7.37	0.032	4	-1.06	5	0	6	0.52
P48047	ATPO	7	45.54	4.19	0.073	4	-0.46	5	0	7	0.21
Q9UNZ2	NSF1C	7	27.03	0.78	0.502	4	-0.25	5	0	7	0.16
Q04637	IF4G1	7	6.38	5.14	0.061	4	-0.07	5	0	7	1.05
Q99829	CPNE1	7	16.57	1.45	0.306	4	-0.5	5	0	7	0.42
P52272	HNRPM	7	12.60	13.87	0.006	4	-1.21	6	0	4	0.79
P09429	HMGB1	7	34.88	3.31	0.107	4	-0.98	6	0	5	0
Q15257	PTPA	7	30.45	0.7	0.532	4	-0.68	6	0	5	-0.46
P19827	ITIH1	7	10.54	0.26	0.779	4	-0.18	6	0	6	0.2
P05155	IC1	7	17.80	1.43	0.31	4	0.05	6	0	6	1.26
O14818	PSA7	7	38.71	2.28	0.184	4	-0.56	6	0	7	0.4
Q9Y3A5	SBDS	7	40.40	0.1	0.908	5	0.09	3	0	6	0.21
P20591	MX1	7	18.13	11.49	0.009	5	-0.05	4	0	1	-2.11
Q9BZV1	UBXN6	7	29.93	0.79	0.498	5	-0.59	4	0	4	-1.03
P00441	SODC	7	64.29	3.11	0.119	5	0.88	4	0	6	0.89
Q15046	SYK	7	14.91	1.72	0.256	5	-1.15	4	0	6	0.05
P19623	SPEE	7	40.40	0.15	0.861	5	0.29	4	0	6	-0.05
Q9UBQ7	GRHPR	7	37.20	0.17	0.85	5	0.19	4	0	7	0.03
Q14847	LASP1	7	38.31	0.69	0.538	5	0.27	4	0	7	0.58
Q08431	MFGM	7	24.81	1.17	0.384	5	0.61	5	0	5	0.22
Q9BWM7	SFXN3	7	32.00	2.18	0.194	5	-1.01	5	0	6	0.35
Q15366	PCBP2	7	29.59	1.79	0.245	5	0.11	5	0	6	0.59
P55884	EIF3B	7	13.64	2.66	0.149	5	-0.32	5	0	6	0.45
Q9UNF0	PACN2	7	16.67	1.4	0.316	5	-1.73	5	0	6	-0.73
O43813	LANC1	7	27.57	2.98	0.126	5	0.13	5	0	7	0.99
P62826	RAN	7	36.11	2.59	0.155	5	-0.44	5	0	7	0.17

P12268	IMDH2	7	22.76	4.56	0.062	5	0.92	5	0	7	1.91
P11464	PSG1	7	21.96	0.04	0.965	5	-0.01	5	0	7	-0.21
P61019	RAB2A	7	45.75	3.27	0.11	5	-0.37	6	0	7	0.54
P17066	HSP76	7	13.84	3.76	0.087	5	-0.51	6	0	7	0.07
Q9Y277	VDAC3	7	32.16	15.83	0.004	5	-1.22	6	0	7	-0.18
P15531	NDKA	7	47.37	1.97	0.22	5	-1.8	6	0	7	0.02
A5A3E0	POTEF	7	7.81	1.57	0.282	5	-0.43	7	0	6	0.02
Q9NSD9	SYFB	7	14.94	1.75	0.266	6	-0.58	3	0	6	0.76
P06748	NPM	7	38.44	0.21	0.817	6	0.58	3	0	7	0.59
Q9NQW7	XPP1	7	18.78	3.55	0.096	6	-0.6	4	0	7	0.25
P36405	ARL3	7	50.00	3.22	0.112	6	-0.23	4	0	7	0.69
Q96I99	SUCB2	7	25.00	1.29	0.341	6	-0.48	5	0	6	0.12
P20073	ANXA7	7	21.11	1.88	0.232	6	-0.68	5	0	7	-0.06
P22392	NDKB	7	44.08	0.89	0.458	6	-0.96	5	0	7	0.1
Q8IWE2	NXP20	7	19.18	0.13	0.878	6	-0.33	6	0	5	-0.11
P30488	1B50	7	30.94	5.16	0.05	6	-1.13	6	0	5	-0.91
P30487	1B49	7	30.94	5.16	0.05	6	-1.13	6	0	5	-0.91
Q16836	HCDH	7	39.49	0.17	0.851	6	0.23	6	0	7	0.27
O75368	SH3L1	7	84.21	3.39	0.104	6	0.53	6	0	7	0.57
Q00839	HNRPU	7	10.79	4.19	0.073	6	0.23	6	0	7	0.91
P61224	RAP1B	7	42.39	1.8	0.244	6	-0.27	7	0	7	0.35
P62834	RAP1A	7	42.39	3.64	0.092	6	-0.22	7	0	7	0.51
P62158	CALM	7	59.06	5.44	0.045	7	0.98	4	0	6	1.08
P01834	IGKC	7	82.08	1.32	0.336	7	-0.17	7	0	7	0.01
P30048	PRDX3	7	48.05	1.86	0.236	7	0.56	7	0	7	0.41
P02763	A1AG1	7	40.80	2.06	0.208	7	0.49	7	0	7	0.78
P35555	FBN1	6	3.03	0	-1	0	-10	0	-10	6	10
P05783	K1C18	6	16.28	0	-1	0	-10	0	-10	6	10
P00746	CFAD	6	42.29	2.42	0.195	0	-10	2	0	6	0.73
O60271	JIP4	6	9.24	146.97	0.058	1	0	1	0	4	2.7
P13807	GYS1	6	10.18	48.99	0.02	1	2.32	1	0	6	2.72
P46976	GLYG	6	16.57	20.4	0.018	1	-0.29	1	0	6	1.8
O75165	DJC13	6	3.74	22.35	0.016	1	-1	2	0	5	1.6
Q14118	DAG1	6	11.96	3.4	0.17	1	-1.53	2	0	6	0.34
Q9C0C2	TB182	6	5.61	0.3	0.759	1	-1	3	0	4	-0.25
P63000	RAC1	6	30.73	3.29	0.123	1	-2.19	3	0	5	-0.2
Q15386	UBE3C	6	7.39	5.64	0.052	1	0.95	3	0	5	1.39
Q9UJS0	CMC2	6	12.00	0.35	0.729	1	1.18	3	0	6	0.85
Q16643	DREB	6	15.56	4.66	0.09	1	-2.39	4	0	6	0.76
Q12904	AIMP1	6	33.01	1.64	0.283	1	-1.39	4	0	6	-0.91
Q13510	ASAH1	6	20.51	1.65	0.378	2	-1	1	0	4	1.23
Q9UJZ1	STML2	6	27.25	1.53	0.32	2	-0.58	2	0	5	1.48

P17174	AATC	6	24.94	0.07	0.937	2	-0.45	2	0	5	-0.2
P29144	TPP2	6	8.41	0.69	0.544	2	-0.4	2	0	5	0.64
P43490	NAMPT	6	21.79	8.72	0.017	2	-0.51	2	0	6	0.59
O75534	CSDE1	6	12.53	2.02	0.227	2	-0.27	3	0	4	1.28
P43686	PRS6B	6	25.84	0.27	0.772	2	0.39	3	0	4	0.6
P43243	MATR3	6	12.16	9.63	0.019	2	-0.13	3	0	5	1.22
Q9HDC9	APMAP	6	22.12	28.22	0.001	2	-0.69	3	0	6	1.24
P54619	AAKG1	6	24.77	2.57	0.17	2	-1.38	4	0	4	0
P30084	ECHM	6	32.41	3.21	0.113	2	-0.33	4	0	5	1.37
Q96C19	EFHD2	6	27.50	0.95	0.437	2	-1.01	4	0	5	0.32
Q9UJW0	DCTN4	6	21.74	5.88	0.064	2	-2.19	4	0	6	0.11
P16402	H13	6	15.38	2.27	0.22	2	-2.54	4	0	6	0.51
P16403	H12	6	15.96	2.27	0.22	2	-2.54	4	0	6	0.51
P10412	H14	6	15.53	2.27	0.22	2	-2.54	4	0	6	0.51
P06703	S10A6	6	47.78	1.78	0.26	2	0.01	5	0	4	-1.25
P51148	RAB5C	6	37.50	2.42	0.169	2	-0.93	5	0	5	0.88
P62979	RS27A	6	41.67	0.02	0.979	2	0.05	5	0	5	0.11
O14579	COPE	6	24.35	6.94	0.036	2	-1.89	5	0	6	0.06
Q13838	DX39B	6	17.99	4.57	0.093	2	1.28	5	0	6	2.71
P16435	NCPR	6	13.74	2.22	0.225	3	1.64	1	0	5	2.38
P22061	PIMT	6	45.81	0.29	0.758	3	-0.34	2	0	4	0.32
P35858	ALS	6	16.36	0.28	0.772	3	-0.26	2	0	4	0.5
P36269	GGT5	6	18.09	0.73	0.537	3	0.9	2	0	4	1.5
P13693	TCTP	6	35.47	0.95	0.44	3	0.5	2	0	5	0.81
Q9BT78	CSN4	6	21.43	3.85	0.148	3	-2.08	2	0	6	0.03
Q9NUQ9	FA49B	6	24.69	8.49	0.018	3	-1.44	3	0	4	0.72
O75436	VP26A	6	25.99	0.44	0.664	3	-0.29	3	0	4	0.01
P56192	SYMC	6	12.89	1.36	0.337	3	-0.21	3	0	5	0.49
Q96A65	EXOC4	6	9.65	3.12	0.132	3	0.44	3	0	5	2.26
P22234	PUR6	6	19.76	9.96	0.012	3	1.32	3	0	6	1.86
Q9UNF1	MAGD2	6	19.31	1.45	0.307	3	-1.07	3	0	6	-0.3
P32455	GBP1	6	11.82	2.43	0.169	3	-1.65	3	0	6	-0.49
P27144	KAD4	6	44.84	0.52	0.623	3	-0.3	3	0	6	0.53
Q7Z5L7	PODN	6	13.70	4.03	0.078	3	-0.28	3	0	6	1.99
Q96CW1	AP2M1	6	17.70	0.4	0.684	3	-0.2	4	0	4	0.63
P25789	PSA4	6	40.23	0.9	0.463	3	-0.17	4	0	5	1.12
P25325	THTM	6	37.37	1.07	0.399	3	-0.68	4	0	5	0.42
P35613	BASI	6	18.44	1.45	0.307	3	0.36	4	0	5	0.94
Q9Y2Q3	GSTK1	6	34.96	0.89	0.499	3	-0.9	4	0	5	0.89
Q9BYX7	ACTBM	6	23.47	0.86	0.471	3	-0.34	4	0	5	-0.03
P21810	PGS1	6	23.91	3.99	0.079	3	-1.42	4	0	5	0.45
P68036	UB2L3	6	63.64	1.1	0.391	3	-0.31	4	0	6	0.48

P55290	CAD13	6	11.64	2.05	0.21	3	0.17	4	0	6	0.99
Q9Y2J2	E41L3	6	9.57	3.84	0.098	3	-0.89	4	0	6	1.2
Q9UFN0	NPS3A	6	31.58	5.52	0.044	3	0.89	4	0	6	1.23
Q9NP72	RAB18	6	37.86	27.43	0.001	3	-1.38	5	0	4	-0.09
Q9Y6G9	DC1L1	6	18.16	5.06	0.052	3	-1.23	5	0	4	-0.28
Q86UX2	ITIH5	6	8.70	4.28	0.083	3	-0.84	5	0	4	0.1
P00918	CAH2	6	32.31	1.6	0.277	3	-0.77	5	0	5	-0.08
Q14914	PTGR1	6	30.09	0.83	0.481	3	-0.89	5	0	5	0.96
P02786	TFR1	6	10.13	11	0.01	3	-3.07	5	0	5	-0.08
P30520	PURA2	6	19.52	4.76	0.058	3	-1.3	5	0	5	-0.12
P46781	RS9	6	22.68	0.08	0.926	3	-0.25	5	0	5	-0.09
Q9Y5X1	SNX9	6	17.48	2.45	0.167	3	-0.94	5	0	6	0.75
O75947	ATP5H	6	52.80	1.13	0.382	3	-0.23	5	0	6	1.02
P17931	LEG3	6	28.40	0.91	0.452	3	-1.17	5	0	6	-0.3
Q8TBC4	UBA3	6	25.05	1.58	0.28	4	0.55	2	0	3	1.92
Q66K74	MAP1S	6	9.44	0.68	0.543	4	-0.07	2	0	6	0.82
P13798	ACPH	6	11.48	0.43	0.673	4	-0.03	3	0	4	0.9
P07339	CATD	6	22.33	0.61	0.572	4	-0.57	3	0	5	0.19
P00966	ASSY	6	17.23	0.32	0.74	4	0.61	3	0	5	0.75
Q13616	CUL1	6	12.76	0.05	0.952	4	0.18	3	0	5	0.25
O43175	SERA	6	14.63	0.04	0.961	4	0.27	3	0	5	0.25
P39023	RL3	6	22.08	0.33	0.731	4	-0.14	3	0	5	0.76
Q9P0V9	41527	6	22.69	0.22	0.806	4	0.19	3	0	5	0.33
Q9BXS5	AP1M1	6	20.57	0.11	0.901	4	0.65	3	0	5	0.28
Q7Z434	MAVS	6	22.22	2.79	0.139	4	0.45	3	0	6	0.99
Q4L180	FIL1L	6	6.17	2.3	0.182	4	-0.21	3	0	6	0.52
Q07021	C1QBP	6	36.88	2.82	0.137	4	-1.09	4	0	4	-0.34
P38606	VATA	6	17.02	3.98	0.079	4	1.39	4	0	5	1.65
Q13310	PABP4	6	11.96	1.26	0.35	4	-0.71	4	0	5	0.32
Q9H993	CF211	6	16.10	0.68	0.541	4	-0.33	4	0	5	0.62
P00748	FA12	6	16.75	1.89	0.264	4	-0.87	4	0	5	-0.61
P0CG39	POTEJ	6	7.42	1.21	0.361	4	-1.2	4	0	5	-0.4
P41250	SYG	6	12.99	0.31	0.741	4	-0.04	4	0	6	0.74
P62241	RS8	6	37.98	4.94	0.054	4	-0.15	4	0	6	0.57
O43488	ARK72	6	27.02	7.34	0.024	4	0.12	4	0	6	1.61
P19652	A1AG2	6	39.80	0.87	0.466	4	0.94	4	0	6	1.48
P07203	GPX1	6	42.86	1.29	0.354	4	-0.95	5	0	3	-0.28
O60841	IF2P	6	8.52	1.88	0.232	4	-0.95	5	0	4	0.65
P36957	ODO2	6	17.66	2.67	0.148	4	-0.86	5	0	5	-0.16
P30050	RL12	6	54.55	0.55	0.601	4	-0.3	5	0	6	-0.37
P55036	PSMD4	6	27.59	0.73	0.522	4	-0.28	5	0	6	0.16
O75351	VPS4B	6	23.20	1.73	0.255	4	-0.43	5	0	6	0.49

Q13126	MTAP	6	37.10	1.27	0.347	4	-0.24	6	0	4	0.21
Q9BXN1	ASPN	6	24.21	5.59	0.043	4	-1.67	6	0	5	-0.42
P25786	PSA1	6	30.42	1.96	0.221	4	0.07	6	0	5	0.65
P50213	IDH3A	6	21.31	2.63	0.151	4	-0.48	6	0	5	0.72
P30040	ERP29	6	22.99	0.06	0.944	4	0.16	6	0	5	0.07
Q8TDQ7	GNPI2	6	44.93	1.52	0.292	5	1.01	2	0	6	1.08
Q13263	TIF1B	6	18.68	1.56	0.315	5	-0.95	3	0	4	-1.98
Q9HB71	CYBP	6	36.84	5.41	0.045	5	1.33	3	0	5	2.5
Q13557	KCC2D	6	19.44	0.87	0.465	5	0.43	3	0	5	0.77
Q9NSE4	SYIM	6	7.61	0.8	0.492	5	0.57	3	0	6	1.15
O43681	ASNA	6	32.18	0.28	0.767	5	0.11	3	0	6	0.73
Q9BR39	JPH2	6	11.78	0.08	0.929	5	0.21	4	0	5	0.2
P07741	APT	6	48.33	1.06	0.402	5	-0.25	4	0	5	0.54
Q15293	RCN1	6	20.24	1.2	0.364	5	-1.21	4	0	6	0.13
O14498	ISLR	6	20.79	2.5	0.162	5	0.43	4	0	6	0.98
Q9NTK5	OLA1	6	24.24	2.93	0.129	5	-0.29	5	0	4	1.09
O43396	TXNL1	6	26.64	0.67	0.547	5	-0.23	5	0	4	0.21
P59998	ARPC4	6	47.62	0.64	0.559	5	-0.55	5	0	4	0.31
A6NHL2	TBAL3	6	8.30	0.18	0.842	5	-0.55	5	0	4	-0.26
P11908	PRPS2	6	29.87	2.64	0.151	5	-1.32	5	0	6	0.21
Q92896	GSLG1	6	7.63	1.4	0.329	5	0.21	5	0	6	0.34
P61088	UBE2N	6	46.71	0.1	0.909	5	0.19	5	0	6	0.12
P52565	GDIR1	6	31.86	0.6	0.579	5	-0.22	6	0	4	-0.23
P02760	AMBP	6	21.88	0.1	0.905	5	0.31	6	0	5	0.02
O95865	DDAH2	6	37.89	0.86	0.469	5	0.12	6	0	6	0.36
P04004	VTNC	6	19.87	3.36	0.105	5	0.41	6	0	6	0.74
P08134	RHOC	6	33.16	0.18	0.837	5	0.14	6	0	6	0.03
P61586	RHOA	6	33.16	0.15	0.865	5	0.03	6	0	6	-0.12
Q03013	GSTM4	6	29.36	9.12	0.015	6	1.58	3	0	4	0.53
P52294	IMA1	6	16.17	1.5	0.296	6	-0.84	4	0	4	-0.4
P15374	UCHL3	6	36.09	1.45	0.306	6	-0.71	5	0	4	-0.14
P26599	PTBP1	6	22.41	0.65	0.554	6	0.11	5	0	5	0.55
P09972	ALDOC	6	17.86	3.95	0.08	6	0.69	5	0	6	0.22
P25787	PSA2	6	38.46	0.11	0.893	6	0.04	5	0	6	0.16
P84085	ARF5	6	42.22	5.49	0.044	6	0.38	5	0	6	0.37
P37235	HPCL1	6	35.23	4.67	0.06	6	-0.85	6	0	6	0.58
P10599	THIO	6	57.14	2.36	0.176	6	-0.12	6	0	6	0.73
P42704	LPPRC	5	4.88	0	-1	0	-10	0	-10	5	10
Q27J81	INF2	5	6.73	0.9	0.443	0	-10	1	0	5	0.78
Q9Y6F6	MRVI1	5	8.25	0.01	0.931	0	-10	2	0	3	0.11
Q9NSB2	KRT84	5	10.33	0	-1	0	-10	3	0	2	-0.42
Q4G0F5	VP26B	5	16.07	0.2	0.697	0	-10	3	0	3	-0.63

Q8IWA5	CTL2	5	9.77	1.27	0.323	0	-10	3	0	4	0.89
Q9UBQ0	VPS29	5	39.56	3.64	0.153	0	-10	3	0	4	1.57
P42226	STAT6	5	8.85	0.39	0.577	0	-10	3	0	5	0.71
Q8NBJ5	GT251	5	9.97	8.77	0.035	1	-1.45	1	0	5	0.95
Q03001	DYST	5	1.37	1.62	0.382	1	0.58	2	0	3	-0.5
P42566	EPS15	5	8.26	3.06	0.247	1	-1	2	0	4	1.95
Q99733	NP1L4	5	17.07	2.56	0.157	1	0.24	2	0	5	1.4
Q14165	MLEC	5	17.81	64.67	0.001	1	-1.88	2	0	5	0.81
P19525	E2AK2	5	12.16	17.37	0.022	1	-1.48	3	0	3	0.21
Q8NE71	ABCF1	5	6.51	0.37	0.728	1	-0.66	3	0	3	-0.87
P29966	MARCS	5	34.94	1.29	0.342	1	-1.38	3	0	4	0.06
P02649	APOE	5	24.61	2.2	0.258	1	-1.67	3	0	4	1.13
Q9BRF8	CPPED	5	24.20	0	1	1	0	3	0	4	0.03
P36542	ATPG	5	19.13	0.84	0.477	1	-1.53	3	0	4	-0.3
Q9BVG4	CX026	5	26.18	1.78	0.309	1	-2.16	3	0	4	-1.05
Q9P2B2	FPRP	5	8.42	0.08	0.926	1	-0.27	3	0	4	-0.48
Q96N66	MBOA7	5	14.62	0.49	0.645	1	-1.11	3	0	4	0.48
Q13404	UB2V1	5	32.65	0.46	0.655	1	-1.33	3	0	4	-0.41
P27105	STOM	5	23.96	12.16	0.02	1	-2.04	3	0	5	1.91
Q14019	COTL1	5	48.59	22.16	0.003	1	0.79	3	0	5	3.6
P17844	DDX5	5	10.10	1.36	0.355	1	-1.89	3	0	5	-0.5
P49023	PAXI	5	15.40	0.79	0.56	1	-1.44	4	0	1	-1.44
Q8TE77	SSH3	5	14.42	0.16	0.857	1	-0.51	4	0	3	-0.3
O60504	VINEX	5	11.62	2.64	0.165	1	-0.77	4	0	3	1.06
O00303	EIF3F	5	19.89	0.4	0.69	1	-0.45	4	0	4	0.03
Q9UHB6	LIMA1	5	10.67	1.82	0.303	2	0.79	1	0	4	1.86
Q5VT25	MRCKA	5	5.31	0.38	0.711	2	-0.5	1	0	4	0.53
P00325	ADH1B	5	18.67	0.57	0.604	2	-0.71	1	0	5	0.89
Q03591	FHR1	5	20.61	2.51	0.197	2	1.2	1	0	5	0.9
Q99426	TBCB	5	34.43	0.35	0.727	2	-0.2	2	0	2	-0.03
P34949	MPI	5	14.42	0.46	0.661	2	0.1	2	0	3	1.16
P49755	TMEDA	5	22.37	0.13	0.883	2	-0.14	2	0	3	-0.34
Q96RF0	SNX18	5	9.71	1.77	0.311	2	0.17	2	0	3	0.75
Q9Y262	EIF3L	5	12.41	0.48	0.641	2	-0.09	2	0	4	0.42
P00736	C1R	5	10.78	3.55	0.11	2	-1.49	2	0	4	0.2
O95219	SNX4	5	14.89	0.01	0.995	2	0.05	2	0	4	0
P15170	ERF3A	5	16.83	0.5	0.64	2	-0.13	2	0	4	-0.78
P29590	PML	5	10.20	7.2	0.047	2	-1.17	2	0	4	0.79
P52597	HNRPF	5	19.52	3.93	0.081	2	0.37	2	0	5	1.02
P50453	SPB9	5	13.83	5.67	0.096	2	0.58	2	0	5	2.41
P98082	DAB2	5	10.65	6.35	0.057	2	-1.14	2	0	5	0.57
P62269	RS18	5	25.00	11.64	0.009	2	0.04	2	0	5	1.33

P26373	RL13	5	22.75	7.65	0.022	2	0.49	2	0	5	1.33
O60493	SNX3	5	27.78	0.88	0.471	2	-0.57	2	0	5	0.25
Q9Y6Q2	STON1	5	7.89	0.12	0.894	2	-0.97	3	0	1	-0.38
O95967	FBLN4	5	17.83	1.02	0.416	2	-1.24	3	0	3	0.15
Q02790	FKBP4	5	18.95	3.62	0.127	2	-2.08	3	0	3	-0.88
Q15819	UB2V2	5	37.93	0.25	0.785	2	-1.05	3	0	3	-0.85
Q8NCA5	FA98A	5	14.26	5.79	0.04	2	-2.2	3	0	4	0.17
O00264	PGRC1	5	32.82	2.39	0.172	2	-1.15	3	0	4	-0.17
Q9HAV0	GBB4	5	16.18	2.95	0.128	2	-0.89	3	0	4	0.12
Q8IUX7	AEBP1	5	5.27	5.64	0.068	2	-2.08	3	0	4	-0.26
Q9NUU7	DD19A	5	10.04	0.85	0.491	2	0.71	3	0	5	1.66
P62249	RS16	5	30.14	1.33	0.332	2	-0.24	3	0	5	0.62
Q9NR46	SHLB2	5	16.20	1.45	0.319	2	-1.12	3	0	5	0.67
Q13586	STIM1	5	9.93	4.65	0.06	2	-1.33	4	0	3	-0.14
Q6BCY4	NB5R2	5	33.70	2.42	0.184	2	-0.54	4	0	3	-1.39
P21281	VATB2	5	14.29	10.05	0.018	2	0.75	4	0	3	1.51
Q9H8Y8	GORS2	5	19.91	0.5	0.631	2	-0.24	4	0	4	0.2
Q8WUD1	RAB2B	5	32.87	5.52	0.044	2	-0.71	4	0	4	0.59
O15371	EIF3D	5	9.31	4.58	0.122	2	-0.94	4	0	4	1.68
Q92629	SGCD	5	23.18	0.55	0.601	2	-0.53	4	0	4	-0.07
P35914	HMGCL	5	20.92	1.5	0.326	2	-0.73	4	0	5	0.87
Q14444	CAPR1	5	12.83	0.07	0.936	2	0.4	4	0	5	0.41
P78417	GSTO1	5	25.31	0.43	0.672	2	-0.55	4	0	5	0.19
P30566	PUR8	5	19.21	1.06	0.403	2	-1.33	5	0	3	-0.15
O43301	HS12A	5	9.93	0.58	0.595	2	-0.61	5	0	4	-0.14
O60313	OPA1	5	7.71	1.15	0.379	2	-1.27	5	0	4	-0.07
P20774	MIME	5	23.83	1.52	0.324	2	-2.83	5	0	5	-2.14
P35625	TIMP3	5	24.64	0.71	0.537	2	-1.51	5	0	5	0.07
Q8NDH3	PEPL1	5	16.25	0	-1	3	10	0	-10	4	10
P55795	HNRH2	5	17.15	1.21	0.363	3	-0.07	1	0	4	0.71
Q13177	PAK2	5	18.13	0.02	0.976	3	0.21	1	0	4	-0.02
P13674	P4HA1	5	13.67	0.66	0.566	3	-1.22	2	0	3	-1.32
P00403	COX2	5	27.75	0.05	0.948	3	-0.05	2	0	3	0.16
Q01105	SET	5	18.28	0.33	0.729	3	0.12	2	0	4	0.42
O00232	PSD12	5	15.57	0.03	0.97	3	-0.18	2	0	4	-0.11
Q9UJU6	DBNL	5	16.51	0.51	0.624	3	-0.17	2	0	5	0.8
P08571	CD14	5	18.93	5.22	0.049	3	-0.6	2	0	5	1.52
Q9H0U4	RAB1B	5	40.30	0.05	0.948	3	0.07	2	0	5	-0.08
Q13618	CUL3	5	8.72	2.42	0.17	3	-1.36	2	0	5	0.77
P25685	DNJB1	5	18.82	1.87	0.233	3	-0.61	3	0	3	0.09
P49773	HINT1	5	60.32	2.51	0.161	3	1.21	3	0	4	0.73
P35270	SPRE	5	31.03	0.08	0.925	3	-0.47	3	0	4	0.12

O95834	EMAL2	5	14.95	0.18	0.842	3	0.1	3	0	4	0.34
O15173	PGRC2	5	22.87	2.42	0.17	3	-0.89	3	0	4	0.02
P49354	FNTA	5	16.36	0.38	0.702	3	-0.49	3	0	4	0.07
Q02818	NUCB1	5	15.18	3.36	0.139	3	-0.11	3	0	4	0.8
P38117	ETFB	5	25.49	0.53	0.613	3	0.26	3	0	4	0.84
Q00688	FKBP3	5	22.32	1.13	0.393	3	-1.15	3	0	4	0.2
Q03135	CAV1	5	38.76	3.96	0.08	3	-1.24	3	0	5	0.38
P04181	OAT	5	17.08	1.02	0.424	3	0.57	3	0	5	1.46
P08697	A2AP	5	17.52	4.63	0.061	3	-0.42	3	0	5	1.13
P55899	FCGRN	5	29.32	0.5	0.632	3	-0.64	3	0	5	0.33
P18428	LBP	5	14.76	1.85	0.27	3	0.98	3	0	5	1.34
Q9UL25	RAB21	5	27.56	1.06	0.404	3	-0.15	3	0	5	0.65
Q9Y6E0	STK24	5	11.96	2.5	0.177	3	1.02	3	0	5	1.27
P07602	SAP	5	11.07	6.66	0.039	3	1.59	3	0	5	3.02
Q969X5	ERGI1	5	22.07	9.14	0.021	3	1.08	3	0	5	0.94
P04278	SHBG	5	19.65	1.88	0.246	3	-0.82	4	0	3	0.03
P61201	CSN2	5	13.77	0.02	0.982	3	0.05	4	0	3	0.29
Q9NVJ2	ARL8B	5	34.95	1.76	0.25	3	-0.09	4	0	4	0.96
P62753	RS6	5	25.70	1.09	0.395	3	-0.88	4	0	4	-0.07
P62277	RS13	5	32.45	4.32	0.069	3	-1.48	4	0	4	0.49
P53007	TXTP	5	17.68	0.04	0.959	3	-0.27	4	0	4	0.06
B9A064	IGLL5	5	35.98	1.65	0.268	3	-0.26	4	0	5	0.14
O75396	SC22B	5	21.86	0.5	0.629	3	-0.28	4	0	5	0.14
Q53GQ0	DHB12	5	21.79	6.43	0.032	3	-0.8	4	0	5	0.02
P05198	IF2A	5	26.35	0.5	0.628	3	0.34	4	0	5	1.08
P60891	PRPS1	5	23.58	2.12	0.201	3	-1.69	4	0	5	-0.03
P62081	RS7	5	28.35	5.55	0.043	3	-0.4	4	0	5	0.73
P46777	RL5	5	23.91	3.92	0.082	3	-1.31	5	0	3	0.18
Q9H8H3	MET7A	5	31.56	0.69	0.535	3	0.37	5	0	4	-0.05
Q9UNH7	SNX6	5	15.52	0.3	0.753	3	-0.27	5	0	4	-0.08
P18621	RL17	5	27.72	2.67	0.163	3	-2.22	5	0	4	-0.37
Q96HE7	ERO1A	5	12.39	2.91	0.131	3	-0.02	5	0	4	1.11
P61020	RAB5B	5	32.09	3.67	0.091	3	-1.35	5	0	5	0.38
O15511	ARPC5	5	62.25	0.06	0.944	4	0.53	2	0	4	0.33
Q12907	LMAN2	5	22.75	3.19	0.114	4	0.92	2	0	5	1.15
P46926	GNPI1	5	37.37	3.68	0.091	4	1.44	2	0	5	1.15
P30042	ES1	5	35.07	2.59	0.154	4	1.35	2	0	5	1.76
Q9UDY4	DNJB4	5	19.58	2.67	0.148	4	0.95	2	0	5	1.15
Q16576	RBBP7	5	18.82	1.2	0.39	4	1.46	2	0	5	1.22
O60684	IMA7	5	13.43	1.91	0.228	4	-0.81	3	0	4	-0.14
Q96CN7	ISOC1	5	25.84	0.33	0.733	4	0.46	3	0	4	-0.38
Q13011	ECH1	5	17.68	22.09	0.002	4	-1.32	3	0	4	0.45

P32969	RL9	5	28.65	16.92	0.003	4	-0.66	3	0	5	0.59
Q96IU4	ABHEB	5	34.76	3.57	0.095	4	-0.58	3	0	5	1.52
Q00577	PURA	5	27.02	0.84	0.477	4	0.1	4	0	4	0.54
Q8NCW5	AIBP	5	30.56	0.13	0.876	4	-0.18	4	0	4	-0.29
P09622	DLDH	5	13.56	1.81	0.243	4	0.61	4	0	4	1.94
Q9Y570	PPME1	5	17.10	0.42	0.674	4	-0.59	4	0	4	0.52
P58546	MTPN	5	66.95	8.24	0.019	4	1.25	4	0	5	1.35
Q12765	SCRN1	5	18.60	0.38	0.697	4	-0.14	4	0	5	0.3
P61026	RAB10	5	27.00	0.56	0.598	4	-0.45	4	0	5	0.27
P48739	PIPNB	5	33.21	3.38	0.104	4	0.85	4	0	5	1.23
P49593	PPM1F	5	18.28	0.18	0.843	4	0.1	4	0	5	0.6
O00116	ADAS	5	11.55	0.27	0.775	4	-0.93	4	0	5	-0.59
P31153	METK2	5	21.52	2.76	0.156	4	-2.05	4	0	5	-0.64
P15880	RS2	5	21.84	2.06	0.208	4	-0.21	4	0	5	0.71
O95292	VAPB	5	30.45	2.13	0.2	4	-0.3	4	0	5	0.36
P49720	PSB3	5	34.15	3.03	0.123	4	-0.76	5	0	4	-0.1
Q9BW30	TPPP3	5	34.09	0.71	0.53	4	-0.32	5	0	4	-0.32
Q14141	41523	5	20.05	1.33	0.333	4	-1.13	5	0	4	0.05
P20042	IF2B	5	20.42	23.2	0.002	4	-1.43	5	0	4	-0.15
Q2M2I8	AAK1	5	8.53	1.81	0.243	4	0.04	5	0	4	0.93
P21912	DHSB	5	20.36	0.38	0.698	4	-0.91	5	0	4	-0.07
O14773	TPP1	5	15.45	17.06	0.003	4	-1.03	5	0	5	0.65
Q9UL46	PSME2	5	30.54	6.14	0.035	4	-2	5	0	5	0.35
Q15121	PEA15	5	44.62	0.63	0.566	4	-0.22	5	0	5	0.56
P09471	GNAO	5	18.93	7.99	0.02	4	-0.89	5	0	5	0.09
O75390	CISY	5	12.66	3.84	0.084	4	-0.9	5	0	5	0.36
P46108	CRK	5	29.61	2.17	0.195	5	1.6	3	0	4	1.27
Q99439	CNN2	5	17.80	0.19	0.831	5	0.1	3	0	4	0.45
P09455	RET1	5	44.44	0.13	0.881	5	0.51	3	0	5	0.43
P56537	IF6	5	42.45	0.57	0.591	5	-0.59	5	0	4	0
P52943	CRIP2	5	45.67	0.43	0.671	5	-0.15	5	0	5	0.08
P50502	F10A1	5	17.89	0.08	0.92	5	0.13	5	0	5	0.11
P24158	PRTN3	4	27.73	0	-1	0	-10	0	-10	4	10
P05107	ITB2	4	6.11	0	-1	0	-10	0	-10	4	10
P08572	CO4A2	4	2.92	0	-1	0	-10	0	-10	4	10
P05771	KPCB	4	9.39	0.97	0.429	0	-10	1	0	3	1.92
Q13217	DNJC3	4	14.09	0.26	0.643	0	-10	1	0	3	0.36
Q15029	U5S1	4	4.53	0	-1	0	-10	1	0	3	2
O43790	KRT86	4	16.26	0	-1	0	-10	1	0	4	1.14
O14744	ANM5	4	8.32	9.57	0.091	0	-10	1	0	4	2.33
Q641Q2	FA21A	4	4.40	4.3	0.286	0	-10	1	0	4	2.2
Q9Y4E1	FA21C	4	4.48	4.3	0.286	0	-10	1	0	4	2.2

Q5SNT6	FA21B	4	4.71	4.3	0.286	0	-10	1	0	4	2.2
Q13098	CSN1	4	9.98	0.02	0.917	0	-10	1	0	4	-0.29
Q01546	K22O	4	6.74	1.24	0.466	0	-10	2	0	2	1.53
Q3KQU3	MA7D1	4	6.42	0.43	0.581	0	-10	2	0	3	0.63
Q07075	AMPE	4	6.48	0.2	0.697	0	-10	2	0	3	0.63
P29622	KAIN	4	13.58	0.01	0.931	0	-10	2	0	3	0.06
Q8WXF7	ATLA1	4	11.11	160.35	0.001	0	-10	2	0	4	2.65
P02792	FRIL	4	28.57	45.03	0.007	0	-10	2	0	4	2.5
Q13564	ULA1	4	15.54	0.77	0.473	0	-10	2	0	4	0.72
P62328	TYB4	4	45.45	0.17	0.719	0	-10	2	0	4	1.46
A8MW06	TMSL3	4	45.45	0.17	0.719	0	-10	2	0	4	1.46
O00468	AGRIN	4	2.79	0.16	0.72	0	-10	2	0	4	-0.37
Q969V3	NCLN	4	9.24	0.04	0.867	0	-10	2	0	4	0.13
Q13630	FCL	4	16.20	11.41	0.078	0	-10	4	0	2	2.25
P62805	H4	4	40.78	0.14	0.725	0	-10	4	0	4	0.23
P00167	CYB5	4	42.54	0.06	0.832	0	-10	4	0	4	0.39
P09543	CN37	4	17.58	0.25	0.816	1	0	1	0	2	-0.21
Q13459	MYO9B	4	4.36	0.21	0.818	1	-0.5	1	0	2	-0.17
Q14739	LBR	4	8.46	6.61	0.131	1	-0.71	1	0	3	0.45
P62917	RL8	4	22.57	0.4	0.715	1	-0.5	1	0	3	1.35
O00505	IMA3	4	13.82	5580.67	0.009	1	-0.42	1	0	4	0.81
O95394	AGM1	4	11.81	8.43	0.037	1	-0.67	1	0	4	1.76
Q29974	2B1G	4	22.18	2.15	0.232	1	-1.14	1	0	4	0.39
Q9Y295	DRG1	4	15.53	1.99	0.252	1	-1.72	1	0	4	0.25
P52306	GDS1	4	11.20	4.88	0.17	1	-1	1	0	4	-0.28
P24666	PPAC	4	33.54	1.4	0.372	1	0	1	0	4	1.83
P42356	PI4KA	4	3.28	18.05	0.052	1	-1	1	0	4	1.55
P11279	LAMP1	4	10.55	0.03	0.968	1	-0.33	1	0	4	-0.44
P52594	AGFG1	4	14.06	1.41	0.37	1	-2	1	0	4	-0.14
P38919	IF4A3	4	8.27	0.26	0.778	1	-0.4	1	0	4	0.02
Q9NTJ5	SAC1	4	6.81	0.35	0.723	1	-0.95	1	0	4	-0.13
P61619	S61A1	4	10.29	2.67	0.148	1	0.95	1	0	4	1.37
P14923	PLAK	4	9.80	29.06	0.001	1	-1.97	1	0	4	0.77
Q99961	SH3G1	4	12.23	1.71	0.29	1	-0.89	1	0	4	0.45
O14787	TNPO2	4	6.24	2.78	0.208	1	0.79	1	0	4	1.65
P31689	DNJA1	4	19.65	0.21	0.825	1	-1.5	2	0	2	-0.34
Q15208	STK38	4	11.18	1.4	0.417	1	2	2	0	2	1
Q6WCQ1	MPRIP	4	7.41	1.4	0.417	1	0.5	2	0	3	-0.5
P21397	AOFA	4	13.09	0.72	0.54	1	0.7	2	0	3	1.24
Q16539	MK14	4	15.00	1.01	0.462	1	0.39	2	0	3	-1.09
P05166	PCCB	4	10.95	0.18	0.843	1	-0.68	2	0	3	-0.42
P10606	COX5B	4	35.66	0.24	0.799	1	0.33	2	0	3	0.43

P16284	PECA1	4	9.49	1.52	0.349	1	-0.33	2	0	4	0.31
P51808	DYLT3	4	73.28	2.83	0.172	1	-2.2	2	0	4	-0.47
P26368	U2AF2	4	13.26	1.78	0.261	1	-0.93	2	0	4	1.12
P01033	TIMP1	4	32.37	19.33	0.049	1	-2.81	2	0	4	0.72
Q9Y4J8	DTNA	4	8.88	1.01	0.442	1	-0.79	2	0	4	0.18
Q9Y315	DEOC	4	19.18	0.16	0.864	1	0.26	2	0	4	0.64
Q02809	PLOD1	4	7.98	1.45	0.507	1	-2.32	2	0	4	0.13
Q9P035	HACD3	4	15.47	1.55	0.3	1	-1.44	2	0	4	-0.22
P13073	COX41	4	26.04	0.69	0.543	1	-1.24	2	0	4	-0.38
O60568	PLOD3	4	7.59	4.38	0.129	1	0.21	2	0	4	2.21
P16298	PP2BB	4	9.16	1.02	0.439	1	-0.89	2	0	4	0.25
Q99613	EIF3C	4	5.15	1.47	0.314	1	-0.47	2	0	4	0.77
Q9H3U7	SMOC2	4	13.23	6.16	0.14	1	-1.08	3	0	1	-2.08
O60884	DNJA2	4	15.53	0.69	0.568	1	-1.64	3	0	2	0.03
P00491	PNPH	4	20.76	5.01	0.081	1	-2.55	3	0	2	-0.56
P49746	TSP3	4	8.37	0.88	0.484	1	-0.83	3	0	3	0.5
Q8IZ83	A16A1	4	7.11	5.26	0.076	1	-1.53	3	0	3	0.96
P51178	PLCD1	4	8.20	0.5	0.65	1	0.79	3	0	3	1.29
Q13619	CUL4A	4	6.06	1.13	0.409	1	0.47	3	0	3	1.36
P62191	PRS4	4	15.23	2.27	0.184	1	-1.15	3	0	4	0.28
P16989	DBPA	4	18.82	1.13	0.408	1	-1.08	3	0	4	0.12
Q9H4G4	GAPR1	4	42.21	0.7	0.531	1	0.35	3	0	4	0.75
Q9Y5Z4	HEBP2	4	23.90	2.5	0.177	1	-0.11	3	0	4	1.7
O94826	TOM70	4	9.21	1.18	0.42	1	0.11	3	0	4	0.8
P62166	NCS1	4	31.05	0.56	0.601	1	-0.47	3	0	4	0.47
Q8TCJ2	STT3B	4	6.90	17.95	0.005	1	-1.61	3	0	4	1.37
P62263	RS14	4	36.42	4.85	0.085	1	-1.24	3	0	4	0.18
O75569	PRKRA	4	19.81	15.39	0.026	1	0.39	3	0	4	1.39
Q86X55	CARM1	4	9.70	0.86	0.507	1	0.7	3	0	4	1.28
P46977	STT3A	4	5.53	1.64	0.283	1	-0.73	3	0	4	0.38
Q96JJ7	TMX3	4	13.00	1.44	0.364	1	-0.08	4	0	2	-1.42
Q9C0E8	LNP	4	16.36	3.22	0.112	1	1.77	4	0	2	0.44
O43293	DAPK3	4	12.33	1.15	0.404	1	-1.57	4	0	2	-1.57
P52566	GDIR2	4	40.30	1	0.422	1	-1	4	0	3	-0.15
Q9BS26	ERP44	4	15.27	0.8	0.49	1	-0.82	4	0	3	-0.23
Q8TD55	PKHO2	4	18.57	0.95	0.459	1	1.36	4	0	3	1.22
Q86UX7	URP2	4	11.84	7.6	0.043	1	-2.3	4	0	3	-0.67
O75477	ERLN1	4	15.32	1.85	0.237	1	-0.85	4	0	3	-0.05
O60888	CUTA	4	40.78	0.42	0.678	1	-0.84	4	0	4	0.58
P67809	YBOX1	4	25.00	0.76	0.516	1	-1.58	4	0	4	-1.18
Q765P7	MTSSL	4	10.04	0	-1	2	10	0	-10	4	10
Q9Y680	FKBP7	4	18.15	0	-1	2	10	0	-10	4	10

Q9UH65	SWP70	4	10.94	0.2	0.833	2	0.5	1	0	2	0.5
Q3LXA3	DHAK	4	14.78	1.23	0.368	2	0.66	1	0	3	1.4
P27361	MK03	4	16.36	0.2	0.833	2	-0.21	1	0	3	-0.21
P48163	MAOX	4	11.71	0.37	0.73	2	1.58	1	0	3	0.5
P14324	FPPS	4	12.89	3.26	0.144	2	0.33	1	0	3	1.86
P49006	MRP	4	51.28	0.94	0.464	2	1.39	1	0	4	1.71
P14866	HNRPL	4	11.21	2.2	0.192	2	-0.03	1	0	4	1.31
Q9Y285	SYFA	4	12.01	2.81	0.263	2	2.81	1	0	4	2.58
Q5T6V5	CI064	4	16.42	0.36	0.717	2	0.79	1	0	4	0.55
Q9Y2A7	NCKP1	4	6.38	1.27	0.44	2	-0.89	1	0	4	-0.57
P07686	HEXB	4	10.61	8.77	0.034	2	-0.79	1	0	4	1.65
P33121	ACSL1	4	5.73	10.2	0.046	2	0.5	1	0	4	2.66
Q03169	TNAP2	4	6.42	5.23	0.076	2	-0.53	2	0	1	1.47
P30419	NMT1	4	13.31	8.54	0.058	2	-1.82	2	0	2	-1.03
P39687	AN32A	4	18.07	1.18	0.369	2	-0.25	2	0	2	-1.42
O15460	P4HA2	4	11.21	0.87	0.476	2	-0.16	2	0	2	-1.1
P62820	RAB1A	4	35.61	0.17	0.846	2	-0.24	2	0	3	-0.15
Q9H7Z7	PGES2	4	20.42	1.06	0.427	2	1	2	0	3	1.64
P54727	RD23B	4	18.34	0.55	0.608	2	-0.85	2	0	3	0.42
Q9H444	CHM4B	4	30.36	0.29	0.766	2	-1.08	2	0	3	-0.81
P61086	UBE2K	4	28.00	0.95	0.479	2	0.21	2	0	3	0.9
P61221	ABCE1	4	10.85	0.29	0.758	2	0.43	2	0	3	0.5
Q12959	DLG1	4	8.52	0.11	0.902	2	0.79	2	0	3	0.37
Q9UKS6	PACN3	4	12.97	10.08	0.012	2	1.41	2	0	3	2.26
P48637	GSHB	4	9.70	1.49	0.329	2	1.79	2	0	3	1.14
P61764	STXB1	4	11.62	0.94	0.464	2	-1.81	2	0	3	-0.98
Q14738	2A5D	4	8.64	3.66	0.105	2	0.04	2	0	3	-1.26
Q9Y263	PLAP	4	9.06	7.82	0.041	2	-1.29	2	0	4	1.37
Q16585	SGCB	4	22.64	1.95	0.223	2	0.05	2	0	4	1.11
P02652	APOA2	4	63.00	7.8	0.021	2	1.25	2	0	4	1.5
Q92599	41525	4	15.53	5.05	0.052	2	0.53	2	0	4	1.68
O43741	AAKB2	4	29.04	0.2	0.821	2	-0.3	2	0	4	0.55
Q07020	RL18	4	25.00	1.44	0.309	2	0	2	0	4	0.48
Q99627	CSN8	4	28.71	4.17	0.136	2	-1.35	2	0	4	-0.45
P49721	PSB2	4	28.86	1.54	0.288	2	-0.93	2	0	4	0.08
Q15654	TRIP6	4	12.39	0.16	0.856	2	-0.6	2	0	4	-0.2
P05109	S10A8	4	32.26	34.15	0.001	2	-1.29	2	0	4	1.67
P61313	RL15	4	20.59	2.95	0.128	2	-1.45	2	0	4	-0.24
O75340	PDCD6	4	21.99	5.91	0.048	2	-1.23	2	0	4	1.7
P05156	CFAI	4	7.55	0.86	0.476	2	-0.99	2	0	4	-0.84
P99999	CYC	4	32.38	0.87	0.467	2	0.46	2	0	4	1.21
O14737	PDCD5	4	28.80	0.64	0.56	2	-0.37	2	0	4	0.45

Q02252	MMSA	4	11.03	1.94	0.257	2	-1.37	2	0	4	-1.3
O00442	RTC1	4	14.75	1.16	0.385	2	-1.2	2	0	4	-0.09
Q9H3N1	TMX1	4	15.00	1.13	0.47	2	0.84	2	0	4	1.86
P05546	HEP2	4	8.42	1	0.445	2	-0.42	2	0	4	1.27
O43598	RCL	4	38.51	9.5	0.03	2	-1.96	3	0	2	-1.17
Q92890	UFD1	4	16.94	0.31	0.749	2	-0.7	3	0	2	-0.23
Q9UMY4	SNX12	4	22.09	0.46	0.657	2	1.34	3	0	2	0.31
Q6ZMI0	PPR21	4	10.90	1.48	0.312	2	-0.91	3	0	3	0.79
P12270	TPR	4	3.09	0.19	0.831	2	0.5	3	0	3	0.04
P48426	PI42A	4	12.32	0.94	0.451	2	-1.41	3	0	3	-0.33
O15145	ARPC3	4	19.10	1.56	0.284	2	-1	3	0	3	0.6
P08559	ODPA	4	16.67	10.88	0.01	2	-2.18	3	0	3	-0.18
O76003	GLRX3	4	16.42	0.31	0.744	2	-0.47	3	0	3	-0.17
P25788	PSA3	4	18.04	2.72	0.144	2	-1.26	3	0	3	0.66
Q8N335	GPD1L	4	16.52	5.74	0.04	2	-0.58	3	0	4	1.12
Q16718	NDUA5	4	57.76	0.36	0.715	2	0.08	3	0	4	0.69
A1L0T0	ILVBL	4	12.82	1.27	0.346	2	0.36	3	0	4	1.65
P54725	RD23A	4	15.43	1.16	0.401	2	-1.98	3	0	4	-1.75
P46937	YAP1	4	16.07	0.6	0.586	2	-0.44	3	0	4	0.68
O75821	EIF3G	4	17.81	2.66	0.149	2	1.01	3	0	4	1.93
Q8TC12	RDH11	4	18.87	3.57	0.095	2	-0.47	3	0	4	0.89
Q96AM1	MRGRF	4	13.70	1.66	0.299	2	-0.43	3	0	4	0.71
P50914	RL14	4	20.93	1.42	0.312	2	0.09	3	0	4	0.82
P63208	SKP1	4	20.86	1.91	0.228	2	-1.2	3	0	4	-0.15
P02743	SAMP	4	20.63	10.48	0.016	2	-1.45	3	0	4	0.08
P06865	HEXA	4	8.51	2.65	0.165	2	-1.7	3	0	4	0.41
Q9H0B6	KLC2	4	11.90	1.56	0.285	2	1.48	4	0	2	1.23
P83731	RL24	4	25.48	0.57	0.597	2	-0.18	4	0	2	1.06
P16070	CD44	4	6.33	0.57	0.591	2	-0.13	4	0	3	0.34
P20339	RAB5A	4	22.33	3.32	0.107	2	-1.8	4	0	3	0.4
Q9UKG1	DP13A	4	7.62	0.24	0.791	2	0.39	4	0	3	0.69
Q9NTX5	ECHD1	4	16.61	0	-1	3	10	0	-10	2	10
P29218	IMPA1	4	22.02	0	-1	3	10	0	-10	2	10
Q14515	SPRL1	4	10.09	0	-1	3	10	0	-10	4	10
P02452	CO1A1	4	6.63	0.3	0.756	3	0.64	1	0	1	-0.23
O00391	QSOX1	4	7.36	1.95	0.287	3	0	1	0	3	1.01
Q8N3F8	MILK1	4	10.43	2.58	0.191	3	0.33	1	0	3	1.66
Q04323	UBXN1	4	26.60	0.8	0.501	3	-0.7	1	0	3	-0.96
Q13637	RAB32	4	24.00	29.44	0.002	3	-0.72	1	0	3	0.91
Q8NB37	PDDC1	4	35.91	1.3	0.368	3	-1.67	1	0	4	-0.07
O15075	DCLK1	4	8.78	0.89	0.468	3	-0.77	1	0	4	0.83
Q00169	PIPNA	4	25.56	0.03	0.974	3	-0.01	1	0	4	0.12

P09110	THIK	4	13.68	6.53	0.081	3	0.79	1	0	4	2.48
P46782	RS5	4	27.94	0.25	0.784	3	-0.37	2	0	3	-0.11
Q9NRX4	PHP14	4	37.60	3.15	0.151	3	1.46	2	0	3	0.83
P26885	FKBP2	4	38.73	0.17	0.845	3	-0.67	2	0	3	-0.33
O00339	MATN2	4	8.79	0.5	0.628	3	0.83	2	0	3	0.95
Q9H008	LHPP	4	24.07	0.65	0.556	3	0.39	2	0	3	0.38
P35659	DEK	4	13.87	0.79	0.505	3	0.52	2	0	3	-0.84
Q6YN16	HSDL2	4	17.70	0.5	0.632	3	-0.15	2	0	4	-1
P22694	KAPCB	4	20.51	1.06	0.403	3	0.32	2	0	4	1.14
Q96S97	MYADM	4	13.66	0.05	0.951	3	-0.03	2	0	4	0.21
Q9BWD1	THIC	4	20.65	0.44	0.665	3	-0.22	2	0	4	0.68
Q09028	RBBP4	4	13.18	0.78	0.516	3	1.25	2	0	4	1.08
O75828	CBR3	4	25.63	0.64	0.56	3	-0.03	3	0	2	0.26
P63151	2ABA	4	16.78	2.86	0.169	3	-1.23	3	0	2	-0.5
Q13683	ITA7	4	6.52	0.51	0.628	3	-0.67	3	0	2	0.27
Q9H0W9	CK054	4	20.63	3.04	0.122	3	1.07	3	0	2	1.64
P40121	CAPG	4	24.71	2.05	0.224	3	1.36	3	0	3	2.12
P24534	EF1B	4	34.67	9.05	0.015	3	-0.63	3	0	3	0.63
P51692	STA5B	4	5.72	1.12	0.395	3	-0.47	3	0	3	0.66
Q16619	CTF1	4	40.30	0.14	0.87	3	-0.69	3	0	3	-0.95
Q9H9A6	LRC40	4	10.63	0.5	0.631	3	-0.91	3	0	3	-0.42
P63173	RL38	4	35.71	0.84	0.477	3	-0.78	3	0	3	-0.17
Q9H1E5	TMX4	4	11.75	1.56	0.285	3	1.01	3	0	3	1.99
Q7L5N1	CSN6	4	20.80	0.22	0.814	3	0.58	3	0	3	-0.12
P09417	DHPR	4	26.23	2.21	0.226	3	0.15	3	0	3	1.2
P29373	RABP2	4	34.78	1.01	0.43	3	0	3	0	3	1.62
Q9UKY7	CDV3	4	36.82	2.79	0.139	3	-0.89	3	0	4	-0.94
Q13765	NACA	4	25.58	0.75	0.511	3	0.17	3	0	4	0.46
P62330	ARF6	4	40.00	1.87	0.234	3	-1.09	3	0	4	0.16
P60983	GMFB	4	41.55	0.82	0.485	3	-0.42	3	0	4	-0.38
P08185	CBG	4	14.81	2.2	0.192	3	-0.82	3	0	4	0.58
P04080	CYTB	4	55.10	0.34	0.727	3	0.47	3	0	4	0.59
P25398	RS12	4	40.15	0.6	0.58	3	-0.81	3	0	4	0.36
P18124	RL7	4	21.37	2.92	0.13	3	-0.72	3	0	4	0.49
Q14980	NUMA1	4	3.97	1.39	0.332	3	-1.1	3	0	4	0.11
P62993	GRB2	4	20.74	1.75	0.252	3	-0.73	3	0	4	0.74
P30626	SORCN	4	26.77	1.09	0.404	3	0.38	3	0	4	1.71
P24539	AT5F1	4	19.14	2.08	0.206	3	-0.97	3	0	4	-0.19
P14649	MYL6B	4	15.38	0.47	0.645	3	-0.43	3	0	4	-0.43
Q9BRA2	TXD17	4	38.21	0.08	0.928	3	-0.16	3	0	4	0.07
Q8NBX0	SCPDL	4	11.19	4.03	0.091	3	-0.38	3	0	4	0.96
Q53T59	H1BP3	4	14.54	0.09	0.915	3	-0.28	4	0	2	0.11

Q16543	CDC37	4	16.93	0.83	0.48	3	0.42	4	0	3	0.05
P51858	HDGF	4	25.42	0.08	0.926	3	0.16	4	0	3	0
O95299	NDUAA	4	16.06	1.71	0.272	3	-1.59	4	0	3	0.22
O75915	PRAF3	4	21.28	0.06	0.944	3	-0.28	4	0	3	0
P54709	AT1B3	4	19.35	1.81	0.243	3	-1.17	4	0	3	-0.23
Q9NWV4	CA123	4	40.00	0.81	0.487	3	0.19	4	0	3	0.41
Q96MM6	HS12B	4	9.62	1.14	0.38	3	-1.55	4	0	3	-1.22
P55145	MANF	4	31.87	0.13	0.881	3	-0.33	4	0	3	-0.01
P13929	ENOB	4	16.13	2.54	0.159	3	0.23	4	0	4	0.39
P0CG06	LAC3	4	65.09	2.06	0.208	3	-0.11	4	0	4	0.22
P0CG05	LAC2	4	65.09	2.06	0.208	3	-0.11	4	0	4	0.22
Q8N163	K1967	4	9.10	0.04	0.965	3	-0.29	4	0	4	-0.1
Q12905	ILF2	4	15.90	1.43	0.322	3	0.55	4	0	4	1.28
P29692	EF1D	4	21.71	2.3	0.181	3	-1.03	4	0	4	-0.3
Q96D15	RCN3	4	21.04	2.02	0.214	3	-1.71	4	0	4	-0.47
P61970	NTF2	4	50.39	0.13	0.877	3	0.83	4	0	4	0.18
Q02543	RL18A	4	24.43	2.85	0.135	3	-1.55	4	0	4	1.19
P31947	1433S	4	10.08	0.13	0.88	3	0.23	4	0	4	0.56
P54819	KAD2	4	23.01	8.24	0.038	4	1.33	1	0	3	2.44
P11177	ODPB	4	21.73	0.06	0.94	4	0.24	2	0	2	-0.03
Q9NR31	SAR1A	4	20.71	3.56	0.096	4	0.4	2	0	3	0.93
Q12929	EPS8	4	8.64	2.69	0.147	4	-1.06	2	0	4	-0.28
P35754	GLRX1	4	43.40	13.44	0.01	4	2.04	2	0	4	3.4
Q2TAA2	IAH1	4	27.42	1.6	0.277	4	0.4	2	0	4	1.05
Q8NE86	MCU	4	18.23	0.82	0.484	4	0.2	2	0	4	1.35
P60033	CD81	4	27.54	0.14	0.874	4	-0.13	3	0	3	-0.02
Q13155	AIMP2	4	20.94	0.37	0.704	4	-0.44	3	0	3	0.29
P01625	KV402	4	36.84	3.9	0.082	4	0.05	3	0	3	1.25
O75347	TBCA	4	26.85	0.73	0.518	4	-0.71	3	0	4	0.32
Q9UBY9	HSPB7	4	33.53	9.06	0.015	4	0.46	3	0	4	0.77
P04196	HRG	4	11.05	0.46	0.653	4	-0.96	4	0	1	-0.34
Q9Y371	SHLB1	4	10.96	0.67	0.548	4	-0.27	4	0	3	0.06
P04216	THY1	4	24.84	1.85	0.236	4	-0.26	4	0	4	0.52
P46783	RS10	4	32.12	0.97	0.43	4	-1.01	4	0	4	0.03
Q9NQP4	PFD4	4	37.31	0.15	0.861	4	-0.66	4	0	4	-0.16
Q9ULZ3	ASC	3	22.56	0	-1	0	-10	0	-10	3	10
Q16082	HSPB2	3	29.67	0	-1	0	-10	0	-10	3	10
Q10471	GALT2	3	7.53	0	-1	0	-10	0	-10	3	10
P08246	ELNE	3	24.34	0	-1	0	-10	0	-10	3	10
O75112	LDB3	3	6.88	0	-1	0	-10	0	-10	3	10
P41218	MNDA	3	8.60	0	-1	0	-10	0	-10	3	10
P42345	MTOR	3	1.77	0	-1	0	-10	0	-10	3	10

P06681	CO2	3	5.72	0	-1	0	-10	0	-10	3	10
Q96L92	SNX27	3	7.76	0	-1	0	-10	0	-10	3	10
P55058	PLTP	3	10.75	0	-1	0	-10	0	-10	3	10
Q8N0X7	SPG20	3	7.36	0	-1	0	-10	0	-10	3	10
P54289	CA2D1	3	4.17	0	-1	0	-10	0	-10	3	10
P20700	LMNB1	3	8.70	0	-1	0	-10	0	-10	3	10
Q9NTI5	PDS5B	3	3.18	0	-1	0	-10	0	-10	3	10
Q96JB5	CK5P3	3	6.13	0	-1	0	-10	0	-10	3	10
Q12906	ILF3	3	4.70	0	-1	0	-10	0	-10	3	10
P11277	SPTB1	3	1.36	0	-1	0	-10	0	-10	3	10
Q5JRX3	PREP	3	4.44	0	-1	0	-10	0	-10	3	10
Q8NBQ5	DHB11	3	13.67	0	-1	0	-10	0	-10	3	10
P59666	DEF3	3	25.53	0	-1	0	-10	0	-10	3	10
P59665	DEF1	3	25.53	0	-1	0	-10	0	-10	3	10
Q15459	SF3A1	3	7.06	0.99	0.424	0	-10	1	0	2	1.8
O14756	H17B6	3	11.99	12.7	0.07	0	-10	1	0	2	1.39
Q52LJ0	FA98B	3	12.12	0.44	0.577	0	-10	1	0	2	-0.8
Q93009	UBP7	3	4.81	0.03	0.895	0	-10	1	0	2	0.4
Q15006	TTC35	3	13.47	0.35	0.614	0	-10	1	0	2	-0.5
Q6XQN6	PNCB	3	7.25	0	-1	0	-10	1	0	2	0
Q9UPT5	EXOC7	3	6.12	0	-1	0	-10	1	0	2	0
Q9UHX1	PUF60	3	10.02	1	0.423	0	-10	1	0	2	0.67
Q12846	STX4	3	15.49	2.32	0.267	0	-10	1	0	2	-1.21
Q9BUL8	PDC10	3	15.57	0	-1	0	-10	1	0	2	-0.32
O00469	PLOD2	3	5.16	0	-1	0	-10	1	0	2	0
P22830	HEMH	3	9.22	0.33	0.667	0	-10	1	0	2	1
O60879	DIAP2	3	3.81	0	-1	0	-10	1	0	2	0
Q92905	CSN5	3	12.57	1.86	0.402	0	-10	1	0	2	2.75
Q53FA7	QORX	3	12.65	0	-1	0	-10	1	0	2	0.58
P49407	ARRB1	3	13.40	0.33	0.667	0	-10	1	0	2	-0.79
Q9Y5L0	TNPO3	3	5.09	0.33	0.667	0	-10	1	0	2	1.16
Q9Y5P6	GMPPB	3	15.83	9.39	0.092	0	-10	1	0	3	1.2
Q6DKJ4	NXN	3	13.10	0.08	0.823	0	-10	1	0	3	-0.86
P31146	COR1A	3	11.93	11.82	0.18	0	-10	1	0	3	2.4
Q6IAA8	LTOR1	3	34.78	31.49	0.011	0	-10	1	0	3	2.16
O95837	GNA14	3	12.96	1.9	0.302	0	-10	1	0	3	1.29
P08582	TRFM	3	6.64	0.07	0.809	0	-10	1	0	3	-0.33
Q9UBR2	CATZ	3	12.54	1.33	0.333	0	-10	1	0	3	1.17
Q03252	LMNB2	3	5.50	0.33	0.667	0	-10	1	0	3	-0.37
O60762	DPM1	3	16.92	0.01	0.949	0	-10	1	0	3	0.16
Q9NR28	DBLOH	3	12.97	6.51	0.238	0	-10	1	0	3	1.29
Q7L1Q6	BZW1	3	6.92	0.61	0.516	0	-10	1	0	3	0.72

P08833	IBP1	3	16.60	0.33	0.667	0	-10	2	0	1	-1.4
P37198	NUP62	3	9.96	6666.67	0.008	0	-10	2	0	2	1
Q9P2R7	SUCB1	3	10.37	8.94	0.205	0	-10	2	0	2	-1.51
Q16666	IF16	3	6.62	0.01	0.931	0	-10	2	0	2	-0.16
P16401	H15	3	10.62	28.56	0.118	0	-10	2	0	2	2.71
Q9Y4E8	UBP15	3	3.98	0.77	0.541	0	-10	2	0	2	1.21
Q15642	CIP4	3	8.65	0	-1	0	-10	2	0	2	-0.42
P26006	ITA3	3	3.33	1.11	0.402	0	-10	2	0	2	1.29
P09466	PAEP	3	23.89	13.19	0.036	0	-10	2	0	3	2.33
P15104	GLNA	3	12.06	1.98	0.232	0	-10	2	0	3	0.87
P08195	4F2	3	6.19	0	0.95	0	-10	2	0	3	-0.06
Q96QV6	H2A1A	3	29.77	1.45	0.315	0	-10	2	0	3	1.46
P16104	H2AX	3	27.27	1.45	0.315	0	-10	2	0	3	1.46
P57053	H2BFS	3	19.84	1.77	0.276	0	-10	2	0	3	0.96
P58876	H2B1D	3	19.84	1.77	0.276	0	-10	2	0	3	0.96
P62807	H2B1C	3	19.84	1.77	0.276	0	-10	2	0	3	0.96
Q5QNW6	H2B2F	3	19.84	1.77	0.276	0	-10	2	0	3	0.96
Q93079	H2B1H	3	19.84	1.77	0.276	0	-10	2	0	3	0.96
Q99877	H2B1N	3	19.84	1.77	0.276	0	-10	2	0	3	0.96
Q99879	H2B1M	3	19.84	1.77	0.276	0	-10	2	0	3	0.96
Q99880	H2B1L	3	19.84	1.77	0.276	0	-10	2	0	3	0.96
O60814	H2B1K	3	19.84	1.77	0.276	0	-10	2	0	3	0.96
O95182	NDUA7	3	32.74	7.88	0.107	0	-10	2	0	3	1.72
Q9Y6Y8	S23IP	3	2.90	0.88	0.52	0	-10	2	0	3	1.52
Q08378	GOGA3	3	4.01	0	-1	0	-10	3	10	0	-10
P20039	2B1B	3	18.42	0.04	0.871	0	-10	3	0	1	-0.18
Q9UN37	VPS4A	3	10.98	1.49	0.347	0	-10	3	0	1	1
Q8TED1	GPX8	3	15.31	26666.7	0.004	0	-10	3	0	1	-2
Q13057	COASY	3	9.04	0.31	0.608	0	-10	3	0	2	0.27
P53985	MOT1	3	6.40	2.49	0.36	0	-10	3	0	3	0.3
P62851	RS25	3	22.40	0.73	0.55	0	-10	3	0	3	-0.6
Q8NBF2	NHLC2	3	8.68	0	-1	1	10	0	-10	2	10
O76070	SYUG	3	29.13	0	-1	1	10	0	-10	2	10
Q9UPU9	SMAG1	3	8.50	0	-1	1	10	0	-10	2	10
P01111	RASN	3	24.87	0	-1	1	10	0	-10	2	10
Q9UH99	SUN2	3	9.07	0	-1	1	10	0	-10	3	10
Q09013	DMPK	3	6.68	0	-1	1	10	0	-10	3	10
Q9Y6W5	WASF2	3	10.24	0	-1	1	10	0	-10	3	10
Q96QR8	PURB	3	14.74	0	-1	1	10	0	-10	3	10
Q9UMS4	PRP19	3	8.73	0	-1	1	10	0	-10	3	10
O96000	NDUBA	3	20.35	0	-1	1	10	0	-10	3	10
Q9P0J0	NDUAD	3	22.22	0	-1	1	10	0	-10	3	10

Q13347	EIF3I	3	15.08	0	-1	1	10	0	-10	3	10
P11498	PYC	3	5.18	0	-1	1	-1	1	0	1	-1
P57772	SELB	3	7.55	0.25	0.816	1	0	1	0	1	1.16
O14786	NRP1	3	6.07	0.2	0.83	1	-1	1	0	2	0.16
Q9NZL9	MAT2B	3	14.97	0	-1	1	0	1	0	2	1
P23368	MAOM	3	11.64	1.47	0.404	1	1.66	1	0	2	1.5
Q9NVH1	DJC11	3	7.51	1.4	0.417	1	0.5	1	0	2	2
O95786	DDX58	3	3.14	0.23	0.826	1	-1	1	0	2	-0.21
P47985	UCRI	3	20.44	0.52	0.657	1	-1.58	1	0	2	0.05
Q6ZVM7	TM1L2	3	11.83	5.2	0.106	1	0	1	0	3	1.72
Q15847	APM2	3	69.74	3.34	0.14	1	1.9	1	0	3	1.71
P06702	S10A9	3	37.72	23.66	0.003	1	-0.97	1	0	3	2.45
Q9P000	COMD9	3	34.85	5.99	0.063	1	-1.28	1	0	3	0.07
Q86VS8	HOOK3	3	7.10	0	-1	1	2.32	1	0	3	3.17
P62266	RS23	3	34.97	23.95	0.143	1	-3.81	1	0	3	-0.93
P62854	RS26	3	31.30	2.37	0.241	1	0.5	1	0	3	1.62
Q9BVK6	TMED9	3	17.45	20	0.018	1	-1.82	1	0	3	0.67
P61769	B2MG	3	35.29	3.07	0.121	1	1.34	1	0	3	1.31
O15327	INP4B	3	4.98	6.25	0.272	1	0	1	0	3	2.5
P23743	DGKA	3	6.94	0.35	0.732	1	-0.79	1	0	3	0.21
P28070	PSB4	3	17.05	6.62	0.079	1	0.29	1	0	3	1.4
P06730	IF4E	3	14.75	14.32	0.029	1	-1.2	1	0	3	0.61
Q92734	TFG	3	9.75	0.82	0.615	1	0	1	0	3	2.23
P62750	RL23A	3	20.51	5.45	0.045	1	-0.56	1	0	3	0.33
P43304	GPDM	3	6.05	1.28	0.372	1	0.16	1	0	3	1.5
Q16629	SRSF7	3	12.61	0.04	0.963	1	-0.04	1	0	3	0.08
Q13033	STRN3	3	6.40	0.34	0.771	1	-1.42	1	0	3	-0.55
Q9Y5K5	UCHL5	3	14.59	1283.34	0.02	1	0.58	2	0	1	0
P51570	GALK1	3	11.22	1.58	0.49	1	-1.66	2	0	1	-1.66
Q99747	SNAG	3	18.91	0.13	0.889	1	1	2	0	2	0.29
P78356	PI42B	3	9.62	0.43	0.687	1	-0.71	2	0	2	-0.71
P62256	UBE2H	3	21.86	1.9	0.293	1	-1.53	2	0	2	0.93
Q5JTV8	TOIP1	3	9.09	0.7	0.564	1	0.24	2	0	2	-1.03
Q9NRN5	OLFL3	3	9.61	0.77	0.522	1	0.95	2	0	2	0.14
Q16762	THTR	3	18.52	0.75	0.53	1	-0.62	2	0	2	0.24
Q9H330	CI005	3	5.60	0.62	0.595	1	-1.66	2	0	2	-1.66
P53041	PPP5	3	8.82	0.85	0.475	1	-0.66	2	0	2	-1.33
Q9NS86	LANC2	3	11.33	0.27	0.804	1	-2	2	0	2	-0.6
Q03518	TAP1	3	7.80	0.6	0.625	1	-1	2	0	2	-1
Q9Y316	MEMO1	3	16.50	0	-1	1	-1	2	0	2	1.17
P30533	AMRP	3	14.29	0.14	0.872	1	0.39	2	0	2	0.66
Q15758	AAAT	3	8.13	6.41	0.083	1	-0.53	2	0	2	2.17

O00487	PSDE	3	16.77	1.25	0.363	1	-1.01	2	0	2	0.11
P53634	CATC	3	7.99	2.55	0.158	1	-1.51	2	0	2	0.3
Q9NRW7	VPS45	3	8.42	0.41	0.689	1	0.48	2	0	2	0.85
Q00534	CDK6	3	14.72	0.01	0.993	1	-0.16	2	0	2	-0.16
Q9BY44	EIF2A	3	8.72	1.5	0.354	1	-0.29	2	0	2	1
Q14166	TTL12	3	7.61	0.27	0.788	1	-0.79	2	0	2	0.71
P02100	HBE	3	18.37	6.12	0.036	1	-0.26	2	0	2	0.8
Q6ZSR9	YJ005	3	15.49	4.51	0.125	1	-0.79	2	0	3	1.93
P49841	GSK3B	3	15.00	3.5	0.098	1	-1.92	2	0	3	0.47
O75531	BAF	3	48.31	0.35	0.722	1	-0.93	2	0	3	-0.24
P13671	CO6	3	5.14	1.77	0.361	1	-1.32	2	0	3	-0.79
Q9Y3D6	FIS1	3	23.68	2.41	0.171	1	-1.36	2	0	3	0.74
Q99685	MGLL	3	15.84	0.84	0.485	1	-0.67	2	0	3	0.2
P10620	MGST1	3	19.35	1.43	0.311	1	-1.6	2	0	3	-0.2
O00423	EMAL1	3	6.50	0.69	0.551	1	0.06	2	0	3	0.84
O75832	PSD10	3	24.34	1.31	0.364	1	-1.88	2	0	3	-1.33
P38159	HNRPG	3	10.23	3.95	0.202	1	-0.79	2	0	3	1.87
Q9UNN8	EPCR	3	16.39	0.99	0.426	1	-0.48	2	0	3	0.5
Q9NT62	ATG3	3	10.51	1.06	0.413	1	-0.3	2	0	3	1
P43307	SSRA	3	11.89	1.52	0.322	1	-1.8	2	0	3	-0.74
Q9UI12	VATH	3	9.73	3.18	0.115	1	1.53	2	0	3	1.51
P11234	RALB	3	18.93	0.28	0.777	1	0.58	2	0	3	0.95
P84103	SRSF3	3	18.29	0.36	0.709	1	-0.18	2	0	3	0.14
P08311	CATG	3	13.73	4.34	0.081	1	1.25	2	0	3	2.66
Q9NZJ7	MTCH1	3	8.23	1.44	0.339	1	-0.5	2	0	3	0.71
P23219	PGH1	3	9.18	0.02	0.893	1	-0.21	3	0	0	-10
Q9BY43	CHM4A	3	18.92	0.05	0.948	1	-0.44	3	0	1	0.17
P53999	TCP4	3	19.69	1.61	0.276	1	-0.02	3	0	1	-1.02
Q86W92	LIPB1	3	2.87	2.25	0.426	1	-1.5	3	0	1	-1.5
Q68CZ2	TENS3	3	4.29	0.75	0.543	1	-0.14	3	0	2	0.8
P18084	ITB5	3	6.38	32.5	0.009	1	3	3	0	2	2.5
P62314	SMD1	3	36.97	0.36	0.712	1	-0.33	3	0	2	0.55
Q13451	FKBP5	3	11.16	1.25	0.363	1	-0.39	3	0	2	-0.7
Q9Y4P3	TBL2	3	11.19	3.78	0.12	1	-1.39	3	0	2	-0.72
P31942	HNRH3	3	14.45	0.52	0.623	1	1.49	3	0	2	-0.09
Q16698	DECR	3	15.22	2.08	0.22	1	-0.89	3	0	2	0.66
Q3SY69	AL1L2	3	6.07	5.09	0.062	1	0.74	3	0	2	1.35
Q9NZB2	F120A	3	4.65	5.71	0.051	1	-0.67	3	0	2	1.6
Q9Y6E2	BZW2	3	8.35	1.93	0.289	1	-1.66	3	0	2	-0.03
Q06210	GFPT1	3	6.01	1.38	0.351	1	-2	3	0	2	0.09
O94808	GFPT2	3	6.16	1.38	0.351	1	-2	3	0	2	0.09
P46776	RL27A	3	22.30	1.74	0.254	1	-0.59	3	0	2	0.41

Q9NSK0	KLC4	3	6.79	2.49	0.231	1	-2.16	3	0	2	-1.16
Q9NVZ3	NECP2	3	19.39	2.2	0.226	1	1.48	3	0	3	1.48
Q9UBQ5	EIF3K	3	18.35	2.39	0.208	1	-1.38	3	0	3	0.42
P13987	CD59	3	18.75	0.9	0.494	1	-3.42	3	0	3	0.18
P0C0S8	H2A1	3	26.92	1.51	0.295	1	-0.84	3	0	3	0.42
P20671	H2A1D	3	26.92	1.51	0.295	1	-0.84	3	0	3	0.42
Q16777	H2A2C	3	27.13	1.51	0.295	1	-0.84	3	0	3	0.42
Q6FI13	H2A2A	3	26.92	1.51	0.295	1	-0.84	3	0	3	0.42
Q7L7L0	H2A3	3	26.92	1.51	0.295	1	-0.84	3	0	3	0.42
Q93077	H2A1C	3	26.92	1.51	0.295	1	-0.84	3	0	3	0.42
Q96KK5	H2A1H	3	27.34	1.51	0.295	1	-0.84	3	0	3	0.42
Q99878	H2A1J	3	27.34	1.51	0.295	1	-0.84	3	0	3	0.42
Q9BTM1	H2AJ	3	27.13	1.51	0.295	1	-0.84	3	0	3	0.42
P04908	H2A1B	3	26.92	1.51	0.295	1	-0.84	3	0	3	0.42
O95816	BAG2	3	22.75	0.72	0.531	1	-0.12	3	0	3	0.92
Q9NZL4	HPBP1	3	12.98	0.43	0.678	1	1	3	0	3	0
Q96AB3	ISOC2	3	18.54	0	-1	2	10	0	-10	2	10
Q13308	PTK7	3	5.33	0	-1	2	10	0	-10	2	10
Q16527	CSRP2	3	27.98	0	-1	2	10	0	-10	2	10
Q9UKK9	NUDT5	3	17.81	0	-1	2	10	0	-10	2	10
O95571	ETHE1	3	19.69	0	-1	2	10	0	-10	2	10
O75663	TIPRL	3	12.87	0	-1	2	10	0	-10	2	10
Q9UK41	VPS28	3	23.53	0	-1	2	1.58	1	0	0	-10
P37108	SRP14	3	36.03	25.05	0.14	2	2.81	1	0	1	0.79
Q96EM0	PRCM	3	14.41	1.23	0.358	2	-1	1	0	2	-0.47
Q9NRR5	UBQL4	3	14.14	1.5	0.5	2	1	1	0	2	-0.5
Q96EK6	GNA1	3	33.15	1.92	0.26	2	-0.37	1	0	2	0.55
O60784	TOM1	3	8.13	1.03	0.437	2	0.39	1	0	2	1.26
Q96C86	DCPS	3	15.43	35958	0	2	1.58	1	0	2	2.32
Q14696	MESD	3	21.79	1.07	0.425	2	-0.33	1	0	2	0.83
P80748	LV302	3	37.84	0.53	0.625	2	-0.6	1	0	2	-0.49
P07197	NFM	3	3.82	1.96	0.235	2	-0.9	1	0	2	0.19
P49257	LMAN1	3	15.29	0.41	0.711	2	-0.47	1	0	2	-0.08
O15260	SURF4	3	11.90	0.59	0.59	2	-1.47	1	0	2	0.02
Q9H8S9	MOB1A	3	17.13	0.68	0.547	2	-0.05	1	0	2	1.05
Q7L9L4	MOB1B	3	17.13	0.68	0.547	2	-0.05	1	0	2	1.05
Q9Y6B6	SAR1B	3	16.67	2.52	0.16	2	0.27	1	0	2	0.99
Q9H0R4	HDHD2	3	15.44	2.13	0.266	2	0.95	1	0	2	0.97
Q16134	ETFD	3	8.91	0.72	0.53	2	-0.52	1	0	3	0.76
P62942	FKB1A	3	29.63	12.24	0.012	2	2.4	1	0	3	3.07
O00499	BIN1	3	9.61	3.54	0.13	2	0	1	0	3	1.34
Q13151	ROA0	3	16.72	3.87	0.116	2	-0.82	1	0	3	0.54

O00244	ATOX1	3	50.00	0.7	0.548	2	-1.86	1	0	3	-0.63
Q9Y3B8	ORN	3	14.77	4.48	0.064	2	0.14	1	0	3	1.9
Q5VYK3	ECM29	3	2.22	5.8	0.093	2	-1.92	1	0	3	-0.63
P15090	FABP4	3	36.36	1.83	0.272	2	2.25	1	0	3	0.46
P20674	COX5A	3	18.00	0.49	0.657	2	1.29	1	0	3	1.99
Q13526	PIN1	3	34.36	0	0.982	2	-0.03	2	0	0	-10
Q96M27	PRRC1	3	9.44	2.38	0.208	2	-0.09	2	0	1	-0.87
Q9H3K6	BOLA2	3	51.16	0.71	0.537	2	-0.07	2	0	1	-0.54
Q9H488	OFUT1	3	9.54	3.56	0.351	2	1.96	2	0	1	-0.5
P62280	RS11	3	24.68	1.58	0.281	2	-0.4	2	0	1	0.28
Q13572	ITPK1	3	15.46	0.76	0.525	2	0.4	2	0	2	1.29
O15400	STX7	3	16.09	9.82	0.048	2	-2.16	2	0	2	-0.5
Q13976	KGP1	3	6.56	2.55	0.194	2	0.86	2	0	2	1.5
P02750	A2GL	3	17.29	0.65	0.607	2	1.08	2	0	2	1.32
P50895	BCAM	3	6.37	2.45	0.181	2	-0.9	2	0	2	0.18
Q99729	ROAA	3	8.73	1.26	0.359	2	-0.9	2	0	2	0.45
Q9HCC0	MCCB	3	7.99	1.67	0.326	2	0.66	2	0	2	1.79
P51665	PSD7	3	16.05	0.98	0.427	2	0.14	2	0	3	0.66
P62837	UB2D2	3	36.05	0.69	0.543	2	0.04	2	0	3	1.11
P61077	UB2D3	3	36.05	0.69	0.543	2	0.04	2	0	3	1.11
P61923	COPZ1	3	18.64	2.29	0.183	2	-1.18	2	0	3	1.06
P62888	RL30	3	40.87	3.83	0.085	2	-0.41	2	0	3	0.52
O00764	PDXK	3	15.38	4.9	0.066	2	-0.14	2	0	3	0.68
P08574	CY1	3	16.00	7.78	0.042	2	0.66	2	0	3	1.89
Q687X5	STEA4	3	11.11	0.09	0.917	2	0.13	2	0	3	0.2
Q96PD5	PGRP2	3	10.24	1.26	0.361	2	1.15	2	0	3	0.39
Q9UMX0	UBQL1	3	9.00	3.41	0.136	2	1.66	2	0	3	0.36
O75935	DCTN3	3	21.51	2.14	0.199	2	-0.24	2	0	3	0.33
P07910	HNRPC	3	11.44	2.33	0.178	2	-1.15	2	0	3	0.78
Q9Y639	NPTN	3	10.05	0.56	0.601	2	0	2	0	3	0.77
P13716	HEM2	3	13.94	1.24	0.353	2	-0.09	2	0	3	1.18
Q15661	TRYB1	3	14.91	6.19	0.06	2	-1.24	2	0	3	-1.34
P20231	TRYB2	3	14.91	6.19	0.06	2	-1.24	2	0	3	-1.34
Q9BUP0	EFHD1	3	14.23	2.03	0.246	2	-1.38	2	0	3	0.27
P68400	CSK21	3	13.81	1.05	0.405	2	0.03	2	0	3	1.05
P49961	ENTP1	3	7.25	1.81	0.243	2	-0.96	2	0	3	0.07
P61604	CH10	3	32.35	0.36	0.711	2	-0.77	2	0	3	-0.07
P50583	AP4A	3	21.77	0.48	0.66	2	-0.24	2	0	3	1.06
P46063	RECQ1	3	8.63	1.97	0.254	2	-0.93	2	0	3	-1.12
P61758	PFD3	3	15.23	0.76	0.516	2	-1.24	2	0	3	-0.15
P32456	GBP2	3	7.28	0.47	0.649	2	-0.54	2	0	3	-0.51
Q8NBJ7	SUMF2	3	12.96	0.45	0.66	2	-0.5	2	0	3	-0.56

Q93062	RBPMS	3	23.47	0.28	0.767	2	0.32	2	0	3	0.71
Q8N0U8	VKORL	3	17.05	0.22	0.808	2	0.72	2	0	3	0.39
Q00889	PSG6	3	7.13	0.14	0.875	2	-0.16	2	0	3	0.38
Q00887	PSG9	3	7.28	0.14	0.875	2	-0.16	2	0	3	0.38
Q15477	SKIV2	3	4.33	0.43	0.701	2	-0.13	3	0	1	-1.29
Q9Y394	DHRS7	3	16.52	0.36	0.722	2	0.58	3	0	1	-0.33
Q5ZPR3	CD276	3	11.24	1.52	0.292	2	0.5	3	0	2	1.2
P42167	LAP2B	3	14.32	0.22	0.812	2	-0.25	3	0	2	-0.21
P42166	LAP2A	3	9.37	0.22	0.812	2	-0.25	3	0	2	-0.21
Q8WZA9	IRGQ	3	11.88	1.43	0.324	2	0.97	3	0	2	1.65
P01903	DRA	3	18.11	1.11	0.389	2	-0.14	3	0	2	1.04
P68402	PA1B2	3	20.96	0.32	0.736	2	-0.04	3	0	2	0.27
Q9Y6I3	EPN1	3	9.72	0.06	0.943	2	0.38	3	0	2	0.27
Q63HR2	TENC1	3	3.97	3.67	0.091	2	-0.09	3	0	2	1
Q92688	AN32B	3	16.73	1.17	0.372	2	-0.21	3	0	2	-1.44
Q9HCU0	CD248	3	7.13	0.64	0.564	2	-0.99	3	0	2	-0.93
P51648	AL3A2	3	8.66	1.87	0.268	2	0.33	3	0	2	-0.74
P00492	HPRT	3	17.89	5.04	0.081	2	-2.29	3	0	2	-0.08
P11310	ACADM	3	8.79	0.79	0.496	2	1.14	3	0	2	1.14
Q5JPE7	NOMO2	3	4.26	0.53	0.625	2	1.2	3	0	2	1.44
P69849	NOMO3	3	4.42	0.53	0.625	2	1.2	3	0	2	1.44
P37840	SYUA	3	27.14	1.39	0.32	2	-0.77	3	0	3	0.02
P01623	KV305	3	39.45	19.43	0.002	2	0.67	3	0	3	0.6
P01620	KV302	3	39.45	19.43	0.002	2	0.67	3	0	3	0.6
P62745	RHOB	3	19.39	0.41	0.68	2	-0.21	3	0	3	0.18
P31949	S10AB	3	34.29	1.51	0.294	2	-0.22	3	0	3	0.74
Q9UIJ7	KAD3	3	19.38	1.35	0.339	2	-1.21	3	0	3	-0.37
P35268	RL22	3	30.47	0.13	0.882	2	0.18	3	0	3	-0.2
Q9UBI1	COMD3	3	23.59	1.61	0.275	2	-0.39	3	0	3	0.48
P16930	FAAA	3	9.79	0.77	0.51	2	-1.03	3	0	3	-0.27
P0CW22	RS17L	3	25.19	0.78	0.501	2	-1.33	3	0	3	-0.4
P08708	RS17	3	25.19	0.78	0.501	2	-1.33	3	0	3	-0.4
Q9UBV8	PEF1	3	11.27	3.74	0.088	2	-2.46	3	0	3	-0.7
P35637	FUS	3	4.75	0.88	0.469	2	-0.72	3	0	3	0.08
P51571	SSRD	3	23.12	1.78	0.247	2	-0.68	3	0	3	0.36
P62913	RL11	3	20.22	3.11	0.118	2	0.06	3	0	3	0.62
Q9BXK5	B2L13	3	12.58	0.71	0.544	2	-0.34	3	0	3	0.06
P62070	RRAS2	3	19.12	0.28	0.764	2	0.42	3	0	3	0.94
Q9HC38	GLOD4	3	15.34	0.87	0.466	2	-0.54	3	0	3	-0.03
P12955	PEPD	3	7.30	4.79	0.069	2	-1.15	3	0	3	1.26
Q14108	SCRB2	3	6.90	1.05	0.407	2	-1.13	3	0	3	-0.11
Q16563	SYPL1	3	19.69	1.61	0.275	2	-1.23	3	0	3	0.5

Q9H9S4	CB39L	3	8.90	6.09	0.036	2	-1.06	3	0	3	0.41
O43920	NDUS5	3	29.25	1	0.421	2	-0.8	3	0	3	0.02
P13473	LAMP2	3	7.07	4.18	0.105	2	-1.11	3	0	3	0
Q9BTW9	TBCD	3	5.37	4.76	0.308	3	2.81	1	0	1	0.5
Q15811	ITSN1	3	3.37	0.99	0.425	3	0.91	1	0	3	0.55
Q14558	KPRA	3	13.76	41.31	0.024	3	2.3	1	0	3	3.7
P30038	AL4A1	3	10.83	1.57	0.429	3	1.08	2	0	0	-10
Q9NR45	SIAS	3	13.65	2.89	0.146	3	0.39	2	0	1	0.58
P63027	VAMP2	3	45.69	0.33	0.732	3	0.34	2	0	2	0.24
P09871	C1S	3	6.69	0.92	0.458	3	-0.07	2	0	2	0.77
P01617	KV204	3	32.74	1.19	0.367	3	-0.22	2	0	2	-0.57
Q13442	HAP28	3	16.57	3.96	0.08	3	0.96	2	0	2	0
P62244	RS15A	3	33.08	5.81	0.039	3	-1.41	2	0	2	0.55
Q96IJ6	GMPPA	3	10.71	0.68	0.542	3	-1.04	2	0	2	-1.41
Q9NP97	DLRB1	3	51.04	5.09	0.062	3	-0.86	2	0	2	0.71
Q5VSL9	FA40A	3	6.21	2.58	0.17	3	1.49	2	0	2	1.22
O94760	DDAH1	3	15.79	0.98	0.438	3	1.13	2	0	2	0.11
Q6NVY1	HIBCH	3	9.07	0.18	0.838	3	0.28	2	0	2	0.54
Q9Y243	AKT3	3	7.52	1.54	0.346	3	-0.92	2	0	2	-1.53
O14880	MGST3	3	33.55	0.61	0.575	3	-0.18	2	0	3	0.36
P61626	LYSC	3	35.14	6.08	0.036	3	0.9	2	0	3	1.84
P14854	CX6B1	3	47.67	0.45	0.667	3	-0.22	2	0	3	0.61
Q86Y82	STX12	3	16.67	5.42	0.045	3	1.81	2	0	3	2.4
P56134	ATPK	3	25.53	1.46	0.305	3	-1.3	2	0	3	0.22
Q15056	IF4H	3	20.16	1.23	0.357	3	-0.62	2	0	3	-0.1
P07947	YES	3	9.58	0.74	0.525	3	-0.06	2	0	3	1.44
P07108	ACBP	3	50.57	3.52	0.111	3	1.77	2	0	3	2.16
P53597	SUCA	3	15.90	0.03	0.972	3	0.08	3	0	2	0.08
Q9UNS2	CSN3	3	13.71	2.35	0.191	3	0.1	3	0	2	1.85
O43169	CYB5B	3	44.52	0.5	0.629	3	-0.32	3	0	2	-0.07
Q969H8	CS010	3	20.81	2.25	0.187	3	-0.95	3	0	2	0.04
P61960	UFM1	3	58.82	1.91	0.228	3	0.54	3	0	3	1.14
P55809	SCOT1	3	11.92	1.22	0.358	3	0.69	3	0	3	0.5
P48539	PCP4	3	43.55	0.26	0.776	3	0.1	3	0	3	0.61
P10515	ODP2	3	6.80	0.77	0.512	3	-0.71	3	0	3	0.43
P02746	C1QB	3	17.00	0.91	0.453	3	0.06	3	0	3	0.46
Q9P0L0	VAPA	3	11.24	0.91	0.451	3	0.1	3	0	3	0.74
Q15185	TEBP	3	26.25	0.94	0.442	3	0.64	3	0	3	0.55
Q13363	CTBP1	3	12.95	2.4	0.207	3	-0.33	3	0	3	1.89
P61081	UBC12	3	20.77	0.12	0.886	3	0.24	3	0	3	0.23
O75964	ATP5L	3	35.92	0.23	0.799	3	-0.31	3	0	3	-0.41
Q9Y512	SAM50	3	8.10	2.09	0.205	3	-1.92	3	0	3	0.02

P11233	RALA	3	17.48	0.15	0.867	3	0.26	3	0	3	0.57
P30046	DOPD	3	32.20	0.92	0.447	3	-0.28	3	0	3	0.54
Q14554	PDIA5	3	8.48	0.42	0.676	3	0.42	3	0	3	0.51
P43487	RANG	3	22.39	0.23	0.802	3	0.48	3	0	3	0.6
Q9Y3B3	TMED7	3	19.64	7.36	0.032	3	-2.2	3	0	3	-0.47
P01833	PIGR	2	5.10	0	-1	0	-10	0	-10	2	10
Q9Y3D0	MIP18	2	26.38	0	-1	0	-10	0	-10	2	10
P09601	HMOX1	2	13.19	0	-1	0	-10	0	-10	2	10
P63172	DYLT1	2	30.09	0	-1	0	-10	0	-10	2	10
Q99471	PFD5	2	21.43	0	-1	0	-10	0	-10	2	10
P80188	NGAL	2	14.14	0	-1	0	-10	0	-10	2	10
P51809	VAMP7	2	12.73	0	-1	0	-10	0	-10	2	10
Q9P2W9	STX18	2	10.45	0	-1	0	-10	0	-10	2	10
Q9UN86	G3BP2	2	6.22	0	-1	0	-10	0	-10	2	10
O95747	OXSR1	2	5.50	0	-1	0	-10	0	-10	2	10
P11182	ODB2	2	7.88	0	-1	0	-10	0	-10	2	10
P78386	KRT85	2	7.50	0	-1	0	-10	0	-10	2	10
Q7L5N7	PCAT2	2	8.09	0	-1	0	-10	0	-10	2	10
P51812	KS6A3	2	4.86	0	-1	0	-10	0	-10	2	10
O75695	XRP2	2	8.86	0	-1	0	-10	0	-10	2	10
P81605	DCD	2	12.73	0	-1	0	-10	0	-10	2	10
O00186	STXB3	2	5.07	0	-1	0	-10	0	-10	2	10
P62316	SMD2	2	24.58	0	-1	0	-10	0	-10	2	10
Q8N1F7	NUP93	2	4.40	0	-1	0	-10	0	-10	2	10
Q9Y6C2	EMIL1	2	3.54	0	-1	0	-10	0	-10	2	10
Q9NP79	VTA1	2	14.33	0	-1	0	-10	0	-10	2	10
Q8WU76	SCFD2	2	4.97	0	-1	0	-10	0	-10	2	10
Q8TEA8	DTD1	2	14.83	0	-1	0	-10	0	-10	2	10
Q9NPH2	INO1	2	5.38	0	-1	0	-10	0	-10	2	10
Q9BQA1	MEP50	2	11.40	0	-1	0	-10	0	-10	2	10
Q8IXJ6	SIRT2	2	9.25	0	-1	0	-10	0	-10	2	10
Q96P70	IPO9	2	2.59	0	-1	0	-10	0	-10	2	10
O94832	MYO1D	2	2.09	0	-1	0	-10	0	-10	2	10
Q96A72	MGN2	2	18.24	0	-1	0	-10	0	-10	2	10
P61326	MGN	2	18.49	0	-1	0	-10	0	-10	2	10
Q9NPJ3	ACO13	2	15.71	0	-1	0	-10	0	-10	2	10
Q13201	MMRN1	2	2.44	0	-1	0	-10	0	-10	2	10
Q9P266	K1462	2	2.21	0	-1	0	-10	0	-10	2	10
Q6H9L7	ISM2	2	5.95	0	-1	0	-10	0	-10	2	10
P42126	ECI1	2	6.95	0	-1	0	-10	0	-10	2	10
Q8TEX9	IPO4	2	2.96	0	-1	0	-10	0	-10	2	10
Q9UBB6	NCDN	2	3.16	0	-1	0	-10	0	-10	2	10

Q9NP74	PALMD	2	4.90	0	-1	0	-10	0	-10	2	10
P56385	ATP5I	2	34.78	0	-1	0	-10	0	-10	2	10
P00533	EGFR	2	2.89	0	-1	0	-10	0	-10	2	10
Q96Q11	TRNT1	2	8.99	0	-1	0	-10	0	-10	2	10
Q92542	NICA	2	2.82	0	-1	0	-10	0	-10	2	10
P09497	CLCB	2	7.86	0	-1	0	-10	0	-10	2	10
P45877	PPIC	2	9.91	0	-1	0	-10	0	-10	2	10
Q9NZ01	TECR	2	9.42	0	-1	0	-10	0	-10	2	10
Q96N67	DOCK7	2	1.45	0	-1	0	-10	0	-10	2	10
Q9HC35	EMAL4	2	2.55	0	-1	0	-10	0	-10	2	10
O00233	PSMD9	2	12.56	0	-1	0	-10	0	-10	2	10
Q8N1A0	KT222	2	6.78	0	-1	0	-10	0	-10	2	10
P27708	PYR1	2	2.07	0	-1	0	-10	0	-10	2	10
P52888	THOP1	2	3.19	0	-1	0	-10	0	-10	2	10
O15013	ARHGA	2	2.34	0	-1	0	-10	0	-10	2	10
P12429	ANXA3	2	6.19	0	-1	0	-10	0	-10	2	10
Q9GZP4	PITH1	2	7.58	0	-1	0	-10	0	-10	2	10
Q9HB90	RRAGC	2	4.51	0	-1	0	-10	0	-10	2	10
Q96AE4	FUBP1	2	3.11	0	-1	0	-10	0	-10	2	10
O43676	NDUB3	2	21.43	0	-1	0	-10	0	-10	2	10
P05165	PCCA	2	3.71	0	-1	0	-10	0	-10	2	10
Q9H7C9	CK067	2	22.13	0	-1	0	-10	0	-10	2	10
O75431	MTX2	2	15.59	0.33	0.667	0	-10	1	0	1	1.16
Q7Z4G1	COMD6	2	29.41	0.1	0.805	0	-10	1	0	1	-0.71
Q92621	NU205	2	2.29	0	-1	0	-10	1	0	1	0
Q5JSH3	WDR44	2	3.94	0	-1	0	-10	1	0	1	-2
Q9UEW8	STK39	2	7.34	0	-1	0	-10	1	0	1	0
Q07666	KHDR1	2	7.67	0.11	0.793	0	-10	1	0	1	-0.58
Q96HY6	DDRGK	2	11.78	0	-1	0	-10	1	0	1	2.81
Q9BY32	ITPA	2	10.82	0	-1	0	-10	1	0	1	1
P53990	IST1	2	10.44	0.39	0.575	0	-10	1	0	1	-0.4
Q9Y608	LRRF2	2	3.61	0	-1	0	-10	1	0	1	1
Q8N556	AFAP1	2	5.48	0	-1	0	-10	1	0	1	1
P00519	ABL1	2	3.98	0	-1	0	-10	1	0	1	-1
Q9H0A8	COMD4	2	20.60	0	-1	0	-10	1	0	1	-2
Q8IWV7	UBR1	2	1.83	16748.2	0.005	0	-10	1	0	1	1.58
Q9Y5J7	TIM9	2	29.21	0	-1	0	-10	1	0	1	-1
Q9H3H3	CK068	2	9.56	0	-1	0	-10	1	0	1	-1
O14936	CSKP	2	3.35	0	-1	0	-10	1	0	1	0
Q13576	IQGA2	2	1.52	0	-1	0	-10	1	0	1	0
Q8IZP0	ABI1	2	5.31	0.33	0.667	0	-10	1	0	1	-0.79
O75718	CRTAP	2	3.74	0	-1	0	-10	1	0	1	-1.58

Q9BQE5	APOL2	2	6.23	0	-1	0	-10	1	0	1	2
Q96JG6	CC132	2	3.22	0	-1	0	-10	1	0	1	1.58
Q13617	CUL2	2	2.28	0	-1	0	-10	1	0	1	1
Q8WUH6	CL023	2	22.41	0.33	0.667	0	-10	1	0	2	0.29
P33241	LSP1	2	12.98	1.57	0.429	0	-10	1	0	2	1.08
P55039	DRG2	2	7.97	0.98	0.503	0	-10	1	0	2	-0.63
P03915	NU5M	2	6.14	0.47	0.541	0	-10	1	0	2	0.36
Q8WTS6	SETD7	2	7.38	0.93	0.511	0	-10	1	0	2	1.45
Q8IVM0	CCD50	2	9.80	0.33	0.667	0	-10	1	0	2	-0.5
Q9NYL9	TMOD3	2	8.52	0.33	0.667	0	-10	1	0	2	1.29
Q9BV57	MTND	2	18.44	2.4	0.219	0	-10	1	0	2	0.67
Q9BXP5	SRRT	2	3.65	16748.2	0.005	0	-10	1	0	2	-1.58
A7E2Y1	MYH7B	2	1.70	0.25	0.651	0	-10	1	0	2	-0.66
Q06136	KDSR	2	8.13	0.29	0.646	0	-10	1	0	2	0.63
Q9BYM8	HOIL1	2	7.06	0	-1	0	-10	1	0	2	1.32
Q15233	NONO	2	5.31	2.11	0.384	0	-10	1	0	2	1.66
P23527	H2B1O	2	19.05	0.03	0.885	0	-10	1	0	2	-0.34
P33778	H2B1B	2	19.05	0.03	0.885	0	-10	1	0	2	-0.34
Q16778	H2B2E	2	19.05	0.03	0.885	0	-10	1	0	2	-0.34
Q8N257	H2B3B	2	19.05	0.03	0.885	0	-10	1	0	2	-0.34
P06899	H2B1J	2	19.05	0.03	0.885	0	-10	1	0	2	-0.34
Q53FT3	CK073	2	11.17	6.17	0.131	0	-10	1	0	2	1.66
O94925	GLSK	2	4.48	0.53	0.521	0	-10	1	0	2	-0.9
Q5VW32	BROX	2	7.30	20.48	0.138	0	-10	1	0	2	2.29
O14672	ADA10	2	4.01	3	0.333	0	-10	1	0	2	1.5
Q9BQB6	VKOR1	2	20.86	0.6	0.519	0	-10	1	0	2	-0.79
Q6IQ22	RAB12	2	8.61	2	0.293	0	-10	1	0	2	1
Q16186	ADRM1	2	6.14	0.58	0.585	0	-10	1	0	2	-1.32
Q9Y2H1	ST38L	2	6.03	0.33	0.667	0	-10	1	0	2	-0.5
Q9Y6M9	NDUB9	2	12.85	24.87	0.126	0	-10	1	0	2	1.79
Q6ZMR3	LDH6A	2	7.53	0.99	0.424	0	-10	1	0	2	-1.95
Q14699	RFTN1	2	4.84	0.33	0.667	0	-10	1	0	2	0.24
Q9Y266	NUDC	2	7.85	0	0.958	0	-10	1	0	2	0.08
Q9Y3P9	RBGP1	2	2.53	0.1	0.784	0	-10	1	0	2	-0.29
P49356	FNTB	2	4.12	0.02	0.917	0	-10	1	0	2	0.29
P55268	LAMB2	2	2.17	0	-1	0	-10	1	0	2	0
Q8TCT9	HM13	2	5.04	0.01	0.931	0	-10	1	0	2	-0.06
P58658	CU063	2	6.58	0.1	0.784	0	-10	1	0	2	0.29
P02724	GLPA	2	20.67	0	-1	0	-10	2	10	0	-10
Q9NZ45	CISD1	2	25.93	0	-1	0	-10	2	10	0	-10
Q9H3P7	GCP60	2	7.39	0	-1	0	-10	2	10	0	-10
P16157	ANK1	2	1.65	0	-1	0	-10	2	10	0	-10

Q8N5K1	CISD2	2	21.48	0	-1	0	-10	2	10	0	-10
Q86UU1	PHLB1	2	1.74	0	-1	0	-10	2	10	0	-10
P12821	ACE	2	2.37	0	-1	0	-10	2	10	0	-10
Q8N129	CNPY4	2	16.13	0	-1	0	-10	2	10	0	-10
Q9NVE7	PANK4	2	4.27	0	-1	0	-10	2	10	0	-10
Q8WZ42	TITIN	2	0.12	0	-1	0	-10	2	10	0	-10
P17302	CXA1	2	7.85	0	-1	0	-10	2	10	0	-10
Q9UBP9	GULP1	2	9.21	0	-1	0	-10	2	10	0	-10
O95352	ATG7	2	4.13	0.33	0.667	0	-10	2	0	1	0.29
Q9NX40	OCAD1	2	12.65	0.33	0.667	0	-10	2	0	1	-0.5
Q14112	NID2	2	2.84	0.03	0.869	0	-10	2	0	1	-0.2
Q8TEY5	CR3L4	2	4.81	1.71	0.416	0	-10	2	0	1	1.79
Q9H6R3	ACSS3	2	5.69	2.4	0.219	0	-10	2	0	1	0.67
P21283	VATC1	2	6.54	8.94	0.205	0	-10	2	0	1	1.51
P07357	CO8A	2	5.82	0.01	0.953	0	-10	2	0	1	0.18
Q92520	FAM3C	2	14.98	0.26	0.663	0	-10	2	0	1	-0.58
P04433	KV309	2	26.09	0.07	0.834	0	-10	2	0	1	-0.5
Q99719	41522	2	8.94	26666.7	0.004	0	-10	2	0	1	-2
O95168	NDUB4	2	16.28	2.39	0.22	0	-10	2	0	1	0.7
Q96DB5	RMD1	2	6.37	0.33	0.667	0	-10	2	0	1	-0.5
P50579	AMPM2	2	7.74	0.29	0.643	0	-10	2	0	2	-0.29
Q8N3V7	SYNPO	2	3.77	6.51	0.238	0	-10	2	0	2	-1.29
P21926	CD9	2	15.35	0.47	0.563	0	-10	2	0	2	0.61
Q96JY6	PDLI2	2	9.09	0.45	0.55	0	-10	2	0	2	-0.63
P61009	SPCS3	2	12.78	0.25	0.667	0	-10	2	0	2	0.47
O75306	NDUS2	2	4.97	0.34	0.599	0	-10	2	0	2	0.95
Q16774	KGUA	2	17.26	1.04	0.415	0	-10	2	0	2	-1.2
Q3ZCQ8	TIM50	2	7.65	0.58	0.585	0	-10	2	0	2	1.32
Q92882	OSTF1	2	9.35	0.94	0.405	0	-10	2	0	2	1.16
O75352	MPU1	2	9.72	16	0.057	0	-10	2	0	2	-2.67
Q9HD45	TM9S3	2	3.74	0.09	0.781	0	-10	2	0	2	0.38
O75367	H2AY	2	10.75	0.33	0.667	0	-10	2	0	2	0.9
Q9UNX3	RL26L	2	11.03	0.56	0.531	0	-10	2	0	2	0.48
P61254	RL26	2	11.03	0.56	0.531	0	-10	2	0	2	0.48
Q9UL18	AGO1	2	4.90	0	-1	1	10	0	-10	1	10
Q86TC9	MYPN	2	3.18	0	-1	1	10	0	-10	1	10
Q96F86	EDC3	2	7.28	0	-1	1	10	0	-10	1	10
Q14232	EI2BA	2	8.20	0	-1	1	10	0	-10	1	10
Q9HCU5	PREB	2	10.79	0	-1	1	10	0	-10	1	10
P07358	CO8B	2	4.40	0	-1	1	10	0	-10	1	10
Q9BUJ2	HNRL1	2	4.91	0	-1	1	10	0	-10	1	10
O43592	XPOT	2	3.01	0	-1	1	10	0	-10	1	10

Q8IYI6	EXOC8	2	6.76	0	-1	1	10	0	-10	1	10
P14735	IDE	2	3.14	0	-1	1	10	0	-10	1	10
Q9BRG1	VPS25	2	17.05	0	-1	1	10	0	-10	1	10
Q9P2X3	IMPCT	2	9.69	0	-1	1	10	0	-10	1	10
Q9NTJ4	MA2C1	2	2.69	0	-1	1	10	0	-10	1	10
Q86U42	PABP2	2	6.86	0	-1	1	10	0	-10	1	10
Q13496	MTM1	2	3.98	0	-1	1	10	0	-10	1	10
P28072	PSB6	2	8.37	0	-1	1	10	0	-10	1	10
P16949	STMN1	2	18.12	0	-1	1	10	0	-10	1	10
Q86XP3	DDX42	2	4.16	0	-1	1	10	0	-10	1	10
Q5CZC0	FSIP2	2	0.54	0	-1	1	10	0	-10	1	10
P45954	ACDSB	2	8.56	0	-1	1	10	0	-10	1	10
Q7RTS7	K2C74	2	6.43	0	-1	1	10	0	-10	1	10
Q5SY16	NOL9	2	3.56	0	-1	1	10	0	-10	1	10
P48556	PSMD8	2	13.14	0	-1	1	10	0	-10	2	10
O14828	SCAM3	2	12.10	0	-1	1	10	0	-10	2	10
Q14257	RCN2	2	9.78	0	-1	1	10	0	-10	2	10
O43866	CD5L	2	9.51	0	-1	1	10	0	-10	2	10
Q8IWB7	WDFY1	2	6.34	0	-1	1	10	0	-10	2	10
Q9UKP3	ITBP2	2	12.39	0	-1	1	10	0	-10	2	10
Q15057	ACAP2	2	4.24	0	-1	1	10	0	-10	2	10
Q9HA64	KT3K	2	8.09	0	-1	1	10	0	-10	2	10
P49903	SPS1	2	9.18	0	-1	1	10	0	-10	2	10
P52815	RM12	2	12.63	0	-1	1	10	0	-10	2	10
O14732	IMPA2	2	12.15	0	-1	1	10	0	-10	2	10
P07225	PROS	2	5.03	0	-1	1	10	0	-10	2	10
O75223	GGCT	2	11.17	0	-1	1	10	0	-10	2	10
Q9ULC4	MCTS1	2	14.36	0	-1	1	10	0	-10	2	10
Q9NUQ6	SPS2L	2	6.45	0	-1	1	10	0	-10	2	10
Q9UM22	EPDR1	2	8.04	0	-1	1	10	0	-10	2	10
Q9Y5Y2	NUBP2	2	8.86	0	-1	1	10	0	-10	2	10
O75694	NU155	2	1.80	0	-1	1	10	0	-10	2	10
P35052	GPC1	2	6.09	0	-1	1	10	0	-10	2	10
O95169	NDUB8	2	12.37	0	-1	1	10	0	-10	2	10
P61513	RL37A	2	28.26	0	-1	1	10	0	-10	2	10
Q9NX62	IMPA3	2	6.96	0	-1	1	10	0	-10	2	10
P51572	BAP31	2	6.10	0	-1	1	10	0	-10	2	10
P02654	APOC1	2	24.10	0	-1	1	10	0	-10	2	10
Q9BZF1	OSBL8	2	2.47	0	-1	1	10	0	-10	2	10
P47813	IF1AX	2	20.83	0	-1	1	0	1	0	0	-10
O14602	IF1AY	2	20.83	0	-1	1	0	1	0	0	-10
Q6PGP7	TTC37	2	1.53	0	-1	1	-1	1	0	0	-10

O95573	ACSL3	2	5.14	0.33	0.667	1	-0.79	1	0	0	-10
Q96A33	CCD47	2	6.63	0	-1	1	0	1	0	0	-10
O75521	ECI2	2	7.11	0.2	0.833	1	0.5	1	0	1	0
Q8N7X1	RMXL3	2	3.94	0	-1	1	0	1	0	1	2
Q96GG9	DCNL1	2	11.20	0	-1	1	-0.58	1	0	1	0.42
P51610	HCFC1	2	1.92	3750	0.012	1	0	1	0	1	1
P36507	MP2K2	2	12.25	0	-1	1	-1	1	0	1	0.58
P41567	EIF1	2	23.89	0.2	0.833	1	-0.29	1	0	1	-0.29
P55263	ADK	2	12.15	0	-1	1	0	1	0	1	0
Q9H3S7	PTN23	2	2.38	3.06	0.375	1	2.2	1	0	1	2.81
Q9NUQ7	UFSP2	2	6.40	0	-1	1	0.58	1	0	1	0.58
Q06278	ADO	2	2.47	0.77	0.565	1	1.14	1	0	1	0.14
P80217	IN35	2	9.09	0	-1	1	0	1	0	1	0
P56211	ARP19	2	25.00	0	-1	1	0.58	1	0	1	-2
P20338	RAB4A	2	12.68	0	-1	1	-1	1	0	1	0.58
O43747	AP1G1	2	2.80	10000	0.007	1	-1	1	0	1	-2
P18031	PTN1	2	5.29	3750	0.012	1	-1	1	0	1	-1
P24310	CX7A1	2	29.11	0.55	0.644	1	-0.16	1	0	1	-1.16
Q2M389	WASH7	2	1.79	0	-1	1	1	1	0	1	0
Q13283	G3BP1	2	4.94	0	-1	1	0	1	0	1	0
P61457	PHS	2	25.00	8.27	0.06	1	-0.67	1	0	1	1.63
O60547	GMDS	2	8.60	13750	0.006	1	-1	1	0	1	1
P05362	ICAM1	2	8.08	0	-1	1	0	1	0	1	0
P60059	SC61G	2	36.76	0	-1	1	-1.58	1	0	1	-1.17
Q9Y5K3	PCY1B	2	10.03	0	-1	1	0	1	0	1	1
P49585	PCY1A	2	10.08	0	-1	1	0	1	0	1	1
P05090	APOD	2	12.70	3750	0.012	1	0	1	0	1	1
O00471	EXOC5	2	2.68	0	-1	1	0	1	0	1	0
P09619	PGFRB	2	2.08	0	-1	1	-1	1	0	1	0.58
P14621	ACYP2	2	18.18	0	-1	1	0	1	0	1	0
O96005	CLPT1	2	6.28	0	-1	1	0	1	0	1	0.58
Q9C005	DPY30	2	36.36	2.32	0.301	1	-0.42	1	0	2	0.3
Q9HC07	TM165	2	15.74	1.93	0.258	1	0.45	1	0	2	1.25
P18859	ATP5J	2	30.56	3.62	0.159	1	0.58	1	0	2	2.24
Q53H12	AGK	2	11.61	0.16	0.856	1	-0.86	1	0	2	-0.28
Q99614	TTC1	2	13.01	0.65	0.57	1	-0.83	1	0	2	0.17
Q8NF37	PCAT1	2	7.12	0.26	0.812	1	1.58	1	0	2	1.16
P42229	STA5A	2	3.15	1.5	0.399	1	1.32	1	0	2	0.33
P18065	IBP2	2	10.77	0.49	0.645	1	-0.5	1	0	2	0.6
Q8IUD2	RB6I2	2	2.24	0.25	0.816	1	0	1	0	2	0.16
O60237	MYPT2	2	2.95	4.56	0.062	1	1.63	1	0	2	1.73
Q8WWX9	SELM	2	19.31	0.77	0.503	1	-0.72	1	0	2	0.36

Q8IW45	CARKD	2	12.10	12.6	0.195	1	-1	1	0	2	0.79
O00401	WASL	2	9.70	10.18	0.089	1	1.58	1	0	2	1.29
P60510	PP4C	2	9.77	0.21	0.84	1	-1.32	1	0	2	-1.16
Q9NRV9	HEBP1	2	17.46	0.11	0.898	1	0.38	1	0	2	0.38
Q9Y5X3	SNX5	2	9.65	0.25	0.816	1	0	1	0	2	0.29
Q12931	TRAP1	2	3.41	12.42	0.035	1	0	1	0	2	1.92
Q9NUV9	GIMA4	2	8.81	18.33	0.052	1	-1.29	1	0	2	0.71
P62899	RL31	2	19.20	5.16	0.05	1	-0.67	1	0	2	0.82
Q8IV08	PLD3	2	7.35	1.08	0.442	1	-1.82	1	0	2	-0.99
Q96C90	PP14B	2	14.97	0.3	0.767	1	-0.66	1	0	2	-0.37
P01598	KV106	2	26.85	0.09	0.916	1	-0.61	1	0	2	-0.65
Q15370	ELOB	2	31.36	1.69	0.294	1	0.45	1	0	2	0.88
P14927	QCR7	2	20.72	0.09	0.918	1	-0.29	1	0	2	-0.23
P08493	MGP	2	23.30	0.58	0.612	1	-0.53	1	0	2	-1.08
Q53SF7	COBL1	2	2.74	0.68	0.594	1	0	1	0	2	1.39
Q9UBV2	SE1L1	2	4.03	1.83	0.463	1	-2	1	0	2	0.29
O60645	EXOC3	2	4.10	0.22	0.82	1	-0.79	1	0	2	-0.13
Q8N1G4	LRC47	2	5.66	5.79	0.066	1	-1.16	1	0	2	0.78
P63098	CANB1	2	10.59	24.2	0.142	1	0	1	0	2	2.88
O15498	YKT6	2	17.68	1.49	0.355	1	-0.28	1	0	2	1.22
P35080	PROF2	2	20.71	6.19	0.086	1	1.03	1	0	2	0
P61006	RAB8A	2	10.14	0.59	0.582	1	-0.59	1	0	2	0.25
Q6UXV4	APOOL	2	11.57	0.13	0.884	1	-0.02	1	0	2	0.28
P0CG30	GSTT2	2	11.48	0.24	0.797	1	0.31	1	0	2	0.9
P0CG29	GST2	2	11.48	0.24	0.797	1	0.31	1	0	2	0.9
Q68EM7	RHG17	2	4.54	0.72	0.555	1	0.21	1	0	2	0.49
Q5VWZ2	LYPL1	2	11.39	29.27	0.004	1	0	1	0	2	2.5
O75953	DNJB5	2	8.62	0.01	0.994	1	-0.13	1	0	2	0
Q32P28	P3H1	2	2.99	0.04	0.961	1	0.21	1	0	2	0.09
Q15631	TSN	2	15.35	0.02	0.982	1	-0.18	1	0	2	-0.17
Q96KP1	EXOC2	2	2.38	0.6	0.625	1	0.79	1	0	2	0.79
P01764	HV303	2	18.80	1.4	0.318	1	-0.79	1	0	2	-0.52
Q8TDX7	NEK7	2	9.93	1.17	0.422	1	-0.15	1	0	2	-1.16
Q9UKK3	PARP4	2	1.68	0.5	0.707	1	1	1	0	2	0.5
Q9NX63	CHCH3	2	10.13	0.4	0.746	1	-1	1	0	2	-1.21
Q9BXW6	OSBL1	2	3.68	0	-1	1	0	1	0	2	1
Q04941	PLP2	2	18.42	3.05	0.19	1	-0.79	1	0	2	0.49
Q92643	GPI8	2	5.82	2.14	0.264	1	-0.5	1	0	2	0.67
P07738	PMGE	2	10.42	1.5	0.5	1	-1	1	0	2	0.5
Q92930	RAB8B	2	10.14	1.08	0.397	1	-0.2	1	0	2	0.46
Q6NUM9	RETST	2	4.92	0.76	0.631	1	1	1	0	2	1.9
Q8TDZ2	MICA1	2	2.34	1.28	0.439	1	-1.16	1	0	2	1.13

Q9UJC5	SH3L2	2	24.30	1.72	0.367	1	2.58	1	0	2	1
O75608	LYPA1	2	10.87	1.59	0.311	1	1.16	1	0	2	1.33
O75533	SF3B1	2	2.53	1.82	0.274	1	0.19	1	0	2	0.9
Q7RTP6	MICA3	2	1.60	1.5	0.4	1	-1.08	1	0	2	-0.29
Q8NF91	SYNE1	2	0.40	1.1	0.416	1	1.2	1	0	2	-0.41
P42677	RS27	2	28.57	0.13	0.882	1	-0.49	1	0	2	-0.37
Q13547	HDAC1	2	4.36	26956.1	0.004	1	0	1	0	2	2.32
Q71UM5	RS27L	2	28.57	0.13	0.882	1	-0.49	1	0	2	-0.37
Q9UHQ9	NB5R1	2	7.87	2.58	0.403	1	-1.46	1	0	2	-1.96
Q9NQT8	KI13B	2	1.20	11.82	0.078	1	-1.58	1	0	2	0.82
P48454	PP2BC	2	5.27	5.29	0.075	1	-0.37	1	0	2	0.63
O43615	TIM44	2	5.75	0.5	0.638	1	-0.95	1	0	2	-1.2
Q9Y376	CAB39	2	6.45	0.26	0.783	1	0.61	1	0	2	0.15
Q86VR2	F134C	2	7.30	0	-1	1	0	1	0	2	2.32
O95861	BPNT1	2	9.09	0.5	0.707	1	1	1	0	2	0.5
P28062	PSB8	2	9.06	0.16	0.86	1	0.08	1	0	2	-0.3
O75380	NDUS6	2	21.77	2.65	0.217	1	-1.45	1	0	2	-0.06
P11215	ITAM	2	2.00	0.41	0.69	1	0.7	1	0	2	1
P31751	AKT2	2	5.41	0.65	0.605	1	-0.34	1	0	2	0.58
O95793	STAU1	2	5.89	0.93	0.518	1	0.79	1	0	2	1.79
Q96HN2	SAHH3	2	3.27	4.4	0.319	1	-1.58	1	0	2	-0.29
O43865	SAHH2	2	3.77	4.4	0.319	1	-1.58	1	0	2	-0.29
O43556	SGCE	2	6.41	1.13	0.409	1	-1.72	1	0	2	-1.25
P58335	ANTR2	2	4.70	0.25	0.785	1	-0.72	1	0	2	-0.12
O75822	EIF3J	2	9.30	10000	0.007	1	-2	1	0	2	-1
Q96FJ2	DYL2	2	20.22	1.13	0.394	1	-1.2	1	0	2	0.51
Q9NR56	MBNL1	2	4.38	0.43	0.677	1	-0.89	1	0	2	-0.28
Q5VZF2	MBNL2	2	4.56	0.43	0.677	1	-0.89	1	0	2	-0.28
Q9NYL2	MLTK	2	3.25	10.4	0.088	1	0.5	1	0	2	2.45
P26447	S10A4	2	18.81	0.16	0.854	1	0.97	1	0	2	0.72
Q12768	STRUM	2	2.59	0.33	0.667	1	-0.5	2	0	0	-10
P63220	RS21	2	34.94	0	-1	1	0	2	0	0	-10
Q8WXF1	PSPC1	2	4.78	0.01	0.949	1	-0.16	2	0	0	-10
P51153	RAB13	2	10.34	6.51	0.238	1	-1.29	2	0	0	-10
P50135	HNMT	2	14.38	1.57	0.283	1	0.42	2	0	1	-0.11
O43633	CHM2A	2	8.56	2.26	0.252	1	-1.08	2	0	1	0.08
Q9BXF6	RFIP5	2	7.04	0.1	0.909	1	0	2	0	1	0.39
P62829	RL23	2	25.00	3.42	0.102	1	-0.54	2	0	1	-0.04
P15559	NQO1	2	9.49	2.72	0.159	1	1.95	2	0	1	1
Q9H0E2	TOLIP	2	9.85	7.28	0.121	1	-2.08	2	0	1	-0.42
Q9H0Q0	FA49A	2	8.05	1.34	0.521	1	-0.5	2	0	1	1.08
Q07955	SRSF1	2	10.48	0	-1	1	-1.58	2	0	1	-1.58

Q9Y2B0	CNPY2	2	17.03	13750	0.006	1	-1	2	0	1	1
Q9Y3E0	GOT1B	2	10.87	2.11	0.267	1	-2.08	2	0	1	-1.03
Q16740	CLPP	2	12.27	1283.34	0.02	1	0	2	0	1	-0.58
O43768	ENSA	2	23.14	0.66	0.564	1	-0.66	2	0	1	-0.19
P67812	SC11A	2	11.17	0.46	0.662	1	-0.86	2	0	1	0.41
P22352	GPX3	2	11.06	0.24	0.797	1	-0.11	2	0	1	0.27
Q6UWY5	OLFL1	2	5.72	10.43	0.087	1	-1.06	2	0	1	-1.77
O15127	SCAM2	2	9.73	4.4	0.185	1	-2.08	2	0	1	0
Q96DZ1	ERLEC	2	7.87	0.2	0.833	1	0	2	0	1	-0.79
Q9NVI7	ATD3A	2	4.73	4.97	0.167	1	0.5	2	0	1	1.79
Q9H254	SPTN4	2	1.01	5.43	0.045	1	-0.28	2	0	1	1.62
P01779	HV318	2	26.72	17.63	0.003	1	-0.49	2	0	2	0.35
P01766	HV305	2	25.00	1.66	0.267	1	0.35	2	0	2	0.22
P62318	SMD3	2	24.60	0.36	0.723	1	-1.16	2	0	2	0.23
P08123	CO1A2	2	2.27	1.9	0.244	1	-1.39	2	0	2	-0.75
Q96A49	SYAP1	2	9.94	0.03	0.975	1	-0.58	2	0	2	0
Q96F85	CNRP1	2	23.78	0.1	0.91	1	-0.69	2	0	2	-0.09
P14406	CX7A2	2	27.71	1.43	0.31	1	1.05	2	0	2	1.8
P60866	RS20	2	19.33	0.3	0.754	1	-0.08	2	0	2	0.36
Q5M775	CYTSB	2	2.34	1.26	0.402	1	-0.08	2	0	2	0.83
P61353	RL27	2	22.06	0.5	0.635	1	-0.36	2	0	2	0.64
Q15843	NEDD8	2	34.57	0.66	0.563	1	1.37	2	0	2	0.14
Q9H2U2	IPYR2	2	8.08	1.24	0.405	1	-1.17	2	0	2	-0.89
Q93034	CUL5	2	2.69	0.22	0.813	1	0.65	2	0	2	-0.43
P84022	SMAD3	2	5.65	4.23	0.084	1	-1.9	2	0	2	-0.41
Q15796	SMAD2	2	5.14	4.23	0.084	1	-1.9	2	0	2	-0.41
O15198	SMAD9	2	5.14	4.23	0.084	1	-1.9	2	0	2	-0.41
P08253	MMP2	2	4.55	0.44	0.678	1	-0.71	2	0	2	0
Q14157	UBP2L	2	2.76	1.18	0.396	1	-1.38	2	0	2	-0.99
O43324	MCA3	2	20.11	3.69	0.124	1	-1.11	2	0	2	0.48
Q9NVS9	PNPO	2	12.64	0.64	0.576	1	-0.95	2	0	2	-1.53
P55083	MFAP4	2	9.80	5.49	0.055	1	-1.61	2	0	2	-1.8
Q99584	S10AD	2	23.47	3.74	0.101	1	-0.86	2	0	2	0.77
P61225	RAP2B	2	12.02	1.95	0.236	1	-1.17	2	0	2	0.44
P67870	CSK2B	2	11.63	1.53	0.321	1	-0.57	2	0	2	0.52
Q8WU90	ZC3HF	2	6.34	2.62	0.219	1	-1.4	2	0	2	1.47
Q12965	MYO1E	2	1.90	1.04	0.434	1	-0.29	2	0	2	0.57
P42766	RL35	2	18.70	0.76	0.54	1	-1.34	2	0	2	-0.42
Q9UHA4	LTOR3	2	30.65	3.37	0.171	1	0.58	2	0	2	0.48
Q5NDL2	AER61	2	3.42	0.81	0.506	1	1.16	2	0	2	1.2
O95278	EPM2A	2	11.78	0.8	0.556	1	-1.58	2	0	2	-0.42
Q9UDW1	QCR9	2	38.10	5.09	0.164	1	-0.58	2	0	2	-1.66

P27169	PON1	2	8.45	0	-1	2	10	0	-10	0	-10
P07451	CAH3	2	14.62	0	-1	2	10	0	-10	0	-10
Q9P2R3	ANFY1	2	4.70	0	-1	2	10	0	-10	1	10
P35244	RFA3	2	29.75	0	-1	2	10	0	-10	1	10
Q96EP5	DAZP1	2	7.86	0	-1	2	10	0	-10	1	10
Q9NX08	COMD8	2	14.75	0	-1	2	10	0	-10	1	10
O75884	RBBP9	2	17.74	0	-1	2	10	0	-10	1	10
P19022	CADH2	2	4.86	0	-1	2	10	0	-10	2	10
Q14767	LTBP2	2	2.75	0	-1	2	10	0	-10	2	10
P05026	AT1B1	2	8.25	0	-1	2	10	0	-10	2	10
Q8IXL7	MSRB3	2	31.77	3.86	0.144	2	-1.57	1	0	0	-10
Q01484	ANK2	2	0.79	1.8	0.272	2	-0.66	1	0	0	-10
Q6NYC8	PPR18	2	6.85	2.59	0.354	2	2.21	1	0	0	-10
A6NDU8	CE051	2	14.63	0.4	0.746	2	-0.21	1	0	1	1
P49902	5NTC	2	7.49	17.48	0.022	2	-1.58	1	0	1	0.25
Q9BZK3	NACP1	2	13.15	1.04	0.41	2	0.45	1	0	1	0.71
Q9GZZ9	UBA5	2	10.15	0.21	0.822	2	-0.49	1	0	1	-0.21
O60331	PI51C	2	6.74	3.36	0.229	2	-0.79	1	0	1	1.03
P07360	CO8G	2	16.34	0.79	0.504	2	1.16	1	0	1	1.2
P27635	RL10	2	6.54	1.91	0.455	2	-0.82	1	0	1	0.85
P48634	PRC2A	2	2.18	1.12	0.434	2	1.3	1	0	1	1.79
Q8NFW8	NEUA	2	8.76	0.23	0.826	2	0.79	1	0	1	1
P0CW20	LIM3L	2	23.93	0.13	0.885	2	-0.58	1	0	1	-0.79
P0CW19	LIMS3	2	23.93	0.13	0.885	2	-0.58	1	0	1	-0.79
P26583	HMGB2	2	13.40	0.1	0.91	2	-0.29	1	0	1	-0.84
Q9BX68	HINT2	2	21.47	1.78	0.248	2	-0.23	1	0	1	1.72
O14972	DSCR3	2	8.08	0.66	0.658	2	0.66	1	0	1	0.32
Q96T76	MMS19	2	3.30	8737.1	0.008	2	0	1	0	1	-1.32
Q13153	PAK1	2	6.97	1711.12	0.017	2	0.58	1	0	1	0
Q9BS40	LXN	2	12.16	13607.6	0.006	2	1	1	0	1	2.32
Q9P1F3	CF115	2	35.80	2.21	0.312	2	0.53	1	0	2	1.46
Q8WUP2	FBLI1	2	9.12	1.1	0.417	2	-0.2	1	0	2	1.15
P24592	IBP6	2	18.33	1.25	0.403	2	-0.35	1	0	2	0.87
Q14011	CIRBP	2	14.53	2.18	0.195	2	-0.59	1	0	2	0.23
P46109	CRKL	2	10.56	0.6	0.625	2	-1.5	1	0	2	-1
Q76M96	CCD80	2	4.21	3.16	0.15	2	1.53	1	0	2	0.79
P35813	PPM1A	2	10.99	0.01	0.988	2	0.17	1	0	2	0.14
Q9UHV9	PFD2	2	16.88	0.03	0.974	2	-0.21	1	0	2	0
Q9UBI6	GBG12	2	25.00	3.76	0.088	2	-0.22	1	0	2	0.83
Q99816	TS101	2	8.46	0.86	0.47	2	-0.11	1	0	2	0.69
Q9Y3E1	HDGR3	2	15.27	6.42	0.082	2	0.05	1	0	2	-1.62
Q86X76	NIT1	2	7.65	3.65	0.157	2	-0.49	1	0	2	0.11

P62304	RUXE	2	25.00	23.98	0.014	2	-2.58	1	0	2	0.02
Q15628	TRADD	2	9.62	8.97	0.23	2	1	1	0	2	3.02
Q9Y2Z0	SUGT1	2	8.22	3.29	0.143	2	-0.07	1	0	2	1.27
Q8IXQ6	PARP9	2	2.46	3.68	0.214	2	-1.58	1	0	2	0.08
Q9BTE1	DCTN5	2	9.34	19.7	0.019	2	-1	1	0	2	-2.99
P63167	DYL1	2	37.08	0.1	0.909	2	-0.47	2	0	1	-0.56
Q8TAT6	NPL4	2	5.26	0.11	0.897	2	0.74	2	0	1	0.34
P08236	BGLR	2	4.45	3.36	0.229	2	-1.58	2	0	1	0.24
Q9H9B4	SFXN1	2	8.70	5.48	0.1	2	-2.16	2	0	1	-1.37
Q9UBW8	CSN7A	2	11.27	0.09	0.921	2	-0.77	2	0	1	-0.26
P23786	CPT2	2	6.08	0.21	0.82	2	-0.14	2	0	1	0.33
Q05397	FAK1	2	2.76	0.16	0.854	2	-0.67	2	0	1	-0.13
P05386	RLA1	2	51.75	0.92	0.447	2	0.76	2	0	2	0.56
Q9Y333	LSM2	2	40.00	1.23	0.407	2	0.76	2	0	2	1.83
Q9Y3E5	PTH2	2	21.23	0.01	0.993	2	0.05	2	0	2	0.07
O75781	PALM	2	8.53	0.13	0.883	2	0.04	2	0	2	-0.3
Q8NC51	PAIRB	2	8.33	2.69	0.146	2	-1.19	2	0	2	-0.14
P40222	TXLNA	2	11.72	0.33	0.73	2	-0.39	2	0	2	0.14
P17612	KAPCA	2	8.83	1.01	0.419	2	-0.65	2	0	2	0.59
P02656	APOC3	2	27.27	7.38	0.024	2	-0.57	2	0	2	0.76
O60613	41532	2	17.90	0.43	0.674	2	-0.91	2	0	2	0.14
O95433	AHSA1	2	10.06	7.69	0.022	2	-1.17	2	0	2	0.45
Q13636	RAB31	2	12.89	0.73	0.519	2	-0.76	2	0	2	0.73
Q96AT9	RPE	2	17.54	1.29	0.354	2	1.21	2	0	2	0.67
Q9UGJ0	AAKG2	2	4.92	0.05	0.951	2	-0.51	2	0	2	-0.06
P02753	RET4	2	13.93	1.03	0.423	2	-1.11	2	0	2	-0.06
Q96BJ3	AIDA	2	12.09	0.56	0.596	2	-0.44	2	0	2	0.36
Q6P587	FAHD1	2	13.39	11.49	0.039	2	1.27	2	0	2	1.4
Q9H299	SH3L3	2	20.43	3.66	0.092	2	0.11	2	0	2	0.47
Q13148	TADBP	2	7.25	5.23	0.048	2	0.17	2	0	2	1.04
P02747	C1QC	2	11.02	4.05	0.077	2	0.56	2	0	2	0.75
Q9BPX5	ARP5L	2	16.34	0.96	0.434	2	-1.2	2	0	2	-0.13
Q14344	GNA13	2	6.37	0.41	0.684	2	-0.73	2	0	2	-0.12
O15372	EIF3H	2	9.09	4.06	0.14	2	-1.47	2	0	2	-0.92
P80303	NUCB2	2	7.14	0.66	0.578	2	2	2	0	2	0.66
Q4KMQ2	ANO6	2	3.74	0.13	0.878	2	0.23	2	0	2	0.37
P62847	RS24	2	20.30	0.44	0.669	2	-0.67	2	0	2	-0.96
O95674	CDS2	2	8.99	1.08	0.399	2	-0.25	2	0	2	1.43
Q9NQE9	HINT3	2	21.43	1.3	0.368	2	1.24	2	0	2	0.79
P51553	IDH3G	2	8.65	1.62	0.288	2	-0.64	2	0	2	1.32
Q96T51	RUFY1	2	4.38	0.07	0.934	2	0.52	2	0	2	0.39
Q9UHY7	ENOPH	2	13.41	5.2	0.077	2	-1.92	2	0	2	-1.79

P19404	NDUV2	2	9.24	0.1	0.909	2	-0.04	2	0	2	0.18
P43155	CACP	2	4.79	2.34	0.213	2	1.33	2	0	2	1.29
P01781	HV320	2	17.24	0.4	0.689	2	0.3	2	0	2	0.3
P05543	THBG	2	9.40	0.6	0.58	2	0.4	2	0	2	0.77
Q5GLZ8	HERC4	2	3.03	0.32	0.74	2	0.64	2	0	2	0.71
O00483	NDUA4	2	27.16	2.89	0.146	2	-1.95	2	0	2	-0.02
P40429	RL13A	2	11.33	0.21	0.816	2	-0.5	2	0	2	0.1
P36969	GPX4	2	12.69	0.14	0.878	2	0.58	2	0	2	-0.06
P11166	GTR1	2	3.66	0.56	0.604	2	-1.35	2	0	2	-0.81
O43929	ORC4	2	4.82	3.45	0.114	2	2.08	2	0	2	0.2
P31749	AKT1	2	5.63	0.28	0.767	2	0.36	2	0	2	-0.19

SECTION III- The Human Uterine Smooth Muscle S-Nitrosoproteome

Table S4.1. The S-nitrosoproteome in pregnancy.

UniProt ID	Sequence Name	Main Function	Total Peps	L Log2 Rel Exp	PTL Log2 Rel Exp
P21333	Filamin-A	Cytoskeletal dynamics	175	-0.22	0.55
P02768	Serum albumin	Transporter	78	-0.16	-1.44
P63267	Actin, gamma-enteric smooth muscle	Smooth muscle contraction	48	0.11	0.53
P63261	Actin, cytoplasmic 2	Cytoskeletal dynamics	44	0.13	0.14
P17661	Desmin	Cytoskeletal dynamics	39	0.1	1.25
Q9Y490	Talin-1	Cytoskeletal dynamics	33	-0.71	-2.48
P68871	Hemoglobin subunit beta	Transporter	26	-0.14	-2.22
P18206	Vinculin	Cytoskeletal dynamics	26	-0.65	-1.53
P51911	Calponin-1	Smooth muscle contraction	26	-0.78	1.4
Q14315	Filamin-C	Cytoskeletal dynamics	27	0	0.2
P04264	Keratin, type II cytoskeletal 1	Structural	25	-0.19	0.99
P14618	Pyruvate kinase isozymes M1/M2	Metabolic enzyme	23	0.41	-1.32
P35527	Keratin, type I cytoskeletal 9	Structural	21	-0.19	1.31
Q8WX93	Palladin	Cytoskeletal dynamics	20	0.27	-1.42
Q93052	Lipoma-preferred partner	Transporter and scaffolding	21	-0.08	-1.35
Q01995	Transgelin	Cytoskeletal dynamics	18	-0.1	1.69
P06733	Alpha-enolase	Metabolic enzyme	16	0.38	0.09
P04406	Glyceraldehyde-3-phosphate dehydrogenase	Metabolic enzyme	15	-0.18	-0.12
P09211	Glutathione S-transferase P	Nitric oxide signaling	13	0.39	-2.53
P02042	Hemoglobin subunit delta	Transporter	16	0.09	-1.83
P08670	Vimentin	Cytoskeletal dynamics	17	-0.18	0.21
P09382	Galectin-1	Scaffolding	15	-0.26	-2.04
P13645	Keratin, type I cytoskeletal 10	Structural	13	-0.63	0.45
P35908	Keratin, type II cytoskeletal 2 epidermal	Structural	13	0.22	0.9

P04792	Heat shock protein beta-1	Cytoskeletal dynamics	12	0.09	0.63
P12277	Creatine kinase B-type	Metabolic enzyme	12	-0.25	-1.19
P69905	Hemoglobin subunit alpha	Transporter	13	-0.29	0.03
P12814	Alpha-actinin-1	Cytoskeletal dynamics	12	-0.36	-1.13
P67936	Tropomyosin alpha-4 chain	Smooth muscle contraction	13	0.31	0.78
P13639	Elongation factor 2	Transcriptional regulation	10	0.05	-1.09
P10768	S-formylglutathione hydrolase	Metabolic enzyme	10	0.4	-1.16
O00151	PDZ and LIM domain protein 1	Transcriptional regulation	10	-0.04	-1.27
P68363	Tubulin alpha-1B chain	Structural	9	0.09	0.43
Q71U36	Tubulin alpha-1A chain	Structural	9	0.09	0.43
O14558	Heat shock protein beta-6	Smooth muscle contraction	9	0.09	0.76
Q14195	Dihydropyrimidinase-related protein 3	Cytoskeletal dynamics	11	0.08	-0.04
P08133	Annexin A6	Smooth muscle contraction	10	0.25	-1.47
P07437	Tubulin beta chain	Structural	9	-0.06	0.23
P07951	Tropomyosin beta chain	Smooth muscle contraction	11	0.31	0.78
Q15746	Myosin light chain kinase, smooth muscle	Smooth muscle contraction	9	0.17	-0.3
P62937	Peptidyl-prolyl cis-trans isomerase A	Protein binding	9	-0.03	1.15
P48668	Keratin, type II cytoskeletal 6C	Structural	9	0.06	1.29
P68371	Tubulin beta-4B chain	Protein binding	8	-0.09	0.2
P21291	Cysteine and glycine-rich protein 1	Cytoskeletal dynamics	10	0.29	0.48
Q562R1	Beta-actin-like protein 2	Cytoskeletal dynamics	9	0.43	0.19
P01009	Alpha-1-antitrypsin	Peptidase inhibitor	7	0.24	0.37
P55072	Transitional endoplasmic reticulum ATPase	Protein binding and transport	8	-0.05	-0.76
P09493	Tropomyosin alpha-1 chain	Cytoskeletal dynamics	9	0.31	0.78
Q6PEY2	Tubulin alpha-3E chain	Structural	7	0.11	0.55
P54652	Heat shock-related 70 kDa protein 2	Protein binding	7	0.42	-1.55

P08779	Keratin, type I cytoskeletal 16	Structural	7	0.57	1.5
P04075	Fructose-bisphosphate aldolase A	Metabolic enzyme	7	0.26	0.79
Q9NZN4	EH domain-containing protein 2	Cytoskeletal dynamics	6	0.12	-0.77
P07355	Annexin A2	Cytoskeletal dynamics	5	-0.42	-0.49
P13647	Keratin, type II cytoskeletal 5	Structural	6	-0.25	1.21
P02533	Keratin, type I cytoskeletal 14	Structural	6	0.43	1.7
P06396	Gelsolin	Cytoskeletal dynamics	4	-0.28	0.67

Q15942	Zyxin	Cytoskeletal dynamics	5	0.08	-0.56
P60660	Myosin light polypeptide 6	Smooth muscle contraction	6	0.21	1.58
P68104	Elongation factor 1-alpha 1	Transcriptional regulation	4	-0.07	-0.65
Q5VTE0	Putative elongation factor 1-alpha-like 3	Transcriptional regulation	4	-0.07	-0.65
P13489	Ribonuclease inhibitor	Protein binding	4	0.21	-0.36
P07737	Profilin-1	Cytoskeletal dynamics	5	0.48	2.23
Q53GG5	PDZ and LIM domain protein 3	Cytoskeletal dynamics	5	-0.39	0.36
P23142	Fibulin-1	Protein binding	4	-0.55	-0.91
P37802	Transgelin-2	Cytoskeletal dynamics	5	0.48	1
Q01518	Adenylyl cyclase-associated protein 1	Cytoskeletal dynamics	4	0.3	-0.28
P21980	Protein-glutamine gamma-glutamyltransferase 2	Protein crosslinking	4	0.11	-2.34
Q09666	Neuroblast differentiation-associated protein AHNAK	Protein binding	5	-0.18	0.46
Q15124	Phosphoglucomutase-like protein 5	Metabolic enzyme	4	0.16	-0.29
O43707	Alpha-actinin-4	Cytoskeletal dynamics	4	-0.38	-0.89
P31949	Protein S100-A11	Calcium signaling	4	0.45	0.26
P01857	Ig gamma-1 chain C region	Protein binding	5	-0.53	0.34
P24844	Myosin regulatory light	Smooth muscle contraction	3	0.37	1.82

	polypeptide 9				
Q99497	Protein DJ-1	Redox response	4	0.14	-1.11
P00387	NADH-cytochrome b5 reductase 3	Biosynthesis	4	0.6	-0.33
Q05682	Caldesmon	Smooth muscle contraction	5	0.4	0.9
P00338	L-lactate dehydrogenase A chain	Metabolic enzyme	3	-0.3	-0.41
P10809	60 kDa heat shock protein, mitochondrial	Chaperone	2	-0.19	-0.5
Q9NR12	PDZ and LIM domain protein 7	Cytoskeletal dynamics	4	-0.6	0.13
Q16881	Thioredoxin reductase 1, cytoplasmic	Redox response	3	0.21	-0.67
P01834	Ig kappa chain C region	Protein binding	3	-0.32	0.33
P49419	Alpha-aminoadipic semialdehyde dehydrogenase	Metabolic enzyme	3	0.69	-1.45
P02787	Serotransferrin	Transporter	2	-0.44	0.31
O00299	Chloride intracellular channel protein 1	Redox response	3	0.46	-0.55
P02766	Transthyretin	Transporter	3	-0.23	0.34
P04083	Annexin A1	Phospholipid binding	2	0.69	0.98
P50395	Rab GDP dissociation inhibitor beta	GTPase regulation	2	0.38	-0.95
P04179	Superoxide dismutase [Mn], mitochondrial	Redox response	2	0.66	0.07
Q9UBQ7	Glyoxylate reductase/hydroxypyruvate reductase	Metabolic enzyme	2	0.1	-1.72
O60478	Integral membrane protein GPR137B	G-Protein receptor	3	-0.72	0.83
P00441	Superoxide dismutase [Cu-Zn]	Redox response	2	-0.22	0.5
P01861	Ig gamma-4 chain C region	Protein binding	3	-0.24	0.66
P14550	Alcohol dehydrogenase [NADP+]	Metabolic enzyme	2	0.74	-0.52

P02652	Apolipoprotein A-II	Transporter	2	-1.51	-0.24

P62508	Estrogen-related receptor gamma	Hormone receptor	3	-1.92	-2.04
P10599	Thioredoxin	Redox response	2	0.22	1.04
P16591	Tyrosine-protein kinase Fer	Cytoskeletal dynamics	3	-0.05	-1
P35754	Glutaredoxin-1	Redox response	2	-0.78	-0.28
P47756	F-actin-capping protein subunit beta	Cytoskeletal dynamics	2	-0.3	-1.1
P60953	Cell division control protein 42 homolog	Cytoskeletal dynamics	2	0.12	-1.09
P31040	Succinate dehydrogenase [ubiquinone] flavoprotein subunit, mitochondrial	Metabolic enzyme	2	-0.89	-2.42
Q13371	Phosducin-like protein	Protein binding	2	-0.23	-0.33
P01876	Ig alpha-1 chain C region	Protein binding	2	-0.17	-0.35
P06703	Protein S100-A6	Calcium signaling	2	-0.96	-0.06
Q9UMS6	Synaptopodin-2	Cytoskeletal dynamics	2	Not Id'd	10
Q6IE37	Ovostatin homolog 1	Proteinase inhibito	2	-1.11	-0.15
Q5SVZ6	Zinc finger MYM-type protein 1	Protein binding	2	-0.28	0.71
O75083	WD repeat-containing protein 1	Cytoskeletal dynamics	2	0.15	-1.08
Q9ULJ3	Zinc finger protein 295	Transcriptional regulation	2	-0.09	-1.34

Legend: 110 S-nitrosated proteins were identified with 2 or more unique peptides. Log2 relative expressions (L/PTL Rel Ex) for these 110 proteins are based on area under the curve analysis of all identified peptides using the non-laboring state as reference. Note Synaptopodin-2 was only positively identified in PTL.

Table S4.2. S-nitrosated or reversibly oxidized cysteine residues identified by mass shift labeling.

Sequence Id	Sequence Name	SNO Peptide(s)	Mod-Cysteine(s)
P02768	Serum albumin	ALVLIAFAQYLQQC*PFEDHVKLVNEVTEFAK	C*58
P21333	Filamin-A	AEISC*TDNQDGTC*SVSYLPVLPGDYSILVK	C*1912, C*1920
		AHVVPC*FDASK	C*1157
		ALGALVDSC*APGLC*PDWDSWDASKPVTNAR	C*205, C*210
		ALGALVDSC*APGLC#PDWDSWDASKPVTNAR	C*205, C#210
		APLRVQVQDNEGC*PVEALVK	C*717
		APSVANVGSHC*DLSLKIPEISIQDMTAQVTSPSGK	C*2160
		ATC*APQHGAPGPGPADASK	C*2543
		C*APGVVGPAEADIDFDIIRNDNDTFTVK	C*810
		C*SGPGLSPGMVR	C*1453
		IVGPSGAAVPC*KVEPGLGADNSVVRFLPR	C*1018
		LQVEPAVDTSGVQC*YGPGIEGQGVFR	C*1260
		MDC*QEC*PEGYRVTYTPMAPGSYLISIK	C*2476, C*2479
		MDC#QEC*PEGYRVTYTPMAPGSYLISIK	C#2479, C*2479
		SPYTVTVGQAC*NPSAC*R	C*478, C*483
		SPYTVTVGQAC*NPSAC#RAVGRGLQPK	C*478, C#483

		SPYTVTVGQAC#NPSAC*R	C#478, C*483
		THEAEIVEGENHTYC*IR	C*2199
		VEYTPYEEGLHSVDVTYDGSPVPSSPFQVPVTEGC*DPSR	C*1353
		VGSAADIPINISETDLSLLTATVVPPSGREEPC*LLK	C*1997
		VQVQDNEGC*PVEALVKDNGNGTYSC#SYVPR	C*717
		VTYC*PTEPGNYIINIK	C*2107
		YWPQEAGEYAVHVLC*NSEDIR	C*649
P60709	Actin, cytoplasmic 1	C*DVDIRKDLYANTVLSGGTTMYPGIADR	C*285
		FRC*PEALFQPSFLGMESC*GIHETTFNSIMK	C*257, C*272
		FRC#PEALFQPSFLGMESC*GIHETTFNSIMK	C#257, C*272
		FRC*PEALFQPSFLGMESC#GIHETTFNSIMK	C*257, C#272
		EKLC*YVALDFEQEMATAASSSSLEK	C*217
P62736	Actin, aortic smooth muscle	C*DIDIRKDLYANNVLSGGTTMYPGIADR	C*287
		C*PETLFQPSFIGMESAGIHETTYNSIMK	C*259
		EKLC*YVALDFENEMATAASSSSLEK	C*219
P51911	Calponin-1	IGNNFMDGLKDGIILC*EFINKLQPGSVK	C*61
		RQIFEPGLGMEHC*DTLNVSLQMGSNKGASQR	C*238
		YC*LTPEYPELGEPAHNHHAHNYYNSA	C*273

Q93052	Lipoma-preferred partner	AYC#EPC#YINTLEQC*NVC*SKPIMER	C#465, C#468, C*476, C*480
		AYHPHC*FTC*VMC*HR	C*499, C*502, C*505
		AYHPHC#FTC*VMC*HR	C#499, C*502, C*505
		C*SVC*KEPIMPAPGQEETVR	C*536, C*539
		IVALDRDFHVHC*YR	C*566
		KTYITDPVSAPC*APPLQPK	C*364
		SAQPSPHYMAAPSSGQIYGSGPQGYNTQPVPVSGQC*PPPSTR	C*262
		SLDGIPFTVDAGGLIHC*IEDFHKK	C*524
P68871	Hemoglobin subunit beta	VLGAFSDGLAHLDNLKGTFATLSELHC*DKLHVDPENFR	C*94
		LLGNVLVC*VLAHHFGKEFTPPVQAAYQK	C*113
P14618	Pyruvate kinase isozymes M1/M2	AEGSDVANAVLDGADC*IMLSGETAKGDYPLEAVR	C*358
		AGKPVIC*ATQMLESMIK	C*326
		GIFPVLC*KDPVQEAWAEDVDLRVNFAMNVGK	C*474
		NTGIIC*TIGPASR	C*497
P09382	Galectin-1	SFVLNLGKDSNNLC*LHFNPR	C*43
		FNAHGDANTIVC*NSKDGGAWGTEQR	C*61
		EAVFPFQPGSVAEVC*ITFDQANLTVK	C*89

P13489	Ribonuclease inhibitor	ELDLSNNC*LGDAGILQLVESVR	C*409
		TLPTLQELHLSDNLLGDAGLQLLC*EGLLDPQC*RLEK	C*134, C*142
		WAELLPLLQQC*QVVR	C*30
P17661	Desmin	QEMMEYRHQIQSYTC*EIDALKGTNDSLMR	C*333
P04264	Keratin, type II cytoskeletal 1	MSGEC*APNVSVSVSTSHTTISGGGSR	C*497
		SGGGGGRFSSC*GGGGGSFGAGGGFGSR	C*49
Q15746	Myosin light chain kinase, smooth muscle	FDC*KIEGYPDPEVVWFKDDQSIR	C*1830
		HFQIDYDEDGNC*SLIISDVC*GDDDAKYTC*K	C*1865, C*1873, C*1882
		QAQVNLTVVDKPDPPAGTPC*ASDIR	C*1339
Q9Y490	Talin-1	ALC*GFTEAAAQAAYLVGVSDPNSQAGQQGLVEPTQFAR	C*1434
		EC*ANGYLELLDHVLLTLQKPSPELK	C*2243
		TMQFEPSTMVYDAC*R	C*29
P13645	Keratin, type I cytoskeletal 10	GSSGGGC*FGGSSGGYGGLGGFGGGSFR	C*66
		YC*VQLSQIQAQISALEEQLQQIR	C*401
O14558	Heat shock protein beta-6	LFDQRFGEGLLEAELAALC*PTTLAPYYLR	C*46

P68363	Tubulin alpha-1B chain	AVC*MLSNTTAIAEAWAR	C*376
		AYHEQLSVAEITNAC*FEPANQMVK	C*295
O00151	PDZ and LIM domain protein 1	AALANLC*IGDVITAIDGENTSNMTHLEAQNR	C*45
		IKGC*TDNLTLTVAR	C*73
P69905	Hemoglobin subunit alpha	LLSHC*LLVTLAAHLPAEFTPAVHASLDKFLASVSTVLTSK	C*105
P68104	Elongation factor 1-alpha 1	NMITGTSQADC*AVLIVAAGVGEFEAGISK	C*111
		SGDAAIVDMVPGKPMC*VESFSDYPPLGR	C*411
Q5VTE0	Putative elongation factor 1-alpha-like 3	NMITGTSQADC*AVLIVAAGVGEFEAGISK	C*111
		SGDAAIVDMVPGKPMC*VESFSDYPPLGR	C*411
P00338	L-lactate dehydrogenase A chain	GLYGIKDDVFLSVPC*ILGQNGISDLVK	C*293
		LGVHPLSC*HGWVLGEHGDSSVPVWSGMNVAGVSLK	C*185
Q53GG5	PDZ and LIM domain protein 3	AAAANLC*PGDVILAIDGFGTESMTHADAQDR	C*44
P08779	Keratin, type I cytoskeletal 16	ISSVLAGGSC*RAPSTYGGGLSVSSR	C*40
		YC*MQLSQIQGLIGSVEEQLAQLR	C*369

Q01518	Adenylyl cyclase-associated protein 1	ALLVTASQC*QQPAENKLSDLLAPISEQIK	C*93
P67936	Tropomyosin alpha-4 chain	EENVGLHQTLDQTLNELNC*I	C*247
P62937	Peptidyl-prolyl cis-trans isomerase A	HTGPGILSMANAGPNTNGSQFFIC*TAK	C*115
		IIPGFMC*QGGDFTR	C*62
P04406	Glyceraldehyde-3-phosphate dehydrogenase	IISNASC*TTNC#LAPLAK	C*152
		IISNASC#TTNC*LAPLAK	C*156
P10768	S-formylglutathione hydrolase	SVSAFAPIC*NPVLC*PWGK	C*176, C*181
		SYPGSQLDILIDQGKDDQFLLDGQLLPDNFIAAC*TEK	C*243
P23142	Fibulin-1	RGYQLSDVDGVTC*EDIDEC*ALPTGGHIC*SYR	C*479, C*485, C*494
		C*LAFEC*PENYRR	C*551, C*556
Q14315	Filamin-C	FGGEHIPNSPFHVLAC*DPLPHEEEPSEVPQLR	C*1735
		SPFPVHVSEAC*NPNAC#R	C*472
P02042	Hemoglobin subunit delta	GTFSQLSELHC*DKLHVDPENFR	C*113
P06733	Alpha-enolase	SGETEDTFIADLVVGLC*TGQIK	C*389

Q9NZN4	EH domain-containing protein 2	FMC*AQLPNQVLESISIIDTPGILSGAK	C*138
P21291	Cysteine and glycine-rich protein 1	GLESTTLADKDGEIYC*K	C*170
		NLDSTTVAVHGEEIYC*K	C*58
P09211	Glutathione S-transferase P	TLGLYGKDQQEAALVDMVNDGVEDLRC*K	C*102
P07355	Annexin A2	EVKGDLENAFLNLVQC*IQNKPLYFADR	C*262
P02787	Serotransferrin	SAGWNIPIGLLYC*DLPEPR	C*156
P07437	Tubulin beta chain	LTTPTYGDLNHLVSATMSGVTTC*LR	C*239
Q8WX93	Palladin	RLLGADSATVFNIQEPEEETANQEYKVSSC*EQR	C*964
P04075	Fructose-bisphosphate aldolase A	ALSDHHIYLEGTLLKPNMVTPGHAC*TQK	C*240
Q01995	Transgelin	LVEWIIVQC*GPDVGRPDR	C*38
P24844	Myosin regulatory light polypeptide 9	NAFAC*FDEEASGFIHEDHLR	C*109
P35527	Keratin, type I cytoskeletal 9	YC*GQLQMIQEQISNLEAQITDVR	C*406
P12277	Creatine kinase B-type	SKDYEFMWNPHLGYILTC*PSNLGTGLR	C*283

P48668	Keratin, type II cytoskeletal 6C	ISIGGGSC*AISGGYGSR	C*77
P08670	Vimentin	QVQSLTC*EVDALKGTNESLER	C*328
Q14195	Dihydropyrimidinase-related protein 3	AITIASQTNC*PLYVTK	C*248
P54652	Heat shock-related 70 kDa protein 2	GPAIGIDLGTTYSC*VGVFQHGK	C*18
Q99497	Protein DJ-1	GLIAAIC*AGPTALLAHEIGFGSK	C*106
P60660	Myosin light polypeptide 6	ILYSQC*GDVMR	C*32
P47756	F-actin-capping protein subunit beta	NLSDLIDLVPSLC*EDLLSSVDQPLK	C*36
P02652	Apolipoprotein A-II	EPC*VESLVSQYFQTVTDYGKDLMEK	C*29
Q15942	Zyxin	C*SVC*SEPIMPEPGRDETVR	C*504, C*507
O00299	Chloride intracellular channel protein 1	EEFASTC*PDDEEIELAYEQVAK	C*223
P01861	Ig gamma-4 chain C region	WQEGNVFSC*SVMHEALHNHYTQK	C*305

Legend: Modified cysteines are marked with a * and non S-nitrosated cysteines are labeled with a #. Note some peptides were found in multiple states of S-nitrosation all of which were included in this table.

Table S4.3. Statistical values for area under the curve analysis of quantitated proteins.

UniProt Id	Sequence Name	F-Stat	P-Value	L Log2 Rel Ex	L Log2 Rel Ex Std Dev	NL Log2 Rel Ex	NL Log2 Rel Ex Std Dev	PTL Log2 Rel Ex	PTL Log2 Rel Ex Std Dev
P02768	ALBU	235.07	0	-0.14	0.58	0	0.33	-2.01	0.95
P60709	ACTB	9.19	0	0.38	0.64	0	0.35	-0.3	0.86
P21333	FLNA	0.03	0.975	-0.01	0.28	0	0.22	-0.02	1.03
P17661	DESM	0.67	0.514	0.01	0.79	0	0.22	0.2	1.17
P68871	HBB	92.08	0	-0.1	0.55	0	0.2	-2.5	1.42
P35527	K1C9	4.47	0.016	-0.12	0.92	0	1	0.69	1.02
P04792	HSPB1	0.91	0.406	0.06	0.62	0	0.26	0.2	1.02
P68363	TBA1B	3.76	0.03	0.31	0.4	0	0.28	-0.19	0.85
P69905	HBA	2.73	0.072	-0.19	0.74	0	0.21	-0.33	1.09
P02042	HBD	67.72	4.4E-16	0.08	0.59	0	0.22	-2.27	1.11
P07437	TBB5	1.24	0.301	-0.03	0.46	0	0.26	-0.24	0.72
P14618	KPYM	137.65	0	0.51	0.53	0	0.33	-2.16	0.48
P08670	VIME	0.13	0.879	-0.06	0.65	0	0.18	0.09	1.26
P06733	ENOA	5.14	0.01	0.46	0.8	0	0.4	-0.15	0.45
P04264	K2C1	2.55	0.093	-0.16	0.86	0	1.02	0.6	0.93
O14558	HSPB6	0.62	0.542	0.11	0.59	0	0.71	0.28	1.22
Q8WX93	PALLD	47.85	5.7E-12	0.33	0.62	0	0.35	-2.13	1.27
Q01995	TAGL	8.72	0.001	-0.05	0.62	0	0.39	1.15	1.43
P06753	TPM3	0.14	0.866	-0.12	1.34	0	0.46	0.14	1.45
P09211	GSTP1	80.82	6.1E-13	0.39	0.73	0	0.23	-2.74	0.79
Q15746	MYLK	19.23	1.11E-4	-0.02	0.9	0	0.35	-1.56	0.82
Q93052	LPP	25.42	3.66E-6	-0.11	0.81	0	0.27	-1.68	0.71
P12277	KCRB	39.49	0	0.19	0.55	0	0.35	-1.49	0.56
P62937	PPIA	5.61	0.01	0.14	0.71	0	0.29	0.69	0.7
Q14315	FLNC	0.87	0.433	0.16	0.16	0	0.24	-0.13	0.79
P04406	G3P	6.63	0.005	0.32	0.98	0	0.29	-0.87	0.82
O00151	PDLI1	9.17	0.001	0.11	0.68	0	0.4	-1.49	1.09
P04083	ANXA1	0.6	0.56	0.33	0.42	0	0.77	-0.06	0.88
P09382	LEG1	22.35	1.79E-	-0.2	0.68	0	0.59	-2.36	0.95

			8						
Q14195	DPYL3	4.5	0.03	0.47	0.73	0	0.27	-0.49	0.56
P60660	MYL6	13.43	3.58E-5	0.01	0.93	0	0.16	1.32	0.65
O43707	ACTN4	12.21	0.001	-0.38	0.32	0	0.21	-1.35	1.04
P21291	CSRP1	0.47	0.633	0.34	0.82	0	0.5	0.11	1.06
Q9NZN4	EHD2	5.24	0.019	0.44	0.48	0	0.33	-0.82	1.05
P18206	VINC	21.99	5.86E-5	-0.59	0.48	0	0.52	-2.15	1.11
P51911	CNN1	11.01	1.87E-4	-0.64	0.54	0	0.36	2.16	1.22
P31949	S10AB	0.26	0.782	0.03	1.06	0	0.34	-0.5	1.59
P08779	K1C16	0	1	-10	0	-10	0	10	0
O00299	CLIC1	7.46	0.014	0.39	0.72	0	0.2	-1.59	0.94
P07355	ANXA2	1.28	0.343	0.2	0.57	0	0.57	-0.66	0.94
P02787	TRFE	2.49	0.164	-0.83	0.36	0	0.48	-0.57	0.91
P68104	EF1A1	3.73	0.089	-0.08	0.61	0	0.51	-1.2	0.86
P00387	NB5R3	1.44	0.309	0.49	1.13	0	0.7	-0.85	1.09
Q15124	PGM5	1.23	0.358	0.16	0.67	0	0.63	-0.76	1.07
P47756	CAPZB	0.38	0.706	0	0.96	0	0.52	-0.72	0
P01009	A1AT	0.12	0.891	0.09	0.26	0	0.09	0.14	0.81
Q53GG5	PDLI3	0.18	0.842	-0.25	0.31	0	0.63	0	0.92
P24844	MYL9	5.14	0.001	0.57	0.58	0	0.29	1.35	0.93
P01857	IGHG1	5.25	0.048	-0.24	0.26	0	0.23	1	0.84
O95678	K2C75	0.74	0.515	0.47	0.91	0	1.25	0.89	1.31
Q9UMS6	SYNP2	0	1	-10	0	-10	0	10	0
P07737	PROF1	13.33	5.76E-5	0.02	0.41	0	0.23	2.12	1.01
Q9NR12	PDLI7	0.46	0.657	-0.19	0.44	0	0.75	0.42	0.96
P08133	ANXA6	16.16	0.002	0.47	0.49	0	0.47	-2.17	0.88
P10599	THIO		0.013	0.22	0.35	0	0.46	1.639	0.54

Legend: Statistical analysis of quantitated proteins showing the F-statistic, P-value, Log_2 Relative Expression, and Log_2 Relative Expression Standard Deviation of Laboring, Non Laboring, and Preterm Laboring samples. Data was extracted from area under the curve analysis of extracted ion chromatograms from ProteoIQ.

References

(2012). "ACOG practice bulletin no. 127: Management of preterm labor." Obstet Gynecol 119(6): 1308-1317.

Ahrens, C. H., E. Brunner, et al. (2010). "Generating and navigating proteome maps using mass spectrometry." Nat Rev Mol Cell Biol 11(11): 789-801.

Alexander, H. A., S. R. Sooranna, et al. (2012). "Myometrial tumor necrosis factor-alpha receptors increase with gestation and labor and modulate gene expression through mitogen-activated kinase and nuclear factor-kappaB." Reprod Sci 19(1): 43-54.

Bantscheff, M., S. Lemeer, et al. (2012). "Quantitative mass spectrometry in proteomics: critical review update from 2007 to the present." Anal Bioanal Chem 404(4): 939-965.

Bartlett, S. R., P. R. Bennett, et al. (1999). "Expression of nitric oxide synthase isoforms in pregnant human myometrium." J Physiol 521 Pt 3: 705-716.

Beck, S., D. Wojdyla, et al. (2010). "The worldwide incidence of preterm birth: a systematic review of maternal mortality and morbidity." Bull World Health Organ 88(1): 31-38.

Behrman, R. E. and A. S. Butler (2006). Preterm Birth: Causes, Consequences, and Prevention. A. S. B. Richard E.Behrman. THE NATIONAL ACADEMIES PRESS, 500 Fifth Street, N.W., Washington, DC 20001 National Academy of Sciences: 1-622.

Behrman, R. E. and A. S. Butler (2007). Preterm Birth: Causes, Consequences, and Prevention, The National Academies Press.

Bradley, K. K., I. L. Buxton, et al. (1998). "Nitric oxide relaxes human myometrium by a cGMP-independent mechanism." Am.J.Physiol 275(6 Pt 1): C1668-C1673.

Brill, L. M., K. Motamedchaboki, et al. (2009). "Comprehensive proteomic analysis of Schizosaccharomyces pombe by two-dimensional HPLC-tandem mass spectrometry." Methods 48(3): 311-319.

Broniowska, K. A., A. R. Diers, et al. (2013). "S-Nitrosoglutathione." Biochim Biophys Acta.

Broniowska, K. A. and N. Hogg (2012). "The chemical biology of s-nitrosothiols." Antioxid Redox Signal 17(7): 969-980.

Buhimschi, C., I. Buhimschi, et al. (1997). "Contrasting effects of diethylenetriamine-nitric oxide, a spontaneously releasing nitric oxide donor, on pregnant rat uterine contractility in vitro versus in vivo." American journal of obstetrics and gynecology 177(3): 690-701.

Buxton, I. L. (2004). "Regulation of uterine function: a biochemical conundrum in the regulation of smooth muscle relaxation." Mol. Pharmacol. 65(5): 1051-1059.

Buxton, I. L. and L. L. Brunton (1983). "Compartments of cyclic AMP and protein kinase in mammalian cardiomyocytes." J. Biol. Chem. 258(17): 10233-10239.

Buxton, I. L., W. Crow, et al. (2000). "Regulation of uterine contraction: mechanisms in preterm labor." AACN.Clin.Issues 11(2): 271-282.

Buxton, I. L., R. A. Kaiser, et al. (2001). "NO-induced relaxation of labouring and non-labouring human myometrium is not mediated by cyclic GMP." British Journal of Pharamcology 134(1): 206-214.

Buxton, I. L., D. Milton, et al. (2010). "Agonist-specific compartmentation of cGMP action in myometrium." JPET 335(1): 256-263.

Buxton, I. L. O., W. Crow, et al. (2000). "Regulation of Uterine Contraction: Mechanisms in Preterm Labor." AACN Clinical Issues 11(2): 271-282.

Carmichael, J. D., S. J. Winder, et al. (1994). "Calponin and smooth muscle regulation." Can J Physiol Pharmacol 72(11): 1415-1419.

Carvajal, J. A., A. M. Germain, et al. (2000). "Molecular mechanism of cGMP-mediated smooth muscle relaxation." J.Cell Physiol 184(3): 409-420.

Cary, S. P., J. A. Winger, et al. (2006). "Nitric oxide signaling: no longer simply on or off." Trends in biochemical sciences 31(4): 231-239.

Choe, Y. S., C. Shim, et al. (1997). "Expression of galectin-1 mRNA in the mouse uterus is under the control of ovarian steroids during blastocyst implantation." Mol Reprod Dev 48(2): 261-266.

Choi, H., T. Glatter, et al. (2012). "SAINT-MS1: protein-protein interaction scoring using label-free intensity data in affinity purification-mass spectrometry experiments." J Proteome Res 11(4): 2619-2624.

Cleeter, M. W., J. M. Cooper, et al. (1994). "Reversible inhibition of cytochrome c oxidase, the terminal enzyme of the mitochondrial respiratory chain, by nitric oxide. Implications for neurodegenerative diseases." FEBS letters 345(1): 50-54.

Daher, S., F. Fonseca, et al. (1999). "Tumor necrosis factor during pregnancy and at the onset of labor and spontaneous abortion." Eur J Obstet Gynecol Reprod Biol 83(1): 77-79.

Dalle-Donne, I., A. Milzani, et al. (2000). "S-NO-actin: S-nitrosylation kinetics and the effect on isolated vascular smooth muscle." J Muscle Res Cell Motil 21(2): 171-181.

Davis, K. L., E. Martin, et al. (2001). "Novel effects of nitric oxide." Annual Review of Pharamacology and Toxicology 41: 203-236.

Dudley, D. J. (1999). "Immunoendocrinology of preterm labor: the link between corticotropin-releasing hormone and inflammation." Am J Obstet Gynecol 180(1 Pt 3): S251-256.

Eiserich, J. P., M. Hristova, et al. "Formation of nitric oxide- derived inflammatory oxidants by myeloperoxidase in neutrophils." Nature 391: 393-397.

Evangelista, A. M., V. S. Rao, et al. (2010). "Direct regulation of striated muscle myosins by nitric oxide and endogenous nitrosothiols." PLoS One 5(6): e11209.

Furchgott, R. F. and J. V. Zawadzki (1980). "The obligatory role of endothelial cells in the relaxation of arterial smooth muscle by acetylcholine." Nature 288: 373-376.

Gaston, B., J. Reilly, et al. (1993). "Endogenous nitrogen oxides and bronchodilator S-nitrosothiols in human airways." Proc Natl Acad Sci U S A 90(23): 10957-10961.

Gaston, B. M. and J. S. Stamler (1999). Biochemistry of Nitric Oxide, Kluwer Academic/Plenum.

Glaser, B. (2010). "Genetic analysis of complex disease--a roadmap to understanding or a colossal waste of money." Pediatr Endocrinol Rev 7(3): 258-265.

Gorenne, I., R. K. Nakamoto, et al. (2003). "LPP, a LIM protein highly expressed in smooth muscle." Am J Physiol Cell Physiol 285(3): C674-685.

Han, M., L. H. Dong, et al. (2009). "Smooth muscle 22 alpha maintains the differentiated phenotype of vascular smooth muscle cells by inducing filamentous actin bundling." Life sciences 84(13-14): 394-401.

Henson, S. E., T. C. Nichols, et al. (1999). "The ectoenzyme gamma-glutamyl transpeptidase regulates antiproliferative effects of S-nitrosoglutathione on human T and B lymphocytes." J Immunol 163(4): 1845-1852.

Hess, D. T., A. Matsumoto, et al. (2005). "Protein S-nitrosylation: purview and parameters." Nat.Rev.Mol.Cell Biol. 6(2): 150-166.

Hooper, C. L., P. R. Dash, et al. (2012). "Lipoma preferred partner is a mechanosensitive protein regulated by nitric oxide in the heart." FEBS Open Bio 2(0): 135-144.

Huie, R. E. and S. Padmaja (1993). "The reaction of NO with superoxide." Free Radic.Res.Commun. 18: 195-199.

Hunt, J. S., H. L. Chen, et al. (1992). "Tumor necrosis factor-alpha messenger ribonucleic acid and protein in human endometrium." Biol Reprod 47(1): 141-147.

Ivanisevic, M., S. Segerer, et al. (2010). "Antigen-presenting cells in pregnant and non-pregnant human myometrium." American journal of reproductive immunology 64(3): 188-196.

Jaffer, S., O. Shynlova, et al. (2009). "Mammalian target of rapamycin is activated in association with myometrial proliferation during pregnancy." Endocrinology 150(10): 4672-4680.

Jaffrey, S. R. and S. H. Snyder (2001). "The biotin switch method for the detection of S-nitrosylated proteins." Sci.STKE. 2001(86): L1.

Je, H. D. and U. D. Sohn (2007). "SM22alpha is required for agonist-induced regulation of contractility: evidence from SM22alpha knockout mice." Mol Cells 23(2): 175-181.

Kakui, K., H. Itoh, et al. (2004). "Augmented endothelial nitric oxide synthase (eNOS) protein expression in human pregnant myometrium: possible

involvement of eNOS promoter activation by estrogen via both estrogen receptor (ER)alpha and ERbeta." Mol Hum Reprod 10(2): 115-122.

Kamm, K. E. and J. T. Stull (1989). "Regulation of smooth muscle contractile elements by second messengers." Annu Rev Physiol 51: 299-313.

Keller, A., A. I. Nesvizhskii, et al. (2002). "Empirical statistical model to estimate the accuracy of peptide identifications made by MS/MS and database search." Anal Chem 74(20): 5383-5392.

Kinney, M. V., C. P. Howsen, et al. (2012). "Executive Summary for Born Too Soon: The Global Action Report on Preterm Birth." March of Dimes, PMNCH, Save the Children, World Health Organization.

Kirsch, M., A. M. Buscher, et al. (2009). "New insights into the S-nitrosothiol-ascorbate reaction. The formation of nitroxyl." Org Biomol Chem 7(9): 1954-1962.

Kluge, I., U. Gutteck-Amsler, et al. (1997). "S-nitrosoglutathione in rat cerebellum: identification and quantification by liquid chromatography-mass spectrometry." J Neurochem 69(6): 2599-2607.

Koh, S. D., K. Monaghan, et al. (2001). "TREK-1 regulation by nitric oxide and cGMP-dependent protein kinase. An essential role in smooth muscle inhibitory neurotransmission." Journal of Biological Chemistry 276(47): 44338-44346.

Kostenko, S. and U. Moens (2009). "Heat shock protein 27 phosphorylation: kinases, phosphatases, functions and pathology." Cellular and Molecular Life Sciences 66(20): 3289-3307.

Kuenzli, K. A., M. E. Bradley, et al. (1996). "Cyclic GMP-independent effects of nitric oxide on guinea-pig uterine contractility." Br J Pharmacol. 119(4): 737-743.

Kuenzli, K. A., I. L. Buxton, et al. (1998). "Nitric oxide regulation of monkey myometrial contractility." Br.J Pharmacol. 124(1): 63-68.

Lawn, J. E., K. Wilczynska-Ketende, et al. (2006). "Estimating the causes of 4 million neonatal deaths in the year 2000." Int J Epidemiol 35(3): 706-718.

Leoni, P., F. Carli, et al. (1990). "Intermediate filaments in smooth muscle from pregnant and non-pregnant human uterus." Biochemical Journal 269: 31-34.

Lim, C. H., P. C. Dedon, et al. (2008). "Kinetic analysis of intracellular concentrations of reactive nitrogen species." Chem Res Toxicol 21(11): 2134-2147.

Littler, D. R., S. J. Harrop, et al. (2004). "The intracellular chloride ion channel protein CLIC1 undergoes a redox-controlled structural transition." J Biol Chem 279(10): 9298-9305.

Lok, H. C., Y. Suryo Rahmanto, et al. (2012). "Nitric oxide storage and transport in cells are mediated by glutathione S-transferase P1-1 and multidrug resistance protein 1 via dinitrosyl iron complexes." J Biol Chem 287(1): 607-618.

MacPherson, J. C., S. A. Comhair, et al. (2001). "Eosinophils are a major source of nitric oxide-derived oxidants in severe asthma: characterization of pathways available to eosinophils for generating reactive nitrogen species." J Immunol 166(9): 5763-5772.

Malinski, T., Z. Taha, et al. (1993). "Diffusion of nitric oxide in the aorta wall monitored in situ by porphyrinic microsensors." Biochem Biophys Res Commun 193(3): 1076-1082.

Meyer, D. J., H. Kramer, et al. (1994). "Kinetics and equilibria of S-nitrosothiol-thiol exchange between glutathione, cysteine, penicillamines and serum albumin." FEBS Lett 345(2-3): 177-180.

Mezgueldi, M., C. Mendre, et al. (1995). "Characterization of the regulatory domain of gizzard calponin. Interactions of the 145-163 region with F-actin, calcium-binding proteins, and tropomyosin." J Biol Chem 270(15): 8867-8876.

Mitchell, B. F. and M. J. Taggart (2009). "Are animal models relevant to key aspects of human parturition?" American journal of physiology. Regulatory, integrative and comparative physiology 297(3): R525-545.

Modzelewska, B. and A. Kostrzewska (2005). "The influence of methylene blue on the spontaneous contractity of the non-pregnant human myometrium and on the myometrial response to DEA/NO." Cell Mol.Biol.Lett. 10(3): 389-400.

Nathan, C. (1992). "Nitric oxide as a secretory product of mammalian cells." FASEB J. 6: 3051-3064.

Nesvizhskii, A. I., A. Keller, et al. (2003). "A statistical model for identifying proteins by tandem mass spectrometry." Anal Chem 75(17): 4646-4658.

Nogueira, L., C. Figueiredo-Freitas, et al. (2009). "Myosin is reversibly inhibited by S-nitrosylation." Biochem J 424(2): 221-231.

Norman, J. E. and I. T. Cameron (1996). "Nitric oxide in the human uterus." Rev.Reprod. 1(1): 61-68.

Okagaki, T., K. Hayakawa, et al. (1999). "Inhibition of the ATP-dependent interaction of actin and myosin by the catalytic domain of the myosin light chain kinase of smooth muscle: possible involvement in smooth muscle relaxation." J Biochem 125(3): 619-626.

Opazo, S. A., W. Zhang, et al. (2004). "Tension development during contractile stimulation of smooth muscle requires recruitment of paxillin and vinculin to the membrane." Am.J.Physiol Cell Physiol 286(2): C433-C447.

Padgett, C. M. and A. R. Whorton (1995). "S-nitrosoglutathione reversibly inhibits GAPDH by S-nitrosylation." Am J Physiol 269(3 Pt 1): C739-749.

Petit, M. M., J. Fradelizi, et al. (2000). "LPP, an actin cytoskeleton protein related to zyxin, harbors a nuclear export signal and transcriptional activation capacity." Mol Biol Cell 11(1): 117-129.

Price, S. A. and A. L. Bernal (2001). "Uterine quiescence: the role of cyclic AMP." Exp Physiol 86(2): 265-272.

Ramachandran, N., S. Jacob, et al. (1999). "N-dansyl-S-nitrosohomocysteine a fluorescent probe for intracellular thiols and S-nitrosothiols." Biochim Biophys Acta 1430(1): 149-154.

Ramachandran, N., P. Root, et al. (2001). "Mechanism of transfer of NO from extracellular S-nitrosothiols into the cytosol by cell-surface protein disulfide isomerase." Proc Natl Acad Sci U S A 98(17): 9539-9544.

Rosenfeld, J., J. Capdevielle, et al. (1992). "In-gel digestion of proteins for internal sequence analysis after one- or two-dimensional gel electrophoresis." Anal Biochem 203(1): 173-179.

Sandoz, G., S. C. Bell, et al. (2011). "Optical probing of a dynamic membrane interaction that regulates the TREK1 channel." Proceedings of the National Academy of Sciences of the United States of America 108(6): 2605-2610.

Santolini, J., S. Adak, et al. (2001). "A kinetic simulation model that describes catalysis and regulation in nitric-oxide synthase." J Biol Chem 276(2): 1233-1243.

Santolini, J., A. L. Meade, et al. (2001). "Differences in three kinetic parameters underpin the unique catalytic profiles of nitric-oxide synthases I, II, and III." J Biol Chem 276(52): 48887-48898.

Schnitzer, J. E. and P. Oh (1994). "Albondin-mediated capillary permeability to albumin. Differential role of receptors in endothelial transcytosis and endocytosis of native and modified albumins." J Biol Chem 269(8): 6072-6082.

Shi, Q., J. Feng, et al. (2008). "A proteomic study of S-nitrosylation in the rat cardiac proteins in vitro." Biol Pharm Bull 31(8): 1536-1540.

Shynlova, O., T. Nedd-Roderique, et al. (2012). "Myometrial immune cells contribute to term parturition, preterm labour and post-partum involution in mice." Journal of cellular and molecular medicine.

Shynlova, O., P. Tsui, et al. (2009). "Integration of endocrine and mechanical signals in the regulation of myometrial functions during pregnancy and labour." Eur J Obstet Gynecol Reprod Biol 144 Suppl 1: S2-10.

Singh, H., M. A. Cousin, et al. (2007). "Functional reconstitution of mammalian 'chloride intracellular channels' CLIC1, CLIC4 and CLIC5 reveals differential regulation by cytoskeletal actin." FEBS J 274(24): 6306-6316.

Smith, B. C. and M. A. Marletta (2012). "Mechanisms of S-nitrosothiol formation and selectivity in nitric oxide signaling." Curr Opin Chem Biol.

Somara, S., R. Gilmont, et al. (2009). "Role of thin-filament regulatory proteins in relaxation of colonic smooth muscle contraction." American Journal of Physiology-Gastrointestinal and Liver Physiology 297(5): G958-G966.

Stamler, J. S., O. Jaraki, et al. (1992). "Nitric oxide circulates in mammalian plasma primarily as an S-nitroso adduct of serum albumin." Proc Natl Acad Sci U S A 89(16): 7674-7677.

Steinborn, A., M. Kuhnert, et al. (1996). "Immunmodulating cytokines induce term and preterm parturition." J Perinat Med 24(4): 381-390.

Stuehr, D. J., J. Santolini, et al. (2004). "Update on mechanism and catalytic regulation in the NO synthases." J Biol Chem 279(35): 36167-36170.

Suzuki, T., C. Mori, et al. (2009). "Changes in nitric oxide production levels and expression of nitric oxide synthase isoforms in the rat uterus during pregnancy." Biosci Biotechnol Biochem 73(10): 2163-2166.

Tabibzadeh, S. (1991). "Ubiquitous expression of TNF-alpha/cachectin immunoreactivity in human endometrium." Am J Reprod Immunol 26(1): 1-4.

Tang, D. D. (2008). "Intermediate filaments in smooth muscle." Am J Physiol Cell Physiol 294(4): C869-878.

Tattersall, M., N. Engineer, et al. (2008). "Pro-labour myometrial gene expression: are preterm labour and term labour the same?" Reproduction. 135(4): 569-579.

Tichenor, S. D., N. A. Malmquist, et al. (2003). "Dissociation of cGMP accumulation and relaxation in myometrial smooth muscle: effects of S-nitroso-N-acetylpenicillamine and 3-morpholinosyndonimine." Cell Signal. 15(8): 763-772.

Ulrich, C., D. R. Quillici, et al. (2012). "Uterine smooth muscle S-nitrosylproteome in pregnancy." Mol. Pharmacol. 81(2): 143-153.

Valdes, G. and J. Corthorn (2011). "Review: The angiogenic and vasodilatory utero-placental network." Placenta 32 Suppl 2: S170-175.

Voltolini, C., M. Torricelli, et al. (2013). "Understanding Spontaneous Preterm Birth: From Underlying Mechanisms to Predictive and Preventive Interventions." Reprod Sci.

Wang, R., Q. Li, et al. (2006). "Role of vimentin in smooth muscle force development." Am J Physiol Cell Physiol 291(3): C483-489.

White, B. G., S. J. Williams, et al. (2005). "Small heat shock protein 27 (Hsp27) expression is highly induced in rat myometrium during late pregnancy and labour." Reproduction 129(1): 115-126.

Winder, S. J., B. G. Allen, et al. (1998). "Regulation of smooth muscle actin-myosin interaction and force by calponin." Acta Physiol Scand 164(4): 415-426.

Wu, G. and S. M. Morris, Jr. (1998). "Arginine metabolism: nitric oxide and beyond." Biochem J 336 (Pt 1): 1-17.

Xue, Y., Z. Liu, et al. (2010). "GPS-SNO: computational prediction of protein S-nitrosylation sites with a modified GPS algorithm." PLoS One 5(6): e11290.

Yellon, S. M., A. M. Mackler, et al. (2003). "The role of leukocyte traffic and activation in parturition." J.Soc.Gynecol.Investig. 10(6): 323-338.

Yuan, W. and A. Lopez Bernal (2007). "Cyclic AMP signalling pathways in the regulation of uterine relaxation." BMC Pregnancy Childbirth 7 Suppl 1: S10.